

UNIVERSITÄT DUISBURG-ESSEN

LEHRSTUHL FÜR TECHNISCHE CHEMIE II

Thin-Layer Hydrogel Composite Membranes with
Tailored Antifouling and Ultrafiltration Properties:
Preparation, Characterisation and
Performance in Bioseparation

Dissertation

zur Erlangung des akademischen Grades

Dr. rer. nat.

der Fakultät für Chemie

der Universität Duisburg-Essen

vorgelegt von DIPL.-ING. POLINA D. PEEVA

geboren am 29.12.1983 in Bulgarien

Essen 2011

Tag der mündlichen Prüfung: 6. Dezember 2011

Vorsitzender: Prof. Dr. W. Sand

Referent: Prof. Dr. M. Ulbricht

Korreferenten: Prof. Dr. C. Mayer

Prof. Dr. T. Melin

ABSTRACT

Aim of this work was to evaluate the optimum conditions for functionalisation of polyethersulfone (PES) ultrafiltration (UF) membranes, as such modified membranes have been already viewed as very promising “new generation” low-fouling materials [1]. Anti-fouling composite membranes were prepared via photo-initiated “grafting-from” of the hydrophilic monomer poly(ethylene glycol) methacrylate (PEGMA) on commercial PES UF membranes with wide range of nominal molecular weight cut-off (MWCO). A fine adjustment of the sieving properties of the modified membranes was achieved by addition of suited crosslinker monomers in appropriate ratio to the reaction mixture. In this study, two crosslinkers were used: N,N'-methylene bisacrylamide (MBAA) and pentaerythritol triallyl ether (PETAE). Systematic variations of UV intensity and UV irradiation dose in combination with different monomer mixtures were performed in order to examine the effect of UV irradiation and crosslinker type and amount on the fouling and selectivity behaviour of the composite membranes. Therefore, a comprehensive study of the membrane properties via contact angle (CA), zeta potential (ZP), water permeability, selectivity/rejection and microscopic measurements was performed.

The results showed that at same UV irradiation dose, increasing the UV irradiation intensity led to increased degree of grafting (DG), higher water permeability but also increased MWCO. By this means, at higher UV intensity, the synthesis of more hydrogel on the membrane surface did not lead to lower membrane cut-off due to the more aggressive conditions at relatively high UV intensity leading to more open membrane structure. The type and amount of the used crosslinkers had an impact on the membrane performance as well. Crosslinking with MBAA led to lower flux and cut-off values; by increasing the amount of MBAA this effect was amplified. In contrast, the crosslinking with PETAE increased the flux and cut-off. Applying the optimised functionalisation conditions made it possible to prepare membranes with similar water flux and sieving properties to virgin membranes but with better fouling resistance.

Furthermore, the fouling behaviour and principles, and the membrane performance of virgin and modified membranes were evaluated during filtration experiments with proteins (myoglobin, bovine serum albumin, γ -globulin, fibrinogen and thyroglobulin), humic substances and polyphenolics as well as during cleaning and long term stability tests.

Membrane properties (membrane chemistry, morphology and charge), solution properties (solute nature, size, concentration and charge) as well as operating parameters (hydrodynamics and operation mode) had an impact on the membrane performance during filtration, since these parameters influence the membrane-solute and solute-solute interactions governing fouling. The modification with hydrogel layer increased the fouling resistance of the membranes. Modified membranes with similar water flux and cut-off to virgin membranes showed higher permeate fluxes and more stable rejection properties during filtration. After several cleaning steps, functionalised membranes showed more stable behaviour and better filtration performance.

The obtained results suggested that by adapting the membrane characteristics and operation conditions to the properties of the feed to be filtered, the performance of the desired process can be well controlled by minimising fouling effects.

This work was performed during the period from February 2008 to May 2011 at the Lehrstuhl für Technische Chemie II, Universität Duisburg-Essen, under the supervision of Prof. Dr. Mathias Ulbricht.

I declare that this dissertation represents my own work, except where due acknowledgement is made.

Polina Peeva

ACKNOWLEDGEMENTS

First of all, I am grateful to Prof. Dr. Mathias Ulbricht for giving me the great opportunity to work in his research group. He always supported me through the difficulties of my research work and encouraged me.

Secondly, I would like to thank Prof. Dr. Christian Mayer and Prof. Dr. Thomas Melin (Rheinisch-Westfälische Technische Hochschule Aachen) for being the co-referents of my work.

I am very thankful to Dr. Heru Susanto and Dr. Eva Maria Berndt for their help, support and inspiring discussions on my work.

The work with Dr. Eva Maria Berndt, Dr. Marcel Gawenda, Dr. Monica Sallai, Dr. Haofei Guo, Nadia Adrus, Karin Klingelhöller and Sven Behnke was a pleasure for me and I would like to thank them all for the nice time we spent together.

I also want to acknowledge Inge Danielzik, Claudia Schenk, Roswitha Nordmann-Silberg, Tobias Kallweit and Jürgen Schulze-Braucks for their support.

I would like to thank Andreas Niermann, Anna Tarasova, Kathryn Marshall, Thorsten Pieper, Dr. Aisyah Endah Palupi, Nina Million and Thomas Knoche for their effort working with me.

All members of the Lehrstuhl für Technische Chemie II are deeply acknowledged for the nice atmosphere they provided me during my PhD research.

Furthermore, I am grateful to Dr. Volkmar Thom, Dr. Eberhard Wünn and Dr. Tobias Schleuß from Sartorius-Stedim Biotech GmbH for supporting me with the base membranes. They are acknowledged for performing of GPC measurements relevant to my work and the discussion on my research.

I want to thank Smail Boukercha (Zentrallabor für Rasterelektronenmikroskopie), Dieter Jacobi (Lehrstuhl für Technische Chemie) and Dr. Daniel Schunk (Arbeitskreis Prof. Dr. Christian Mayer) who performed important analysis for my work. Special thanks go to Prof. Dr. Ranil Wickramasinghe (Colorado State University, Ft. Collins, CO, USA), who helped with the fouling mechanism analysis.

Deutsche Bundesstiftung Umwelt (DBU) is acknowledged for supporting me and my work with a PhD scholarship.

I would like to thank my good friend Valentina Dontcheva for the revision of my English text and Dr. Wolfgang Laarz (Lehrstuhl für Technische Chemie I) for helping me with the printing of this work.

Special thanks are dedicated to Mathias Quilitzsch for supporting me and being patient through the difficult moments of my PhD study. He and his family are giving me a warm and familial atmosphere in Germany.

Finally, my deep thanks go to my family in Bulgaria for making me the person I am, giving me all their love and supporting me from far away.

CONTENT

ABSTRACT..... I

ACKNOWLEDGEMENTS..... III

CONTENT..... IV

1 INTRODUCTION IN MEMBRANE FILTRATION 1

2 THEORY 3

 2.1 FLUX DECLINE 3

 2.1.1 CONCENTRATION POLARISATION 3

 2.1.2 FOULING 5

 2.1.2.1 Fouling models 7

 2.1.2.2 General membrane equation 8

 2.1.3 FACTORS AFFECTING FOULING 9

 2.2 STRATEGIES FOR FLUX IMPROVEMENT 12

 2.3 MEMBRANE MODIFICATION 13

 2.3.1 OVERVIEW OF GENERAL STRATEGIES 13

 2.3.2 GRAFTING-FROM SURFACE MODIFICATION USING ULTRAVIOLET LIGHT 16

 2.3.3 REQUIREMENTS FOR FOULING RESISTANT SURFACES 17

3 CONCEPT 18

4 EXPERIMENTAL..... 22

 4.1 MATERIALS AND CHEMICALS 22

 4.1.1 MEMBRANES..... 22

 4.1.2 MODIFIER COMPOSITIONS..... 23

 4.1.3 HYDROGEL COMPOSITIONS..... 24

 4.1.4 TEST SOLUTIONS 24

 4.1.4.1 Rejection experiments 24

 4.1.4.2 Adsorption, diffusion and filtration experiments..... 25

 4.1.5 OTHERS..... 27

 4.2 EXPERIMENTS..... 27

4.2.1	BULK HYDROGELS	27
4.2.1.1	Preparation	27
4.2.1.2	Swelling experiments	27
4.2.1.3	Calculation of the mesh size.....	28
4.2.1.4	Absorption of test solutes	28
4.2.2	PREPARATION OF NON-POROUS PES FILMS.....	29
4.2.3	FUNCTIONALISATION VIA PHOTO-GRAFTING	29
4.2.4	MEMBRANE SURFACE CHARACTERISATION	30
4.2.4.1	Degree of grafting	30
4.2.4.2	Modification depth	30
4.2.4.3	Estimation of the average radical density.....	30
4.2.4.4	Contact angle.....	31
4.2.4.5	Attenuated total reflection infrared spectroscopy.....	31
4.2.4.6	Zeta potential.....	31
4.2.4.6.1	Measurement with consideration of the cell conductivity.....	32
4.2.4.6.2	Measurement without consideration of the cell conductivity.....	32
4.2.4.7	Atomic force microscopy	33
4.2.4.8	Scanning electron microscopy.....	33
4.2.5	CHARACTERISATION OF MEMBRANE PERFORMANCE.....	33
4.2.5.1	Water permeability	33
4.2.5.2	Rejection experiments	34
4.2.5.3	Adsorption of test solutes	35
4.2.5.4	Diffusion experiments	35
4.2.5.5	Filtration	37
4.2.5.5.1	Stirred dead-end filtration	37
4.2.5.5.1.1	Short stirred dead-end filtration	37
4.2.5.5.1.1.1	Two fold volume reduction	37
4.2.5.5.1.1.2	20 fold volume reduction	37
4.2.5.5.1.2	Stirred dead-end filtration over 24 hours.....	37
4.2.5.5.2	Cross-flow filtration	38

4.2.5.5.3	Stability tests.....	39
4.2.5.6	Membrane cleaning	39
4.2.5.6.1	Cleaning after dead-end filtration.....	40
4.2.5.6.2	Cleaning after cross-flow filtration.....	40
5	RESULTS.....	41
5.1	BULK HYDROGELS.....	41
5.1.1	CHARACTERISATION.....	41
5.1.2	ABSORPTION OF TEST SUBSTANCES.....	42
5.2	MEMBRANE PROPERTIES	43
5.2.1	DEGREE OF GRAFTING	43
5.2.2	WETTABILITY	44
5.2.3	CHARACTERISATION OF THE MEMBRANE COMPOSITION USING ATR-IR.....	45
5.2.4	SURFACE CHARGE.....	45
5.2.5	MEMBRANE ROUGHNESS	48
5.2.6	MEMBRANE MORPHOLOGY.....	49
5.2.6.1	Virgin membranes	49
5.2.6.2	Functionalised membranes	51
5.2.6.2.1	PES 50	51
5.2.6.2.2	PES 100	52
5.2.7	MEMBRANE MODIFICATION DEPTH (EDX-SEM)	53
5.2.8	ESTIMATION OF THE AVERAGE RADICAL DENSITY	54
5.3	MEMBRANE PERFORMANCE.....	54
5.3.1	WATER PERMEABILITY	54
5.3.1.1	PES 10	56
5.3.1.2	PES 50	57
5.3.1.3	PES 100	58
5.3.1.4	PES 300	59
5.3.2	REJECTION CURVES	59
5.3.2.1	Virgin membranes	59
5.3.2.2	Modified membranes without crosslinkers.....	62

5.3.2.3	Modified membranes with crosslinkers	65
5.3.2.3.1	PES 10	65
5.3.2.3.2	PES 50	66
5.3.2.3.3	PES 100	67
5.3.2.3.4	PES 300	68
5.3.3	ADSORPTION OF TEST SOLUTES	69
5.3.4	DIFFUSION OF TEST SOLUTES	70
5.3.5	PROTEIN FILTRATION	71
5.3.5.1	Stirred dead-end protein filtration	71
5.3.5.1.1	Short stirred dead-end filtration	71
5.3.5.1.1.1	Two fold volume reduction	71
5.3.5.1.1.1.1	PES 30	72
5.3.5.1.1.1.2	PES 50	73
5.3.5.1.1.1.3	PES 100	76
5.3.5.1.1.1.4	PES 300	78
5.3.5.1.1.2	20 fold volume reduction	79
5.3.5.1.2	Stirred dead-end filtration over 24 hours and cleaning	80
5.3.5.1.2.1	PES 10	80
5.3.5.1.2.2	PES 30	82
5.3.5.1.2.3	PES 50	83
5.3.5.1.2.3.1	Filtration with virgin membranes	83
5.3.5.1.2.3.2	Filtration with functionalised membranes	84
5.3.5.1.2.4	PES 100	88
5.3.5.2	Cross-flow filtration and cleaning	90
5.3.5.2.1	PES 10	91
5.3.5.2.2	PES 30	92
5.3.5.2.3	PES 50	94
5.3.5.2.3.1	Virgin membranes	94
5.3.5.2.3.2	Functionalised membranes	95
5.3.5.3	Stability	97

5.3.5.3.1	Virgin membranes	97
5.3.5.3.2	Functionalised membranes	98
5.3.6	FILTRATION OF HUMIC ACID	99
5.3.6.1	Virgin membranes	99
5.3.6.2	Functionalised membranes	101
5.3.7	FILTRATION OF POLYPHENOLICS	104
5.3.7.1	Short stirred dead-end filtration.....	104
5.3.7.2	Cross-flow filtration	105
6	DISCUSSION.....	106
6.1	MEMBRANE CHARACTERISATION	106
6.1.1	VIRGIN MEMBRANES – MEMBRANE MORPHOLOGY AND CHEMISTRY	106
6.1.2	FUNCTIONALISED MEMBRANES	107
6.1.2.1	Effect of the UV irradiation on membrane structure	107
6.1.2.2	Effect of the crosslinker type and amount	109
6.1.3	VALIDATION OF THE IMPROVEMENT OF MEMBRANE PERFORMANCE BY COMPOSITE MEMBRANES	111
6.1.3.1	Fouling and rejection during rejection curve measurements	111
6.1.3.2	Rejection properties of membranes with similar water fluxes	113
6.2	PROTEIN FILTRATION.....	116
6.2.1	GENERAL	116
6.2.1.1	Charge effects	116
6.2.1.2	Fouling mechanisms study	118
6.2.2	VIRGIN MEMBRANES.....	119
6.2.3	COMPOSITE MEMBRANES.....	126
6.2.4	VALIDATION OF THE IMPROVEMENT OF MEMBRANE PERFORMANCE BY COMPOSITE MEMBRANES	135
6.2.4.1	Effect of the modification on fouling behaviour	135
6.2.4.2	Effect of the test solution properties.....	140
6.2.4.3	Effect of the operating parameters.....	142
6.2.4.4	Effect of cleaning and long term stability.....	144
6.3	FILTRATION OF HUMIC ACID	145

6.3.1	EFFECT OF PORE SIZE.....	145
6.3.2	EFFECT OF PREFILTRATION.....	148
6.3.3	COMPARISON OF VIRGIN AND MODIFIED MEMBRANES.....	151
6.3.3.1	Permeate flux and rejection during filtration.....	151
6.3.3.2	Fouling regimes and parameters.....	153
6.3.3.3	Effect of cleaning	154
6.4	FILTRATION OF POLYPHENOLICS	156
7	CONCLUSIONS AND OUTLOOK.....	158
	REFERENCES.....	162
	APPENDIX A	176
	APPENDIX B.....	209
	LIST OF TABLES	209
	LIST OF FIGURES	211
	ABBREVIATIONS	219
	APPENDIX C.....	221
	CURRICULUM VITAE.....	221
	LIST OF PUBLICATIONS	222

1 INTRODUCTION IN MEMBRANE FILTRATION

Filtration is a powerful technique that can be used in a variety of applications such as food processing, waste water treatment, biotechnology, desalination and other process stream separations [2,3]. Membrane processes are preferred to common separation techniques due to their beneficial characteristics such as low energy consumption, easy control of operation and lower waste production. Membranes with wide variety of pore sizes are used: microfiltration (MF) membranes remove dispersed solids or bacteria; UF is important for the removal of viruses, proteins, natural organic matter (NOM) and other biomacromolecules; nanofiltration (NF) removes effectively NOM, polyphenolic compounds and divalent cations [4,5].

As mentioned above, ultrafiltration processes are widely used in the biotechnology for separation and purification of bioactive substances [6], in the waste water treatment [7] and production of drinking water [8] as well as in the food industry for the improvement of taste and stability of beverages for production of high quality products [9]. UF membranes act as selective barriers where rejection is dependent on the pore size compared to the size of the molecule being recovered, i.e., the main filtration principle is the size exclusion [6]. Among wide variety of polymers commonly used for preparation of membranes, such as cellulose acetate (CAc), polycarbonates, polyamides, polyolefins (polyethylene, polypropylene) etc., membranes made of polysulfone (PSf) and PES are mostly used because of their mechanical, chemical and thermal stability [10-14]. Besides their moderate stability against organic solvents, another disadvantage of these materials is their hydrophobicity and consequently low surface wettability.

However, complications such as non-uniform pore size, concentration polarisation (CP), and fouling often occur and cause less performance of the filtration processes. Due to the importance of these problems, many strategies have been developed in order to increase the process performance. It has been found that CP and fouling can be controlled by varying the hydrodynamics [15-18], the feed solution properties as well as the membrane material properties such as roughness [19,20], charge [14,21-23], surface tension [24-29], etc. Strong material hydrophilicity has been identified to be beneficial for the performance during filtration of many biocompounds (e.g., proteins [30,31] or NOM [11]). Due to other disadvantages of some hydrophilic materials (e.g., the moderate chemical and thermal stability of cellulose based membranes), many research works were dedicated to hydrophilisation of already established hydrophobic materials [26,27,29,32-38].

In order to apply novel materials in the industry, aside from the membrane material properties itself (such as pore size, surface roughness, porosity, charge, hydrophilicity), there are other important factors posing a challenge. The hydraulic resistance (water permeability) and separation performance

(selectivity) are major characteristics that influence the process performance. Important factors regarding the applicability of materials are the mechanical and chemical stability. Thus, the membranes should meet the requirements of the chemical and hydrodynamic environment [39]. Depending on the application sphere, i.e., required membrane area (e.g., for big elements in desalination and waste water treatment) or high selectivity (downstream processing and pharmaceutical industry), the costs and flexibility of the membrane manufacturing should be taken into account. For the exploitation of small amounts of valuable (expensive) products with high purity, the high material costs could be compensated, whereas when large areas of membranes are required, the production should be kept cost-effective.

In terms of profitability, there is a need of effective long-term-stable, cheap and low-effort high-quality membranes. Therefore, a systematic and comprehensive study of the properties of these novel membranes as well as their applicability in relevant processing areas is necessary.

In the present work, main goal was to describe the basic properties of the new established low-fouling thin-layer hydrogel composite membranes (e.g., wettability, charge, morphology, and selectivity) as well as to evaluate the long term performance and stability of such membranes during filtration of model compounds related to biotechnology (proteins with different size), water treatment (humic acid sodium salt; HA) and food processing (polyphenolic extract from green tea). The effects of other factors, such as environmental (feed properties) and operating parameters (pressure, CF velocity, operating mode), on the filtration behaviour of the novel composite membranes has to be also taken into account.

This work should be relevant to wide variety of separation areas and deliver results for the optimisation of the membranes operational mode leading to cost-effective and high-quality technological applications.

2 THEORY

2.1 FLUX DECLINE

One of the major problems accompanying UF and MF is loss of flux with time. The membrane flux behaviour over a filtration process can be divided in three stages as presented in Figure 2.1 [40].

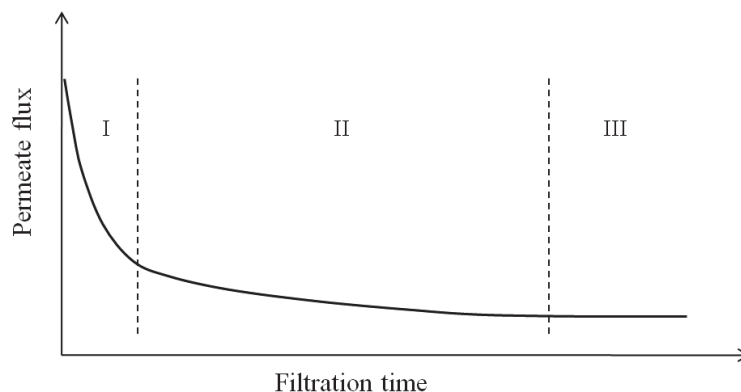


Figure 2.1 Schematic view of the three stages in flux decline.

The flux curve starts with a rapid drop of the flux from the pure water flux (I) followed by long-term moderate flux decline (II) and ends with a steady state flux (III). Flux decline in membrane filtration is caused by the increase of the membrane resistance by formation of CP layer and the development of another resistance layer by deposition of feed solutes (mainly in terms of pore blockage and subsequent cake formation). The strong flux decline in stage I is attributed to the quick pore blocking of membrane pores by the retained molecules/particles [41]. The subsequent cake formation and growth decrease the permeate flux further in stage II. Stage III (steady state) is typical for cross-flow (CF) filtration, since an equilibrium cake layer thickness is reached depending on the applied pressure and CF velocity [40]. In case of dead-end (DE) filtration mode (closed system) the permeate flux may tend to zero due to the increasing osmotic pressure [18].

2.1.1 CONCENTRATION POLARISATION

When filtration through a retentive membrane is performed, feed solutes are enriched on the membrane surface. This phenomenon is called CP and occurs immediately after the filtration run was started. Several models have been developed to describe CP: boundary layer model, gel-polarisation models, osmotic pressure models and resistance models [42]; some of them will be discussed further.

The building of CP can be explained by the film theory (boundary layer model). The fluid flow velocity in a channel decreases in the vicinity of the wall due to friction. The bulk is well mixed by the

convective flow, whereas the motion in the boundary layer close to the wall is governed by diffusion resulting in slow mixing [43]. During filtration the retained solutes are enriched close to the membrane surface as a result of convection and the semipermeable properties of the membrane, building the CP layer. Due to the concentration gradient in the CP layer solutes will be transported back to the bulk by diffusion against the convective flow (Figure 2.2).

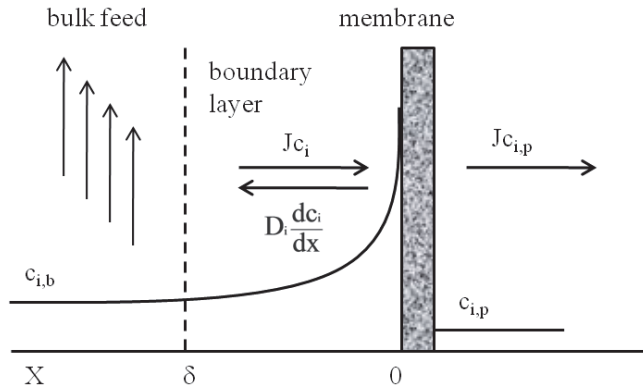


Figure 2.2 Schematic view of the mass transport within a boundary layer.

This transport in the boundary layer can be expressed by mass balance implementing the 1st Fick's law described by Eq.(2.1):

$$Jc_i - D_i \frac{dc_i}{dx} = Jc_{i,p} \quad (2.1)$$

J is the volume flux, c_i is the concentration of the solute i in the boundary layer, D_i is its diffusion coefficient, x is the coordinate perpendicular to the membrane surface and $c_{i,p}$ is the solute concentration in the permeate. Integrating Eq.(2.1) to the whole boundary layer thickness δ leads to the polarisation equation [2] (Eq.(2.2)):

$$\frac{c_{i,0} - c_{i,p}}{c_{i,b} - c_{i,p}} = e^{J\delta D_i} \quad (2.2)$$

$c_{i,0}$ is the solute concentration on the membrane surface and $c_{i,b}$ the bulk concentration.

Furthermore, the build-up of CP layer can be explained on the basis of thermodynamic considerations. The change in free energy (Gibbs energy) dG of a system depending on the change in pressure, temperature and amount of substance dp , dT and dN , respectively, is given by Eq.(2.3):

$$dG = Vdp - SdT + \mu dN \quad (2.3)$$

V is the system volume, S is the entropy and μ the chemical potential. If there is no change in the amount of substance and temperature, $dG = Vdp$. Since during filtration of particles the pressure in the CP layer decreases from the bulk towards the membrane surface, compounds on the membrane surface

have minimum Gibbs energy, thus particles tend to move to the surface. The accumulation of particles near the membrane surface is hindered by their thermal motion. The thermal motion can be measured by osmotic energy which is function of the solute concentration. Hence, the osmotic energy gradient is from the membrane surface to the bulk [18]. The concentration of the particles is determined by the pressure applied to the layer and reaches a maximum determined by the particle nature (closest packing) [18]. At the maximum concentration, a steady state (equilibrium) for the CP layer properties is reached; when the equilibrium state is exceeded, solutes accumulate on the membrane surface and form a cake layer [44] (cf. Section 2.1.2).

Several parameters are known to affect the CP layer thickness and density. The CP layer thickness (and density) depends on the applied pressure, as proposed by the thermodynamic considerations. The density of the CP layer is governed by the solute-solute interactions. It has been shown that permeate flux can be enhanced when repulsive forces are present. The reason is the diffusive back transport of solutes which lowers the concentration on the membrane surface [45]. In case of solute mixtures two phenomena can be discussed where the solutes charge and size have an impact. In case of oppositely charged proteins, an increase of the resistance of the concentrated layer can be observed. If the proteins differ in their size, additional effect can occur – a difference in packing during the solute build-up near the membrane surface (related also to cake formation) [42,46]. Furthermore, hydrodynamics affect the CP properties. Increasing the CF velocity will lead to thinner CP layer [18].

2.1.2 FOULING

The major problem during filtration is the flux decline and loss of selectivity due to membrane fouling. Fouling is the process resulting in loss of performance of a membrane due to the deposition of suspended or dissolved substances on its surface, at its pore openings, or within the pores [47]. Consequently, filtration processes become expensive due to the short lifetime of the membranes, the necessity of frequent cleanings, modest fluxes, and the extra energy required for circulating the solution in an attempt to control fouling [2].

Fouling can occur in two ways: adsorption of foulant (irreversible, cannot be removed by physical cleaning) and cake formation (generally reversible by water washing or back flush) [48]. In the early stage of the filtration process hydrophobic protein-membrane interactions govern the fouling behaviour (deposition on the membrane surface), in later stages protein-protein interaction determine the membrane performance (interactions of the bulk solutes with the deposited) [49,50]. Furthermore, the larger and stronger the fouling, the more intense the required chemical cleaning is.

The deposition of solutes and the build-up of cake layer can be explained from thermodynamic point of view. Depending on the solutes size, charge and nature, a maximum concentration (i.e., maximum

osmotic pressure) in the CP layer exists. A further increase of the applied pressure cannot be balanced by the osmotic energy and particles will tend to move through the CP layer and build a cake layer on the membrane surface [18,44].

The fouling mechanisms are governed by the solute/particle properties, the membrane characteristics and the hydrodynamic conditions during filtration. The schematically presented cases in Figure 2.3 have been described as follows [51,52]:

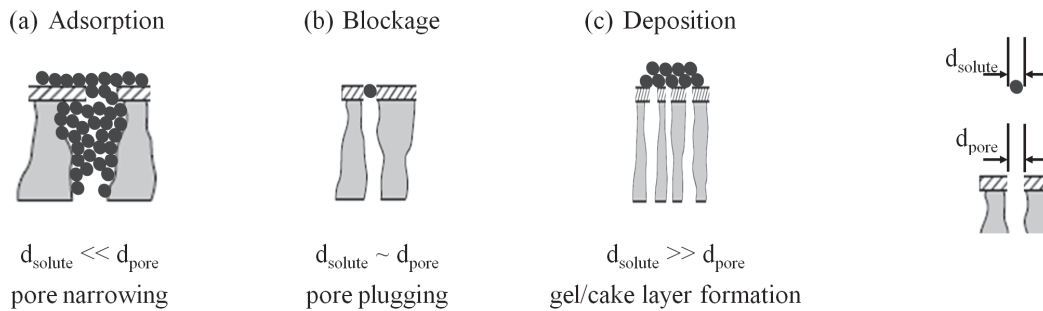


Figure 2.3 Fouling mechanisms depending on the relationship pore size/solute size.

(a) When the membrane pores are much larger than the solute/particle ($d_{solute} \ll d_{pore}$), pore narrowing will occur governed by adsorption. Adsorption occurs when attractive interactions between solute and membrane are present. A monolayer can grow even when there is no permeation flux and increase in the hydraulic resistance. The CP can strengthen the adsorption. Furthermore, pore narrowing can lead to complete loss of pores.

(b) Pore blockage occurs when the solute size is similar to the membrane pore size. In this case the solute can plug the pores leading to a flux reduction.

(c) If high solute retention is provided by the membrane (e.g., $d_{solute} \gg d_{pore}$), the extent of CP may lead to the formation of gel layer which can further lead to cake layer formation due to solutes deposition.

Important issue in fouling studies is the critical flux measurement. The critical flux is defined as the flux point where the permeate flux deviates from the linear dependence of the water flux on pressure [53,54], this is the “first” permeate flux at which fouling becomes noticeable [51]. This means that a critical transmembrane pressure (TMP) corresponds to the critical flux. Above the critical pressure flux raises non-linearly with increasing TMP. It should be noticed that operation below the critical point does not necessarily mean that no fouling will occur during the process, but it can be related to minimising fouling [51]. At very high pressures, a limiting flux can be observed. Beyond this point the

flux becomes independent from the applied pressure, i.e. no further increase in flux can be achieved by applying higher pressure.

2.1.2.1 Fouling models

Furthermore, understanding of fouling causes and mechanisms has been also needed in order to control fouling more efficiently. Fouling mechanisms have been widely studied [55-57]. In order to describe the dominating fouling mechanisms during filtration, several models have been proposed, e.g., the standard pore blocking model [41], the combined pore blocking-cake formation model [58,59], the unifying model for CP, gel-layer formation and particle deposition [60], etc. It has been found that in the early stages of filtration fouling occurs mainly due to pore narrowing and/or pore blocking causing strong flux decline. In the later stages cake formation is dominant. During filtration of NOM pore blockage was the dominant fouling regime at the beginning of the process, later cake formation occurred [56,57,61,62]. Similar results were reported by [58,59] for MF of bovine serum albumin (BSA).

In the following, the classical model equation proposed by Hermia [41] for DE filtration mode will be described (Eq.(2.4)):

$$\frac{d^2 t}{dV^2} = k \left(\frac{dt}{dV} \right)^n \quad (2.4)$$

t is the time, V is the permeate volume, k is a fouling coefficient and n is a dimensionless filtration constant representing the filtration mode. Value of $n = 0$ corresponds to cake formation, $n = 1$ to intermediate blocking, $n = 1.5$ to pore constriction and $n = 2$ indicates the pore blocking regime [41,59]. The differentials are defined as follows (Eq.(2.5) and Eq.(2.6)):

$$\frac{dt}{dV} = \frac{1}{JA} \quad (2.5)$$

$$\frac{d^2 t}{dV^2} = - \frac{1}{J^3 A^2} \frac{dJ}{dt} \quad (2.6)$$

A is the effective membrane surface area. It should be noticed that this model has been developed by assuming uniform, non-connected pores [41], which is not the case with PES membranes. The effect of membrane morphology on the permeate flux decrease during filtration of proteins has been widely studied [27,58,63,64]. It has been found that the mechanisms of fouling depend on the membrane structure [58]. In fact, pore blockage due to deposition of aggregates on the membrane surface has been evaluated for membranes with uniform pores (e.g., track-etched membranes); isotropic membranes fouled more slowly due to the interconnection of pores where the fluid was able to flow through the unblocked pores. In case of asymmetric membranes, the fouling mechanism was dictated

by the membrane skin layer which limited the permeate flux due to pore blockages analogous to the case of membranes with uniform non-connected pores [58,65]. In the literature cases of $n > 2$ have been reported [58,66]. This observation results from the resistance of the support structure of the composite membrane causing fluid to flow through the open pores, leading to more rapid pore blockage [65].

2.1.2.2 General membrane equation

The initial flux of a membrane J_0 (at time 0 of the filtration process) can be expressed with Eq.(2.7):

$$J_0 = \frac{\Delta p}{\mu R_m}, [\text{m}^3/\text{sm}^2] \quad (2.7)$$

μ [Pa.s] is the solution viscosity and R_m [m^{-1}] is the resistance of a clean membrane.

Considering Eq.(2.7), the flux during filtration J could be defined in Eq.(2.8) as [55,57]:

$$J = \frac{\Delta p}{\mu R_t}, [\text{m}^3/\text{sm}^2] \quad (2.8)$$

R_t is the total hydraulic resistance, i.e., represents all resistances which can occur during filtration process [42]. Figure 2.4 shows the possible resistances.

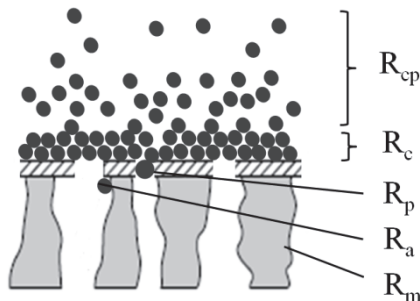


Figure 2.4 Possible resistances against solvent transport occurring during filtration processes.

Aside from the membrane resistance R_m , resistance can occur due to adsorption of solutes on the membrane surface leading to pore narrowing (R_a), resistance caused by pore blocking (R_p), gel layer formation (R_g ; not shown in Figure 2.4) and cake layer deposition (R_p). Another parameter is R_{cp} which results from the built CP layer. The total resistance can be expressed in the so called “resistance in series” model described by Eq.(2.9) [67]:

$$R_t = R_m + R_a + R_p + R_{cp} + R_g + R_c, [\text{m}^{-1}] \quad (2.9)$$

2.1.3 FACTORS AFFECTING FOULING

The wide membrane application in biotechnology and water purification increased the interest in understanding and controlling fouling. Many authors studied the fouling of relevant compounds (proteins and NOM) during MF [10,20,23,61,68-70], UF [14,49,55,71-75], and NF [24,76,77]. It has been found that fouling can be influenced by many factors, especially hydrodynamics and properties of the solution and the membrane, so the solute-solute and membrane-solute interactions can be affected.

Membrane properties

Membrane properties contribute significantly to the overall membrane performance during filtration. Important characteristics are the MWCO, hydrophilicity, surface charge, morphology (pore structure, porosity and roughness) of the membranes.

It has been found that MWCO affects the fouling and rejection of NOM compounds [14]. Membranes with high MWCO have been found to be more affected by fouling; during filtration process the more permeable membranes showed stronger flux decline [11,57,62,68]. The relationship between pore size and solute size plays an important role. From this relationship, the dominating fouling mechanism can be estimated. It has been discussed that pore narrowing and subsequent pore plugging can cause stronger flux decline than outer surface fouling [78]. In another study large fractions of NOM caused severe fouling during operation with 100 kDa membrane, while small fractions affected 10 kDa membranes [79].

The effects of hydrophilicity and surface charge have been comprehensively studied. Hydrophobic materials tend to be fouled preferentially by many biocompounds (e.g., proteins [30,31]). When membranes with varied hydrophilicity have been studied, more hydrophilic membranes showed higher fouling resistance during filtration in aquatic solutions [80,81]. The deposition of humic substances on hydrophobic surfaces occurred preferential due to the prevalent hydrophobic character of these compounds [11]. Moreover, NOM substances were not adsorbed preferentially on negatively charged membranes because electrostatic repulsion of the negative charged humic compounds occurred [14]. Considering these findings, hydrophilic and negatively charged surfaces exhibited less fouling behaviour during filtration of NOM [24,82].

Membrane roughness has been considered as an important factor in fouling influencing the interactions between molecules and the membrane surface, rough surfaces were more affected by fouling [20,68]. As already mentioned, membrane morphology also influenced the membrane performance and rate of flux decline [58,66,69], (cf. Section 2.1.2.1). It has been shown that isotropic membranes maintained high permeate fluxes for longer filtration time [58].

Solution properties

Feed properties which influence fouling include solute nature, size and concentration, solute charge (density), hydrophobicity and functional groups, pH and ionic strength of the solution, presence and concentration of divalent cations.

The solute charge is important characteristic as it determines the solute-solute and membrane-solute interactions. The electrostatic effect has been studied by many authors [22,73-75]. It has been shown that, if repulsion interactions are present (due to the same charge of membrane and solute), the fouling behaviour can be improved. In general, attraction and repulsion forces between membrane surface and solute can govern the membrane selectivity, i.e. transmission will be enhanced for solutes which are oppositely charged compared to the membrane [22,83]. Moreover, studies reported that due to attraction/repulsion the size exclusion properties of a membrane became negligible, i.e., the size selectivity could be inverted, allowing larger molecules with opposite to the membrane charge to pass preferentially instead of small molecules with same charge like the membrane [84,85]. It should be mentioned that this was possible in combination with the adjustment of other parameters, such as ionic strength, permeate flux and system hydrodynamics. The solute-solute interactions are important when cake formation occurs. In this case, when the solutes had same charge, due to repulsion the porosity of the cake layer increased, which led to increased permeate flux [86]. Respectively, dense packing was observed when solutes with opposite charges were mixed [42]. The charge density plays an important role for membrane fouling. The protein charge density is at minimum at its isoelectric point (IEP). Studies demonstrated that membranes were stronger fouled when the pH was adjusted at the proteins IEP [49,75,87].

Some authors studied NOM from different sources [11,20] or others fractionated feed solutions [12,20,88] in order to investigate the effect of molecular weight (MW) and hydrophilicity on the fouling behaviour during filtration. Lin et al. [88] found that the fractions with high MW of both hydrophilic and hydrophobic humic solutions caused the worst flux decline; in contrast, Lee et al. [20] showed that surface water solutions prefiltered through a 0.45 μm filter caused severe fouling in comparison with 1 μm prefiltered solutions. The role of aggregates should also not be underestimated: the changing properties of the cake layer due to aggregation in the feed affected the filtration performance [55,56,61]. The storage of the feed solutions also influenced fouling. After storage the flux decline became more pronounced [23,89]. Aggregation in protein solutions also should be considered when performing protein filtration. For instance, high ionic strength and low pH enhanced protein aggregation and deposition during UF [69].

The influence of divalent cations on the NOM behaviour during filtration is of major interest, since they are present in natural waters. Many authors studied the effect of presence and concentration of

divalent cations [23], and especially Ca^{2+} [90-92]. It has been found that Ca^{2+} ions accelerated the aggregation of NOM compounds, which led to increased fouling behaviour [93,94].

Operating parameters

The hydrodynamic conditions have an impact on the filtration performance. They can be varied by changing the pressure, CF velocity (stirring), equipment design or operation mode.

Amy and Cho [14] reported about the importance of permeate flux and back mass transport by diffusion for minimising fouling and maximising NOM rejection; Seidel and Elimelech [77] found that CP was influenced by the initial permeate flux. Pressure was also found to affect fouling: an increase in operation pressure caused stronger permeate flux decline [10,44,92] increasing the cake resistance [57,71]. Outgoing from the critical flux theory, many studies showed that below the critical flux less fouling occurred; the rate of fouling was greatly reduced because the critical flux was not exceeded [51,53,95].

The CF velocity is of a great importance and an optimum should be found, since different interactions dominate at varied CF rates. If the flow rate is too low, the mixing in the bulk will be not sufficient so that CP and cake formation can become more pronounced. Thus, good mixing is necessary in order to achieve higher permeate fluxes (e.g., increasing in the CF velocity led to increased critical flux in [17]). It should be taken into account that CF is not effective when low retention is present, since the CF does not affect internal fouling. On the other hand, too high CF velocity caused stronger flux decline enhancing fouling due to complex and aggregate formation in protein [96] and NOM solutions [77].

The operating mode of filtration influences the fouling and rejection behaviour of membranes. DE and CF operation modes are schematically viewed in Figure 2.5.

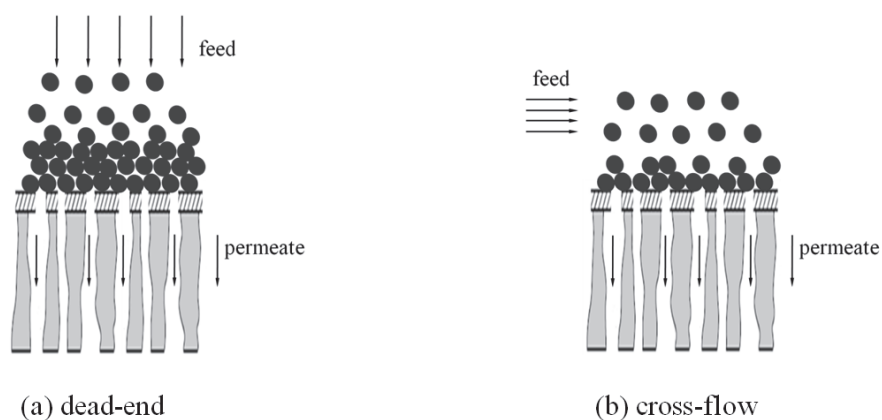


Figure 2.5 Operation modes of filtration; (a) dead-end; (b) cross-flow.

In case of DE mode (Figure 2.5 (a)), the only outlet for the upstream (feed) is through the membrane [47]; the retained solutes accumulate on the membrane surface. CF (Figure 2.5 (b)) is characterised by feed flow parallel to the membrane surface which contributes to the mixing in the upstream side and thus, reduces solutes deposition.

The hydrodynamics can be influenced by the operative design. Protein aggregation and thus increased fouling can be caused by microcavitations in pumps and valves [97].

2.2 STRATEGIES FOR FLUX IMPROVEMENT

Flux can be enhanced mainly by minimising CP and fouling. Therefore, solute-solute and membrane-solute interactions have to be controlled. The methods to improve flux can be classified in: operative methods, solution and membrane related methods as well as membrane cleaning [42].

Equipment related methods for increasing the membrane flux are: variation of the CF velocity, changing the flow channel, decreasing the viscosity by increasing the temperature. Furthermore, rotating equipment or TMP pulsing can be used in order to minimise solutes and particle deposition. Back pulsing allowed frequent back flush with the permeate, which reduced solutes deposition [42]. Electrical current pulsing has been also used for improving flux [98]. The hydrodynamics can be further influenced by changing the membrane surface configuration, e.g., corrugated membranes increase the mass transfer coefficient by increasing the turbulence.

Solution related methods which influence the fouling extent are: concentration of salts or charge changes due to the ionic strength, pH adjustment to achieve the desired electrostatic interactions. Solution composition and concentration can be also varied by prefiltration of the feed solution or dilution.

Cleaning of the membrane can remove the deposited layer and increase membrane flux. Mechanical and chemical cleaning steps are often applied. Mechanical cleaning procedures are membrane outer surface rinsing and back wash with water. Here, only the reversible part of fouling can be removed. Chemical cleaning (enzymatic, alkaline or acidic) can be combined with high temperature in order to increase the effectivity. Disadvantages here are the necessity of interrupting the filtration process in order to perform the cleaning and the reduced membrane life time by the chemicals.

The membrane surface can be chemically treated in order to influence the hydrophilicity. (Increasing the membranes hydrophilicity at the surface of the membrane has been shown to decrease fouling during protein filtration [3]). Membrane surface modification has broad application for minimising fouling or achieving the desired membrane properties.

2.3 MEMBRANE MODIFICATION

Membrane modification has the function to change the basic material properties so that new functionalities are achieved. These can be surface hydrophilisation for minimising fouling tendency or tailoring specific properties (materials with defined selectivity or affinity, i.e., adsorptive or charged membranes, molecular recognition). In the biotechnology, waste water treatment and food processing fouling is major problem, hence, only membrane hydrophilisation will be discussed further. Most of the membranes for MF, UF and NF for industrial applications are prepared from PES, PSf and polyvinylidene fluoride (PVDF). Due to their rather hydrophobic character and consequently fouling tendency, the materials are usually modified. The following general strategies are widely used for changing the material performance: bulk polymer modification and surface modification. During bulk polymer modification other active groups are chemically added to the polymer, thereafter, the membrane can be casted. Surface polymer modifications can be divided in surface treatment with plasma, polymer blending, grafting methods and coating (preadsorption).

2.3.1 OVERVIEW OF GENERAL STRATEGIES

Bulk polymer modification

Bulk modifications are performed by addition of active groups to the polymeric material to increase the hydrophilicity. Sulfonation [99,100] and carboxylation [31] are mainly used. Other works used living polymerisation in order to modify commercial polymers for the preparation of low-fouling membranes, e.g., PVDF has been modified with poly(ethylene glycol) methyl ether methacrylate (PEGMEMA) [101], or polystyrene-block-poly(N,N-dimethylaminoethyl methacrylate) block copolymers have been synthesised [102] for further membrane casting. This method is applicable in the industry but applying appropriate synthesis conditions (e.g., cooling and aggressive chemicals) can be cost intensive.

Plasma treatment

Plasma treatment is used in order to activate the upper molecular layers of a material. Via plasma, radicals are created which can react with the plasma gas molecules leading to the introduction of functional groups on the membrane surface [34]. Possible bonds that can be attacked by gases are C–C, C–H, C–S, except aromatic C–H and C–C bonds. Gases which can be used are CH₄, Ar, O₂, H₂, He, Ne, N₂, CO₂ as well as water [103]. The plasma treatment leads to the formation of functional groups on the membrane surface. Disadvantage of this method is the moderate stability over time, i.e., rearrangement of the functional groups and movement to the bulk in the polymer are possible, as well as chemical reaction with atmospheric oxygen and moisture [34].

Polymer blending

A basic polymer and a polymer with special properties can be dissolved and polymer blend membranes can be prepared. Typically, hydrophobic polymers with good mechanical and chemical stability are mixed with hydrophilic polymers. Casting blends with hydrophilic polymers, such as polyethylene glycol (PEG), polyvinylpyrrolidone (PVP), poly(methyl methacrylate) [80], Pluronics® (PEG-PPG-PEG amphiphilic block copolymer) [104,105] or other amphiphilic polymers [106,107], has been already established. In this way, stable membranes (exhibiting the properties of the main polymer) with appropriate functionalities (delivered from the additive) can be prepared under appropriate conditions.

Coating

Coating of the membrane outer surface can be achieved by adsorption, self assembling [108], layer-by-layer technique [109,110] or entrapment [111,112]. The application of this strategy in the industry is not complicated and no additional special devices are required. In this method the long-term stability is limiting parameter for a broad application [39].

Grafting methods

Grafting involves the chemical attachment of small molecules or, most often, polymers on the membrane surface. It is to distinguish between “grafting-to” and “grafting-from” approaches. “Grafting-to” is performed by coupling polymers to surfaces via functional groups [113]. Advantageous in “grafting-to” methods is that the synthesis of the grafted layer can be well controlled and therefore, its characterisation is easy to establish. However, the slow diffusion of the macromolecules to the surface and the sterical hindrance are limiting for this approach, hence sufficient grafting density would be restricted [114].

During “grafting-from”, monomers are polymerised via initiation of the membrane surface. In this case, high grafting densities and polymer chain lengths can be achieved but the synthesis is less controlled with respect to polymer layer structure. For the initiation of “grafting-from” reaction, the membrane surface has to be activated, i.e., radicals should be present. Here, different methods can be used: plasma treatment, high energy irradiation (e.g., electron beam), reaction with ozone, redox initiation, UV irradiation.

Plasma induced grafting

As already discussed, plasma can be applied for surface modification. The produced free radicals or peroxides can be used as a starter for “grafting-form” reaction [103]. Plasma induced grafting has been already studied by many researchers for the grafting of hydrophilic monomers [33,36,115,116].

Grafting by high energy irradiation

An alternative method to induce grafting is ion beam irradiation. A high-energy source is used to activate the membrane surface. Consequently, the polymer structure and membrane morphology can be changed, e.g., roughness can be reduced [103]; subsequently grafting of a monomer occurs in solution [26]. Furthermore, “grafting-to” of diverse molecules onto PES membranes induced by electron beam has been also performed in an one-step approach [117].

Ozone surface activating

Radicals can be created via reaction with ozone. For instance, the surface of PVDF membranes has been activated by ozone treatment and surface-initiated atom transfer radical polymerisation has been used for modification with zwitterionic polymer [118].

Grafting after redox initiation

Redox initiation is also applied for starting grafting from surfaces. This method can be applied in cases where no direct contact of the membrane surface and the activating source can be provided, e.g., in small channels. Hence, PVP has been grafted onto PSf hollow fibres after redox initiation [119].

UV induced initiation

UV induced grafting is widely used in the research. The mechanism of the initiation is schematically represented in Figure 2.6.

Here, UV light is used for the direct creation of radicals on the surface of UV active polymers, such as PSf or PES [38,120]. That way, degradation of the membrane polymer occurs due to chemical bonds cleavage (e.g., the C–S bond of PES) (Figure 2.6(a)). In cases, when the membrane polymer is not UV sensitive, other reactants are additionally used. Possible mechanisms are the decomposition of an initiator in solution and radical transfer (Figure 2.6(b)) and the adsorption of a photoinitiator on the surface [113] (Figure 2.6(c)). A primary covalent attachment of chemical groups can be also used and these can be further activated [113].

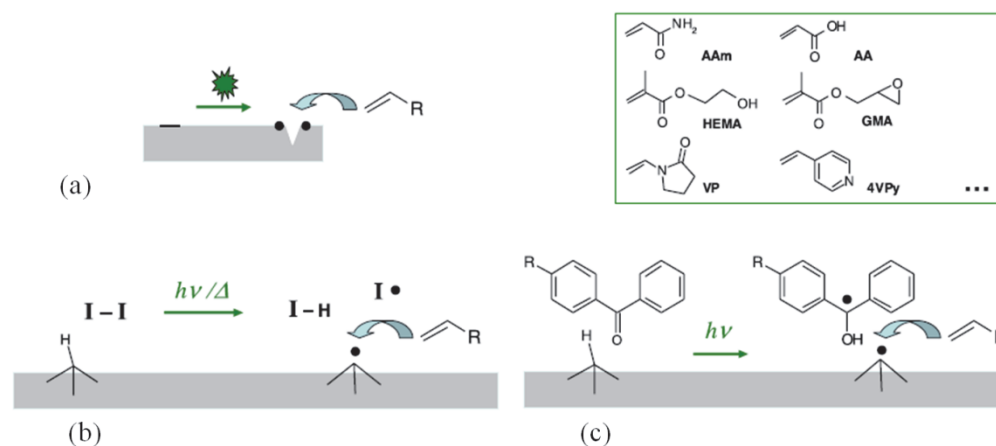


Figure 2.6 Initiation mechanisms for “grafting-from” surface functionalisation; (a) controlled degradation of the membrane polymer; (b) decomposition of an initiator; (c) adsorption of an initiator on the surface.

As it was mentioned above, the polymeric layer structure cannot be well controlled during “grafting-from” modifications. Therefore, in order to control the chain length and density of the grafted layer, living polymerisation techniques are often applied [121,122]. Moreover, the sieving properties of membranes can be further controlled by modification with “smart” (stimuli-responsive) polymers [123] or hydrogels [124]. UV induced grafting will be discussed further in the following section.

2.3.2 GRAFTING-FROM SURFACE MODIFICATION USING ULTRAVIOLET LIGHT

Most commonly used technique for grafting initiation is the direct UV excitation due to its simplicity. Photo-initiated functionalisations of polymeric membranes can be very selective and efficient in combination with low cost for industrial implementation [125]. Ulbricht et al. [37,38,126] grafted via UV initiation acrylic acid (AA) and various acrylates or methacrylates having PEG, carboxyl, sulfopropyl, dimethylaminoethyl or trimethylammoniummethyl side groups onto PSf, PES or polyacrylonitrile UF membranes and studied the resulting membrane hydrophilicity and surface charge and the consequences for membrane performance. The anti-fouling properties of grafted layers from a wide variety of hydrophilic agents had already been investigated. The research group of Belfort has analysed the effects of different monomers, such as 2-hydroxyethyl methacrylate, AA, N-vinyl-2-pyrrolidone (NVP) and many more [35,120,127-129], using UV assisted “grafting-from” modification of PES membranes. According to hydrophilicity, static protein adsorption and filtration measurements, an increased fouling resistance to BSA compared to unmodified PES or regenerated cellulose membranes was found. Susanto and Ulbricht [130] compared the fouling behaviour of PES membranes which had been photo-grafted with the zwitterionic N,N-dimethyl-N-2-(methacryloyloxyethyl)-N-(3-sulfopropyl) ammonium betaine and the hydrophilic PEGMA and found better performance of the polyPEGMA modified membranes.

Very important issue during direct UV initiation is the mechanism of creating radicals. Photoexcitation results in a homolytic cleavage of a bond (C–S in case of PES/PSf) resulting in a simultaneous chain scission and crosslinking affected by temperature. Thus, it has been observed that above 170 °C crosslinking is dominant, while chain scission is much more important at room temperature [131]. Poorly controlled chain scission can lead to pore degradation and thus, to increase in the membrane pore size which may not be completely compensated by the synthesised hydrophilic layer. In this way, loss of rejection/selectivity of the modified membrane may be disadvantageous.

2.3.3 REQUIREMENTS FOR FOULING RESISTANT SURFACES

The interaction of proteins with surfaces has been studied actively to understand the mechanisms of adsorption of proteins to surfaces [132]. It is a complex problem to understand the occurring processes on a surface, since many proteins change their conformation when deposited. Thus, the understanding of the mechanisms behind biocompatibility and protein adsorption is difficult to analyse and is not complete [133]. Numerous works studied different polymer classes with respect to their affinity to proteins. The evaluated results provided a database of material properties which are responsible for reducing or inhibiting fouling. The following features have been identified as essential: the investigated materials were hydrophilic, overall electrically neutral and hydrogen bond acceptors, but *not* hydrogen bond donors [134].

The most studied polymer is PEG which is a charge-neutral polymer that can interact with water via hydrogen bonds creating an energetic barrier to the adsorption of biomolecules at the membrane surface [135]. The reasons why PEGs are fouling resistant to proteins are their kosmotropic properties. Kosmotropes stabilise the native protein structure due to their high hydration [136,137]. However, the water structure near these species has the most important role. The formation of “structured” or “tightly bound” water close to the surface is responsible for their low interactions with protein molecules [134]. Vogler [138] discussed the attractive or repulsive forces between two surfaces immersed in water. The water structure close to more hydrophobic surfaces is disturbed, i.e., the water is “less-dense” with an open hydrogen-bonded network; in this case, the interactions between the surfaces are attractive and replacement of water at the surface by adsorbed solute is enhanced. Close to hydrophilic and kosmotropic surfaces the water structure is similar to the bulk water structure; repulsive forces between surface and solute are observed.

Therefore, polymers with PEG side chains (an anchor group is necessary in order to attach PEG chains onto surfaces) are of great interest for preparation of low-fouling materials. In this regard, the length of the PEG chain is of importance for the resulting surface properties. Hence, thin-film composite membranes with grafted anti-fouling layers made of kosmotropic polymer hydrogels are very promising materials in the field of membrane separations in aquatic systems.

3 CONCEPT

PSf and PES are often used for the preparation of UF membranes due to their mechanical, chemical and thermal stability [6,103]. However, these materials are strongly affected by fouling during filtration, mostly due to their relatively hydrophobic character. By reducing the hydrophobicity, the non-specific binding of product or other components to the membrane surface can be decreased. In this study, PEGMA was attached to the surface of PES UF membranes via “grafting-from” approach, according to next chemical reaction (Figure 3.1):

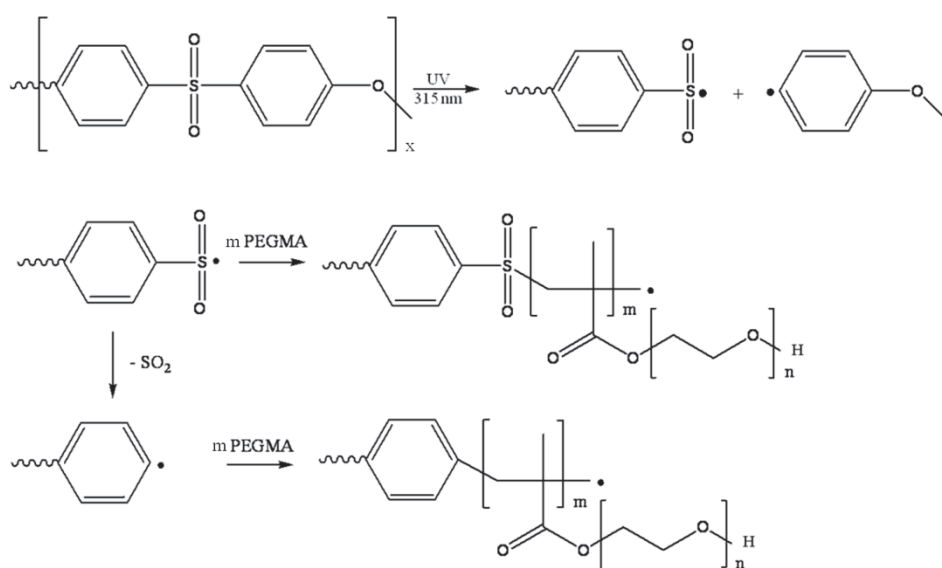


Figure 3.1 Mechanism of the chemical reaction on the membrane surface during “grafting-from” modification of PES with PEGMA.

Among the hydrophilic monomers applied for surface hydrophilisation, PEGMA has already been comprehensively studied. Uchida et al. [139] grafted PEGMA monomers with variable PEG chain lengths onto polyethylene terephthalate film. The modified surfaces exhibited strong hydrophilic properties and a surface charge of nearly zero. Similar results were achieved by Susanto et al. [140] when modifying PES UF membranes with polyPEGMA chains via UV irradiation. In this study, the prepared low-fouling PES-based UF membranes have been analysed with respect to water permeability, hydrophilicity, surface charge and solute rejection, and fouling studies were also performed. The new membranes showed higher rejection and fouling resistance to sugarcane juice polysaccharides and BSA.

The beneficial features of the synthesised composite membranes result in the principle of behaving during an UF process, especially when mixtures of proteins (or other biomacromolecules) with different size have to be treated. The principle of filtration with commercial (i.e., fouling-prone) membranes in comparison to the behaviour of functionalised membranes is illustrated in Figure 3.2.

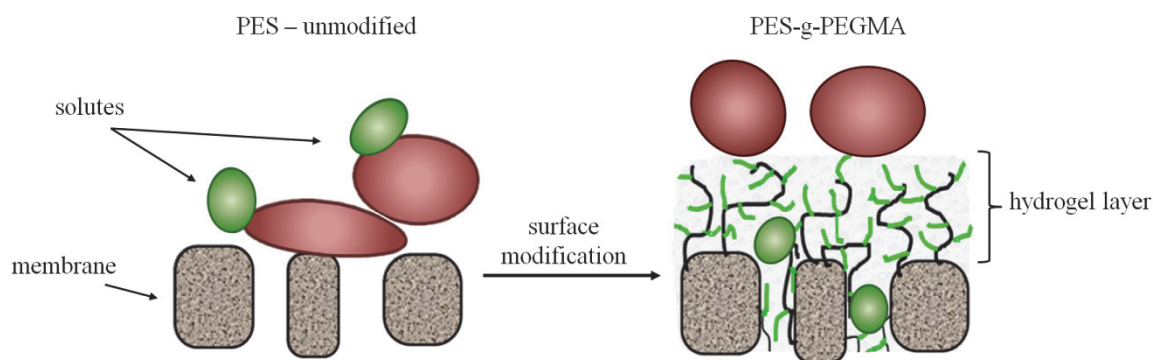


Figure 3.2 Schematic representation of a filtration process with commercial (left) and thin-layer hydrogel composite membranes (right).

When applying filtration, proteins tend to foul on the membrane surface. The consequence is pore narrowing and/or blocking. Thus, membranes lose performance in terms of permeate flux and selectivity (when mixture of differently sized molecules has to be separated, as shown in Figure 3.2 (left)). Due to the deposition of the bigger solutes or particles on the pore openings, smaller solutes/particles are unable to pass through the membrane. When hydrogel layer is applied on the membrane surface (and in the pore openings), the membrane surface is shielded from the foulants, so that they cannot reach the hydrophobic material and deposit (Figure 3.2 (right)). In this way, the pore openings are accessible for smaller solutes that can pass through.

These hydrophilised composite membranes would be even more attractive if the sieving properties of the hydrogel could also be adjusted during “grafting-from” [130]. Using the wide variety of commercially available functional and crosslinker monomers as potential surface modifiers, it should be possible to tune the sieving/rejection properties of the hydrogel layer. Indeed, it has been found that “grafting-from” using mixtures of PEGMA and MBAA reduced the hydraulic permeability and shifted the sieving curve to smaller molecular weights [130]. It is well known that the “mesh” structure of bulk hydrogels can be manipulated by, among other factors, the content of bi- or multifunctional crosslinker monomers in the reaction mixture used for *in situ* radical polymerisation [141]. Fänger et al. [142] used the bifunctional MBAA to crosslink poly(N-isopropylacrylamide) for the preparation of hydrogels with adjustable mesh size, as indicated by different “cut-off” values for biomacromolecules. Wu and Freeman [143] synthesised films of crosslinked NVP/MBAA and analysed their structure, water sorption and transport properties. The results showed that higher crosslinker content in the prepolymerisation mixture led to tighter structures, less water uptake and lower water permeability. Application of “three-armed” crosslinker monomers has been also already studied. For instance, hydrophilisation of self prepared PES membranes has been performed via a thermally induced surface crosslinking polymerisation with poly(ethylene glycol) diacrylate (PEGDA) and trifunctional trimethylolpropane trimethacrylate (TMPTMA) [144]. By adding TMPTMA to the PEGDA solution,

the crosslinking process was accelerated due to the higher amount of double bonds in TMPTMA. The anti-fouling ability and permeability could be well adjusted.

By synthesising a hydrogel with defined mesh size, barrier layers with predetermined and narrow sieving properties could be obtained. In this case, the pore size of the base membrane, the type of functional polymer as well as the hydrogel layer thickness and its crosslinked structure and the resulting hydrogel swelling will affect the sieving characteristics of the new composite membranes. Schematic representation of the possible effects of the base membrane pore size and the hydrogel layer architecture is given in Figure 3.3.

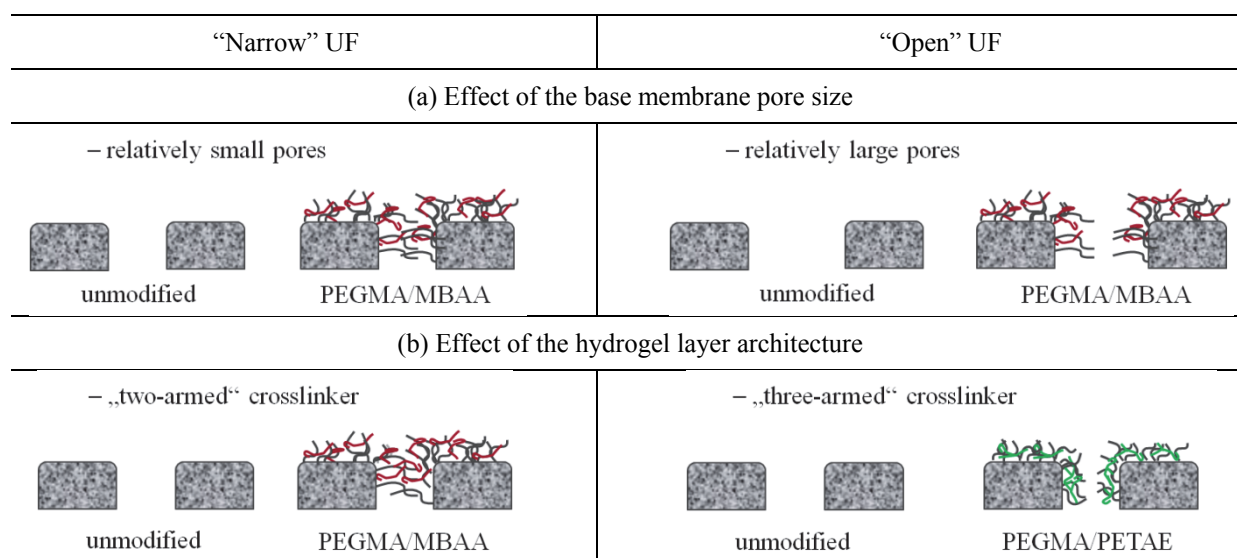


Figure 3.3 Schematic view of UF regimes with composite membranes. Influence of: (a) base membrane pore size and (b) hydrogel layer architecture.

Figure 3.3(a): In case of base membranes with relatively small pores (“narrow” UF), the hydrogel layer would be located on the outer membrane surface and shield the pores completely; the hydrogel layer would determine antifouling and selectivity properties. When membranes with relatively large pores (“open” UF) are used as base membranes, the pores would not be shielded and the grafted layer would cover also the inner pore surface.

Figure 3.3(b): For same base membrane pore size, a variation of the hydrogel layer architecture could lead to the preparation of tailored membranes for “narrow” or “open” UF. The layer architecture could be varied if different crosslinkers are introduced. The amount of double bonds per crosslinker molecule would be important. By applying a crosslinker with two double bonds, the hydrogel layer could cover the pores completely leading to “narrow” UF behaviour for the functionalised membranes (Figure 3.3(b) left). Introducing a crosslinker with three double bonds will lead to a denser hydrogel layer which is located closer to the membrane surface with thereby not completely covering the pores. In this case the membranes would belong to the class of “open” UF (Figure 3.3(b) right). Here, the

degree of crosslinking would be important, since its variation can affect the state of the hydrogel on/in the membrane, and consequently the regime of UF.

Thus, the systematic variation and control of the different UF barrier layer types should be possible for one functional monomer via setting the hydrogel layer thickness in relation to the pore size of the base membrane and the used modifier and crosslinker composition.

In this work PES UF membranes with nominal MWCO of 5 kDa, 10 kDa, 30 kDa, 50 kDa, 100 kDa and 300 kDa were functionalised with the hydrophilic PEGMA. The grafted polyPEGMA brushes on the outer surface of the base membrane were prepared using different crosslinker monomers: MBAA (two crosslinking points per molecule) and PETAE (three crosslinking points). The composite membranes, synthesised by UV-initiated grafting, were characterised with respect to membrane performance using water permeability and batch filtration of PEG and dextran mixtures with broad molecular weight distribution (MWD) as well as proteins (myoglobin, BSA, γ -globulin, fibrinogen and thyroglobulin) in order to characterise their antifouling and sieving properties. To accomplish the characterisation of the prepared composite membranes, bulk hydrogels should be also prepared and characterised. Surface wettability (measured by CA), surface charge (from ZP), surface morphology (from atomic force and scanning electron microscopies) and surface chemistry (from attenuated total reflection infrared spectroscopy; ATR-IR) were other important characteristics for the comparison of base and composite membranes.

Furthermore, filtration of myoglobin, BSA, γ -globulin, HA and polyphenolics (as model systems for processes in the biotechnology, (waste) water treatment and food industry with respect to concentration and fractionation) had to be performed in DE and CF modes (with respect to upscaling). NOM consists mainly of humic substances which contribute strongly to fouling. From this point of view, many authors used HA as model compound [10,62,88] or studied the influence of the NOM composition on fouling. Polyphenolics are interesting because of their ability to precipitate proteins and influence taste. Thus, they have to be separated or removed from the products [145-147].

The influence of operating pressure, CF velocity, operation mode and model solution properties (concentration, pH, composition) on the filtration performance of commercial and novel thin-film hydrogel composite membranes were in the scope of investigation. The resulting fouling mechanisms should be identified by the use of fouling models (classical model). Cleaning tests delivered information about the reversibility of fouling. Further, multiple uses of the membranes in filtration and cleaning tests characterised their long-term stability.

4 EXPERIMENTAL

4.1 MATERIALS AND CHEMICALS

4.1.1 MEMBRANES

In this work, PES UF membranes from Sartorius-Stedim Biotech, Germany with wide range of nominal MWCO were used as base membranes. Figure 4.1 shows the repeating unit of PES.

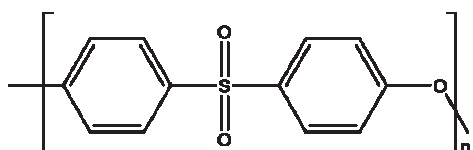


Figure 4.1 Structural formula of PES (repeating unit).

Table 4.1 shows the cross-section structure of the used membranes.

Table 4.1 Cross-section structure of the used membranes

Membrane	PES 5	PES 10	PES 30		PES 50	PES 100	PES 300
			with PVP	w/o PVP			
Structure	finger	finger	finger	sponge	finger	sponge	sponge

The nominal MWCO varied from 5 kDa to 300 kDa. The membranes have been prepared by the manufacturer with PVP as an additive in order to increase the hydrophilic properties. To describe the effects of PVP, PES 30 without PVP was also studied. The used membranes varied also in their cross-section structure: PES 5, PES 10, PES 30 and PES 50 had finger-like structure, whereas PES 30 without PVP, PES 100 and PES 300 were sponge-like.

4.1.2 MODIFIER COMPOSITIONS

For the membrane surface functionalisation, the hydrophilic agent PEGMA from Polysciences Inc., USA (the structure formula is presented in Figure 4.2(a)) was used as modifier. Here, PEGMA monomers with varied PEG chain length were used: PEGMA 200 and PEGMA 400 (the number indicates the MW of the PEG chain in g/mol). “Two-armed” MBAA and “three-armed” PETAE used as crosslinkers were supplied from Sigma-Aldrich, USA. The terminus “arms” indicates the maximum number of crosslinking points per molecule in a hydrogel network. The molecular structures of MBAA and PETAE are shown in Figure 4.2(b) and Figure 4.2(c), respectively.

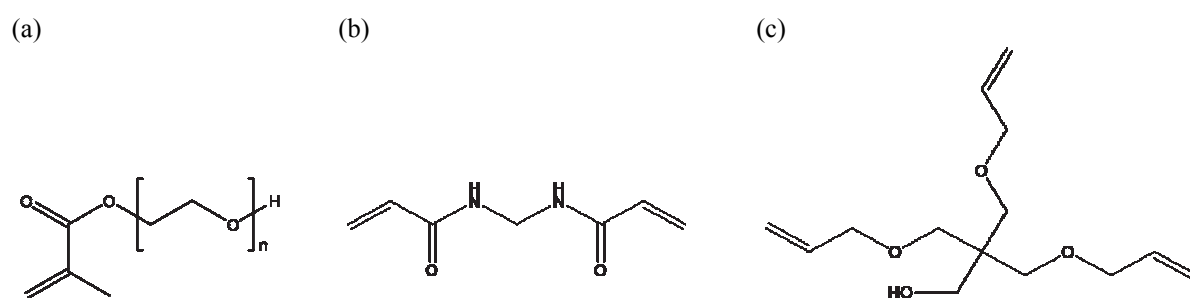


Figure 4.2 Structural formulas of the used modifying monomers; (a) PEGMA; (b) MBAA; (c) PETAE.

The MW of the used modifier agents is given in Table 4.2.

Table 4.2 Molecular weight of the used modifying monomers

Substance	PEGMA 200	PEGMA 400	MBAA	PETAE
Molecular weight [g/mol]	286	486	154	256

Several modifier compositions dissolved in deionised water were used for the membrane surface functionalisation. Table 4.3 shows the concentration of modifier and crosslinker in the mixtures.

Table 4.3 Concentration of the modifier compositions in g/L

Modifier composition	PEGMA	PEGMA/MBAA			PEGMA/PETAE		
PEGMA 200	23	0.4	1	4			
PEGMA 400	40	0.4	1	4	0.66	1.66	6.65

Three main modifying types were applied: using only PEGMA, PEGMA crosslinked with MBAA and PEGMA crosslinked with PETAE. PEGMA 200 and PEGMA 400 were used in equimolar concentrations as well as MBAA and PETAE. In the solutions where crosslinker was applied, the concentration of the crosslinker was varied at three levels. These values will be further used as a code for the nomenclature of the modified membranes - in type 23/0, 40/0.4, 40/6.65, etc., where the first number indicates the concentration of PEGMA followed by the concentration of the used crosslinker.

4.1.3 HYDROGEL COMPOSITIONS

For the preparation of bulk hydrogels, compositions with same ratios of PEGMA/crosslinker as the mixtures used for membrane modification were prepared. The exact values are shown in Table 4.4. The total concentration of the mixtures was increased in order to achieve stable and manageable gels.

Table 4.4 Concentration of the hydrogel compositions in g/L

Gel composition	Code				Concentration [g/L]			
					PEGMA	Crosslinker		
PEMGA 200/MBAA	23/0	23/0.4	23/1	23/4	103.5	1.2	3	12
PEGMA 400/MBAA	40/0	40/0.4	40/1	40/4	120	1.2	3	12
PEGMA 400/PETAE	40/0	40/0.66	40/1.66	40/6.65	120	1.98	4.98	19.92

The polymerisation was initiated using mixture of ammonium persulfate (APS) produced by Merck, Germany and N,N,N',N'-tetra-methylethylene diamine from Sigma-Aldrich, USA with mass ratio 1:4. The amount of APS used was 1.5 mol % related to the PEGMA amount.

4.1.4 TEST SOLUTIONS

4.1.4.1 Rejection experiments

Dextran and PEG solutions in 0.01 M NaN₃ (Sigma-Aldrich, USA) with varied MWD were used to perform rejection experiments. Dextran fractions T4, T35, T100, T500 (numbers indicate the average MW in kg/mol) were purchased from Serva, Sweden, and dextran T2000 was from Sigma-Aldrich, USA. PEG was supplied by Fluka, Germany. The compositions of dextran and PEG feeds with total concentration of 1 g/L used in this work are presented in Table 4.5.

Table 4.5 Composition of the dextran and PEG mixtures

Compound	Feed code	Mixture	Concentration [g/L]
Dextran	A	Dextran T4 + T35	0.4 + 0.6
	B	Dextran T35 + T100 + T500	0.4 + 0.4 + 0.2
	C	Dextran T2000	1
PEG	A	PEG 1 500 + 3 000 + 6 000 + 12 000 + 35 000	0.1 + 0.2 + 0.25 + 0.25 + 0.2
	B	PEG 3 000 + 12 000 + 35 000 + 100 000 + 200 000	0.1 + 0.2 + 0.25 + 0.25 + 0.2
	C	PEG 200 000 + 600 000	0.5 + 0.5

The MWD of these mixtures measured via gel permeation chromatography (GPC) is shown in Figure 4.3.

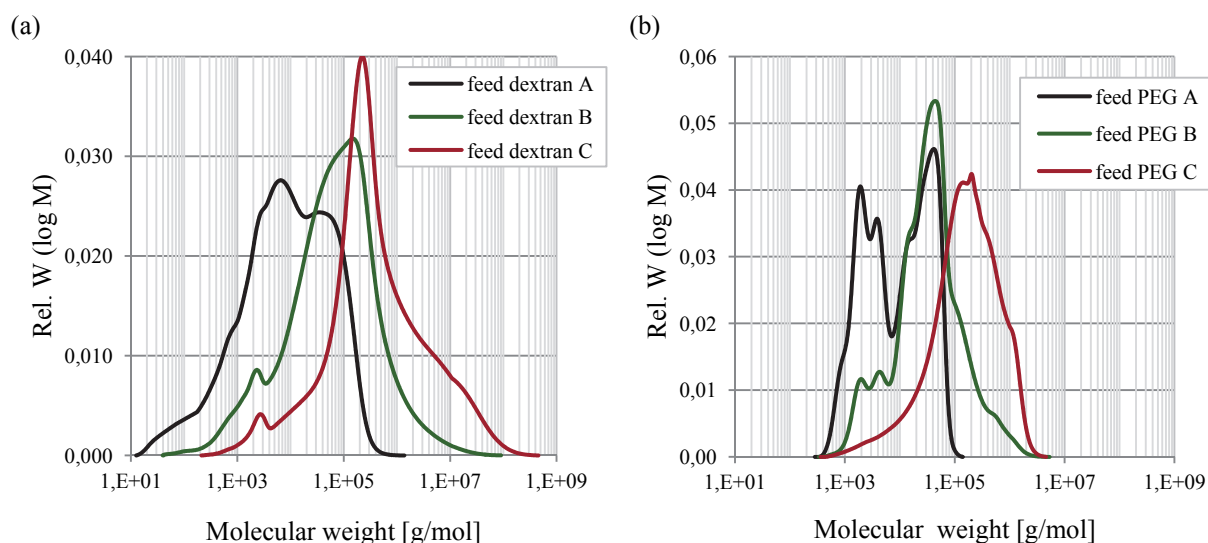


Figure 4.3 Molecular weight distribution of feeds used for the determination of rejection curves; (a) dextran; (b) PEG.

4.1.4.2 Adsorption, diffusion and filtration experiments

Several proteins, HA and polyphenolics were used to perform adsorption, diffusion and filtration tests. The proteins myoglobin, γ -globulin, fibrinogen, thyroglobulin, HA and Polyphenon 60[®] extract from green tea were purchased from Sigma Aldrich, USA. BSA (type HV) was from Gerbu Biotechnik GmbH, Germany. Table 4.6 contains important characteristics of the compounds and the used concentration and pH of their solutions which have been tested in this work.

Table 4.6 Characteristics of the used test solutions

Solute	MW [kg/mol] or [kDa]	IEP [-]	Experiments											
			Adsorption		Diffusion		Short dead-end		Long dead-end		Cross-flow			
			c [g/L]	pH [-]	c [g/L]	pH [-]	c [g/L]	pH [-]	c [g/L]	pH [-]	c [g/L]	pH [-]		
Myoglobin	17	7	1	6	2	6	1	6	0.1	4; 6; 8	0.1	6; 8		
BSA	67	~5	1	6	2	6	1	6	0.1	4; 6; 8	0.1	6; 8		
Equimol. mix BSA + myo	-	-	n.d.	n.d.	2	6	1	6	0.1	4; 6; 8	0.1	6; 8		
γ -Globulin	150	7	1	6	n.d.	n.d.	1	6	0.1	6	n.d.	n.d.		
Fibrinogen	300	5.8	1	7	n.d.	n.d.	1	7	n.d.	n.d.	n.d.	n.d.		
Thyroglobulin	600	4.6	1	6	n.d.	n.d.	1	6	n.d.	n.d.	n.d.	n.d.		
Humic acid	0.5 – 1 000	-	1	7	n.d.	n.d.	n.d.	n.d.	0.1	7	n.d.	n.d.		
Polyphenon 60	< 1	-	1	6	n.d.	n.d.	1	6	n.d.	n.d.	1	6		

n.d.: not done

All solutions except HA were prepared in 0.01 M K-Na-PO₄ buffer in ultrapure water (consisting of KH₂PO₄ and Na₂HPO₄·2H₂O, from Fluka Chemie AG, Germany) and filtered through 0.22 μ m

cellulose membrane filter (Millipore, USA) before use. The solutions of HA were prepared with addition of CaCl_2 (Roth, Germany) to achieve severe fouling [93,94] and prefiltered differently (see below). Figure 4.4 presents the molecular size distribution (MSD) of the used proteins at pH 6 measured via dynamic light scattering (DLS) with the Zetasizer equipment from Malvern, Germany. (Fibrinogen was measured at pH 7 because at pH 6 the solubility decreased due to close proximity to its IEP). The effect of pH on the MSD of myoglobin (as an example) is shown in Figure 4.5. The MSD for the other proteins at varied pH can be found in Appendix A (Figure 1).

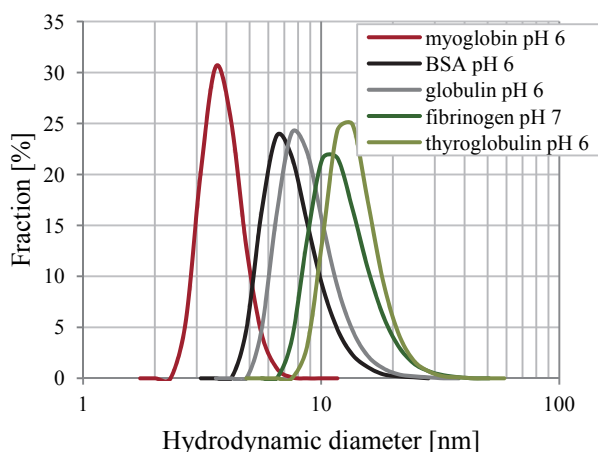


Figure 4.4 Molecular size distribution of the used proteins at pH = 6.

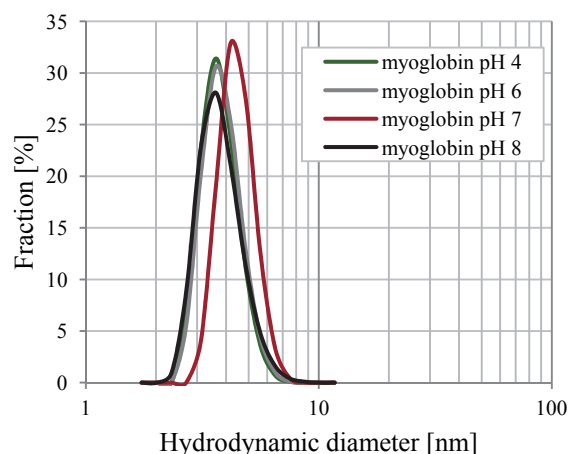


Figure 4.5 Molecular size distribution of myoglobin depending on the pH value.

From Figure 4.5 could be deduced that the molecular size of the protein changed as pH was varied and was the largest at the protein's IEP.

Prior to use, HA solutions were filtered through 8 μm and 0.45 μm membrane filters for different experiments. The particle size distribution (PSD) of untreated and prefiltered solutions at the beginning and after 24 hours of the filtration runs measured via DLS are presented in Figure 4.6.

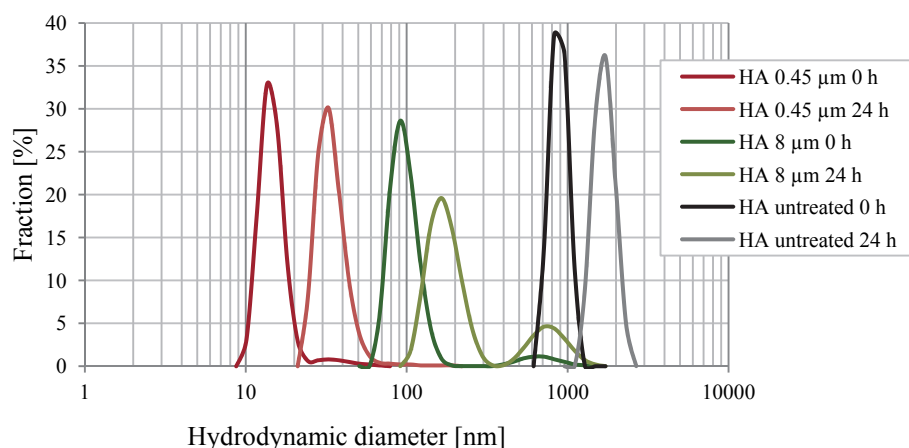


Figure 4.6 Particle size distribution of humic acid at the beginning and after 24 hours of the filtration runs.

A shift in the PSD to higher values was observed after 24 hours.

4.1.5 OTHERS

EtOH p.a. and MeOH p.a. were purchased from VWR, Germany. 1 M solutions of NaOH, KOH and HCl were from Waldeck, Germany, and 1 M KCl from Bernd Kraft GmbH, Germany. N-methyl-2-pyrrolidone (NMP) used to dissolve membranes was supplied from Merck Schuchardt OHG, Germany. Polyacrylic acid (PAA) and CuSO₄ (used for measurement of the modification depth, cf. Section 4.2.4.2) as well as 2,2-diphenyl 1-picryl hydrazyl (DPPH) (used for the estimation of the average radical density, cf. Section 4.2.4.3) were purchased from Sigma-Aldrich, USA. Water purified with a Milli-Q system from Millipore (USA) was used in all experiments. Nitrogen pure gas was from Messer Griesheim GmbH, Germany.

4.2 EXPERIMENTS

4.2.1 BULK HYDROGELS

4.2.1.1 Preparation

The bulk hydrogels were prepared via free radical polymerisation. All compounds were mixed properly in total amount of 25 mL and then let in closed vessels at room temperature for 24 hours. After that time, the gels were taken out, cut into pieces of 1 cm³ and put in 600 mL deionised water to wash out unreacted compounds. The concentration of compounds in the wash water was measured by means of total organic carbon (TOC) with TOC-Vcpn638 equipment from Shimadzu-Siemens, Germany in order to calculate the conversion. The wash water was renewed every 24 hours. Washing was performed until the TOC amount measured was less than 2 mg/L. This level was observed mostly after 8 days of washing.

4.2.1.2 Swelling experiments

To calculate the degree of swelling (DS), the wet hydrogels were weighed, dried in vacuum oven at 45 °C for 24 hours and then weighed again. DS was calculated according to Eq.(4.1) [142]:

$$DS = m_{wet}/m_{dry}, [-] \quad (4.1)$$

m_{wet} and m_{dry} are the masses of the wet and dry gels, respectively.

4.2.1.3 Calculation of the mesh size

The mesh size in a swollen gel ξ was calculated using Eq.(4.2) [148,149]:

$$\xi = r/v_{2m}^{1/3}, [\text{nm}] \quad (4.2)$$

r is the distance between two crosslinking points in a unswollen gel and v_{2m} is the volume fraction of polymer (reciprocal value of DS). The distance between two crosslinking points can be calculated from Eq.(4.3):

$$r = l \left[\frac{2M_c}{M} \right]^{1/2} c_N^{1/2}, [\text{nm}] \quad (4.3)$$

where l is the length of a C–C bond (= 0.154 nm), M_c is the molar mass between two crosslinking points, M is the average molar mass of the monomers mixture and c_N is a characteristic parameter ($c_N = 14.6$ for methacrylates) [150]. Following Eq.(4.4) and Eq.(4.5) were used for the calculation of M_c and M :

$$M_c = \frac{n_{PEGMA}}{n_{crosslinker}} M_{PEGMA} + M_{crosslinker}, [\text{g/mol}] \quad (4.4)$$

$$M = \frac{n_{PEGMA}}{n_{PEGMA} + n_{crosslinker}} M_{PEGMA} + \frac{n_{crosslinker}}{n_{PEGMA} + n_{crosslinker}} M_{crosslinker}, [\text{g/mol}] \quad (4.5)$$

Here n_{PEGMA} and $n_{crosslinker}$ are the amount of substance, and M_{PEGMA} and $M_{crosslinker}$ the molar mass of PEGMA and the used crosslinker, respectively.

It should be noticed that this calculation is applicable for gels including crosslinkers with two crosslinking points. Therefore, in the present work, only the mesh sizes of PEGMA/MBAA gels were calculated and discussed (cf. Table 1 in Appendix A).

4.2.1.4 Absorption of test solutes

Absorption tests in gels with myoglobin, BSA, HA and polyphenolics were performed. A gel piece of 500 mg was placed in 5 mL test solution for 24 hours. In order to calculate the adsorbed amount of solute, the concentration of the test solution was measured before and after the contact with gel by TOC and by UV-Vis spectroscopic measurement using Cary 50 Probe UV-Visible Spectrophotometer from Varian Inc, USA. The partitioning coefficient was calculated using Eq.(4.6):

$$\kappa = c_{gel}/c_{liq.}, [-] \quad (4.6)$$

c_{gel} and $c_{liq.}$ are the solute concentrations after 24 hours in the gel and in the solution, respectively.

4.2.2 PREPARATION OF NON-POROUS PES FILMS

Non-porous PES films were prepared by dissolving a PES 50 membrane in NMP under stirring conditions. Thereafter, from the solution 200 μm thick films were casted and subsequently dried at 60 $^{\circ}\text{C}$ in vacuum oven for three days. The films were stored in 0.01 M NaN_3 solution.

4.2.3 FUNCTIONALISATION VIA PHOTO-GRAFTING

Prior to any experimental use, the membranes/films were cut to circular or rectangular samples (see below), washed in EtOH for 30 minutes to remove preservatives and impurities and soaked overnight in 0.01 M NaN_3 aqueous solution.

The UV irradiation system UVA Cube 2000, Hönle AG, Germany, equipped with a 20 cm long Hg lamp, allowing a homogenous irradiation of 0.1 m^2 area via reflecting walls, was used for the photo-grafting. First, conditioned virgin membranes were placed between papers to remove excess water on the surface. Thereafter, circular membrane samples with diameter up to 47 mm were immersed in 2 ml of the monomer solution in a Petri dish (60 mm x 15 mm) and allowed to equilibrate for 5 minutes. Before performing membrane functionalisation, the monomer solution was bubbled with nitrogen for 10 minutes. Subsequently, a second smaller Petri dish was placed on the sample. The rectangle samples used in CF filtration experiments with area of 84 cm^2 were immersed in 25 mL modifier solution. The experimental configuration is visualised in Figure 4.7.

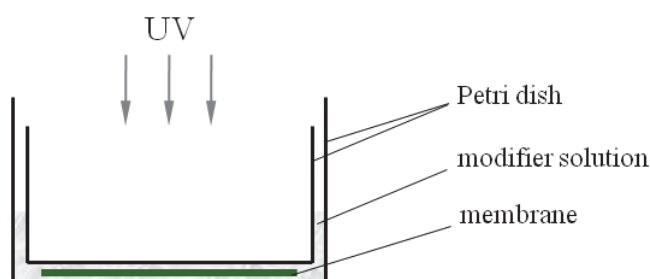


Figure 4.7 Experimental set-up for membrane UV irradiation.

The samples were irradiated with varied irradiation dose (2 – 18 J/cm^2) at different intensities (between 5 mW/cm^2 and 60 mW/cm^2 , measured using the UVA meter from Hönle AG, Germany). The irradiation dose E was controlled by varying the irradiation time according to Eq.(4.7):

$$E = It, [\text{J}/\text{cm}^2] \quad (4.7)$$

I and t are the intensity of the UV waves and the irradiation time, respectively. The desired intensity was adjusted using tarnished glass plates. Since the membrane material could be damaged by UV with too high energy, as already investigated in [127], the UV light was filtered through a special glass

filter so that only UV-A ($\lambda = 315 - 400$ nm) waves reached the samples. After the functionalisation, the samples were placed in a large excess of ultrapure water, shaken overnight to remove unreacted monomer and then stored in 0.01 M NaN_3 solution.

4.2.4 MEMBRANE SURFACE CHARACTERISATION

4.2.4.1 Degree of grafting

DG, also called degree of functionalisation, was measured gravimetrically. Here, samples of virgin membrane were dried in vacuum oven at 40 °C for 24 hours and their mass was taken by a microbalance (Sartorius-Stedim Biotech, Germany). After that, the membranes were soaked in water (in order to achieve the same initial modification conditions like in common modification). Subsequently, the modification was performed as usual. For each modification, three samples were prepared in order to quantify possible result deviations. After membrane washing, the samples were dried in vacuum oven (as described above) and the mass was taken. The DG was calculated according to Eq.(4.8) [140]:

$$DG = (m_{graft} - m_0)/A, [\mu\text{g}/\text{cm}^2] \quad (4.8)$$

m_0 is the initial membrane sample weight, m_{graft} the weight after modification and A the membrane outer surface area. It should be noticed that DG will be later presented in $\mu\text{mol}/\text{cm}^2$ in order to ensure better comparison of the data from different modifications. None of the samples used for the determination of DG were used for further evaluations.

4.2.4.2 Modification depth

The degree of surface modification is not constant in the membrane cross-section when using UV as activator [151]. This is because the intensity of the UV light is decreasing mainly due to adsorption and scattering by the membrane material. In order to characterise this effect, samples were modified with PAA which was further converted to copper complex with CuSO_4 [151,152]. The excess of Cu^{2+} was removed by washing the membranes with NaOH at $\text{pH} = 10$. The amount of Cu^{2+} attached was measured in the membrane cross-section by energy-dispersive X-ray analysis (EDX) combined with scanning electron microscopy (SEM; cf. Section 4.2.4.8).

4.2.4.3 Estimation of the average radical density

Membrane and film samples irradiated in water were placed immediately after the UV treatment into 0.1 mM DPPH solution in MeOH. The samples were incubated for one hour at 50 °C and the change in DPPH absorbance at 520 nm, i.e., the bound amount of DPPH to the samples was subsequently

measured via UV-Vis [29,153]. The average distance between two radicals x was calculated according to Eq.(4.9):

$$x = \frac{1}{\sqrt{\frac{c_{DPPH} N_A \pi}{4A} - 1}}, [\text{nm}] \quad (4.9)$$

c_{DPPH} is the concentration of DPPH bound to the samples, N_A is the Avogadro constant and V is the volume of DPPH solution.

It should be noted that since the samples were kept in the DPPH solution after the UV irradiation process, only the amount of radicals which were present at that time was measured. The amount of radicals which were created during the UV irradiation was not determined.

4.2.4.4 Contact angle

Virgin and modified samples were characterised with respect to their wettability by CA measurement with the system OCA 15 Plus, Dataphysics GmbH, Germany. CA was evaluated in captive bubble mode, where the sample is measured in wet state and there is no damage of the pore structure due to drying [87]. Here, the sample was fixed on a holder and placed in water bath with the active surface to the bottom. Air bubble (ca. 7 μl) was placed on the membrane surface. At least five measurements were performed for each sample and the average value was calculated (deviations within 10 %).

4.2.4.5 Attenuated total reflection infrared spectroscopy

ATR-IR of the outer membrane surfaces was performed using an Equinox 55 instrument (Bruker Optics, Germany). The membranes were dried in vacuum oven at 40 °C for 24 hours. A total of 64 scans were performed with diamond crystal at room temperature, as performed in [140]. This method was used to characterise the membrane chemistry and detect spectroscopically the presence of modifiers on the membrane surface.

4.2.4.6 Zeta potential

The outer surface charge over wide range of pH was characterised by means of ZP. Here, two samples were fixed facing their active surfaces to each other in a defined distance. An aqueous solution of 1 mM KCl was pumped through the channel between the samples at varied flow velocity. The pH was varied in the range 3 – 10 by addition of 0.1 M HCl or KOH, always starting from pH = 3. The ZP was calculated using the Helmholtz-Smoluchowski equation (Eq.(4.10)) [154]:

$$\zeta = \frac{\kappa\eta}{\varepsilon\varepsilon_0} \frac{\Delta E}{\Delta P}, [\text{mV}] \quad (4.10)$$

ΔE is the streaming potential, ΔP the hydrodynamic pressure difference, η the viscosity, ε the dielectric constant of the solvent (water), ε_0 the permittivity of vacuum and κ the solution conductivity. Two different set-ups were used in this study: an automated set-up with consideration of the cell conductivity and a self-made apparatus where the measurement was performed without consideration of the cell conductivity.

4.2.4.6.1 Measurement with consideration of the cell conductivity

SurPASS electrokinetic analyser from Anton Paar GmbH, Germany was used for these measurements. The adjustable gap cell allowed ZP measurement under variation of the gap height. The adjustable gap cell is shown in Figure 4.8 [155].

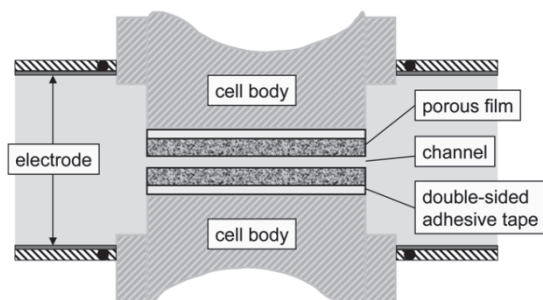


Figure 4.8 Schematic representation of the SurPASS adjustable gap cell [155].

Membrane/film samples were cut into pieces with dimensions 10 mm x 20 mm and attached to the surface of the cell stamps using adhesive tape. Then, the system was equilibrated for 15 minutes by circulating KCl solution. The measurement of streaming current was performed by increasing the pH by increment of 0.25 and the ZP was calculated. Each measurement was repeated with the same sample after complete rinsing of the system and new equilibration.

4.2.4.6.2 Measurement without consideration of the cell conductivity

The measurement of modified samples was impossible with the set-up described above due to bad adhesion. Therefore, similar self-made set-up was used where the cell conductivity was not considered. Here, the samples were fixed by tightening of the measuring cell. To ensure a flow channel was present, a 300 μm thick polytetrafluoroethylene spacer was placed between the samples. The flow and pH were adjusted manually. The measurement was performed in pH intervals of ca. 2.5.

4.2.4.7 Atomic force microscopy

The outer membrane surface was analysed via atomic force microscopy (AFM) in wet and dry state using the NanoWizard instrument from JPK Instruments (Germany) with lateral scan area of $100\ \mu\text{m} \times 100\ \mu\text{m}$, equipped with Si-Cantilever NanoWorld Pointprobe NCH from NanoWorld, Switzerland. Membrane sample of $1\ \text{cm}^2$ was fixed on object holder with adhering tape. Maximal area of $10\ \mu\text{m} \times 10\ \mu\text{m}$ was scanned in non-contact tapping mode. From this method, information about the membrane surface properties such as roughness and homogeneity (distribution of soft and hard segments) was collected. To estimate the surface roughness, the conducted data were analysed in vertical direction. The maximal oscillation in positive and negative direction was taken as characteristic roughness value.

4.2.4.8 Scanning electron microscopy

Membrane surface and cross-section were visualised using SEM instrument Quanta 400 FEG (FEI, Czech Republic) at vacuum conditions. Prior to the measurement, the membrane samples were dried under vacuum conditions (in oven or freeze drier) and dipped in liquid N_2 in order to break the membrane for cross-section analysis. To create a conductive surface, the samples for cross-section analysis were sputtered with 7 nm Au/Pd layer using a K 550 sputter coater (Emitech, UK). In contrast, the membrane active surface was covered by a carbon layer with 5 nm thickness, which allowed more precise visualisation of the pore openings. Visualisations with maximal magnification of 400 000 were taken.

EDX mapping analysis combined with SEM was also used in this work in order to measure the Cu^{2+} amount (cf. Section 4.2.4.2). Here, the membrane cross-section was scanned in 100 nm thick segments and the atomic ratio Cu/S was measured. Since the stainless steel holder contained S, it was covered by $10\ \mu\text{m}$ Au layer via galvanisation.

4.2.5 CHARACTERISATION OF MEMBRANE PERFORMANCE

4.2.5.1 Water permeability

The membrane performance was first characterised by water permeability measurements. Measuring cells Amicon 8010 and Amicon 8050 from Millipore, USA were used for membrane sample diameters of 25 mm and 44 mm, respectively. Prior to the measurement, the membrane was conditioned by filtering ultra pure water at high pressure (mostly 3 bar) for at least 30 minutes. During this process, strong loss of flux was found due to the change in the membrane structure as a consequence of the applied pressure (compacting). Compaction was not done before rejection (Section 4.2.5.2) and short

DE filtration experiments (Section 4.2.5.5.1.1) due to the large amount of samples and time reasons. The water permeability measurements were done under DE stirring conditions at room temperature using the set-up shown in Figure 4.9.

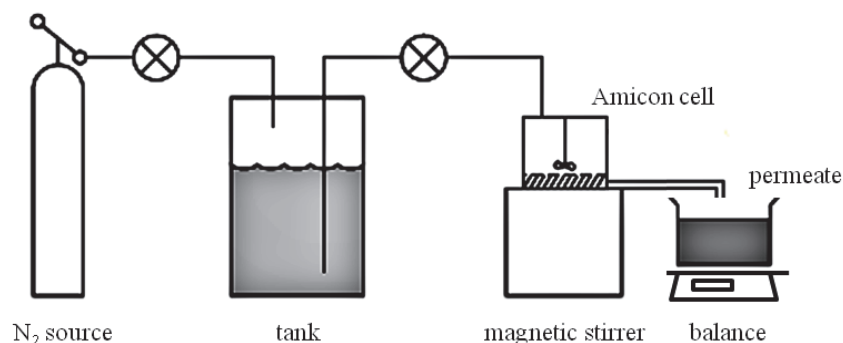


Figure 4.9 Schematic view of DE filtration set-up.

Water was pressurised with nitrogen and filtered through the membrane under stirring conditions (300 min^{-1} , average linear velocity of $0,165 \text{ m/s}$); the mass of permeate collected for 5 minutes was measured using a balance and the permeability was calculated according to Eq.(4.11):

$$L_p = m / \rho t A p, [\text{L}/\text{hm}^2\text{bar}] \quad (4.11)$$

m is the mass of permeate with density ρ collected for time t through membrane surface A at pressure p . Only membranes with flux deviation within 15 % were used for further characterisation.

4.2.5.2 Rejection experiments

Same set-up, as described above, was used for rejection experiments with dextrans and PEG. Membrane samples with diameter of 44 mm were used without precompaction (see above). The initial flux was set to $10 \text{ L}/\text{hm}^2$ by adjusting the pressure in order to minimise the influence of CP and convective flow on the rejection [156]. Amicon cell 8050 was filled with 50 mL feed solution and ca. 3 mL of permeate were collected under stirring at 300 min^{-1} in order to minimise CP effects [156]. The MW of samples from the feed and the collected permeate were analysed via GPC. The GPC column SUPREMA, linear, $10 \mu\text{m}$, $600/8 \text{ mm}$, $100 - 100\,000\,000 \text{ g/mol}$, PSS, Germany was used for the analysis of dextran, and column HEMA Bio, linear, $10 \mu\text{m}$, $600/8 \text{ mm}$, $100 - 3\,000\,000 \text{ g/mol}$, MZ, Germany for PEG solutions. The rejection for each dextran or PEG MW was calculated using Eq.(4.12):

$$R = (1 - c_p/c_f) \cdot 100, [\%] \quad (4.12)$$

c_f and c_p are the concentrations in the feed and permeate, respectively. The MW which was rejected to 90 % is defined as the MWCO of the membrane [47]. By plotting the rejection values for all MW vs. the MW, the rejection curve was built.

The hydrodynamic radii of PEG and dextran could be calculated from their MW using Eq.(4.13) [157] for PEG and Eq.(4.14) [158] for dextran.

$$r(PEG) = 0.262M^{0.5} - 0.3, [\text{\AA}] \quad (4.13)$$

$$r(dextran) = (0.096M^{0.59} + 0.128M^{0.5})/2, [\text{\AA}] \quad (4.14)$$

After the filtration, water permeability was measured again in order to estimate the flux decline caused by adsorbed test solutes. This was calculated by means of fouling resistance after Eq.(4.15):

$$R_f = L_{p,1}/L_{p,0}, [-] \quad (4.15)$$

$L_{p,0}$ and $L_{p,1}$ are the water permeabilities before and after filtration of test solute, respectively. The samples were not used for further characterisation.

4.2.5.3 Adsorption of test solutes

To describe the membrane-solute interactions, adsorption experiments with test solutions were performed using Amicon 8010 cells. First, the initial water flux was collected; thereafter the cell was filled with the test solution. The membranes were incubated for three hours under stirring conditions without any flux through the membrane (the cell outlet was kept closed). After two times rinsing the samples with pure water, the water flux was measured again in order to calculate the fouling resistance (Eq.(4.15)).

The adsorbed amount of test solute on the membrane surface was evaluated by static adsorption experiments for 24 hours in non-stirred conditions using membrane holders similar to the Amicon cells. The concentration of the test solution was measured before and after the experiment by TOC and the adsorbed amount per membrane surface area was calculated.

4.2.5.4 Diffusion experiments

Diffusion tests were performed in order to estimate the effective diffusion coefficient and the amount of solute bound to the membrane under these conditions. The set-up for diffusion experiments is shown in Figure 4.10.

A membrane with surface area of 17.34 cm² was placed between the two cells. The cells were filled with the upstream (buffered protein solution) and downstream (buffer) solutions. The system was

equipped with stirring devices to minimise effects of boundary layers on the solute transport. Cooling bath allowed constant process temperature of 8 ± 0.2 °C minimising biofouling. The diffusion set-up was build asymmetrically – the feed solution volume was larger. In this way, the increase of concentration in the downstream side was larger than the decrease in the upstream side, which facilitated the protein detection in the downstream side.

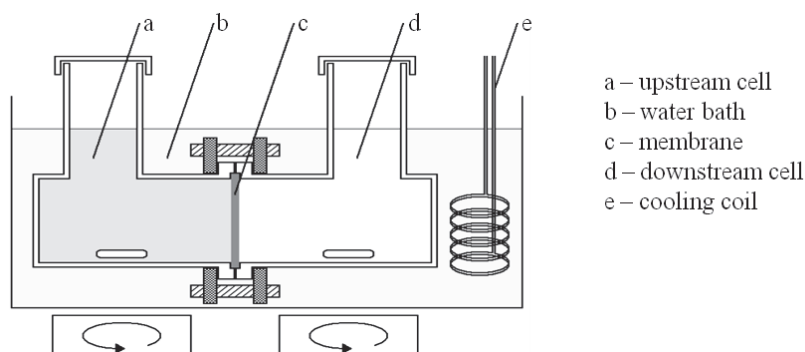


Figure 4.10 Schematic view of diffusion equipment.

Samples from both cells were taken every 4 hours for 48 hours. The concentration was measured by TOC and UV-Vis. The concentration of BSA in mixture was calculated indirectly when the concentration of myoglobin measured by UV at 409 nm in the mixture was subtracted from the total concentration measured by TOC. The effective diffusion coefficient D_{eff} was calculated using Eq.(4.16):

$$D_{eff} = \frac{\delta \Delta N}{A \varepsilon \Delta t \Delta \bar{c}}, [\text{m}^2/\text{s}] \quad (4.16)$$

where δ is the membrane thickness, ΔN the increase in amount of substance between two measurements, ε the membrane volume porosity, Δt the time interval between two measurements and $\Delta \bar{c}$ the concentration difference between upstream and downstream averaged for two measurements. The diffusion coefficient was calculated for every measuring point and a median value was calculated.

Free diffusion coefficients of the proteins were calculated according to the Stokes-Einstein equation, Eq.(4.18):

$$D = \frac{k_B T}{6\pi\eta r}, [\text{m}^2/\text{s}] \quad (4.17)$$

k_B is the Boltzmann constant, T is the absolute temperature, η is the fluid viscosity and r is the radius of a globular protein.

Furthermore, the adsorbed amount of solute on the membranes was calculated via mass balance.

4.2.5.5 Filtration

4.2.5.5.1 Stirred dead-end filtration

Stirred DE filtration experiments were performed with the set-up described in Section 4.2.5.1.

4.2.5.5.1.1 Short stirred dead-end filtration

4.2.5.5.1.1.1 Two fold volume reduction

Non-compacted membrane samples with 44 mm diameter were used for filtration of test substances in short term experiments. Aim was to evaluate the effect of modification degree and type on the fouling resistance and rejection. Due to the large spectrum of variations, these experiments were performed short term. The measuring cell was filled with 50 mL test solution and 25 mL were filtered through the membrane at 1 bar and the time was taken in order to calculate the median permeability during the filtration (Eq.(4.11)). The concentration of permeate was measured via TOC and UV-Vis to calculate the rejection (Eq.(4.12)). The membrane water flux was checked before and after the filtration for the estimation of fouling resistance (Eq.(4.15)).

4.2.5.5.1.1.2 20 fold volume reduction

Short filtration experiments were performed with 20 times feed volume reduction in order to characterise the effect of concentration on fouling resistance. The experiments were performed as described above.

The volume reduction was calculated as follows (Eq.(4.18)):

$$\text{volume reduction} = V_{feed,0} / (V_{feed,0} - V_{permeate}), [-] \quad (4.18)$$

$V_{feed,0}$ is the initial feed volume and $V_{permeate}$ is the volume of collected permeate.

4.2.5.5.1.2 Stirred dead-end filtration over 24 hours

Selected membranes were tested further in long term DE filtration experiments. The membranes were compacted and after that the water flux was measured. The feed vessel was filled with 450 mL test solution and the filtration process was started at initial flux of 100 L/hm² for all tested membranes by adjusting the operation pressure. This allowed the direct comparison of the membrane productivity. A balance was connected to a computer and the mass of permeate was taken for period of 24 hours so that the permeate flux over time could be calculated (Eq.(4.11)). After the process was stopped, samples from permeate and feed were taken and their concentration was measured by TOC and UV-Vis in order to calculate the apparent solute rejection (Eq.(4.12)).

From filtration experiments of HA, the specific cake resistance α , a measure for the contribution of the deposits mass $m_{dep.}$ to the cake resistance R_c , was calculated.

The specific cake resistance is defined according to Eq.(4.19) as [55,57]:

$$\alpha = R_c A / m_{dep.}, [\text{m/g}] \quad (4.19)$$

$m_{dep.}$ is the mass of the deposited foulant on and in the membrane which was calculated via mass balance from all streams and washing tests.

4.2.5.5.2 Cross-flow filtration

Membrane samples with larger area (84 cm²) were tested in CF conditions using the LSta05-2 laboratory CF filtration equipment from Simatec, Germany. Schematic representation of the system is shown in Figure 4.11.

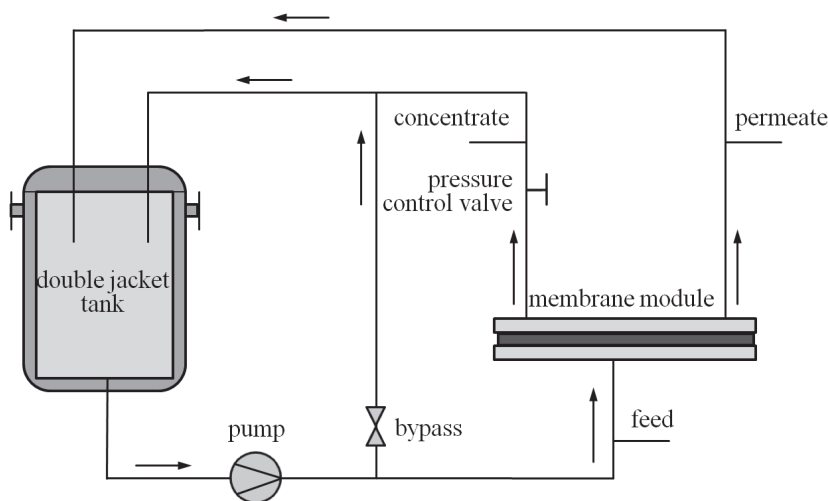


Figure 4.11 Schematic view of the CF filtration set-up.

The CF system consisted of double jacket feed tank (maximal volume of 7 L), membrane module and bypass connection. 2 L test solution was pumped through the membrane module in cycle at 20 ± 1 °C. The experiments were run at initial flux of 100 L/hm², constant pressure and defined CF. Experiments were performed with two CF velocities adjusting of the feed flow to 20 L/h and 60 L/h. The corresponding linear feed velocities were 0.157 m/s and 0.471 m/s. Long term filtration experiments of BSA under CF conditions showed changes in the solution properties, i.e., the solution became turbid. DLS measurements (Figure 4.12) showed increasing hydrodynamic diameter of BSA over time, most pronounced after 8 hours, indicating protein aggregation. Protein aggregation in UF systems has been explained primarily by microcavitation in pumps and valves [97]. For this reason the experiments were performed for 6 hours.

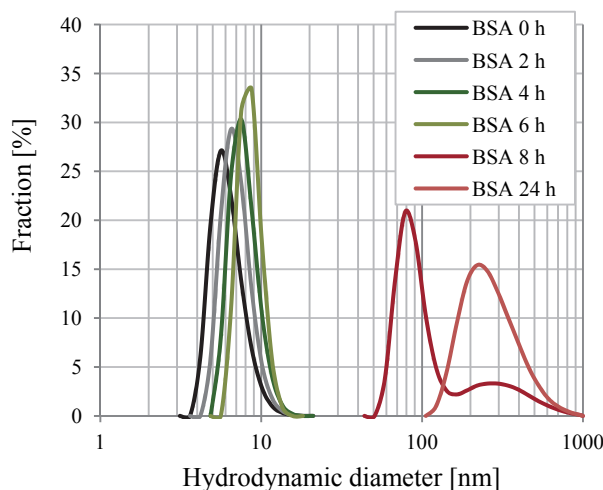


Figure 4.12 Molecular size distribution of BSA during CF filtration depending on the filtration time.

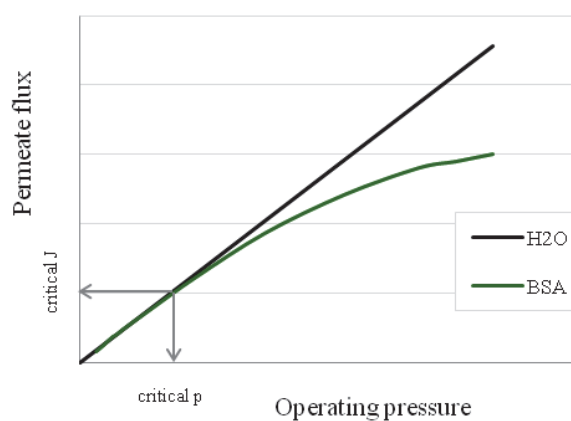


Figure 4.13 Determination of the critical flux and pressure from CF filtration experiments.

Several samples from all streams were taken during the filtration process and analysed by TOC and UV-Vis in order to characterise the current solute rejection. Measuring data about pressure, temperature, feed and permeate fluxes were collected by the DASyLab 9.0 software. The flux over time was determined from the conducted data. The critical flux/pressure was also described by plotting the permeate flux vs. the operating pressure. The deviation of the data from the pure water flux curve gave the critical flux/pressure, as shown in Figure 4.13.

4.2.5.5.3 Stability tests

The membrane stability was tested in CF conditions. Here, three cycles of CF filtration and subsequent cleaning were performed. The results are presented as resistance over filtration time, calculated from the reciprocal value of the actual permeability L_p and the solution viscosity η according to Eq.(4.20):

$$Resistance = \frac{1}{L_p \eta}, [m^{-1}] \quad (4.20)$$

4.2.5.6 Membrane cleaning

Cleaning tests were performed after long term DE and CF filtrations. The effect of mechanical and chemical cleaning on the membrane water flux was studied. The flux recovery from every cleaning step was calculated by comparing the actual water flux to the initial after Eq.(4.21).

$$Flux\ recovery = \frac{L_{p,actual}}{L_{p,0}} \cdot 100, [\%] \quad (4.21)$$

Mechanical cleaning was done by external cleaning and back wash with water. Chemical cleaning was carried out with NaOH at pH = 13 and room temperature (21 °C).

4.2.5.6.1 Cleaning after dead-end filtration

After the filtration procedure, the protein solution was removed from the filtration system and the membrane water flux was measured. Thereafter, the membrane surface was cleaned by filling the Amicon cell with water and stirring for 30 seconds two times; the water flux was determined again. Subsequently, the membrane was turned with the skin side down and water was filtered for 10 minutes at 1 bar. The membrane was placed in its initial position to measure the water flux. At last, NaOH solution (pH = 13) was filtered for 10 minutes at 1 bar and water flux was measured once again.

4.2.5.6.2 Cleaning after cross-flow filtration

The cleaning procedure occurred differently in CF conditions. The contribution of external cleaning and back wash could not be determined due to limitations by the CF equipment. Here, the CF was used for external cleaning in combination with flux through the membrane. After three times washing with water, the permeate flux was determined. Chemical cleaning was performed as described in Section 4.2.5.6.1. After removing the NaOH solution, the water flux was measured.

5 RESULTS

The results obtained in this work are presented in following sections: I. bulk hydrogels, II. membrane properties and III. membrane performance. The last are mainly divided in performance during the filtration of (a) proteins, (b) HA and (c) polyphenolics.

5.1 BULK HYDROGELS

As parallel experiments to the characterisation of the synthesised hydrogels on membrane surfaces, bulk hydrogels were prepared. They were characterised by conversion and DS. In addition, absorption experiments with test solution were also performed.

5.1.1 CHARACTERISATION

The DS depending on the crosslinker concentration is presented in Figure 5.1.

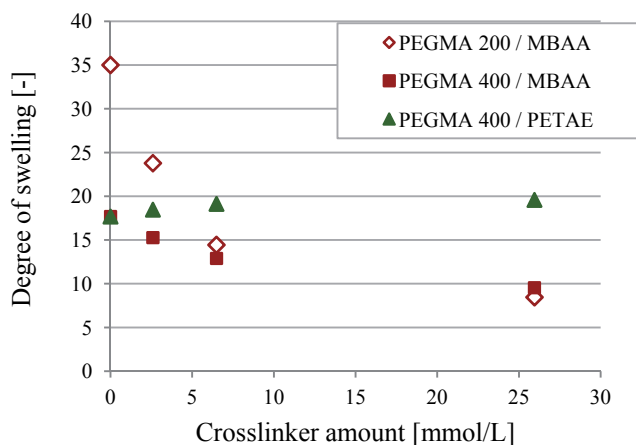


Figure 5.1 Hydrogels degree of swelling depending on the crosslinker amount.

The increase of the crosslinker amount decreased the swelling of PEGMA/MBAA hydrogels. This behaviour was not found for PEGMA/PETAE hydrogels: a slight increase in DS was observed. An overview of all collected data from the hydrogels analysis (incl. mesh size) can be found in Appendix A (Table 1).

5.1.2 ABSORPTION OF TEST SUBSTANCES

Hydrogels prepared from PEGMA 400 with variation of the crosslinking type (at maximal crosslinker amount) were used in absorption experiments with BSA, myoglobin, HA and polyphenolics. The calculated partitioning coefficients are presented in Figure 5.2.

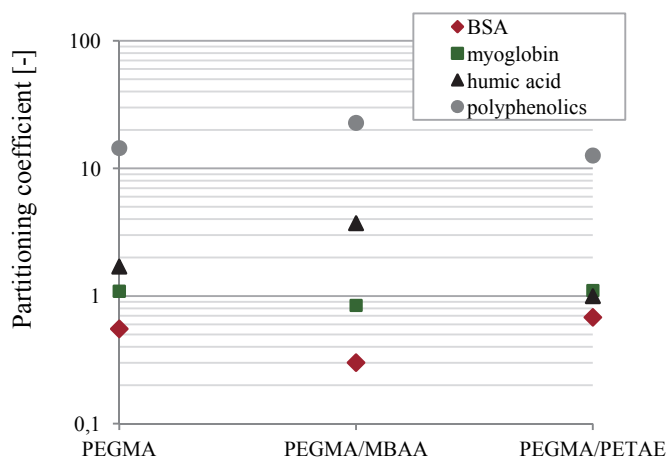


Figure 5.2 Partitioning coefficient after 24 hours absorption of test solutes on hydrogels with maximal crosslinking amount.

For $\kappa < 1$, the concentration of solute is higher in the solution than in the hydrogel; when $\kappa = 1$, the solute is distributed uniformly in the solution and in the gel; in cases when $\kappa > 1$, there is accumulation of solute in the network. As it can be seen from the results, BSA was excluded by the hydrogel network, mostly by PEGMA/MBAA hydrogel which showed the smallest swelling degree. Myoglobin seemed to be slightly excluded by the network crosslinked with MBAA. In case of HA, the solute was a little accumulated in PEGMA/MBAA. Polyphenolic compounds were strongly accumulated in all gels, so that the concentration in the gels exceeded more than 10 times the concentration in the surrounding solution.

Generally speaking, the sorption affinity of the hydrogels to the tested solutes could not be clearly quantified, because washing was not performed after the sorption tests.

5.2 MEMBRANE PROPERTIES

The polymer MWD of the membranes was analysed by dissolving the membranes and subsequent GPC analysis. It was found that the samples showed similar solubility in NMP. Furthermore, similar MWD were observed via GPC (results are presented in Appendix A (Figure 2)). These findings indicate that all samples have been manufactured from PES as a main component. The tested membranes had an average thickness of $130 \pm 20 \mu\text{m}$.

5.2.1 DEGREE OF GRAFTING

An overall increase in the DG with increasing the UV irradiation dose was observed for all tested membranes as confirmation for the occurred hydrogel layer growth. The change in DG with UV irradiation dose is shown in Figure 5.3 for PES 10 modified with PEGMA 400.

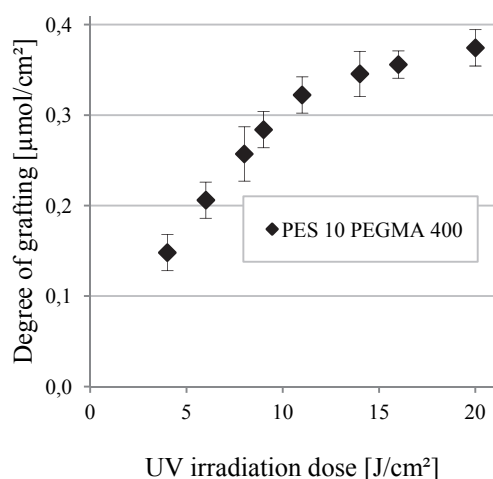


Figure 5.3 DG at varied UV irradiation dose. Example: PES 10 modified with PEGMA 400.

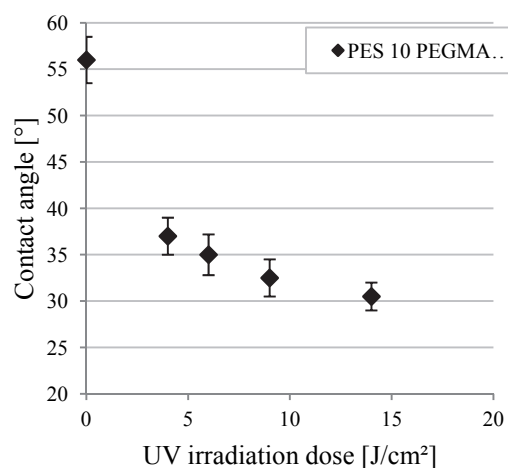


Figure 5.4 CA depending on the UV irradiation dose. Example: PES 10 modified with PEGMA 400.

After initial strong increase of the polymer amount with UV irradiation, a plateau was reached beyond $10 \text{ J}/\text{cm}^2$. DG values for the other membranes can be found in Appendix A (Figure 3).

The DG values at $11 \text{ J}/\text{cm}^2$ UV irradiation dose for all tested membrane types are shown in Table 5.1.

Table 5.1 CA and DG of membranes and film after modification at $11 \text{ J}/\text{cm}^2$. Variation of the UV intensity

Membrane	PES 5	PES 10	PES 30		PES 50			PES 100	PES 300	Film PES 50
			with PVP	w/o PVP	5 mW/cm ²	20 mW/cm ²	60 mW/cm ²			
CA virgin [$^\circ$]	60	58	54	87	48			46	44	55
CA modified [$^\circ$]	29	31	33	45	32	n.d.	n.d.	28	27	36
DG [$\mu\text{mol}/\text{cm}^2$]	0.42	0.29	0.52	n.d.	0.47	0.52	0.57	0.45	0.47	n.d.

n.d.: not determined

It can be seen that similar DG values were measured, except for PES 10. The effect of the UV intensity during the membrane modification on the grafted polymer amount was studied during modification of PES 50. The results showed slightly increased values when higher UV intensity was applied.

Furthermore, the influence of the crosslinking on the modification was tested. The DG values under variation of the monomer and crosslinker type are presented in Table 5.2.

Table 5.2 CA and DG of modified PES 50 with 11 J/cm² depending on the crosslinking type and amount

Modifier composition	PEGMA 200	PEGMA 400	PEGMA/MBAA			PEGMA/PETAE		
Concentration [g/L]	23/0	40/0	40/0.4	40/1	40/4	40/0.66	40/1.66	40/6.65
DG [$\mu\text{mol}/\text{cm}^2$]	0.65	0.46	0.49	0.5	0.54	0.51	0.5	0.57
CA [$^\circ$]	38	32	32	32	32	32	32	33

Comparing the results from the modifications with PEGMA 200 and PEGMA 400, higher amount of PEGMA 200 attached to the membrane surface was found. The addition of crosslinking agents slightly increased the amount of grafted polymers, whereas this effect was more pronounced in modifications with PETAE. Considering the occurred deviations during the measurements ($\pm 0.25 \mu\text{mol}/\text{cm}^2$), the changes caused by the crosslinking were estimated as negligible for low crosslinker amount and small for higher crosslinker amount.

5.2.2 WETTABILITY

CA measurements in captive bubble mode were performed with membranes and non-porous films to measure the wettability. The collected results from the measurements of virgin and modified samples are shown in Table 5.1. Regarding the results obtained from unmodified samples, it was found that the CA decreased with increasing nominal MWCO – from 60° for PES 5 to 44° for PES 300. Furthermore, virgin PES 30 without PVP showed higher CA value (87°) than the corresponding membrane with PVP in the casting solution (54°).

The membrane functionalisation decreased the CA of the tested membranes. Figure 5.4 shows the effect of the UV irradiation dose (as measure for the modification degree) on CA of PES 10. CA increased very rapidly after relatively small irradiations; thereafter a plateau was reached. Data from the measurements of other membranes can be found in Appendix A (Figure 4). In Table 5.1, CA values of all modified membranes at 11 J/cm² are presents. The composite membranes had lower CA than the virgin due to the grafted hydrogel layer – CA decreased to $27 - 36^\circ$. To evaluate the influence of the modifier composition on hydrophilicity, CA of modified PES 50 with varied monomer compositions was measured. The results are presented in Table 5.2. The modifications with

PEGMA 200 resulted in larger CA in comparison to the modification with PEGMA 400. The application of crosslinkers did not have any influence on the CA.

5.2.3 CHARACTERISATION OF THE MEMBRANE COMPOSITION USING ATR-IR

Virgin and modified membranes were analysed by ATR-IR. The results were compared with spectra of PES and PEG solid materials. The collected spectra are shown in Figure 5.5. Grey line indicates virgin membrane, whereas modified membrane spectrum is represented in red.

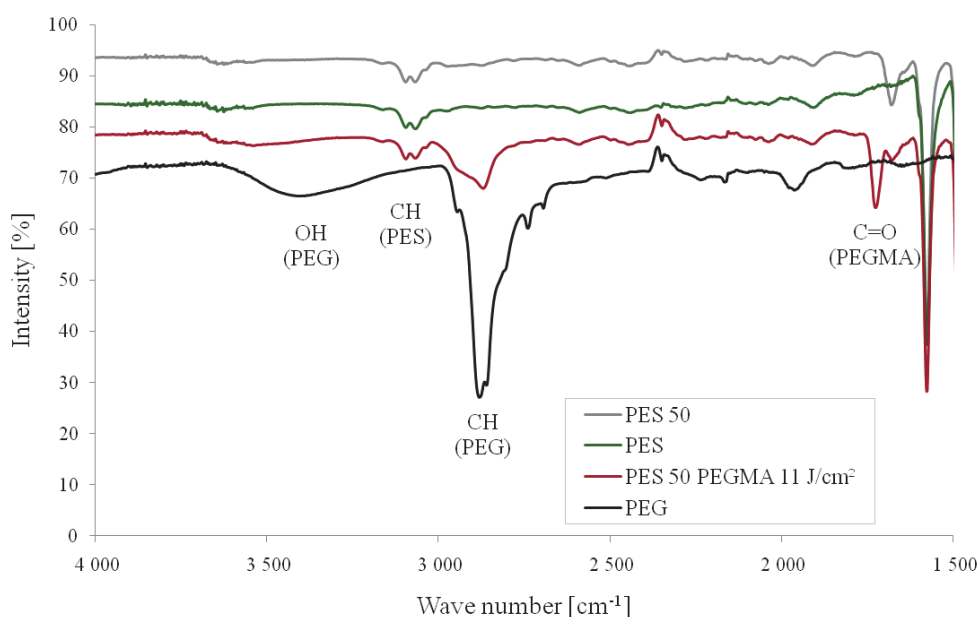


Figure 5.5 ATR-IR spectra of PES, PEG, virgin and modified membranes.

Virgin membrane showed the characteristic peaks for PES at 3069 and 3095 cm⁻¹ and new peak at 1680 cm⁻¹ which was not present in the spectrum of PES solid material. After modification, new peaks appeared: 3500 cm⁻¹ broad band for –OH groups from PEG, 2950 cm⁻¹ for CH bonds from PEG and 1725 cm⁻¹ for C=O from PEGMA.

5.2.4 SURFACE CHARGE

The surface charge of virgin membranes over pH range of 3 – 10 was measured considering the cell conductivity. ZP depending on the pH for PES 30, PES 30 without PVP and film are compared in Figure 5.6. A slight difference was found for PES 30 without PVP and film. It can be seen that the pH value where the surfaces were not charged (ZP = 0) shifted from 3 to 4.5 for these samples. All tested membranes with PVP in the material exhibited zero charge around pH = 3 (see Appendix A (Figure 5)).

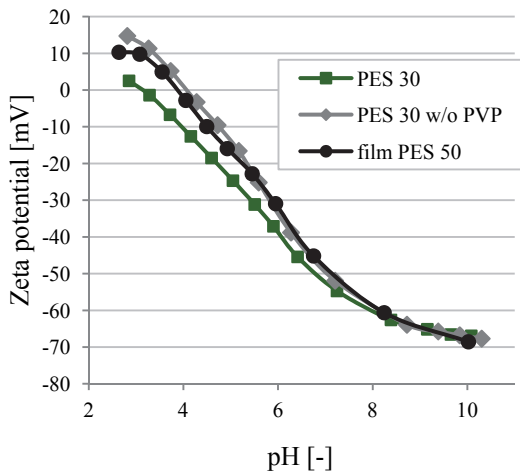


Figure 5.6 ZP of selected virgin membranes and film.

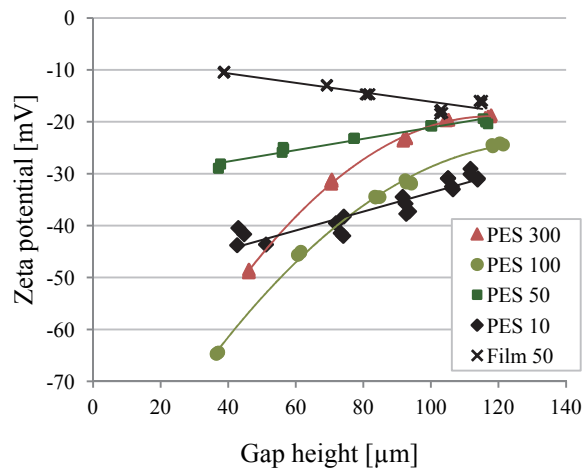


Figure 5.7 ZP at pH = 5.6 as function of the cell gap height.

In further experiments the cell gap height (flow channel height) was varied. The measurements were performed at pH = 5.6. Membranes with varied pore size and cross-section structures as well as film were tested. Figure 5.7 shows that the gap height has an influence on the measured ZP. For porous membranes, ZP decreased in absolute values with increasing gap height, whereas the opposite behaviour was found with film. In detail, the changes for film and membranes with relatively small pores and finger-like cross-section structure (PES 10 and PES 50) were small. In contrast, the dependence of ZP from the gap height was significant for PES 100 and PES 300 which have larger pores and sponge-like structure. Yaroshchuk and Luxbacher [155] studied the effect of the membrane pores on the streaming current and the cell conductance. It has been found that streaming current inside the pores can be measured and its contribution to the apparent streaming current is stronger for bigger pores (microfiltration membranes). In this study negligible change in the streaming current coefficient (shown in Figure 5.8) was found (note Y scale).

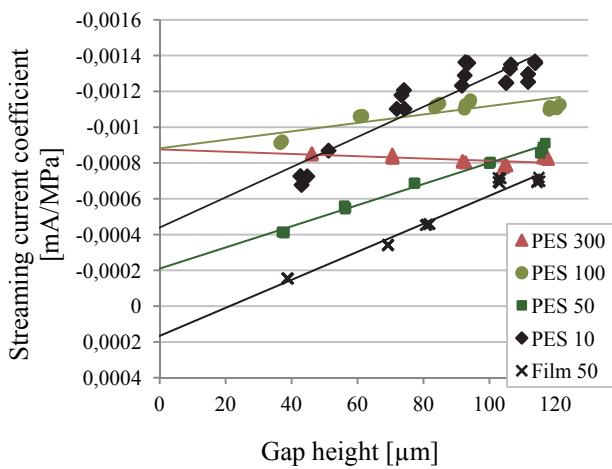


Figure 5.8 Streaming current coefficient of virgin membranes and film vs. cell gap height.

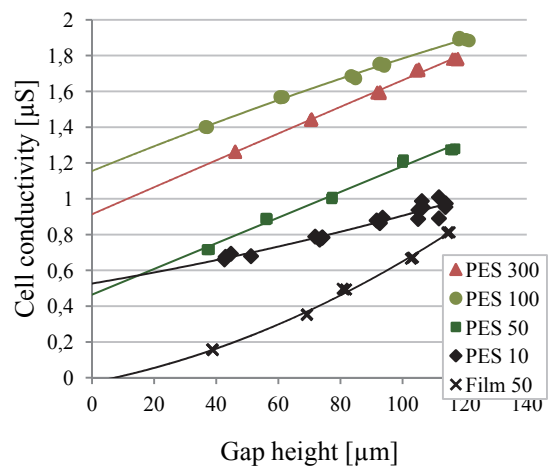


Figure 5.9 Cell conductivity during the ZP measurement at varied cell gap height.

Furthermore, the cell conductivity was measured. It was found to be higher for membranes with larger pores. Similar results have been obtained in [155]. The data extrapolated to zero gap height correspond to the conductivity inside the membrane porous structure. In this study, PES film showed extrapolated value close to zero. This value was higher for membranes with finger-like structure and increased further for sponge-like membranes.

The contribution of the grafted hydrogel layer was tested by measuring the ZP of functionalised membranes without consideration of the cell conductivity. The effect of the modification degree as well as the influence of the crosslinking type (at maximal crosslinker amount) was studied. The obtained results are displayed on Figure 5.10.

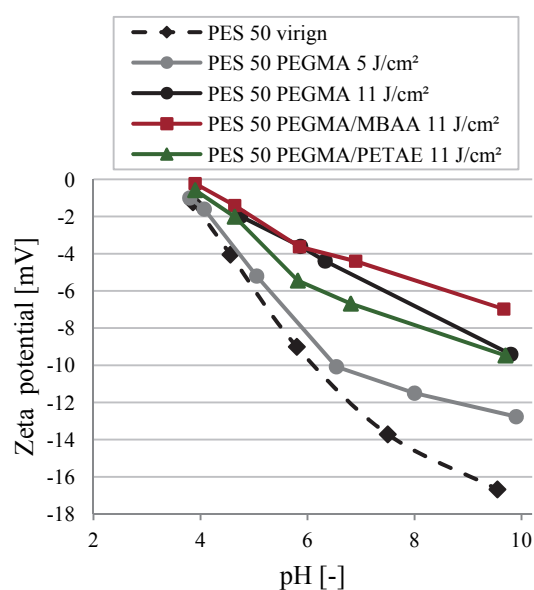


Figure 5.10 ZP of virgin and modified membranes PES 50 at varied UV irradiation dose and crosslinking type.

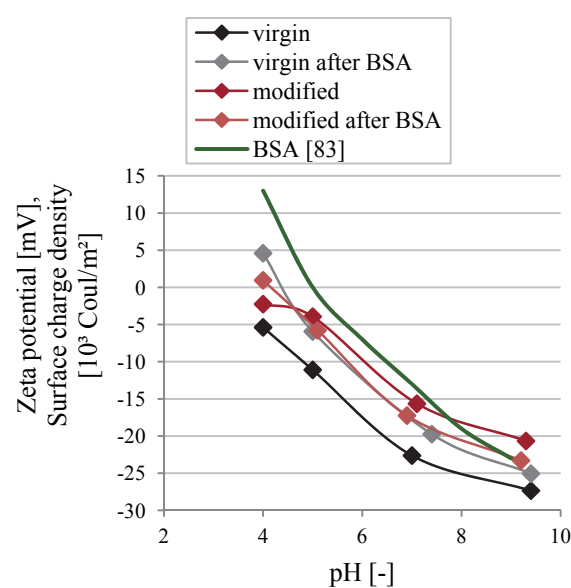


Figure 5.11 ZP of virgin and modified membranes PES 5 (9 J/cm²) before and after static adsorption with 10 g/L BSA at pH 4.8.

The hydrogel layer reduced the membrane surface charge. The stronger the membrane functionalisation, the less charged the membrane surface appeared. Similar finding have been already reported by Susanto et al. [140]. When membranes were modified with crosslinkers, the ZP did not change immensely, i.e., the effect of crosslinking on the membrane surface charge was not significant.

ZP of virgin and modified membranes was measured before and after static adsorption experiments with 10 g/L BSA solution at pH = 4.8 (IEP). The obtained results are shown in Figure 5.11 in comparison with the protein surface charge density (data were adapted from [83]). As it can be seen, after the contact with BSA the membrane ZP changed indicating the charge profile of the protein. Similar results have been found in previous studies [49]. Moreover, this shift of the ZP profile was more significant in case of virgin membranes.

5.2.5 MEMBRANE ROUGHNESS

Analysis of the membrane surface was performed by AFM. Samples of virgin and modified membranes were measured in dry and wet state. Figure 5.12(a) and Figure 5.12(b) present virgin and functionalised surfaces of PES 5 analysed in dry state. Areas of sticky material appeared on the functionalised surface (b). During drying, the PEGMA hydrogel collapsed and built areas with increased PEGMA concentration (soft segments appeared in white). For this reason, further tests in wet state were performed. Results from the analysis of virgin and modified PES 50 are shown in Figure 5.12(c) and Figure 5.12(d).

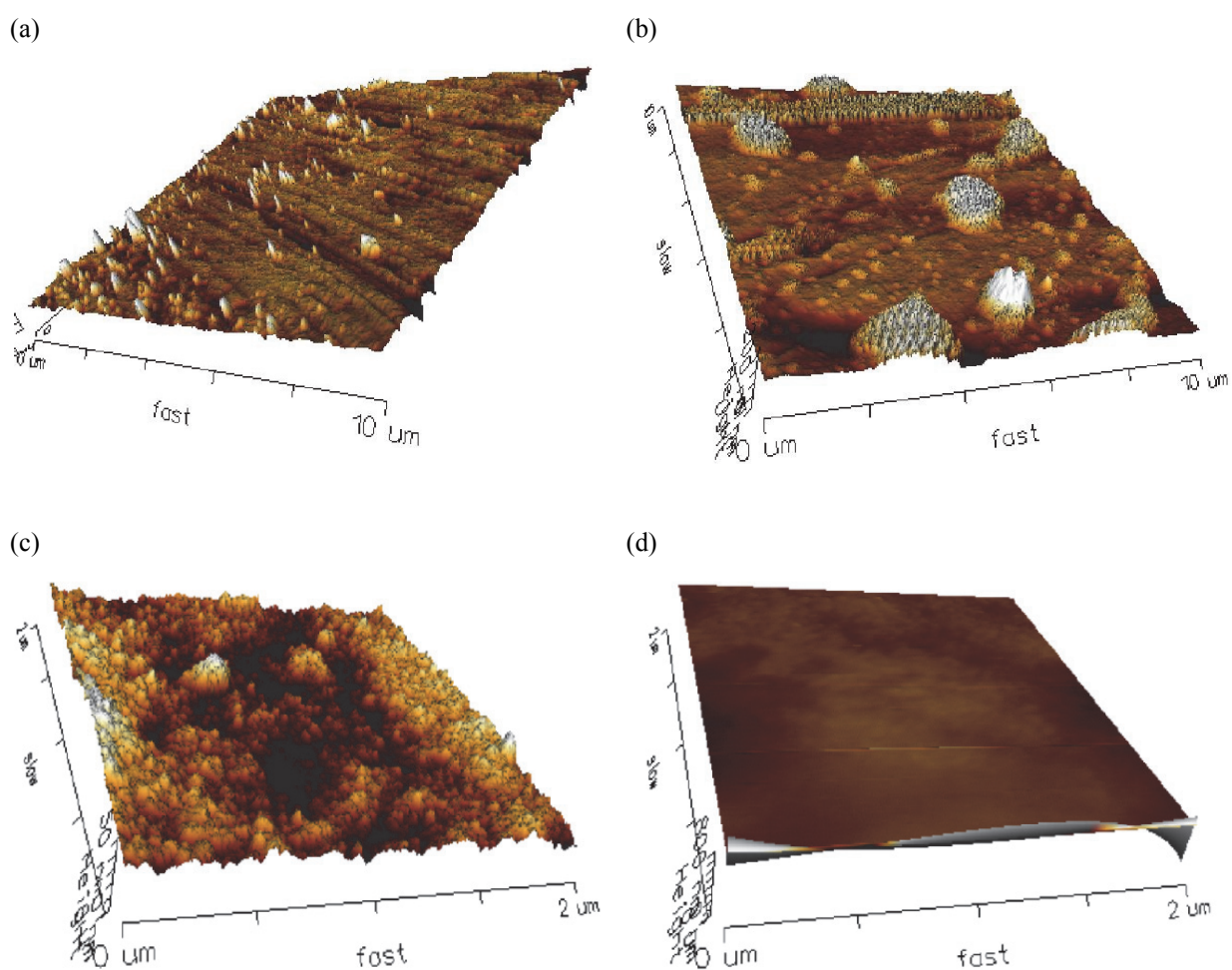


Figure 5.12 AFM 3D visualisation of membranes; (a) PES 5 virgin, dry state; (b) PES 5 modified, dry state; (c) PES 50 virgin, wet state; (d) PES 50 modified, wet state.

Virgin membranes appeared in the typical shape for PES membranes already reported [81,159], whereas functionalised surfaces seemed very smooth and uniform due to the swollen hydrogel. These statements were confirmed by the measured surface roughness values presented in Table 5.3.

Table 5.3 Roughness of virgin and modified membranes measured in wet and dry state

Membrane	Measurement	Roughness [nm]	
		virgin	modified
PES 5	dry state	4	9
PES 50	wet state	14	2.5

In dry state, soft segments increased the membrane roughness from 4 nm to 9 nm. In wet state, it was observed that the functionalised surface became much smoother, i.e., the roughness decreased from 14 nm to 2.5 nm. It should be noted, that PES 50 was measured in wet state but PES 5 was analysed in dry state. This could be the reason for the differences in roughness from both measurements of virgin membranes combined with swelling of PES in water. Images of the cross-section profiles are to find in Appendix A (Figure 7).

5.2.6 MEMBRANE MORPHOLOGY

5.2.6.1 Virgin membranes

Membrane surface and cross-section were analysed by SEM. Typical structures of finger and sponge cross-sections are shown in Figure 5.13.

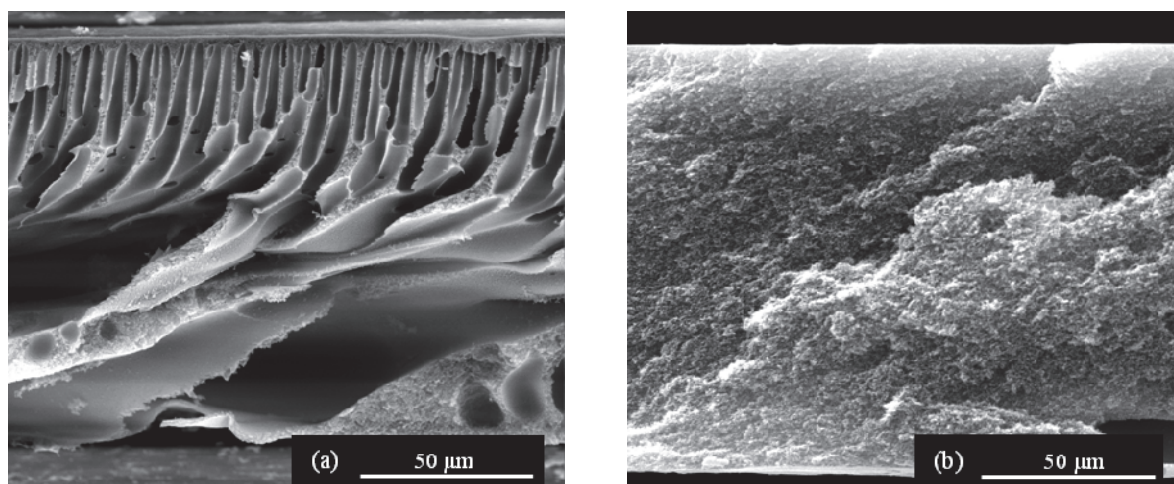


Figure 5.13 SEM cross-section images of selected membranes; (a) PES 50; (b) PES 100.

Membranes with small nominal MWCO (5 – 50 kDa) appeared with finger-like structures (Figure 5.13(a)), i.e., on the top of the membrane the selective (skin) layer was formed, followed by very porous structure with macrovoids acting as a mechanical support. In contrast, the cross-section structure of PES 100 and PES 300 was found to be uniform sponge (Figure 5.13(b)). Cross-section images of PES 5, PES 10 and PES 300 can be found in Appendix A (Figure 8).

Due to instrumental limitations, the visualisation of the pore openings was only possible for membranes with nominal MWCO above 30 kDa. The analysed surfaces are presented in Figure 5.14. With increasing nominal MWCO larger pores were observed. Interesting results were found for PES 30 without PVP (Figure 5.14(b)). Its pores seemed to be much larger than the pores of PES 30 prepared with PVP.

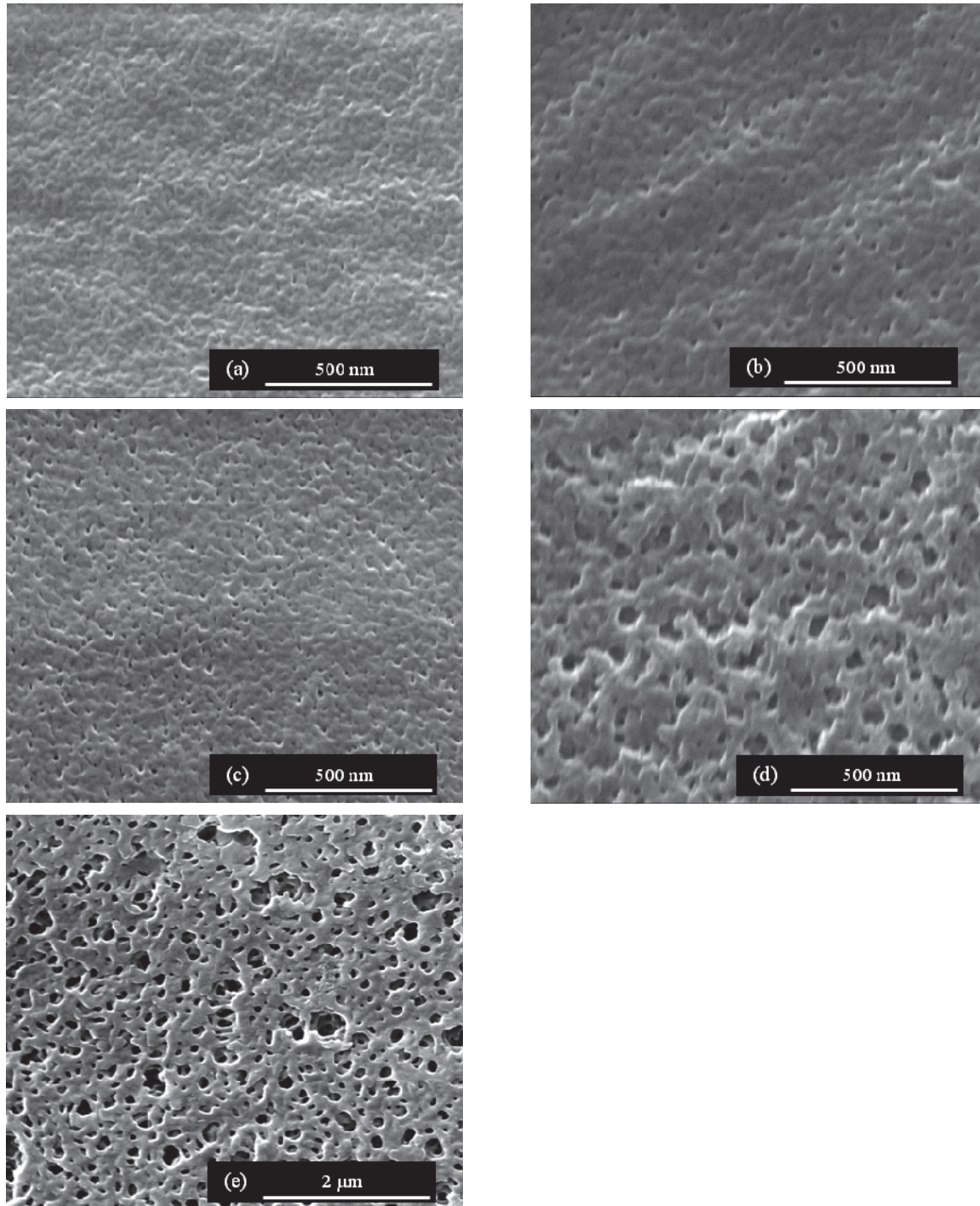


Figure 5.14 SEM surface images of the used virgin membranes; (a) PES 30; (b) PES 30 without PVP; (c) PES 50; (d) PES 100; (e) PES 300.

5.2.6.2 Functionalised membranes

SEM analysis of outer surface and cross-section of modified membranes was performed as supporting characterisation in order to visualise changes caused by the applied UV irradiation and the grafted hydrogel layer. In the next sections, the more important results obtained with modified PES 50 and PES 100 will be presented.

5.2.6.2.1 PES 50

SEM images of the membrane outer surface are presented in Figure 5.15.

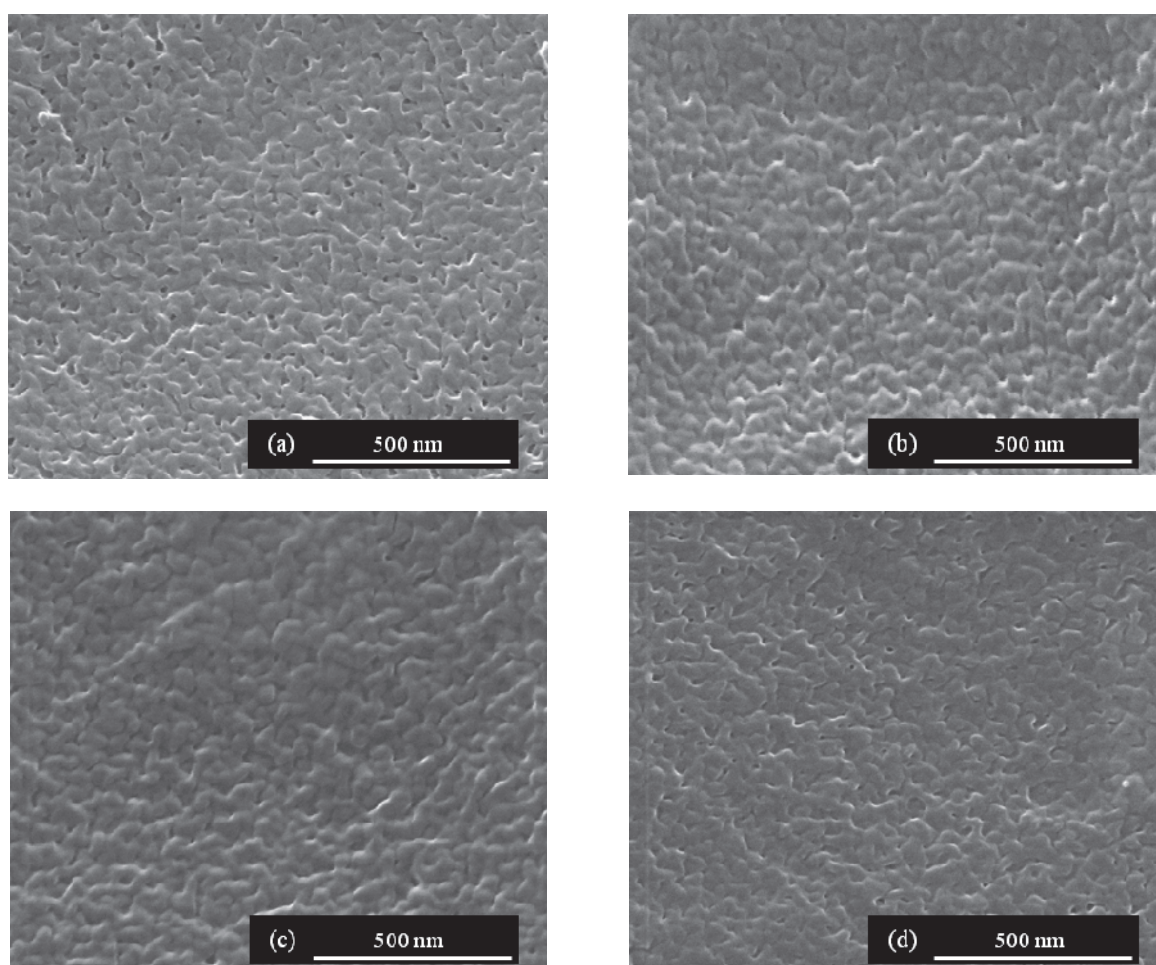


Figure 5.15 SEM surface images of PES 50 UV irradiated with 11 J/cm^2 at 5 mW/cm^2 ; (a) irradiated in water; (b) modified with 40/0; (c) modified with 40/4; (d) modified with 40/6.65.

Figure 5.15(a) shows membrane irradiated in water. Here no difference could be visualised from the outer surface of virgin PES 50 (Figure 5.14(c)). Functionalised membrane samples at 11 J/cm^2 (presented in Figure 5.15(b-d)) seemed to have different surface properties. Overall, the surfaces of the modified membranes appeared smoother than the unmodified. Both pore narrowing and pore blocking because of the surface modification were observed. In Figure 5.15(b) (functionalisation with PEGMA

alone), the grafted polymer seemed to cover the pore openings almost completely. While Figure 5.15(c) was similar to Figure 5.15(b), the pores could be seen very clearly in Figure 5.15(d).

It should be noticed that the carbon layer required for SEM analysis could also cover pores or influence the images otherwise, so that these microscopic analyses gave only some qualitative information about the surface topography and morphology. Further, it should be kept in mind that all SEM images were obtained in dry state; in water, the hydrogel of the modified membranes would be in a swollen state and its structure would deviate from the visualised structure on the images.

5.2.6.2.2 PES 100

SEM images of the outer surface of functionalised PES 100 with varied modifier compositions showed similar structures to each other (Appendix A, Figure 9). The impact of the membrane modification as well as the effect of the crosslinking type on the outer surface structure could not be observed by this analysis. Detailed study of the selective layer structure of PES 100 using SEM cross-section images was performed. The images of virgin, irradiated in water and modified under varied conditions membranes are presented in Figure 5.16.

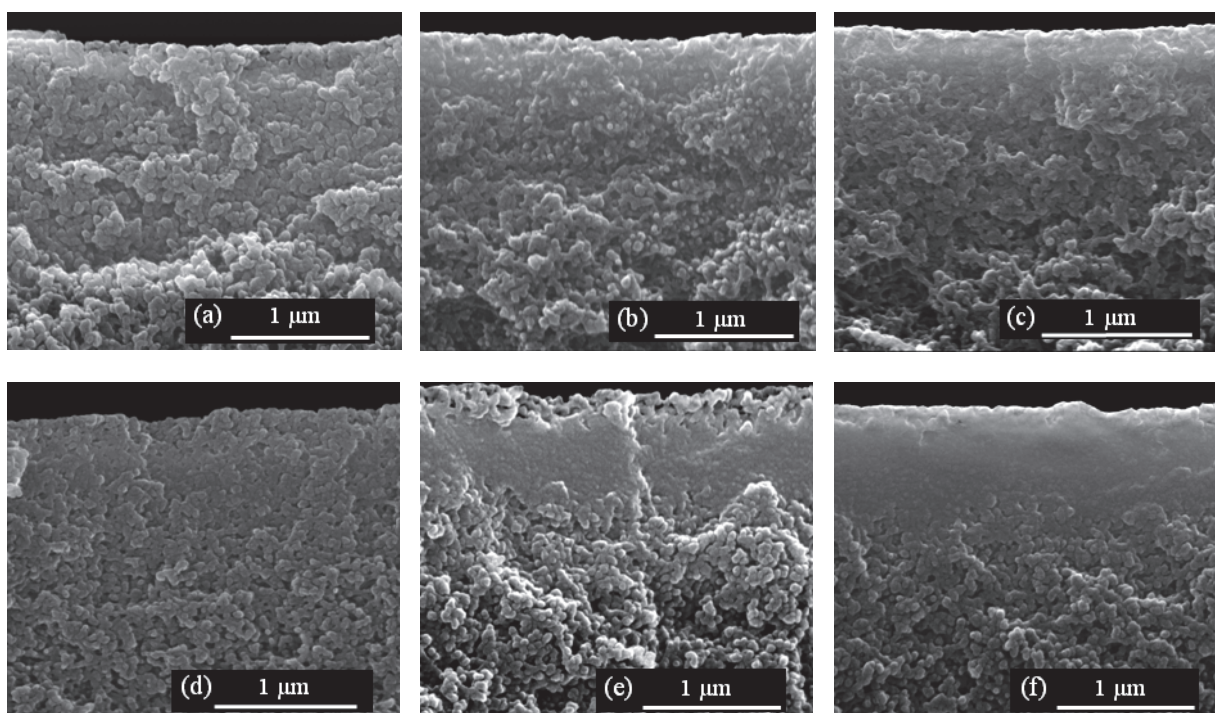


Figure 5.16 SEM cross-section images of the skin layer of PES 100 UV irradiated with 11 J/cm²; (a) virgin; (b) irradiated in water at 5 mW/cm²; (c) irradiated in water at 60 mW/cm²; (d) modified with 40/0 at 5 mW/cm²; (e) modified with 40/1 at 5 mW/cm²; (f) modified with 40/4 at 5 mW/cm².

Compact selective layer with thickness of about 2 µm was present in the image of virgin membrane (Figure 5.16(a)). Irradiation in water at 5 mW/cm² changed the properties of the layer, as it could be

seen in Figure 5.16(b). Irradiation in water with same energy but at 60 mW/cm^2 led to more compact layer in the first $1 \mu\text{m}$ of the membrane cross-section (Figure 5.16(c)). The membrane structure changed significantly after modification with PEGMA (Figure 5.16(d)). Looking at Figure 5.16(e) showing the cross-section of modified membrane with PEGMA/MBAA 40/1, dense layer in the first $1 \mu\text{m}$ was observed. Performing the same modification with increased amount of MBAA (40/4) led to the formation of very compact selective layer, shown in Figure 5.16(f).

5.2.7 MEMBRANE MODIFICATION DEPTH

By using the EDX-SEM method, information about the membrane modification depth could be acquired. The Cu/S atomic ratio in the cross-section of modified membranes with PAA was measured. The obtained results for modification of several membrane types with 11 J/cm^2 are summarised in Figure 5.17. It was found, that Cu was immobilised mostly in the first $5 \mu\text{m}$ of the membrane cross-section and the Cu content decreased very fast in the deeper membrane cross-section regions. Similar results have been published in [151].

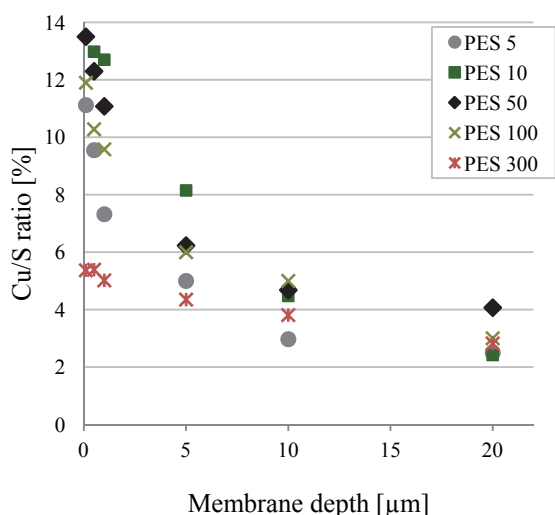


Figure 5.17 Cu/S ratio in the cross-section of modified membranes with 11 J/cm^2 .

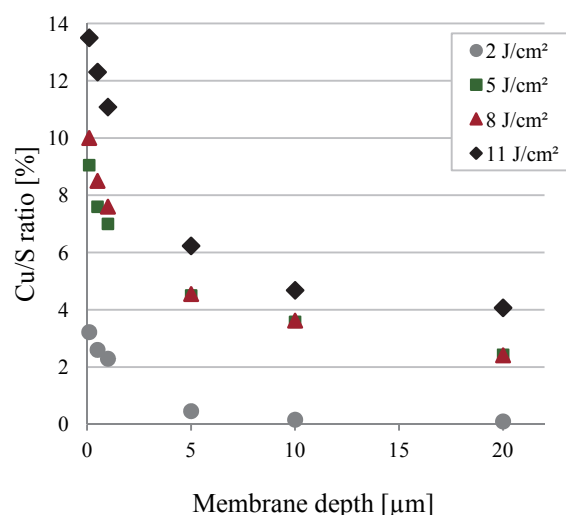


Figure 5.18 Cu/S ratio in the cross-section of PES 50 modified at varied UV irradiation dose.

Furthermore, the amount of Cu was measured depending on the functionalisation degree. The effect of the UV irradiation dose on the amount of Cu in the cross-section of PES 50 is shown in Figure 5.18. The amount of Cu increased when increasing the UV irradiation dose, which corresponded to more PAA grafting with further irradiation.

5.2.8 ESTIMATION OF THE AVERAGE RADICAL DENSITY

The apparent average distance between two radicals produced by the UV irradiation was measured for selected membranes and films (films with varied thickness were tested) using DPPH. The collected results for various samples which were irradiated with 5 J/cm^2 are presented in Figure 5.19. As it can be seen from the results for irradiated membranes, PES 10 exhibited the highest distance between radicals, corresponding to the lowest DG value measured for this membrane (cf. Table 5.1). Moreover, films with thickness of $100 \mu\text{m}$ (comparable to the membranes thickness, see above) showed higher distance between radicals than membrane samples. The distance between radicals for thicker films, e.g., thickness of $500 \mu\text{m}$, was less compared to films with thickness of $100 \mu\text{m}$.

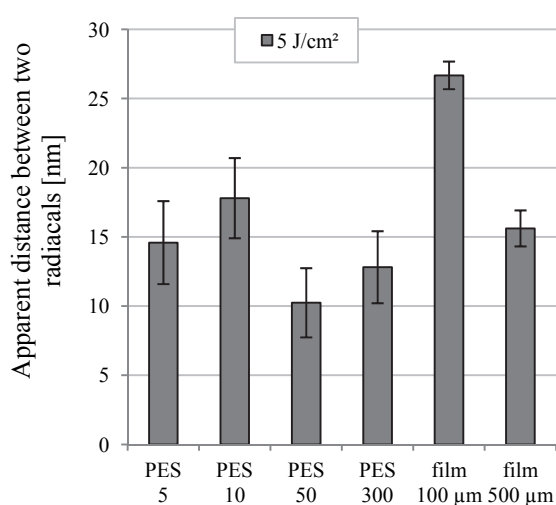


Figure 5.19 Apparent distance between two radicals for selected membranes and films irradiated with 5 J/cm^2 .

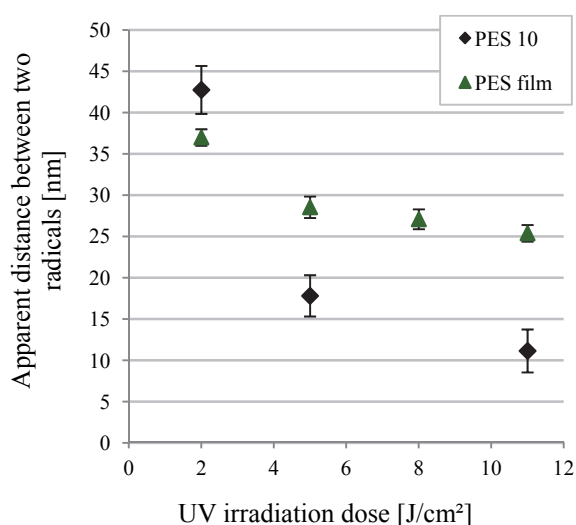


Figure 5.20 Apparent average distance between two radicals for PES 10 and films under variation of the UV irradiation dose.

Furthermore, the effect of the UV irradiation dose for PES 10 and $100 \mu\text{m}$ thick films was also studied. The obtained data are shown in Figure 5.20. It was observed that the apparent distance between two radicals decreased with increasing UV irradiation dose. This effect was more pronounced for membranes, leading to less distance between radicals for membranes than for films after sufficient UV irradiation doses.

5.3 MEMBRANE PERFORMANCE

5.3.1 WATER PERMEABILITY

Membrane performance was first studied by measuring the membrane water permeability before and after modification. Prior to this, the effect of compaction on the membrane water flux was studied. Water permeabilities measured before and after compaction are summarised in Table 5.4.

Table 5.4 Water permeability of virgin membranes and relative flux after modification with 11 J/cm²

Membrane		PES 5	PES 10	PES 30		PES 50			PES 100	PES 300
				with PVP	w/o PVP	PEGMA 200	PEGMA 400	water		
Permeability [L/hm ² bar] virgin membranes	non-compacted	16	230	580	400	1000			930	1600
	compacted	8	100	200	n.d.	500			760	n.d.
Relative flux [-] PEGMA 400 11 J/cm ²		0.03	0.04	0.07	0.33	0.15	0.15	0.83	0.21	0.45

n.d.: not determined

Permeability increased with higher nominal MWCO. During measurements with non-compacted membranes, PES 100 showed lower permeability than PES 50. In contrast, the compaction had less effect on the water flux of PES 100 so that its final permeability was higher than that of PES 50. Another interesting point was the contribution of PVP to the water flux. Comparing the permeabilities of PES 30 with and without PVP, the membrane prepared without PVP showed less flux.

The effect of membrane functionalisation on water flux was also examined. In case of modified membranes, no flux decrease due to compaction was measured. The relative water flux of PES 10 modified with PEGMA 400 depending on the UV dose is shown in Figure 5.21. The membrane functionalisation decreased the water flux strongly. The values reached plateau at relative high UV doses. The obtained relative fluxes for other membrane types can be found in Appendix A (Figure 6).

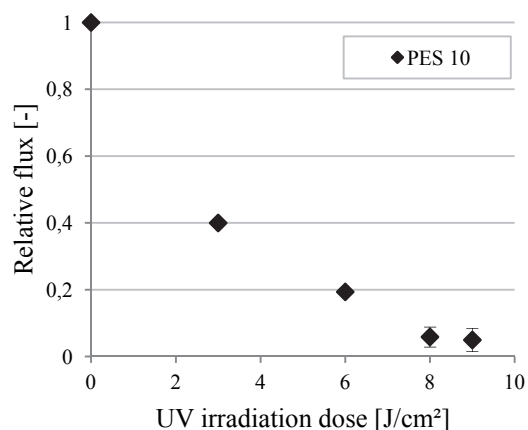


Figure 5.21 Flux ratio at varied UV irradiation dose. Example: PES 10 modified with 40/0.

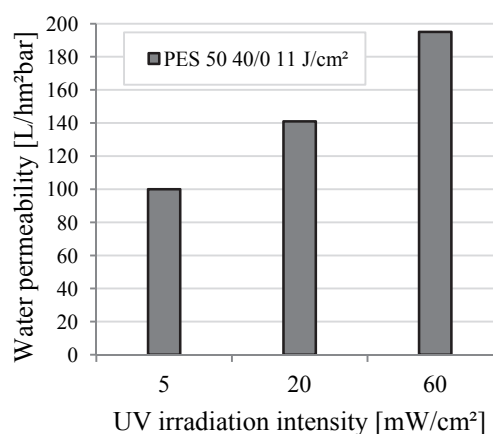


Figure 5.22 Water permeability of PES 50 40/0, 11 J/cm² at varied UV intensity.

The relative flux of membranes after functionalisation with 11 J/cm² is presented in Table 5.4. Membrane functionalisation decreased water permeability depending on the membrane pore size. The larger the pores, the higher the relative water flux. PES 30 prepared without PVP had much higher relative flux after modification than the corresponding membrane with PVP.

Furthermore, the effect of UV irradiation in water was studied. The permeability decreased after UV irradiation dose of 11 J/cm², as it can be seen from the results for PES 50 shown in Table 5.4. Similar effect has been found from comprehensive study of PES 50 from Microdyn-Nadir, Germany in [140] but above 20 J/cm².

Water permeability after modification with same UV irradiation dose at varied UV intensity was also measured (results are presented in Figure 5.22). It was found that irradiation at higher UV intensity led to increased membrane water permeability [160].

The water permeability of modified membranes with crosslinkers was further studied for PES 10, PES 50, PES 100 and PES 300. The results are presented in the following sections.

5.3.1.1 PES 10

PES 10 membranes were UV irradiated with 5 J/cm² and 11 J/cm². Modifications were performed with PEGMA 400 and crosslinkers MBAA and PETAE at their maximal concentrations. The obtained results are presented in Figure 5.23(a) for the crosslinking with MBAA and Figure 5.23(b) for PETAE.

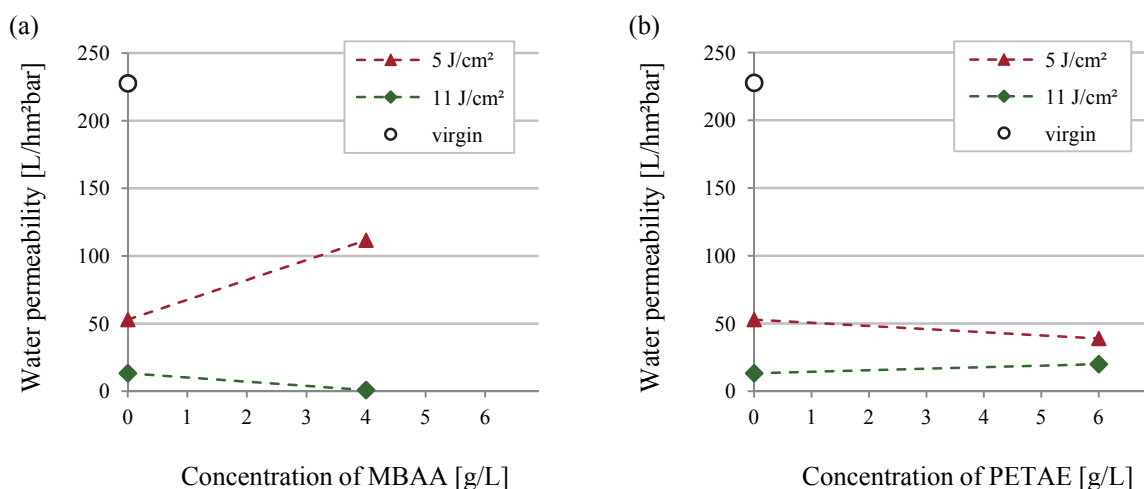


Figure 5.23 Water permeability of PES 10 as function of the crosslinker amount at varied UV irradiation dose; (a) PEGMA 400/MBAA; (b) PEGMA 400/PETAE.

The modified samples with MBAA at 5 J/cm² showed increased flux compared to samples with same irradiation dose without crosslinking. At higher irradiation level (11 J/cm²), crosslinking with MBAA decreased the membrane water flux. Modification of PES 10 with PETAE did not have significant influence on water permeability.

5.3.1.2 PES 50

Surface functionalisation of PES 50 was studied comprehensively under variation of the modifier composition and UV irradiation dose. Modifications with PEGMA 200/MBAA, PEGMA 400/MBAA and PEGMA 400/PETAE were performed. Figure 5.24 shows the water permeability results from modifications with MBAA.

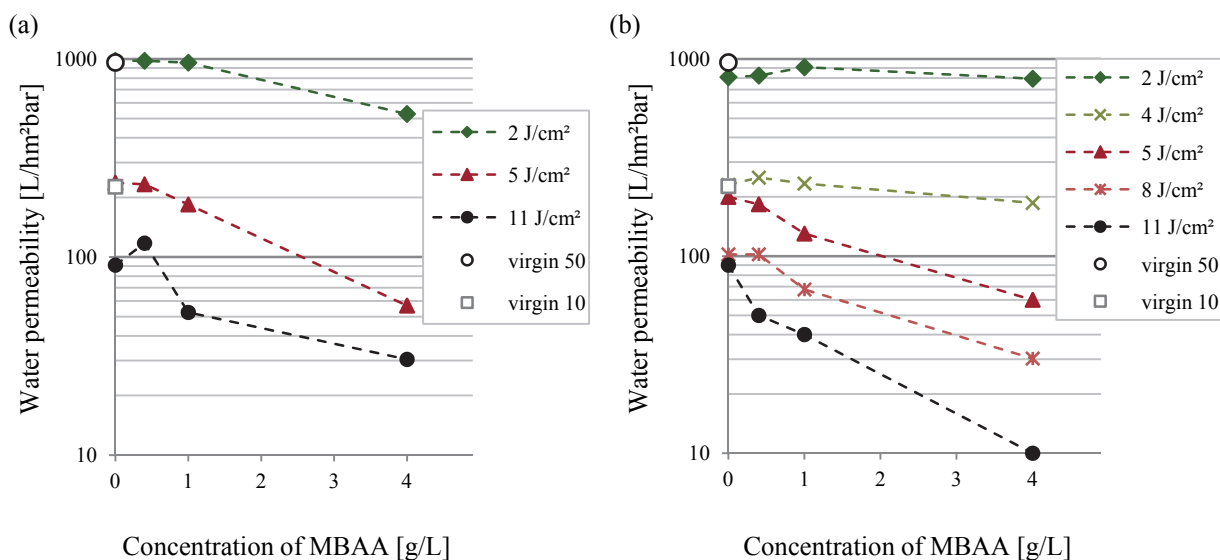


Figure 5.24 Water permeability of PES 50 as function of the crosslinker amount at varied UV irradiation dose; (a) PEGMA 200/MBAA; (b) PEGMA 400/MBAA.

The results are presented in comparison with values of the virgin membranes PES 50 and PES 10 in order to evaluate the resulting changes due to the grafted hydrogel layer. In terms of water flux, the membranes modified with PEGMA 200 (Figure 5.24(a)) and PEGMA 400 (Figure 5.24(b)) performed similar. In the early stages of the modification (2 J/cm^2), slight change in water permeability was observed. After increasing the modification level, there was a strong decrease in water permeability. Furthermore, when increasing the concentration of the crosslinker MBAA in the monomer mixture at same modification level, the water flux decreased significantly.

Looking at the results from the modification with PETAE presented in Figure 5.25, the water permeability decreased consistently when the UV irradiation dose was increased. However, a very different behaviour of PETAE as crosslinking agent was observed. In general, the application of PETAE in the modification mixture led to increased water flux. The effect of varying the PETAE concentration was different depending on the UV irradiation dose. In most cases, modifications with low PETAE amount resulted in decreased water permeability compared to modifications only with PEGMA. The water permeability increased further when more PETAE was used.

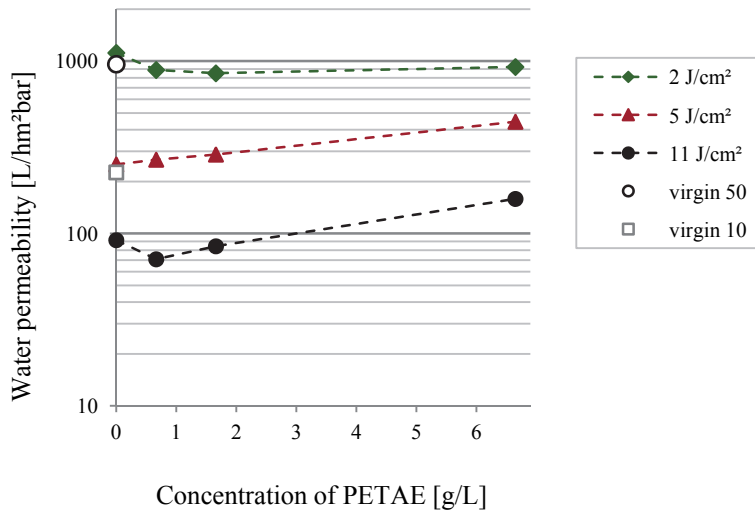


Figure 5.25 Water permeability of PES 50 modified with PEGMA 400 as function of the PETAE amount at varied UV irradiation dose.

5.3.1.3 PES 100

PES 100 was modified with PEGMA 400 and the effect of both crosslinkers was studied. The obtained results are summarised in Figure 5.26.

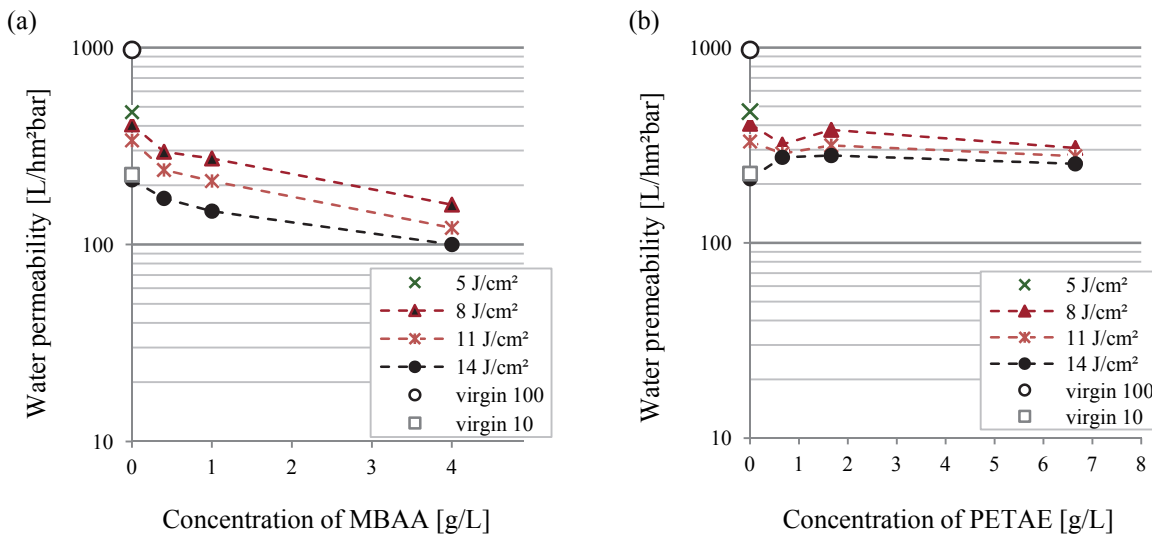


Figure 5.26 Water permeability of PES 100 as function of the crosslinker amount at varied UV irradiation dose; (a) PEGMA 400/MBAA; (b) PEGMA 400/PETAE.

From Figure 5.26(a) can be taken that MBAA decreased the water flux of PES 100. Similar trends to PES 50 were found in the results from the modification with PETAE (Figure 5.26(b)). Certainly, the contribution of PETAE to the water flux change of this membrane type was less pronounced.

5.3.1.4 PES 300

The water permeabilities of PES 300 modified with PEGMA 400/MBAA (Figure 5.27(a)) and PEGMA 400/PETAE (Figure 5.27(b)) will be explained.

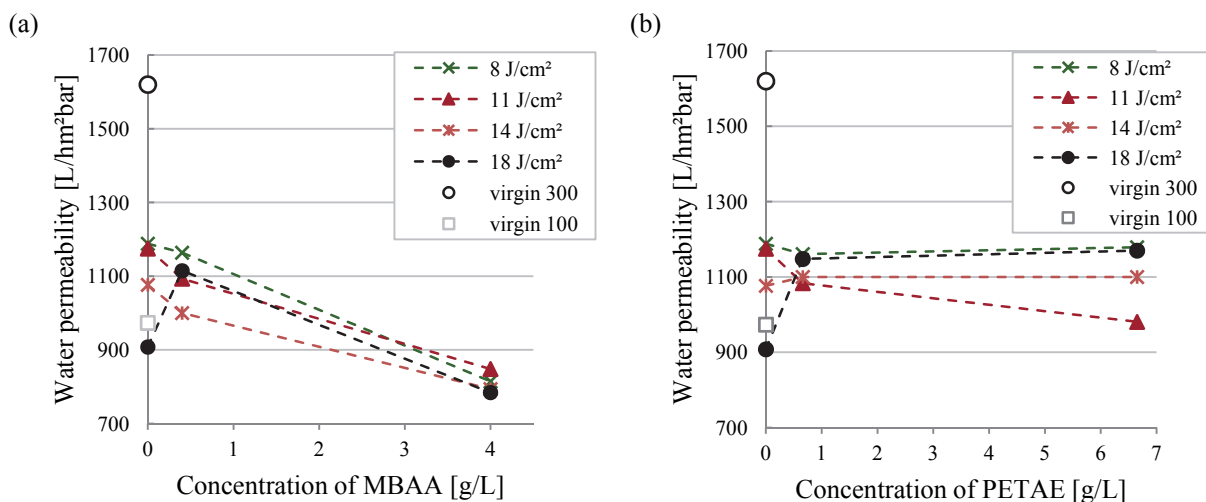


Figure 5.27 Water permeability of PES 300 as function of the crosslinker amount at varied UV irradiation dose; (a) PEGMA 400/MBAA; (b) PEGMA 400/PETAE.

The obtained results were similar to the results from the modification of PES 100 but the crosslinking agents had less pronounced effects on the water flux. Water permeability of membranes modified with MBAA decreased slightly with increasing MBAA amount (Figure 5.27(a)). Crosslinking with PETAE (Figure 5.27(b)) did not lead to significant water flux changes.

5.3.2 REJECTION CURVES

Dextran and PEG mixtures with wide MWD were filtered through virgin and modified membranes. The rejection properties were evaluated by means of rejection curves and cut-off. At least two membrane samples were tested in order to eliminate any possible analysis or membrane instabilities. The reproducibility was quite high, as it can be seen in Figure 10 in Appendix A. The impact of different factors on the membranes fouling and rejection behaviour was studied.

5.3.2.1 Virgin membranes

The rejection curve measurements were performed at 10 L/hm² initial membrane flux. The pressure which was applied in order to achieve the desired initial flux, together with the examined fouling resistance, cut-off values and calculated approximate apparent pore diameter (corresponding to the

hydrodynamic diameter of solutes rejected by 90 %), are summarised in Table 5.5 (upper part for virgin membranes).

Table 5.5 Summary of the parameters and characteristics during the measurement of rejection curves with dextran and PEG (initial flux: 10 L/hm²)

Membrane	Applied pressure [bar]	Fouling resistance [-]		Cut-off [kDa]		Pore diameter from cut-off [nm]		Nominal pore diameter [nm] [161]
		PEG	Dextran	PEG	Dextran	PEG [157]	Dextran [158]	
PES 5 virgin	0.63	0.31	0.63	1	7	2	3	7
PES 10 virgin	0.043	0.63	0.7	3	42	3	8	8.5
PES 30 virgin	0.017	0.72	0.80	7.5	90	4	12	11
PES 30 virgin w/o PVP	0.025	n.d.	0.65	n.d.	150	n.d.	16	
PES 50 virgin	0.01	0.64	0.78	11	95	5	12	15
PES 100 virgin	0.011	0.75	0.82	30	350	9	25	22
PES 300 virgin	0.006	0.78	0.73	100	900	17	43	40
PES 10 modified	1.1	0.99	0.89	0.8	4.4	1	2	
PES 30 modified	0.33	0.94	0.99	1.4	7	2	3	
PES 30 mod. w/o PVP	0.076	n.d.	0.99	n.d.	100	n.d.	13	
PES 50 modified	0.13	0.98	0.99	3	10	3	3	
PES 100 modified	0.05	0.99	1.00	80	120	15	14	
PES 300 modified	0.014	0.96	0.98	bt	bt	n.d.	n.d.	

n.d.: not determined

bt: breakthrough

In most cases, fouling resistance increased when nominal MWCO increased and dextran was filtered. Regarding the calculated cut-off data, higher values were obtained from filtrations with dextran solutions. Nevertheless, the resulting cut-off values from the filtration of both compounds deviated from the nominal values given by the producer. For better comparison with the producer data, apparent pore diameters were estimated using the obtained cut-off values, i.e., by applying Eq.(4.13) and Eq.(4.14), the hydrodynamic diameter of the solutes rejected by 90 % was calculated. The apparent pore diameters calculated from dextran data matched much better the nominal values from the producer.

The effect of PVP on the fouling tendency during filtration of dextrans was also studied. The observed data showed that PES 30 without PVP was fouled by dextran more strongly than PES 30 with PVP.

The corresponding rejection curves for all tested unmodified membranes from filtrations of both dextran and PEG mixtures are shown in Figure 5.28. The abbreviations A, B and C in the legend indicate the applied feed (cf. Table 4.5).

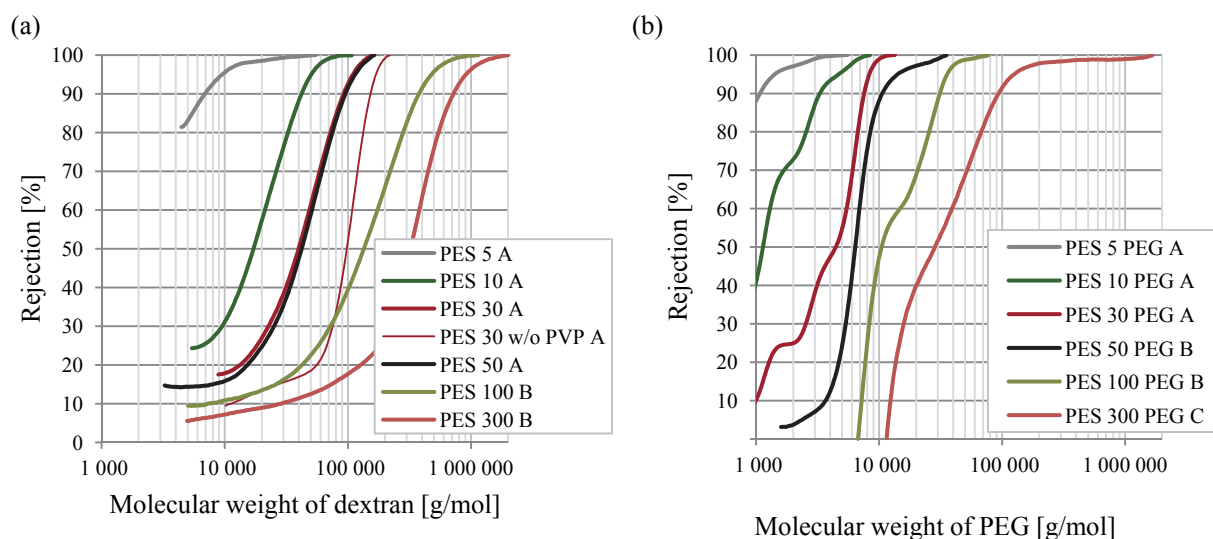


Figure 5.28 Rejection curves of all virgin membranes; (a) with dextran; (b) with PEG.

Moreover, the effect of the initial flux during filtration of PEG and dextran was studied. Fouling resistance and cut-off results from measurements with virgin PES 50 are presented in Table 5.6. It was found that increasing the initial flux led to lower fouling resistance and dramatic increase of the cut-off values for both test solutions. In particular, for filtrations of PEG, this effect was significant for initial fluxes beyond 100 L/hm².

Table 5.6 Characteristics of the rejection curves measurement with dextran and PEG of virgin PES 50 at varied operating pressure

Feed	Pressure [bar]	Initial flux [L/hm ²]	Fouling resistance [-]	Cut-off [kDa]
PEG	0.006	5	0.64	10
PEG	0.027	25	0.62	10
PEG	0.1	100	0.61	12
PEG	0.5	500	0.40	45
PEG	1	1000	0.35	80
Dextran	1*10 ⁻⁵	0.01	0.95	20
Dextran	0.01	10	0.78	100

Taking into account that only rejection results from membranes with fouling resistance higher than 0.7 should be considered as representative, according to [162], further membrane characterisations were performed by experiments with dextran solutions.

The rejection curve shape is important for estimation of the membrane selectivity. Taking a look at the rejection curves resulting from dextran filtration presented in Figure 5.29(a), it can be seen that steeper curve was obtained at lower initial flux. Similar behaviour was found also from the filtration of PEG (Figure 11 in Appendix A).

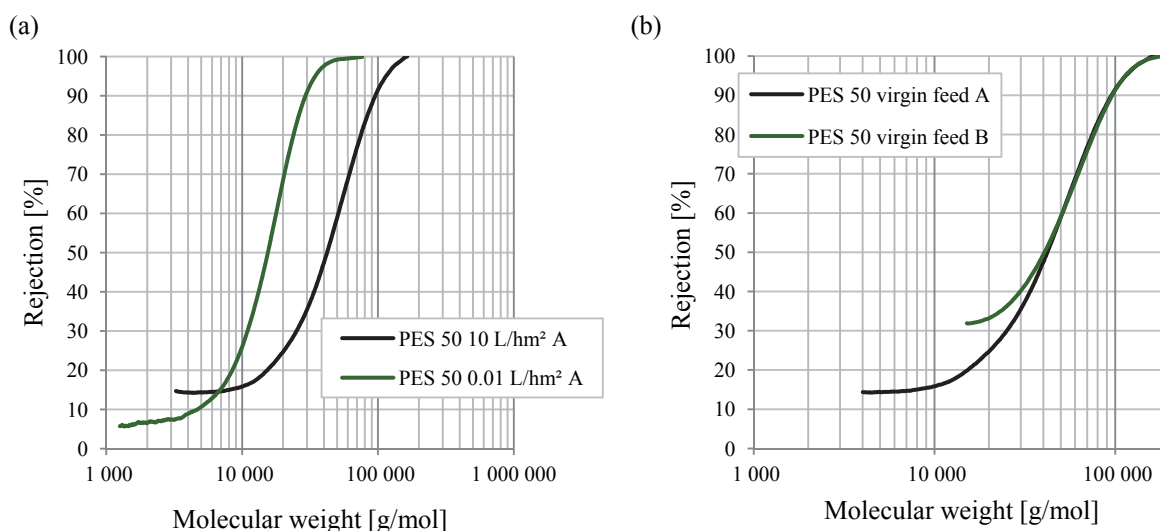


Figure 5.29 Rejection curves of virgin PES 50 with dextran; (a) at varied initial flux; (b) at varied feed.

The impact of the feed composition was also examined. The results from filtration of dextran feeds A and B through PES 50 are shown in Figure 5.29(b). As it can be seen, the feed mixture affected the shape of the rejection curves. Relatively small molecules were rather permeated when in mixtures with lower MW than in mixtures with high MW, whereas the rejection of bigger molecules remained similar (due to sterical hindrance [157]). Similar results were found for modified membranes (Figure 12(a) in Appendix A).

5.3.2.2 Modified membranes without crosslinkers

An overview of the obtained fouling resistance, cut-off values and approximated pore diameter (corresponding to the hydrodynamic diameter of solutes rejected by 90 %) for membranes with varied cut-off irradiated with 11 J/cm² are summarised in Table 5.5 (down panel).

To further understand the contribution of UV irradiation alone to the membrane performance, the effect of UV irradiation on membranes immersed in water was studied. Therefore, dextran was filtered through PES 50 irradiated in water with 11 J/cm². The resulting rejection curve is presented in Figure 5.30 in comparison with a rejection curve of untreated membrane. The slight change in rejection was considered as insignificant, as the examined shift was within the tolerance limit given by Figure 10 in Appendix A.

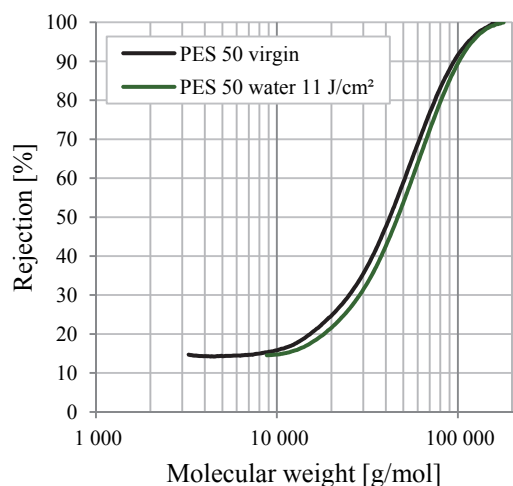


Figure 5.30 Rejection curves with dextran of PES 50. Effect of the irradiation in water.

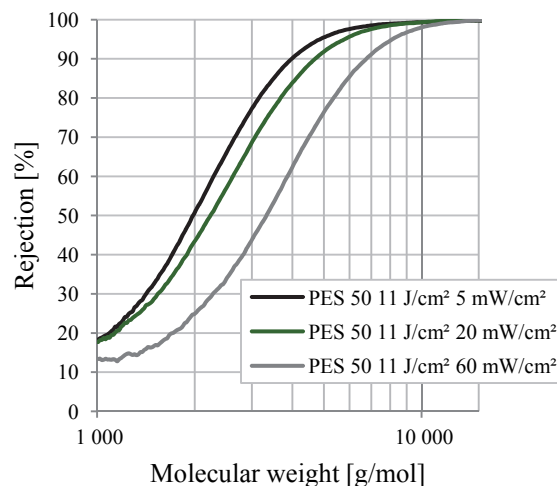


Figure 5.31 Rejection curves with dextran of PES 50 modified with 40/0 at varied UV intensity.

Furthermore, the effect of the UV intensity on the membrane rejection properties was investigated varying the UV intensity from 5 mW/cm² to 60 mW/cm² for PES 50 modified with 11 J/cm². The rejection curves with dextran are shown in Figure 5.31; PEG rejection curves can be found in Appendix A (Figure 12(b)). It was observed that membranes modified at higher UV intensity had lower rejection, i.e., the rejection curves shifted to higher MW.

In the following, rejection curves with dextran for modified membranes with varied nominal MWCO will be presented. Modified PES 5 could not be examined due to limitations by the dextran mixture – the smallest available dextran fraction (Dextran 4) was completely rejected by the membrane. The obtained results for PES 10 at varied UV irradiation dose are presented in Figure 5.32.

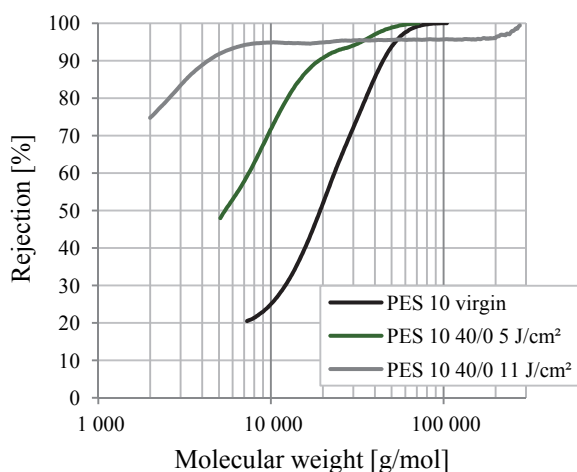


Figure 5.32 Rejection curves of PES 10 modified with varied UV irradiation dose.

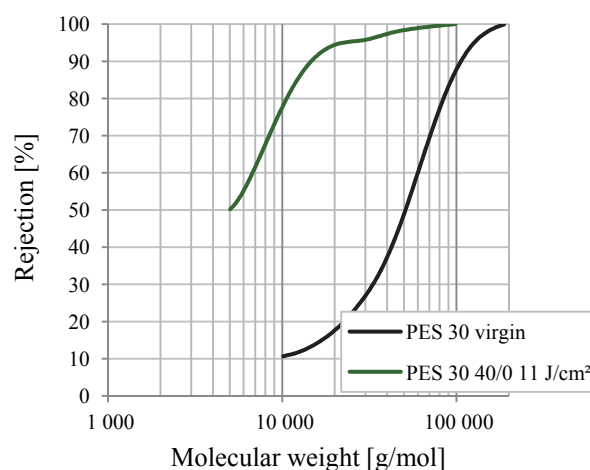


Figure 5.33 Rejection curve of modified PES 30.

It is clearly seen that modification at 5 J/cm² shifted the rejection curve to smaller MW. The curve for higher modification (11 J/cm²) shifted further to smaller MW but changed its shape, i.e., it ended with long tailing in the MW region beyond the curve of virgin membrane.

Typical shifting of the rejection curve due to the performed membrane surface modification was observed for modified PES 30 with PVP. The rejection curve of the modified membrane in Figure 5.33 was shifted to smaller MW and ended with slight tailing above 95 % rejection. Same modification applied to PES 30 without PVP led to smaller shift of the rejection curve (Figure 5.34).

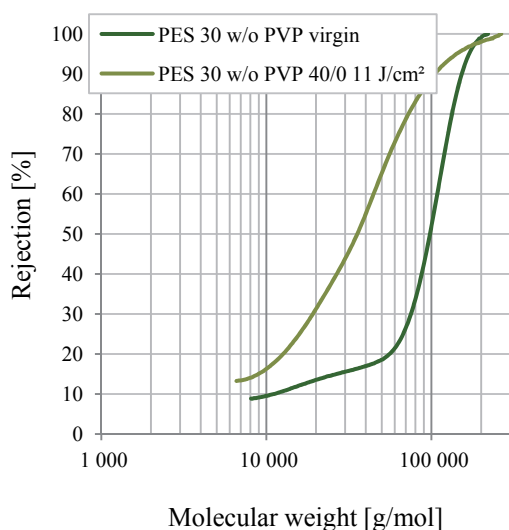


Figure 5.34 Rejection curve of modified PES 30 without PVP.

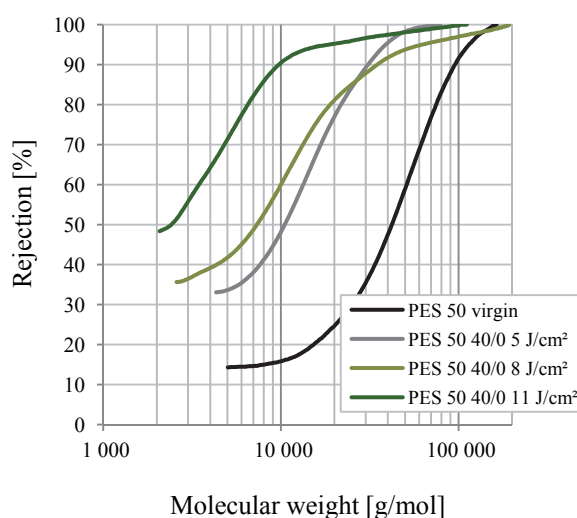


Figure 5.35 Rejection curves of PES 50 modified with varied UV irradiation dose.

Interesting results were obtained from the rejection curves of modified PES 50 at varied UV irradiation dose. In Figure 5.35, the rejection curve of membrane modified with 8 J/cm² was less steep than the curve of membrane modified with 5 J/cm² and crossed also the rejection curve obtained from virgin PES 50. Further modification with 11 J/cm² shifted the curve to lower MW but the shape remained similar to that of modified membrane with 8 J/cm².

Typical rejection curves were obtained for modified PES 100 (Figure 5.36). It was found that further increasing of the UV irradiation from 11 J/cm² to 14 J/cm² did not further change the rejection properties significantly.

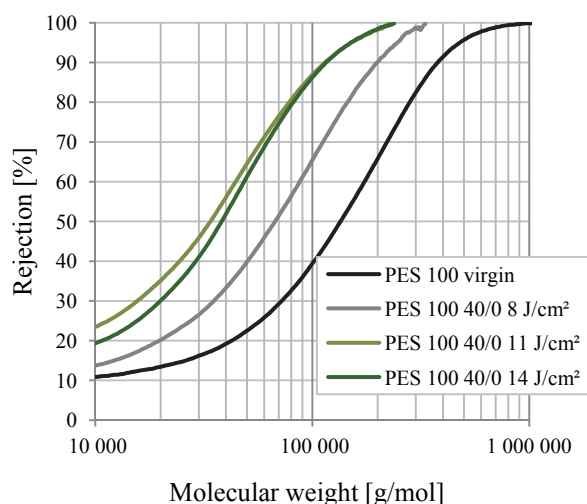


Figure 5.36 Rejection curves of PES 100 modified with varied UV irradiation dose.

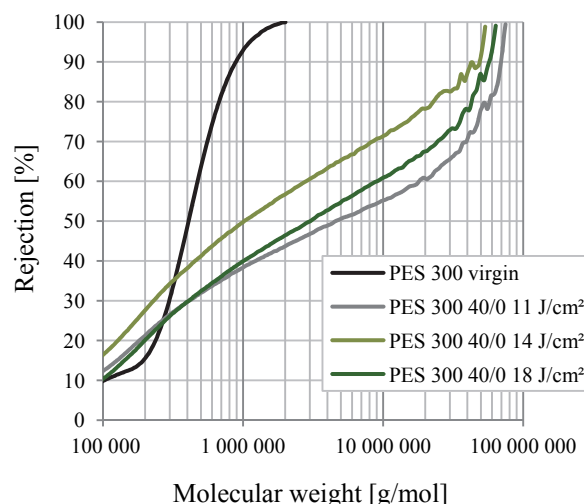


Figure 5.37 Rejection curves of PES 300 modified with varied UV irradiation dose.

In Figure 5.37, the rejection curves of virgin and modified PES 300 are presented. Surprisingly, the rejection curves became less steep and shifted to high MW compared to the result for virgin membrane, indicating breakthrough of also the largest dextrans.

5.3.2.3 Modified membranes with crosslinkers

5.3.2.3.1 PES 10

Modifications of PES 10 with maximum amount of crosslinker were performed with 5 J/cm² and 11 J/cm² UV doses. Since no dextran compound was found in the permeates of modified membranes with 11 J/cm², only the results from modifications with 5 J/cm² are presented (Figure 5.38).

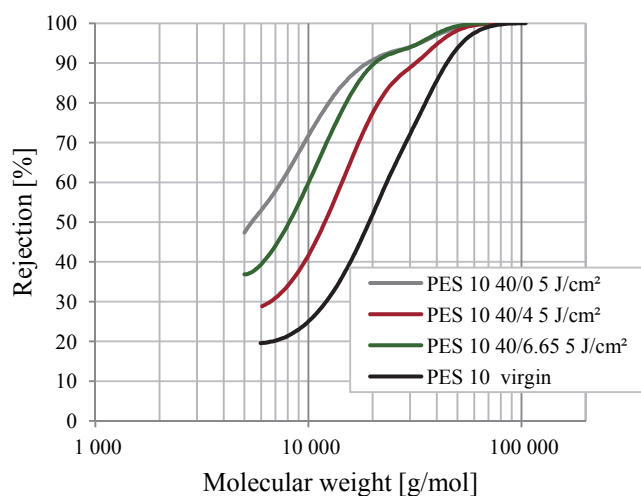


Figure 5.38 Rejection curves of PES 10 modified with different crosslinker type.

For modification with 5 J/cm^2 , the applied crosslinkers caused shift of the rejection curves to higher MW compared to modified membranes with PEGMA only. It should be noted, that the concentration of dextran in the permeate was very low, which could cause difficulties in the GPC analysis. From the aforementioned facts, it could be concluded that this analysis did not yield more detailed information about the hydrogel properties of modified PES 10.

5.3.2.3.2 PES 50

PES 50 was modified with PEGMA 400/MBAA and PEGMA 400/PETAE varying the UV irradiation dose from 5 J/cm^2 to 11 J/cm^2 . The obtained rejection curves at maximum amount of crosslinker are shown in Figure 5.39(a) for crosslinking with MBAA and in Figure 5.39(b) for crosslinking with PETAE.

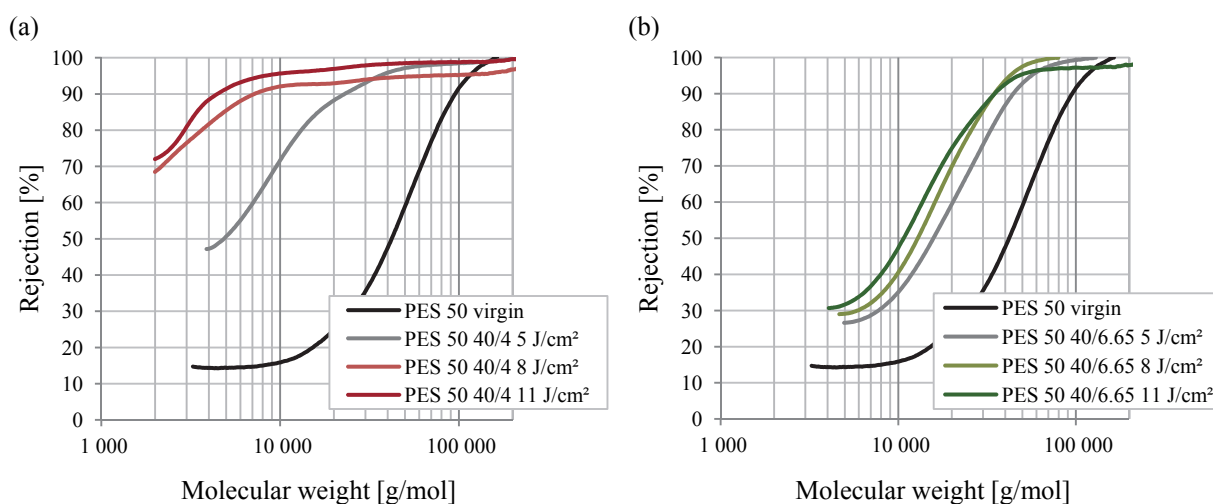


Figure 5.39 Rejection curves of modified PES 50 with varied irradiation dose; (a) PEGMA/MBAA; (b) PEGMA/PETAE.

The expected shift to smaller MW (similar to modifications with PEGMA) was observed in both cases. At closer look, the distance between the curves of membranes modified with 5 J/cm^2 and 8 J/cm^2 with MBAA was larger, i.e., MBAA contributed stronger to the rejection curve shifting than PETAE.

Furthermore, the amount of crosslinker was varied during functionalisation. The rejection curves of modified membranes with varied crosslinker amount (11 J/cm^2) are visualised in Figure 5.40.

Comparing the curves position towards the curve of PEGMA modified membrane, addition of MBAA shifted the curve to lower MW (Figure 5.40(a)). Increase of the MBAA amount resulted in further shift to lower MW.

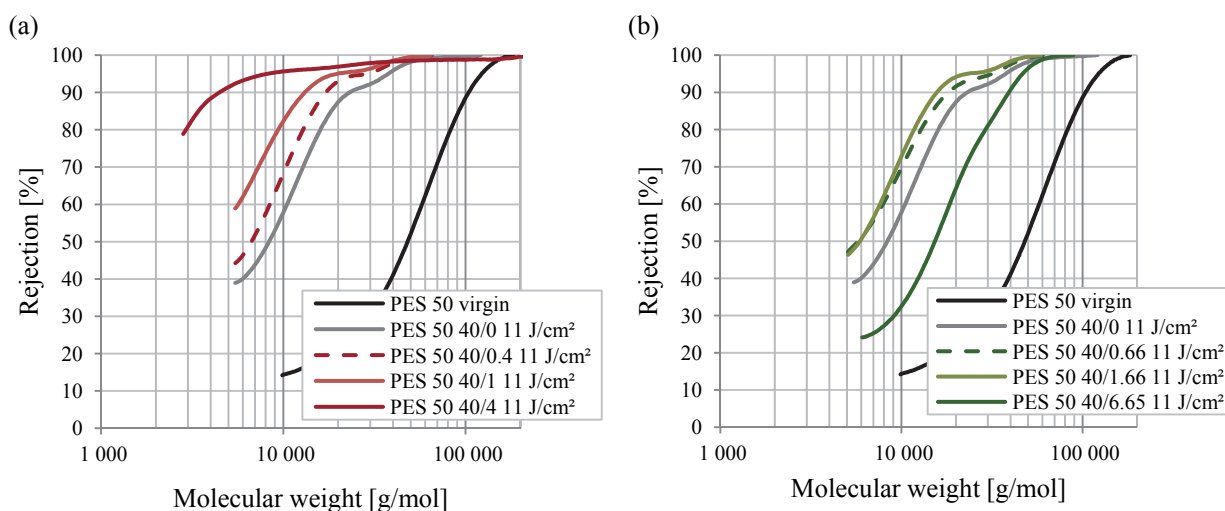


Figure 5.40 Rejection curves of modified PES 50 with variation of the crosslinker amount; (a) PEGMA/MBAA; (b) PEGMA/PETAE.

Different was the case of modifications with PETAE (curves shown in Figure 5.40(b)). Small amounts of PETAE shifted slightly the rejection curve to the left side. In contrast, an increase of the PETAE amount led to rejection curve in the region of higher MW.

Similar results were obtained when modified membranes with 5 J/cm² were tested (see Figure 13 in Appendix A).

5.3.2.3.3 PES 100

The modification of PES 100 with crosslinkers led to interesting results. Rejection curves at maximum amount of MBAA and PETAE were taken (Figure 5.41).

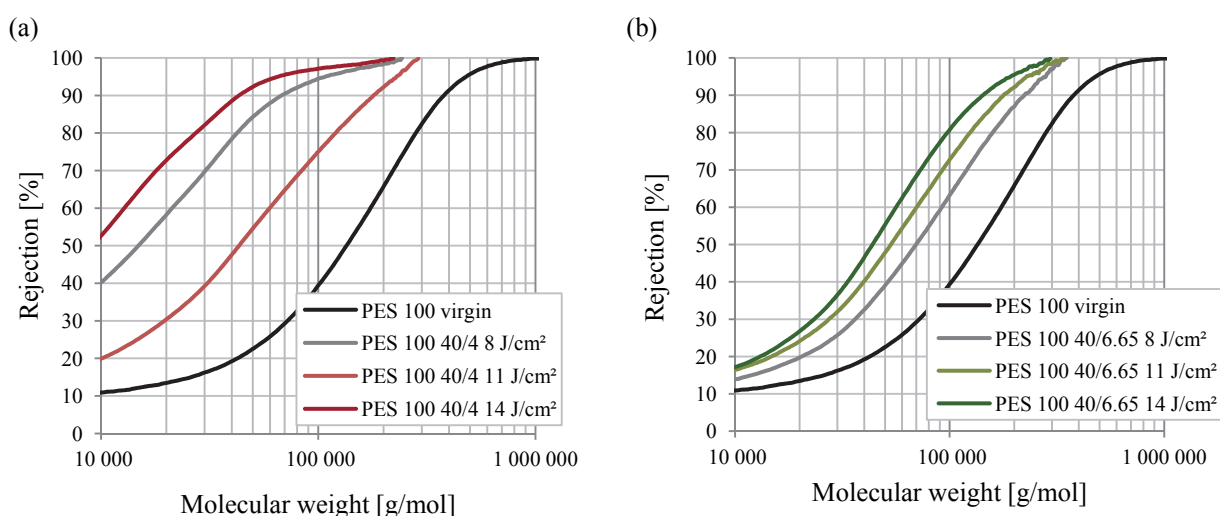


Figure 5.41 Rejection curves of modified PES 100 with varied irradiation dose; (a) PEGMA/MBAA; (b) PEGMA/PETAE.

Modification with MBAA (Figure 5.41(a)) with 8 J/cm² caused curve shift to smaller MW compared to virgin membranes; 11 J/cm² led to rejection curve in higher MW range; modification with 14 J/cm² shifted the curve again to smaller MW. It can be concluded that the rejection properties varied over the modification degree influenced by MBAA. For modified membranes with PETAE at varied functionalisation degree, as it can be seen from Figure 5.41(b), rejection curves were obtained which were consequently shifted to smaller MW with increasing UV irradiation dose.

Results obtained for membranes with varied crosslinker amount (14 J/cm²) are shown in Figure 5.42.

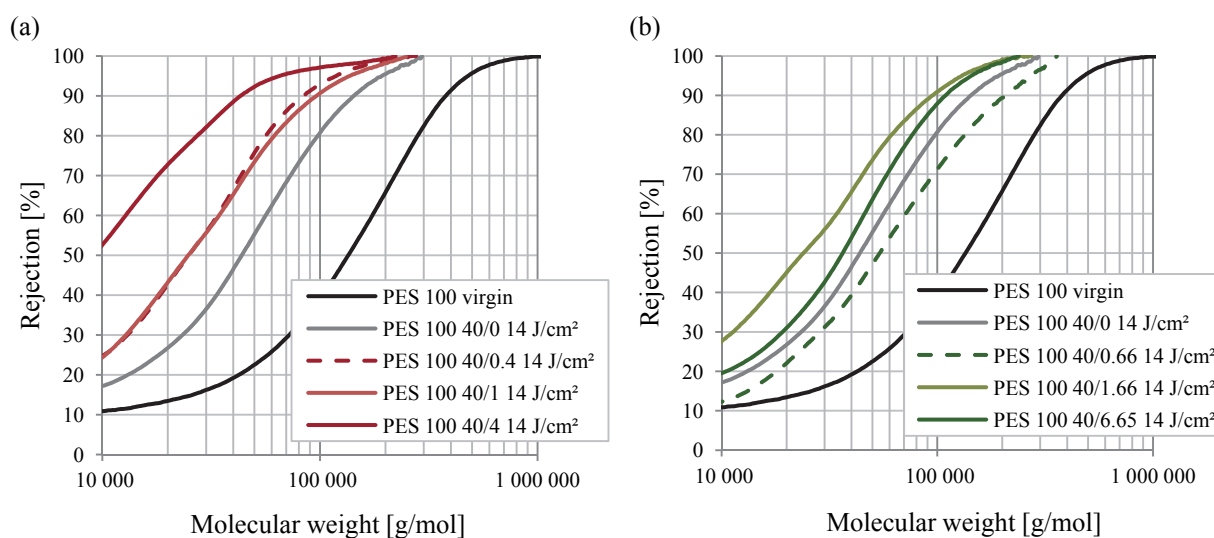


Figure 5.42 Rejection curves of modified PES 100 with variation of the crosslinker amount; (a) PEGMA/MBAA; (b) PEGMA/PETAE.

It was found that the increase of MBAA amount in the modifier solution induced rejection curves moving to smaller MW in relation to modification with PEGMA alone (Figure 5.42(a)). Figure 5.42(b) shows that small amounts of PETAE shifted the rejection curve to higher MW values, whereas further increase of PETAE amount led to rejection curve in range of smaller MW. Similar results were obtained from modifications with 8 J/cm². They can be found in Appendix A (Figure 14).

5.3.2.3.4 PES 300

Modifications with addition of crosslinkers did not influence the rejection curve position of modified membranes (shown in Figure 5.37) relative to the curve of virgin membranes. The rejection curves remained “flat” and shifted to high MW. For comparison, results from the addition of crosslinkers can be found in Figure 15 in Appendix A.

5.3.3 ADSORPTION OF TEST SOLUTES

The effect of adsorbed myoglobin and BSA on the membrane water flux was studied for virgin and modified membranes with varied functionalisation degree. Fouling resistance data from static adsorption tests over 3 hours with virgin PES 10, PES 50 and modified PES 50 with PEGMA 400 are summarised in Figure 5.43. The effect of adsorbed compounds was strong for virgin membranes. In particular, PES 10 was stronger affected than virgin PES 50. Membrane surface functionalisation increased the fouling resistance, reaching a plateau after certain UV irradiation dose. Overall, BSA caused less fouling compared to myoglobin. Consequently, plateau in fouling resistance to BSA was reached already with 5 J/cm², whereas for myoglobin it occurred beyond 6 J/cm².

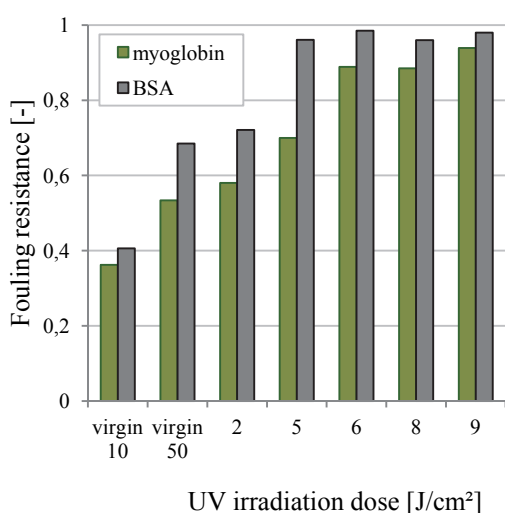


Figure 5.43 Fouling resistance to myoglobin and BSA of virgin PES 10 and PES 50 and modified PES 50 with varied UV irradiation energy.

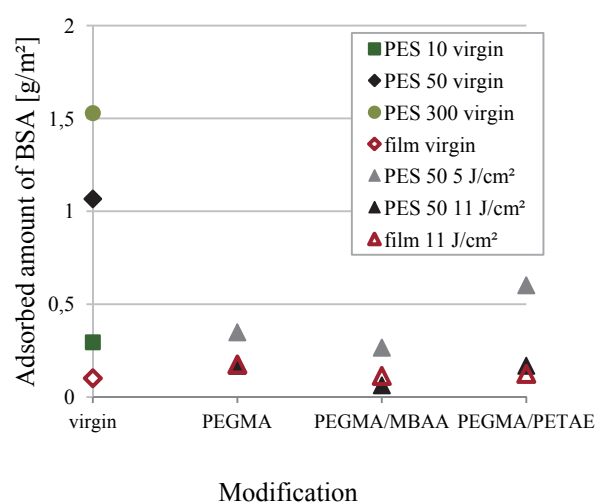


Figure 5.44 Adsorbed amount of BSA after 24 h of static adsorption. Effect of the pore size and the functionalisation.

Adsorption tests over 24 hours were performed with several virgin and modified membranes in order to estimate the adsorbed amount of foulant. Modifications with PEGMA, PEGMA/MBAA and PEGMA/PETAE at varied UV irradiation dose were studied. Results from experiments with BSA are presented in Figure 5.44. Looking at the data obtained with unmodified samples, more BSA was adsorbed on samples with larger pores, i.e., minimum adsorbed solute was found on non-porous film, whereas PES 300 adsorbed maximum BSA. Surface modification reduced the amount of bound BSA. Modified membranes with higher UV irradiation dose adsorbed less amount of BSA. Moreover, the crosslinking type influenced the membrane adsorption behaviour. Less BSA was adsorbed on samples modified with PEGMA/MBAA compared to PEGMA/PETAE.

5.3.4 DIFFUSION OF TEST SOLUTES

Diffusion experiments of BSA, myoglobin and their equimolar mixture were performed with several virgin and modified membranes (5 J/cm²) and with varied MBAA amount. The calculated average diffusion coefficients are summarised in Table 5.7. Calculated free diffusion coefficients (using Eq.(4.17)) are also included. Graphical view of the values contains Figure 16 in Appendix A.

Table 5.7 Summary of the effective diffusion coefficients through virgin and modified membranes of myoglobin and BSA as single solutions and mixture at pH = 6

Membrane	Average diffusion coefficient *10 ⁻¹² [m ² /s]			
	Single proteins		Equimolar mixture	
	Myoglobin	BSA	Myoglobin	BSA
PES 50 virgin	13.4 ± 2.1	1.6 ± 0.9	7.9 ± 2.1	1.8 ± 0.2
PES 30 virgin	10.1 ± 2.2	0.49 ± 0.21	5.3 ± 3.2	0.34 ± 0.25
PES 10 virgin	3.3 ± 1.7	0.46 ± 0.23	1.0 ± 0.7	0.27 ± 0.31
PES 50 40/0 5 J/cm ²	6.0 ± 1.6	0.35 ± 0.26	5.7 ± 2.0	0.57 ± 0.32
PES 50 40/1 5 J/cm ²	4.2 ± 0.8	0.39 ± 0.27	5.3 ± 0.3	0.42 ± 0.05
PES 50 40/4 5 J/cm ²	1.7 ± 0.7	0.20 ± 0.12	0.69 ± 0.15	0.72 ± 0.54
Free diffusion	83.7	48.8	-	-

The measured diffusion coefficients through membranes were much lower than the calculated free diffusion coefficients. In general, higher effective diffusion coefficients were measured for myoglobin. Both diffusion coefficients decreased with decreasing nominal MWCO (for virgin membranes) and increasing MBAA amount (for modified membranes). Comparing diffusion coefficients in single solutes system and in mixture, diffusion of myoglobin was faster when myoglobin was single solute in solution. The diffusion coefficient of BSA slightly increased in some experiments with mixture. It should be noted that difficulties in the detection of BSA in mixture (see Section 4.2.5.4) and high results variation (error) were observed.

Calculated diffusion coefficients over time are presented in Figure 5.45 exemplarily for the diffusion of BSA through virgin PES 10 and modified PES 50 40/1. As clearly seen, the diffusion coefficient through virgin membrane decreased over time, whereas it remained stable for modified membrane.

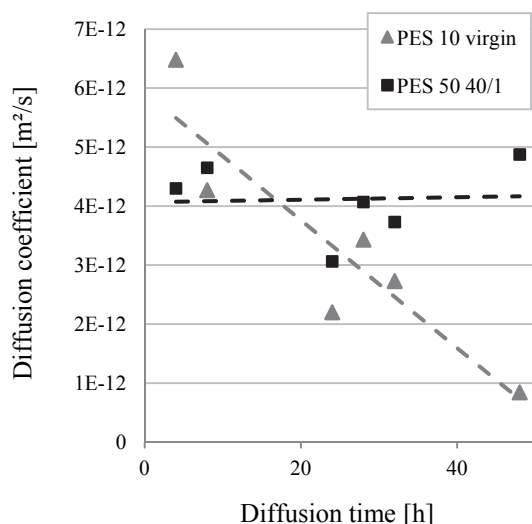


Figure 5.45 Effective diffusion coefficient of BSA over time through virgin and modified membranes.

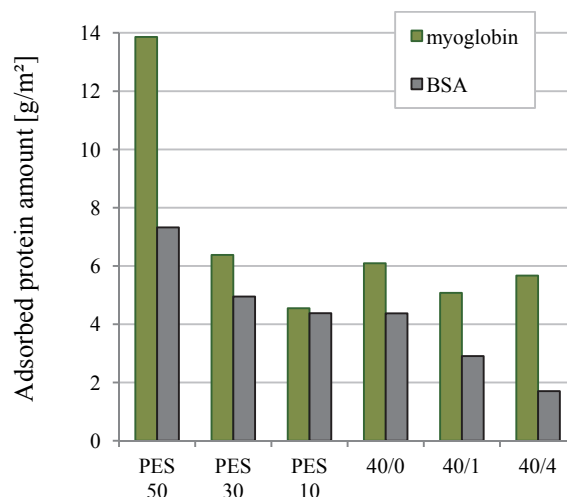


Figure 5.46 Adsorbed amount of solutes as single during 48 h of diffusion.

The adsorbed amount of solutes after 48 hours diffusion was also measured. The amount of adsorbed protein per membrane outer surface area is shown in Figure 5.46. In general, more protein was adsorbed on virgin membranes. It can be seen, that myoglobin was adsorbed stronger than BSA. Furthermore, the adsorbed amount of both proteins decreased as nominal MWCO decreased (for virgin membranes) and MBAA amount increased (for functionalised PES 50).

5.3.5 PROTEIN FILTRATION

In the following section, results obtained from protein filtration experiments will be presented. Stirred DE filtrations in short and long term were performed as well as CF filtrations.

5.3.5.1 Stirred dead-end protein filtration

5.3.5.1.1 Short stirred dead-end filtration

5.3.5.1.1.1 Two fold volume reduction

Short protein filtrations were performed in order to estimate the fouling resistance and apparent rejection for large amount of unmodified and functionalised samples. The experiments were performed with membranes with diameter of 44 mm (11.56 cm² active surface area) at 1 bar and 25 mL permeate from 50 mL feed were collected. The flux behaviour of selected virgin and modified membranes during permeate collection is shown in Figure 5.47 in terms of relative flux.

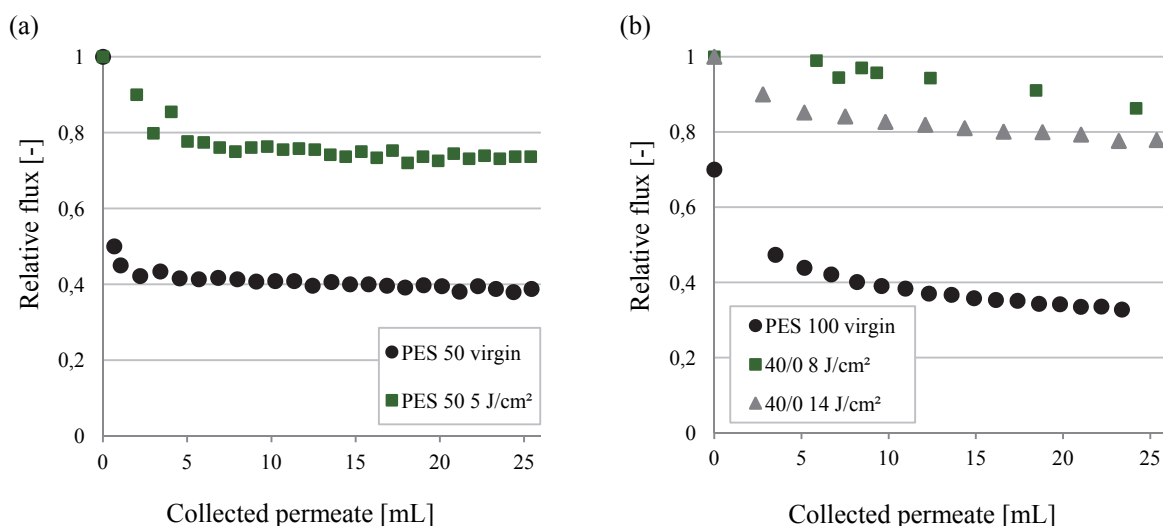


Figure 5.47 Permeate flux behaviour of virgin and modified membranes during short DE filtrations; (a) PES 50; (b) PES 100.

The results from the filtrations with PES 50 (Figure 5.47(a)) showed that stationary conditions were achieved until 25 mL of permeate were collected. This behaviour was not pronounced so clearly in the flux results for PES 100 (Figure 5.47(b)).

5.3.5.1.1.1 PES 30

The effect of the additive PVP on the membrane performance during short filtration experiments was studied. Therefore, PES membranes with nominal MWCO of 30 kDa (nominal MWCO given by the producer) with and without PVP were modified with PEGMA and 11 J/cm². Filtration of BSA was performed with virgin and functionalised membranes. The obtained data about initial water flux, average relative protein flux during filtration, fouling resistance and rejection are summarised in Table 5.8.

Table 5.8 Obtained data from filtration experiments of BSA through virgin and modified PES 30. Effect of PVP

Membranes		Initial water flux [L/hm ²]	Average relative flux during filtration [-]	Fouling resistance [-]	Rejection of BSA [%]
Virgin	with PVP	580	0.16	0.29	100
	w/o PVP	400	0.20	0.21	99.6
Modified with PEGMA 11 J/cm ²	with PVP	40	0.90	0.95	100
	w/o PVP	130	0.88	0.92	83.8

Regarding virgin membranes, the relative protein flux during filtration of PES 30 with PVP was lower compared to the results for PES 30 without PVP. In contrast, after the filtration, the fouling resistance of membrane with PVP was better. The rejection of BSA was found to be similar. Form the tests with

modified membranes was determined that PES 30 with PVP had higher relative flux during filtration and also better fouling resistance. In this case, membranes without PVP had lower BSA rejection compared to membranes with PVP.

5.3.5.1.1.2 PES 50

Prior to the performance investigation of the composite membranes, functionalisations at varied irradiation intensity were performed in order to evaluate the effect of the UV intensity on the membrane structure itself. All membranes were irradiated with same dose at different intensity by variation of the irradiation time according to Eq.(4.7). Table 5.9 shows the rejection of BSA and myoglobin for modified membranes obtained at 20 mW/cm² and 5 mW/cm² compared to virgin membranes.

Table 5.9 Apparent rejection of myoglobin and BSA after short DE filtration through PES 50 depending on the UV irradiation intensity

Test solution	Functionalised membranes			Virgin membranes
	UV irradiation dose [J/cm ²]	UV intensity [mW/cm ²]	Rejection [%]	Rejection [%]
BSA	4	20	75	80
		5	88	
Myoglobin	12	20	14	10
		5	84	

Membranes which were irradiated with same dose at higher UV intensity showed lower protein rejection [160]. All results for modified membranes which will be presented further were obtained after modification at 5 mW/cm².

Myoglobin and BSA were filtered through virgin and modified PES 50 with varied modifier composition: PEGMA 200, PEGMA 200/MBAA, PEGMA 400, PEGMA 400/MBAA, PEGMA 400/PETAE. First, fouling resistance data obtained by measuring the water flux after protein filtration will be presented. Since it has been found in previous work [130] and confirmed in this study that the extent of fouling for certain irradiation level increased with increasing crosslinker amount, Figure 5.48 and Figure 5.49 include only values for membranes at the highest crosslinker concentrations. Results obtained with modified membranes with PEGMA 200 are shown in Figure 5.48(a) for myoglobin and Figure 5.48(b) for BSA, in comparison to data for virgin PES 10 and PES 50.

Virgin membranes lost flux after contact with both proteins. Moreover, the effect on the water flux of PES 10 was more pronounced when myoglobin was filtered. The fouling resistance to BSA was

similar for both membranes. The modification increased the fouling resistance to myoglobin and BSA. It was found that crosslinking did not change this behaviour significantly.

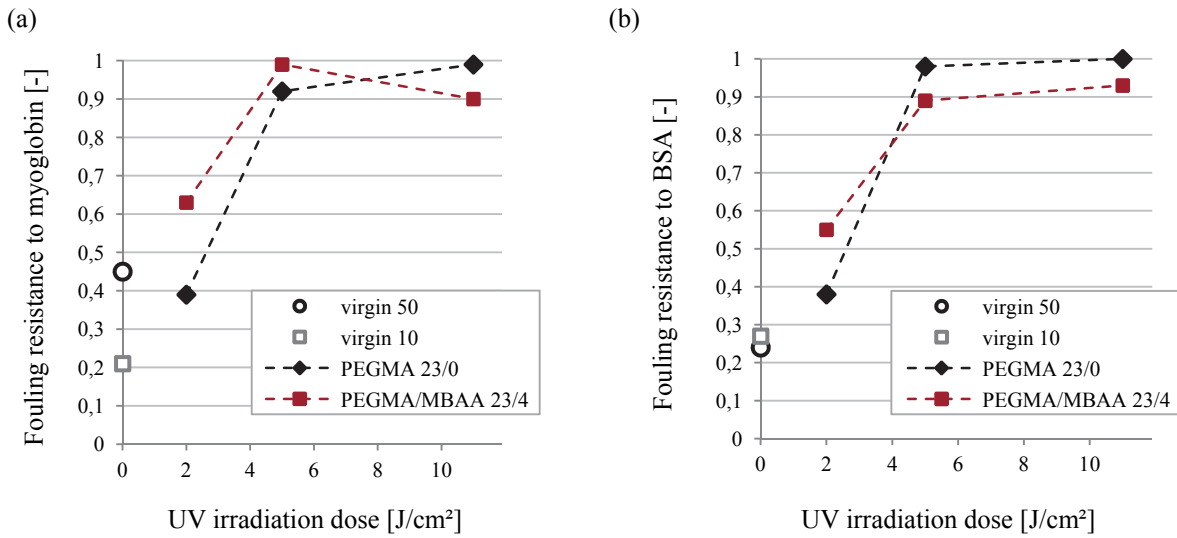


Figure 5.48 Fouling resistance of PES 50 modified with PEGMA 200 depending on the UV irradiation dose; (a) myoglobin; (b) BSA.

Similar results were obtained for membranes modified with PEGMA 400, as shown in Figure 5.49.

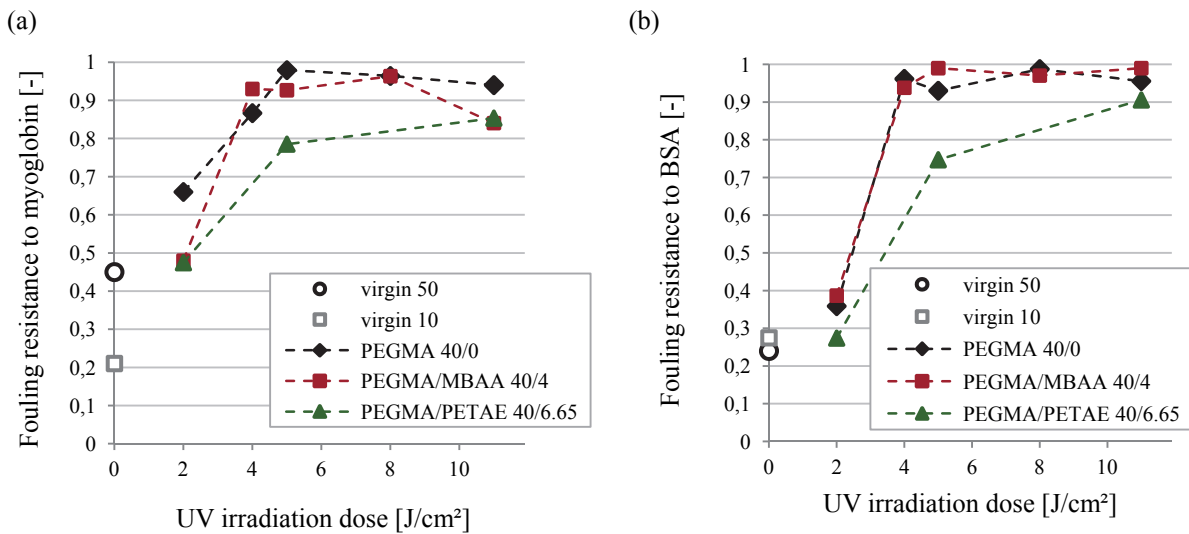


Figure 5.49 Fouling resistance of PES 50 modified with PEGMA 400 depending on the UV irradiation dose; (a) myoglobin; (b) BSA.

In most cases, R_f of 0.9 to both test substances was already achieved at 4-5 J/cm². Modification with PEGMA/PETAE delivered slightly smaller R_f values which were improved by increasing the UV irradiation dose. Additional information regarding the median permeability during the filtration process is included in Appendix A (Figure 17 and Figure 18).

Rejection data for myoglobin and BSA will be presented in combination. Figure 5.50 visualises the rejection behaviour of membranes modified with PEGMA/MBAA with varied MBAA amount depending on the UV irradiation dose. Modifications with PEGMA 200 and PEGMA 400 are included in Figure 5.50(a) and Figure 5.50(b), respectively.

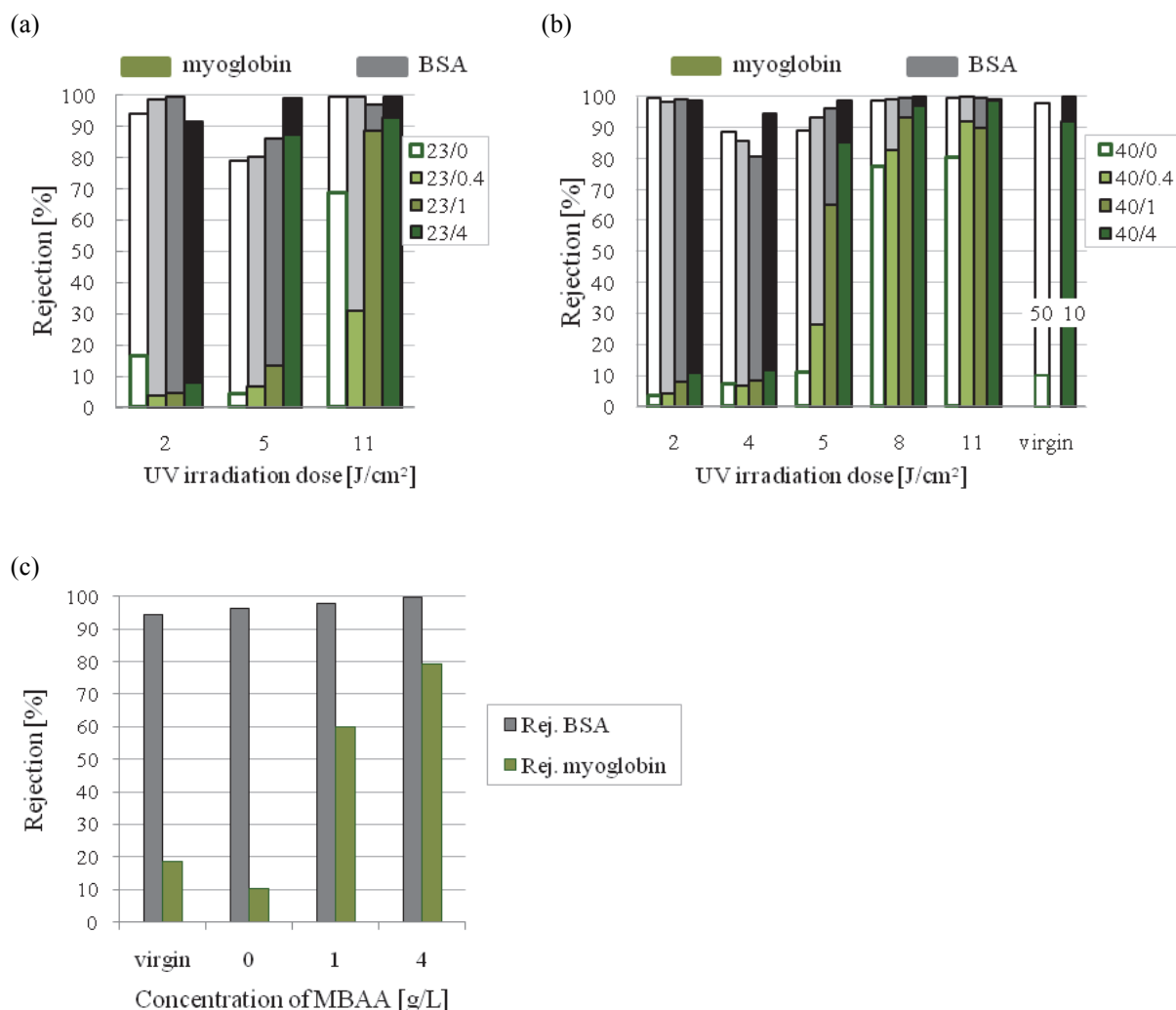


Figure 5.50 Apparent protein rejection of modified PES 50; (a) PEGMA 200/MBAA, single solutions; (b) PEGMA 400/MBAA, single solutions; (c) PEGMA 400/MBAA, UV irradiation dose: 5 J/cm², mixture.

The rejection of BSA was over 80 % during these experiments. At irradiations with 4-5 J/cm², rejection decreased compared to virgin and less modified membranes but could be controlled by addition of crosslinker. At higher UV irradiation dose, the rejection reached 100 %. Myoglobin was rejected by up to 10 % by virgin and slightly modified PES 50. Interesting results were obtained at 5 J/cm². Membranes modified with pure PEGMA showed 5 % (PEGMA 200) to 10 % rejection (PEGMA 400). Using MBAA and increasing its amount could lead to more than 85 % rejection of

myoglobin. In general, slightly lower rejection was measured with membranes modified with PEGMA 200.

Short DE filtrations were performed with equimolar mixture of both proteins with total concentration of 1 g/L. The obtained rejection data are shown in Figure 5.50(c). As it can be seen, the rejection of BSA slightly decreased. Myoglobin was stronger rejected by virgin PES 50, while functionalised membranes rejected myoglobin to same extent as in single solution.

Modifications with PETAE as crosslinking agent were also analysed with respect to protein rejection.

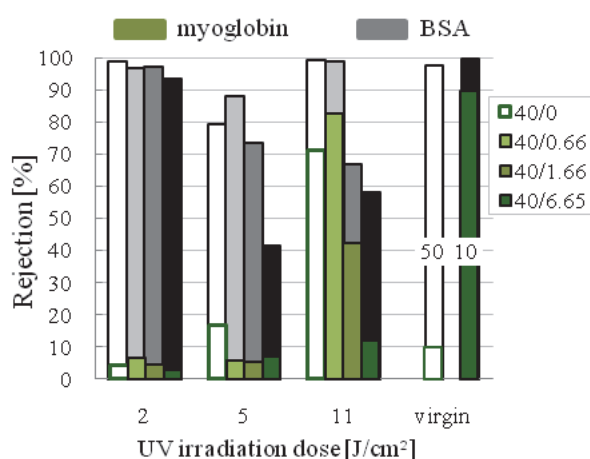


Figure 5.51 Apparent protein rejection of PES 50 modified with PEGMA 400/PETAE.

The results presented in Figure 5.51 were quite different. In general, the addition of PETAE in small amounts increased the rejection slightly. Nevertheless, further increasing the amount of PETAE in the modifier mixture decreased the rejection of the functionalised membranes. At 5 J/cm², the rejection of BSA fell by half from 80 % to 40 %. The rejection of myoglobin changed also dramatically at 11 J/cm²: modification with PEGMA only resulted in 70 % rejection, whereas modification with PETAE at its highest concentration caused rejection decrease to 10 % [160].

5.3.5.1.1.3 PES 100

BSA and γ -globulin solutions were used in filtration experiments with PES 100, and fouling resistance and rejection were determined. Fouling resistance data for the tested membranes (crosslinkers are presented only at maximum amount) to BSA and γ -globulin are presented in Figure 5.52(a) and Figure 5.52(b), respectively.

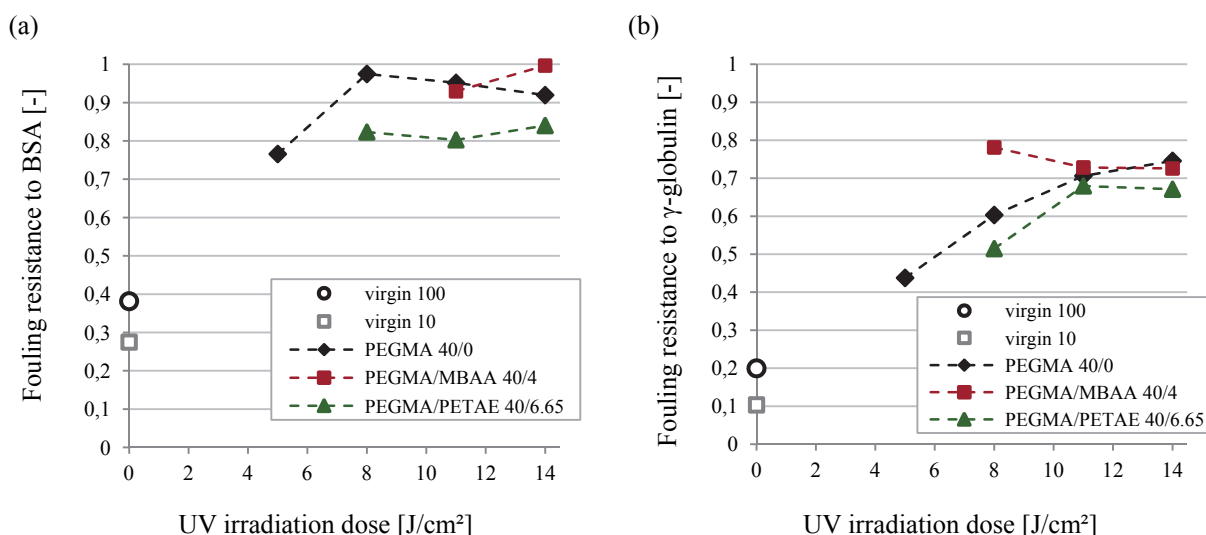


Figure 5.52 Fouling resistance of PES 100 modified with PEGMA 400 depending on the UV irradiation dose; (a) BSA; (b) γ -globulin.

Virgin membranes showed low fouling resistance to the tested proteins. Severe fouling was observed with γ -globulin where R_f of 0.2 and 0.1 were measured for PES 100 and PES 10, respectively. Modification with PEGMA increased the fouling resistance more effectively to BSA in comparison to γ -globulin.

Median permeabilities from the performed filtrations are presented in Figure 19 and Figure 20 in Appendix A.

Apparent rejection data for BSA and γ -globulin are summarised in Figure 5.53.

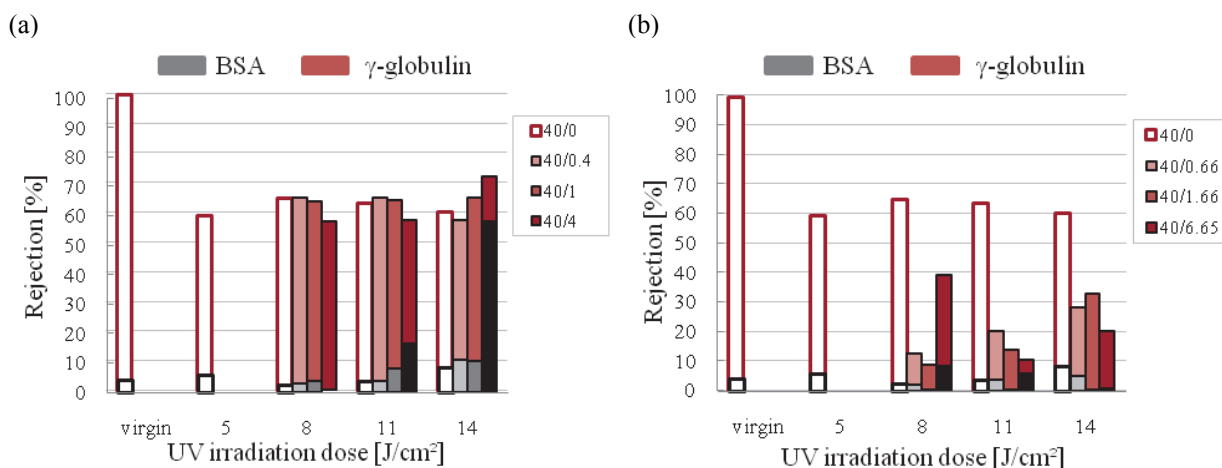


Figure 5.53 Apparent protein rejection of modified PES 100; (a) PEGMA 400/MBAA; (b) PEGMA 400/PETAE.

Virgin PES 100 showed complete rejection of γ -globulin and almost no rejection of BSA. Surface functionalisation with PEGMA caused decrease in rejection. For functionalisations up to 11 J/cm², the addition of MBAA influenced the rejection only partially (Figure 5.53(a)). Higher amount of MBAA slightly decreased the rejection of γ -globulin, whereas the rejection of BSA rose a little but did not exceed 15 %. At 14 J/cm², an increase in the rejection of γ -globulin and BSA was found with increasing MBAA amount.

Different behaviour was found for modified membranes with PETAE. Figure 5.53(b) shows that the application of PETAE caused strong decrease in protein rejection. The measured γ -globulin rejection value of 40 % for modified membrane with PEGMA/PETAE 40/6.65 (8 J/cm²) deviated from the common trend.

5.3.5.1.1.4 PES 300

The filtration performance of PES 300 was tested in short DE filtration experiments with the proteins γ -globulin, fibrinogen and thyroglobulin. Membrane modifications were performed with PEGMA 400 applying MBAA and PETAE for crosslinking. Since the fouling resistance of these membranes was not affected by the crosslinkers, these results will be presented only for modifications with PEGMA 400 without crosslinking. Figure 5.54 summarises the results obtained from the filtrations of the three tested proteins. The proteins affected the fouling resistances of the tested membranes. Thyroglobulin caused the highest flux decline. For this protein, membrane functionalisation improved the fouling resistance to limited extent – R_f was shifted from 0.45 (for virgin membranes) to 0.7. The applied modification improved the fouling resistance to smaller proteins. Results for modified membranes with crosslinkers at maximal concentrations can be found in Appendix A, Figure 21.

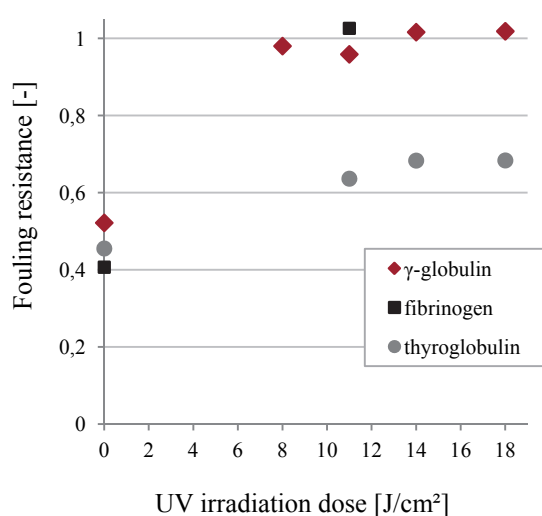


Figure 5.54 Fouling resistance of PES 300 modified with PEGMA 400 depending on the UV dose.

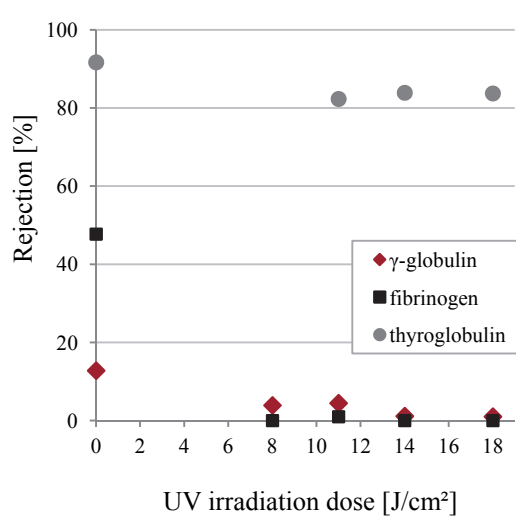


Figure 5.55 Apparent protein rejection of PES 300 modified with PEGMA 400.

Crosslinking did not influence the rejection properties of the tested membranes. For this reason, in Figure 5.55, rejection data only for modifications with PEGMA are presented. The rejection of thyroglobulin was not much changed by the membrane modification. In contrast, γ -globulin and fibrinogen rejections decreased to 0 % due to the functionalisation. Complete data about median permeability during filtration and rejection of membranes modified with MBAA and PETAE are summarised in Figure 22 and Figure 23 in Appendix A, respectively.

5.3.5.1.1.2 20 fold volume reduction

Filtrations of BSA and myoglobin as single solutions and in mixture were performed at pH = 6. Virgin PES 10, PES 30, PES 50 as well as PES 50 modified with 5 J/cm² using PEGMA/MBAA 40/0, 40/1 and 40/4 were tested with respect to flux and rejection behaviour. The permeate flux was taken online. The obtained results from BSA filtrations are summarised in Figure 5.56, sorted by virgin and functionalised samples in Figure 5.56(a) and Figure 5.56(b), respectively.

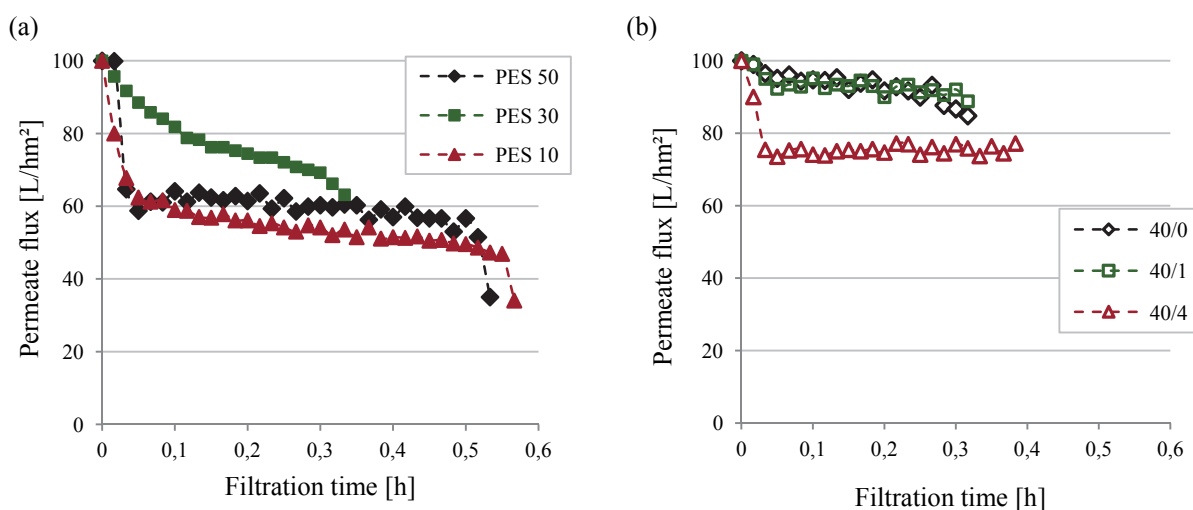


Figure 5.56 Permeate flux of BSA during the 20x volume reduction; (a) virgin membranes; (b) modified PES 50.

The permeate flux of virgin membranes decreased during the filtration process and no steady state was reached, whereas modified membranes behaved more stably.

Protein rejection results from these experiments are shown in Figure 5.57(a) for single solutions and in Figure 5.57(b) for mixture.

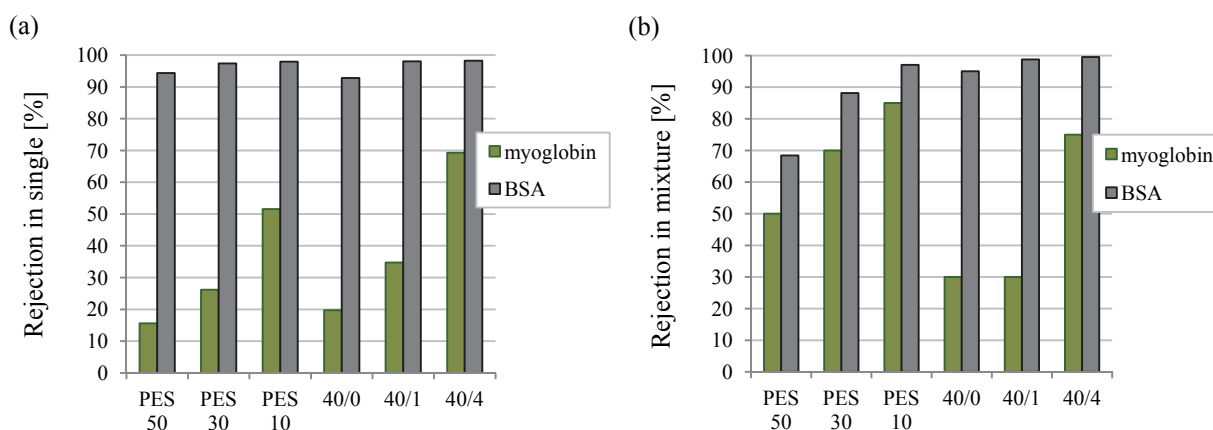


Figure 5.57 Apparent rejection of solutes during 20x volume reduction; (a) single solutions; (b) mixture.

The rejection values increased in accordance to the decreasing nominal MWCO of virgin membranes and the increasing MBAA amount for modified membranes. Comparing the rejection in mixture to that in single solution, increased rejection of myoglobin by virgin membranes was observed, whereas modified membranes behaved in a similar manner. Decreased rejection of BSA by virgin membranes was found when BSA was in mixture.

5.3.5.1.2 Stirred dead-end filtration over 24 hours and cleaning

The performance of virgin PES 10, PES 30, PES 50 and PES 100 during stirred DE filtration and cleaning was studied. In addition, modified PES 50 and PES 100 were also used in these experiments in order to characterise the effect of the surface functionalisation on filtration performance. The results are divided in subsections by the membranes' nominal MWCO.

5.3.5.1.2.1 PES 10

Filtration experiments over 24 hours of BSA, myoglobin and their equimolar mixture were performed with virgin PES 10 at varied pH. Table 5.10 shows the adjusted operating pressure to achieve initial permeate flux of 100 L/hm², the pH as well as the obtained overall rejections.

Table 5.10 Operating parameters and apparent rejection of the tested solutes in all performed DE filtration runs with virgin PES 10

Membrane	Water permeability [L/hm ² bar]	Pressure [bar]	pH	Rejection of single [%]		Rejection in mixture [%]	
				BSA	myoglobin	BSA	myoglobin
PES 10 virgin	100 ± 13	1.0 ± 0.13	8	100	98	100	87
			6	100	88	100	97
			4	100	96	n.d.	n.d.

n.d.: not determined/experiment not done

It was found that BSA was completely rejected by PES 10. The obtained myoglobin rejection data from single solutions showed minimum at pH = 6, while in mixture myoglobin was less rejected at pH = 8.

Permeate fluxes over time at varied pH are presented in Figure 5.58. The results from filtrations with different solutes are presented combined in graphics at same pH, i.e., Figure 5.58(a) presents the results at pH = 4, Figure 5.58(b) and Figure 5.58(c) – at pH = 6 and pH = 8, respectively.

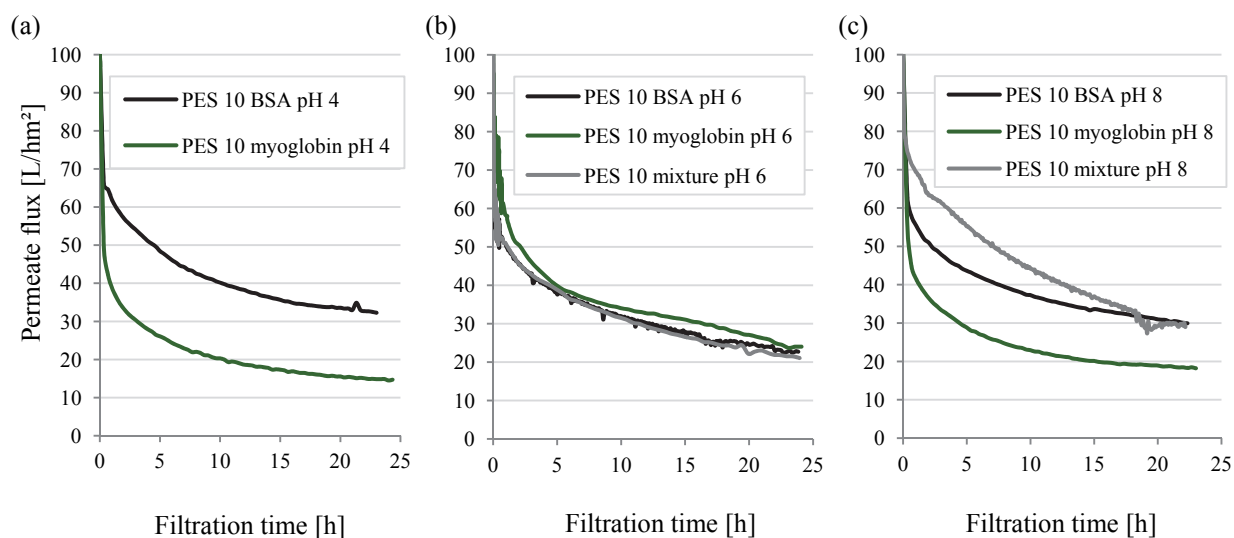


Figure 5.58 Permeate flux behaviour during the DE filtration of BSA, myoglobin and their mixture through virgin PES 10; (a) pH 4; (b) pH 6; (c) pH 8.

In the early stages of the process (up to 2 hours), strong flux decrease was observed. Later, permeate fluxes slightly decreased with tendency to reach plateau. In most cases, filtrate fluxes of BSA (black line) were higher than fluxes during myoglobin filtration (green line). Exceptionally, myoglobin flux at pH = 6 was slightly higher. Overall, higher fluxes were obtained at pH = 8.

Water flux recovery data from mechanical and chemical cleaning are presented in Figure 24 in Appendix A. Mechanical cleaning with water did not change the membrane water flux significantly. Water fluxes of membranes used in myoglobin filtrations remained almost unchanged after external cleaning and back wash, flux recovery was 20-40 %. In case of BSA and mixture cleaning with water slightly increased the membrane water flux. Cleaning with NaOH at pH = 13 led to increase of the flux recovery values but they did not exceed 75 %.

5.3.5.1.2.2 PES 30

Filtration experiments analogous to PES 10 were performed with virgin PES 30. The operation parameters and measured apparent rejection values are summarised in Table 5.11.

Table 5.11 Operating parameters and apparent rejection of the tested solutes in all performed DE filtration runs with virgin PES 30

Membrane	Water permeability [L/hm ² bar]	Pressure [bar]	pH	Rejection of single [%]		Rejection in mixture [%]	
				BSA	myoglobin	BSA	myoglobin
PES 30 virgin	200 ± 22	0.5 ± 0.06	8	100	76	100	76
			6	99.9	40	99.9	69
			4	100	85	n.d.	n.d.

n.d.: not determined/experiment not done

In case of PES 30, BSA was nearly completely rejected. Both in single solution and mixture, myoglobin rejection was at minimum when filtrations were performed at pH = 6.

The permeate fluxes presented in Figure 5.59 decreased rapidly in the first 1-2 hours of the filtration process. Here, filtrations of myoglobin occurred with lower flux compared to filtrations of BSA and mixture. With exception of myoglobin, permeate fluxes increased with increasing pH value during protein filtration through PES 30.

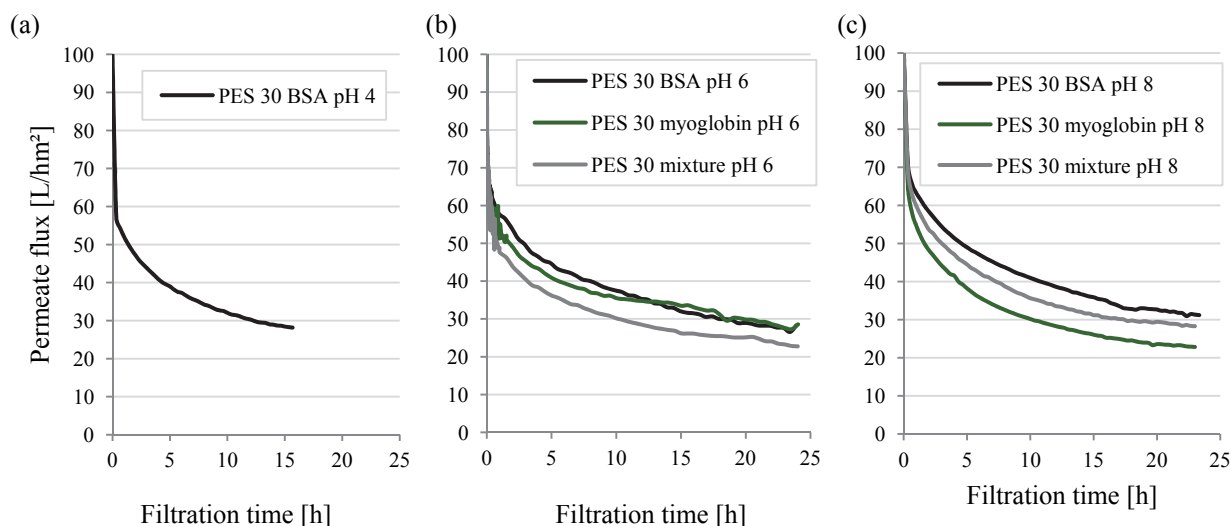


Figure 5.59 Permeate flux behaviour during the DE filtration of BSA, myoglobin and their mixture through virgin PES 30; (a) pH 4; (b) pH 6; (c) pH 8.

Cleaning experiments were also performed. In Figure 25 (Appendix A) could be found that cleaning with water increased slightly the membrane water flux, in most cases flux recovery increased by less than 5 %. Chemical cleaning was more effective and increased the flux recovery by up to 30 %.

5.3.5.1.2.3 PES 50

Long term DE filtration experiments were conducted with virgin and modified membranes PES 50. In the next subsections, the obtained results will be presented.

5.3.5.1.2.3.1 Filtration with virgin membranes

Single solutions of γ -globulin, BSA and myoglobin as well as equimolar mixture of BSA and myoglobin were filtered through virgin PES 50. The operation parameters and the observed rejection values are shown in Table 5.12.

It can be seen that PES 50 rejected γ -globulin to 100 %. BSA was also completely retained at pH = 8 but the apparent rejection decreased with decreasing pH. This trend was also found when myoglobin was filtered as single solute. In contrast, myoglobin in mixture was more strongly rejected at pH = 6.

Table 5.12 Operating parameters and apparent rejection of the tested solutes in all performed DE filtration runs with virgin PES 50

Membrane	Water permeability [L/hm ² bar]	Pressure [bar]	pH	Rejection of single [%]			Rejection in mixture [%]	
				γ -globulin	BSA	myoglobin	BSA	myoglobin
PES 50 virgin	500 ± 53	0.2 ± 0.02	8	n.d.	100	42	100	20
			6	100	99	21	98	47
			4	n.d.	98	19	100	89

n.d.: not determined/experiment not done

The permeate flux behaviour of virgin PES 50 presented in Figure 5.60 was found to be similar to the already presented data for PES 10 and PES 30.

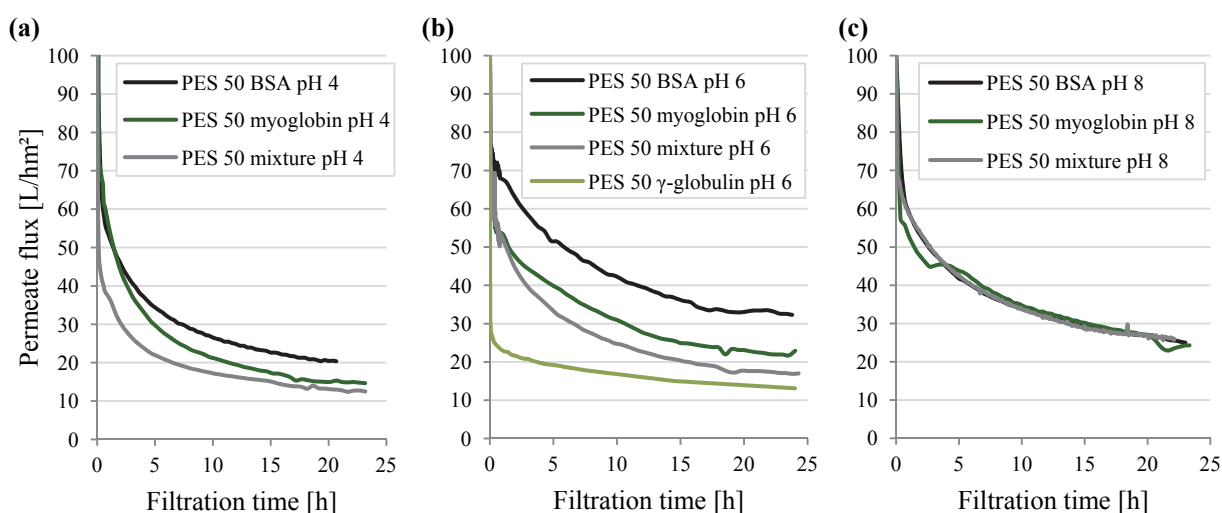


Figure 5.60 Permeate flux behaviour during the DE filtration of globulin, BSA, myoglobin and their mixture through virgin PES 50; (a) pH 4; (b) pH 6; (c) pH 8.

Strong flux decrease at the beginning of the process was measured. As in can be seen from Figure 5.60(b), γ -globulin caused severe flux decline, whereas BSA was filtered with the highest permeate flux, followed by myoglobin. When BSA and myoglobin were in mixture, the membrane flux dropped further. Similar behaviour was detected also at pH = 4. In contrast, at pH = 8 the overall flux performance did not change when filtering different solutions.

Figure 26 in Appendix A contains the obtained flux recovery data during the cleaning procedure of virgin PES 50. Again, insignificant change in the membrane water flux was found during mechanical cleaning, the flux recovery remained mostly below 40 %. Cleaning with NaOH increased the flux recovery to 70 % from the initial membrane water flux.

5.3.5.1.2.3.2 Filtration with functionalised membranes

Protein filtration experiments were performed with modified membranes prepared with varied amount of MBAA and different UV irradiation doses. Here, BSA, myoglobin and their equimolar mixture were used in the filtration procedures. All tested membrane types as well as the operating parameters and obtained apparent rejection values are summarised in Table 5.13.

Membranes modified with 5 J/cm² and PEGMA/MBAA ratios of 40/0, 40/1 and 40/4 were tested. 40/0 and 40/4 were used at varied pH values, whereas 40/1 was tested only at pH = 6. Further experiments were performed with membranes modified with 8 J/cm² from modification type 40/0 (at pH = 4 and pH = 8) and 40/4 (pH = 4).

Table 5.13 Operating parameters and apparent rejection of the tested solutes in all performed DE filtration runs with modified PES 50

UV irradiation dose [J/cm ²]	Concentration of PEGMA/MBAA [g/L]	Water permeability [L/hm ² bar]	Pressure [bar]	pH	Rejection of single [%]		Rejection in mixture [%]	
					BSA	myoglobin	BSA	myoglobin
5 J/cm ²	40/0	200 ± 25	0.5 ± 0.06	8	100	22	100	42
				6	97	12	99.5	50
				4	93	19	100	42
	40/1	130 ± 15	0.77 ± 0.08	6	98	52	100	60
				8	100	91	n.d.	n.d.
				6	99	86	100	92
40/4	60 ± 7	1.7 ± 0.18	4	n.d.	94	n.d.	n.d.	
			4	n.d.	94	n.d.	n.d.	
8 J/cm ²	40/0	100 ± 11	1 ± 0.01	8	99	21	n.d.	n.d.
				4	93	80	85	60
	40/4	30 ± 2	3.3 ± 0.20	4	95	96	n.d.	n.d.

n.d.: not determined/experiment not done

First, results from filtrations through modified membranes with 5 J/cm² will be explained. Membranes modified with MBAA showed increased rejection for both proteins. This trend was amplified for membranes with higher amount of MBAA, e.g., at pH = 6 the rejection of myoglobin increased from 12 % (40/0) to 52 % (40/1) and further to 86 % (40/4). For same functionalisation type, the rejection of BSA as single solute decreased with decreasing pH. In contrast, myoglobin was more strongly rejected when pH decreased (for 40/0 going through minimum at pH = 6). The rejection of the tested proteins increased when they were in mixture. For filtrations with 40/0, maximum of myoglobin rejection in mixture was found at pH = 6.

When modified membranes with 8 J/cm² were tested, 40/4 showed higher rejections than 40/0, similar to membranes modified with 5 J/cm. In single solutions, BSA and myoglobin were rejected similarly to 5 J/cm² modified membranes. In mixtures, the rejection of BSA by 40/0 at pH = 4 dropped; myoglobin was also less rejected than as single solute.

The permeate fluxes of BSA, myoglobin and mixture over filtrations through modified membranes 40/0 with 5 J/cm² are presented in Figure 5.61, ordered according to solution pH.

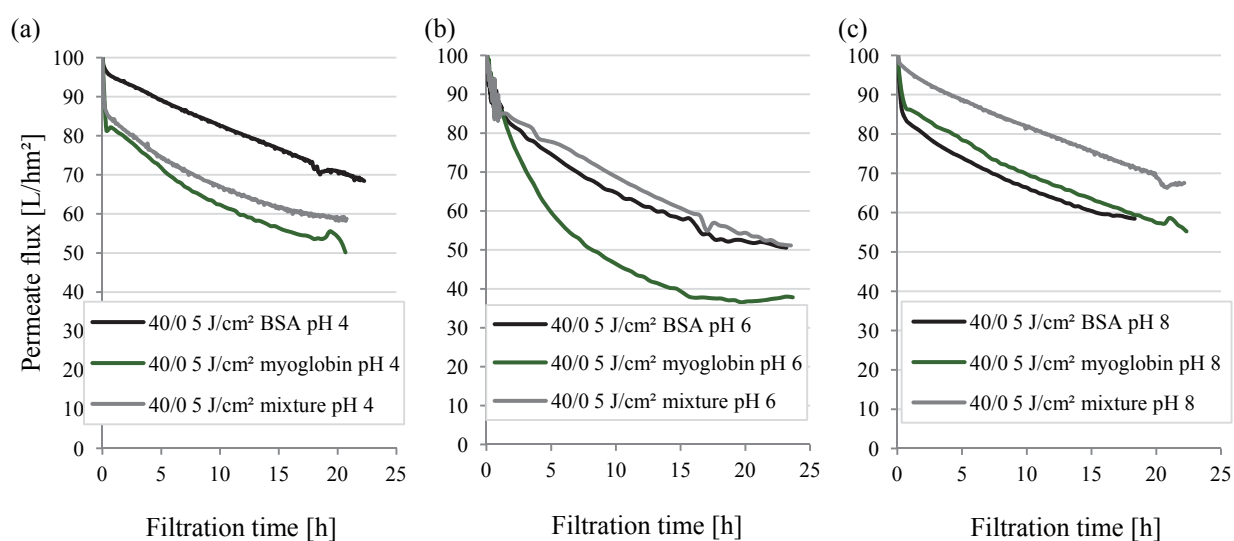


Figure 5.61 Permeate flux behaviour during the DE filtration of BSA, myoglobin and their mixture through modified PES 50; (a) pH 4; (b) pH 6; (c) pH 8.

In the early filtration stages, decrease in the permeate flux to varied extent was found. Later, the flux decreased in most cases linearly with time. Comparing filtration experiments at varied pH value, minimum in permeate flux was measured at pH = 6 for all tested solutions. Strong decrease in permeate flux of myoglobin (green line) over long period of time was detected at this pH value. At pH = 4 and pH = 6, filtration of BSA occurred with higher permeate flux than myoglobin, whereas at pH = 8 similar fluxes were observed for both solutions. Mixture of BSA and myoglobin had the highest flux at pH = 8 (gray line).

Further, results from cleaning of modified membranes with 5 J/cm^2 will be explained. The effect of cleaning on the water flux varied for different test solutions, as it can be taken from Figure 5.62.

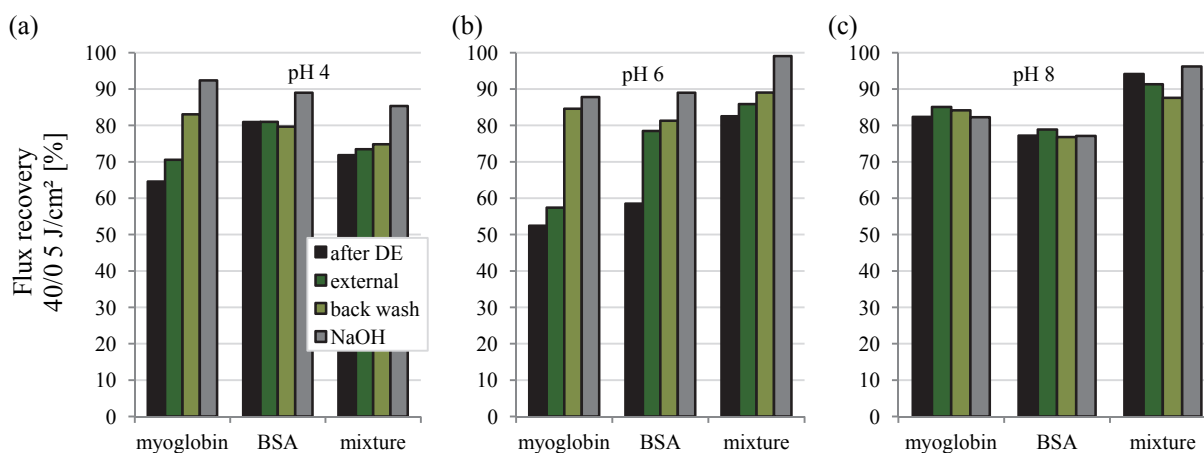


Figure 5.62 Flux recovery of PES 50 modified with $40/0 \text{ 5 J/cm}^2$ during the cleaning process; (a) pH 4; (b) pH 6; (c) pH 8.

Flux recoveries mostly higher than 60 % were measured after the filtration process. At pH = 4 (Figure 5.62(a)), the flux recovery from filtrations of myoglobin increased stepwise after external cleaning and back wash with water, whereas the flux recovery of membranes used for filtration of BSA did not change. The flux of the membrane used for filtration of mixture increased also stepwise but to lower extent. Chemical cleaning increased the flux recovery by 10 %, so that it reached 90 % of the initial water flux. Figure 5.62(b) shows that strong increase in flux recovery resulted from the back wash of myoglobin treated membrane at pH = 6. Flux increase was also measured after external cleaning of membrane used in BSA filtration. The water flux through membrane after filtration of mixture increased stepwise during mechanical cleaning. Treatment with NaOH at pH = 13 increased the membrane water flux further. Very high recovery values were obtained at pH = 8 (data shown in Figure 5.62(c)). Here, the overall effect of chemical cleaning was negligible. Chemical cleaning did not affect the flux recovery significantly.

Similar results from filtration and cleaning experiments were found during tests with $40/1 \text{ 5 J/cm}^2$ at pH = 6 (Figure 27, Appendix A) and $40/4 \text{ 5 J/cm}^2$ at pH = 4, pH = 6 and pH = 8 (Figure 28 and Figure 29, Appendix A).

Further results from filtrations through modified membranes with 8 J/cm^2 were obtained. Figure 5.63 presents the permeate fluxes during filtrations under variation of the membrane modification and pH.

Filtration experiments through membranes modified with 40/0 at pH 8 (Figure 5.63(a)) occurred with similar permeate fluxes for BSA and myoglobin. Over more than 20 hours the flux decreased linearly and reached 70 L/hm^2 . At pH = 4 (Figure 5.63(b)), BSA showed high flux, while myoglobin flux

decreased rapidly. Furthermore, BSA flux decreased constantly over time, whereas the slope of the myoglobin permeate flux curve was changing.

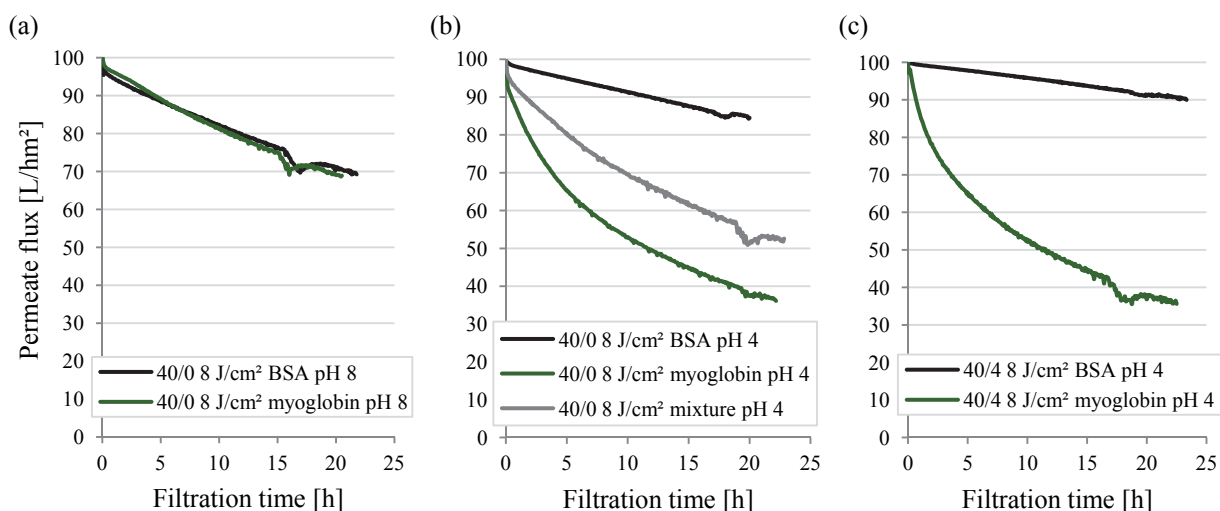


Figure 5.63 Permeate flux behaviour during the DE filtration of BSA, myoglobin and their mixture through modified PES 50 with 8 J/cm^2 ; (a) 40/0 at pH 8; (b) 40/0 at pH 4; (c) 40/4 at pH 4.

The permeate flux curve of mixture behaved similar to the curve of myoglobin permeate but showed higher values. As it can be taken from Figure 5.63(c), modification with 40/4 did not influence the flux behaviour of BSA and myoglobin at $\text{pH} = 4$ significantly compared to 40/0 8 J/cm^2 .

Cleaning data from the upper described tests are summarised in Figure 5.64 in the same sequence.

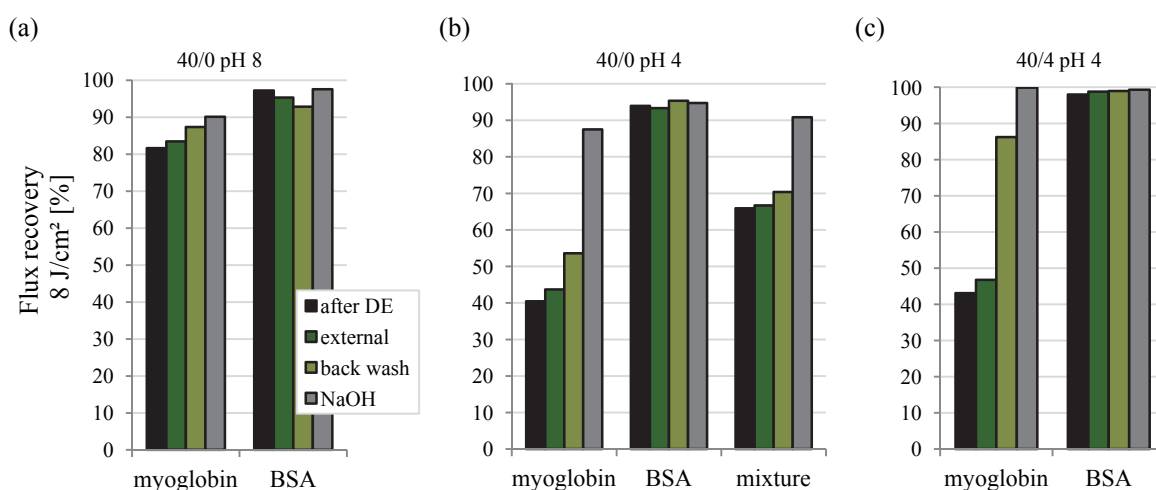


Figure 5.64 Flux recovery of modified PES 50 with 8 J/cm^2 during the cleaning process after DE filtration; (a) 40/0 at pH 8; (b) 40/0 at pH 4; (c) 40/4 at pH 4.

High flux recovery was measured during membrane cleaning after filtrations at pH = 8. After myoglobin filtration, the flux recovery increased continuously after every cleaning step; after BSA, flux recovery remained nearly unchanged (Figure 5.64(a)). At pH = 4, as presented in Figure 5.64(b), 40 % of the initial flux remained after filtration of myoglobin. Flux recovery increased during mechanical cleaning and reached almost 90 % after chemical treatment. BSA flux recovery remained stable during cleaning. The recovery data obtained after filtration of protein mixture were less influenced by mechanical cleaning. Here, chemical cleaning increased the water flux again to 90 %. From Figure 5.64(c) can be taken, that cleaning after filtrations with modified membranes 40/4 at pH 4 led to similar flux recovery results like tests with 40/0. Interesting was the increased effect of back wash for 40/4 treated with myoglobin. This effect was not so strongly pronounced with modified membrane 40/0.

5.3.5.1.2.4 PES 100

Filtration experiments in DE mode were performed with virgin and modified with PEGMA 400 PES 100. Here, the proteins γ -globulin and BSA were tested as single solutions at pH = 6. Table 5.14 presents the used membranes, operation parameters and measured apparent rejection data.

Table 5.14 Operating parameters and apparent rejection of the tested solutes in all performed DE filtration runs with virgin and modified PES 100

Membrane	Water permeability [L/hm ² bar]	Pressure [bar]	pH	Rejection of single [%]	
				γ -globulin	BSA
PES 100 virgin	760 ± 80	0.2 ± 0.02	6	99	34
40/0 11 J/cm ²	225 ± 25	0.44 ± 0.05	6	60	1.5
40/0 14 J/cm ²	170 ± 15	0.59 ± 0.05	6	60	n.d.

n.d.: not determined/experiment not done

Virgin PES 100 rejected γ -globulin to 99 % and BSA to 34 %. These values changed when modified membranes were used. Membranes modified with 11 J/cm² showed 60 % rejection of γ -globulin and nearly no rejection of BSA. The rejection of γ -globulin did not change using modified membranes with 14 J/cm².

The obtained permeate fluxes over the filtration time are shown in Figure 5.65.

Decrease in the permeate flux during filtration through virgin membranes, which was stronger for γ -globulin, was observed in the first few moments of the process (Figure 5.65(a)). Thereafter, the flux decreased continuously over time, more rapidly during filtration of BSA. Nevertheless, over nearly 20 hours, it remained higher than the flux for filtration of γ -globulin. When membranes were modified with 11 J/cm², the permeate flux of γ -globulin decreased strongly over more than 2 hours and after

15 hours reached slightly higher value compared to virgin membrane, as it can be seen in Figure 5.65(b). BSA filtration with modified membranes occurred with higher, linearly decreasing permeate flux. Figure 5.65(c) shows that the initial strong flux decrease during filtration of γ -globulin occurred in longer period of time (around 4 hours). After 15 hours the flux reached 30 L/hm², which was higher than the observed flux with 11 J/cm² modified membranes.

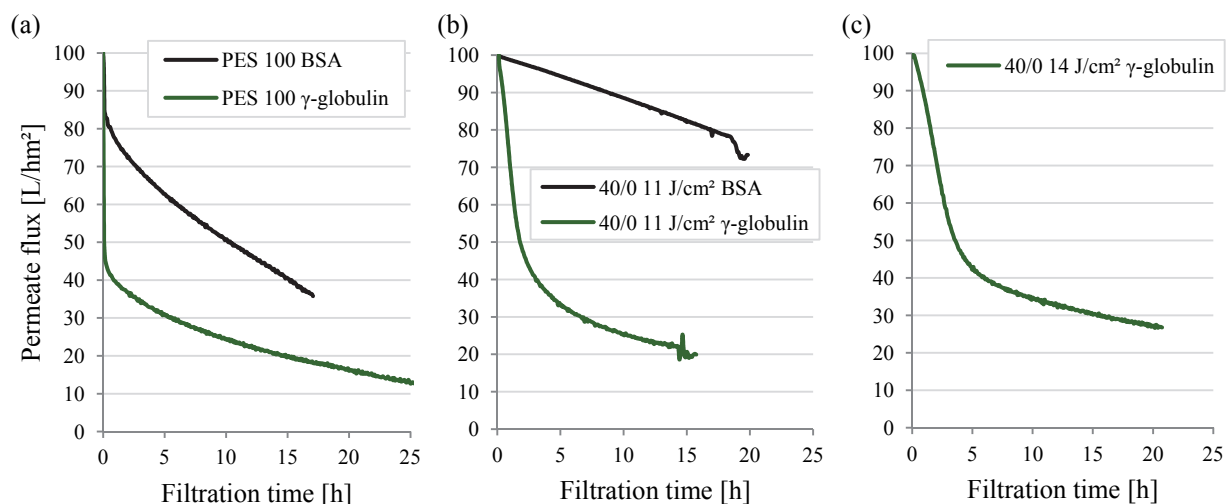


Figure 5.65 Permeate flux behaviour during DE filtration experiments with γ -globulin and BSA through PES 100; (a) virgin PES 100; (b) PES 100 modified with 40/0 11 J/cm²; (c) PES 100 modified with 40/0 14 J/cm².

Mechanical and chemical cleaning were also performed after the filtration experiments. The obtained results from these tests are shown in Figure 5.66 in terms of flux recovery.

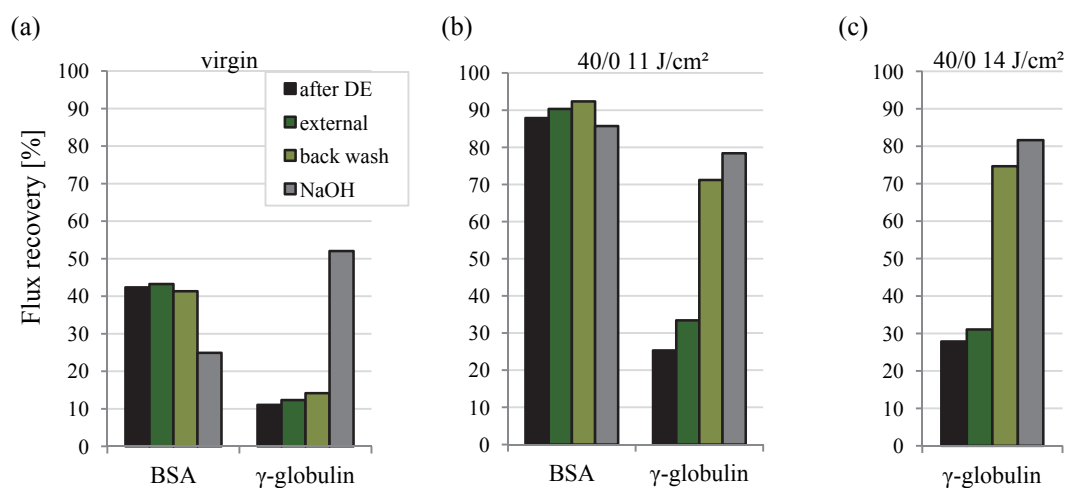


Figure 5.66 Flux recovery of PES 100 during the cleaning process after DE filtration; (a) virgin PES 100; (b) PES 100 modified with 40/0 11 J/cm²; (c) PES 100 modified with 40/0 14 J/cm².

For virgin membranes (Figure 5.66(a)), very low flux recovery was found after γ -globulin filtration. In addition, mechanical cleaning did not have significant effect on water flux. Treatment with NaOH at pH = 13 led to decreased apparent flux recovery in case of BSA but increased values for γ -globulin. When modified membranes were used (Figure 5.66(b,c)), the flux recovery after BSA was 90 %. Moreover, mechanical cleaning, especially back wash, increased the membrane water flux after filtration of γ -globulin.

5.3.5.2 Cross-flow filtration and cleaning

CF filtrations and subsequent cleaning tests were performed with virgin PES 10, PES 30 and PES 50 as well as selected PES 50 functionalised with PEGMA. Modification of large membrane area with PEGMA/MBAA was not successful and no explanation for that result could be found in the present work. BSA, myoglobin and their mixture at pH = 6 and pH = 8 were used as test solutions during the filtrations. Here, the CF was varied in order to evaluate the effect of shear rate on filtration performance. 20 L/h feed flow corresponded to 0.157 m/s linear feed velocity and 60 L/h – to 0.471 m/s. The operating parameters for the experiments and the observed critical data from tests with BSA at pH = 6 are listed in Table 5.15.

Table 5.15 Operating parameters and measured critical data of all tested membranes at pH 6

Membrane	CF [L/h]	Water permeability [L/hm ² bar]	Operating pressure [bar]	Critical pressure [bar]	Critical flux [L/hm ²]
PES 50	20 ^a	500 ± 53	0.2 ± 0.02	0.31	135
	60 ^b			0.46	220
PES 30	20 ^a	200 ± 22	0.5 ± 0.06	0.58	165
	60 ^b			0.88	260
PES 10	20 ^a	100 ± 13	1.0 ± 0.13	0.35	48
	60 ^b			0.54	74
40/0 5 J/cm ²	20 ^a	200 ± 25	0.5 ± 0.06	> 1	> 200
	60 ^b			> 1	> 200
40/0 11 J/cm ²	20 ^a	88	1.15	> 1.2	> 100

^a corresponds to 0.157 m/s linear velocity

^b corresponds to 0.471 m/s linear velocity

From the evaluated data it can be easily seen that performing the experiments at 60 L/h CF increased the critical data. Similar results have been obtained in previous works [17]. In addition, the operating pressure corresponding to initial flux of 100 L/hm² was adjusted below the critical pressure. An exception was PES 10, where the applied pressure exceeded the critical data in all performed experiments. Modified membranes showed higher values compared to virgin membranes. Exact data

for modified membranes were not collected, because the measurements were performed until 1 bar (1.2 bar, respectively) was reached.

In the following, permeate flux and rejection data over filtration runs of 6 hours as well as results from cleaning tests will be presented ordered according to membrane nominal MWCO. In all further plots from CF filtration, peaks in the permeate flux curves were observed as a result from the samples collection.

5.3.5.2.1 PES 10

Virgin membranes PES 10 were used in filtration experiments with BSA, myoglobin and mixture at varied pH and CF velocity. Figure 5.67 shows the obtained results from filtrations at 20 L/h CF.

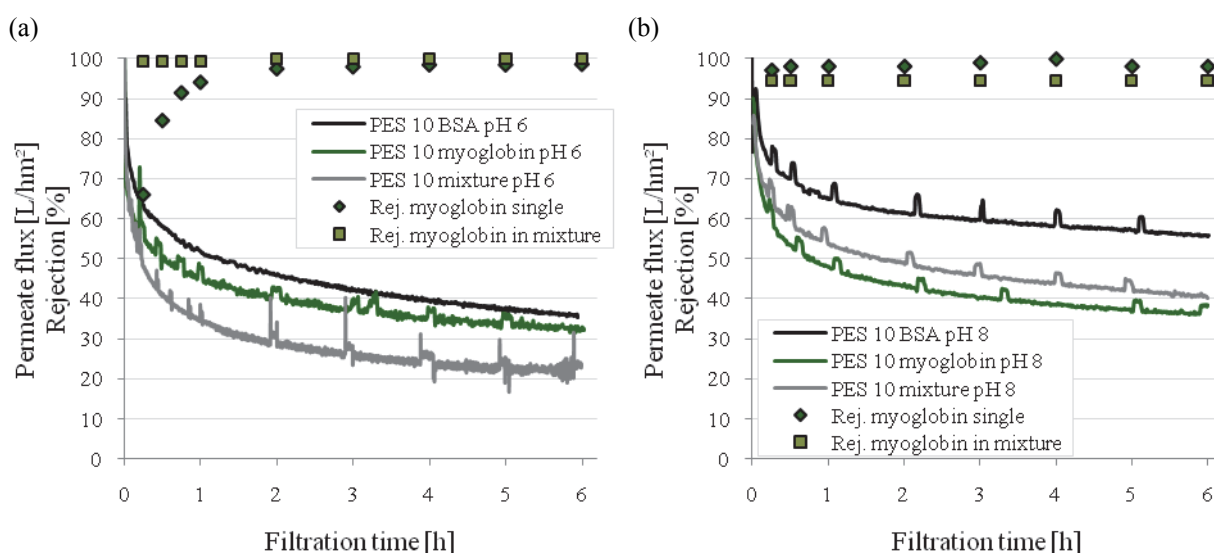


Figure 5.67 Permeate flux and rejection during the CF filtration of BSA, myoglobin and their mixture through virgin PES 10 at 20 L/h CF; (a) pH = 6; (b) pH = 8.

At both pH values, pH = 6 (Figure 5.67(a)) and pH = 8 (Figure 5.67(b)), BSA permeate flux was the highest. Because BSA was rejected to 100 %, the rejection data are not displayed in the plots. It was found, that the rejection of myoglobin as single solution at pH = 6 increased during the filtration process and reached maximum after 1 hour. The flux values of mixture were the lowest and the rejection of myoglobin was 100 %. At pH = 8, myoglobin in single solution showed the lowest flux and constant rejection near 95 %. In general, higher fluxes were observed from tests performed at pH = 8.

Results from filtration experiments at 60 L/h CF are presented in Figure 5.68.

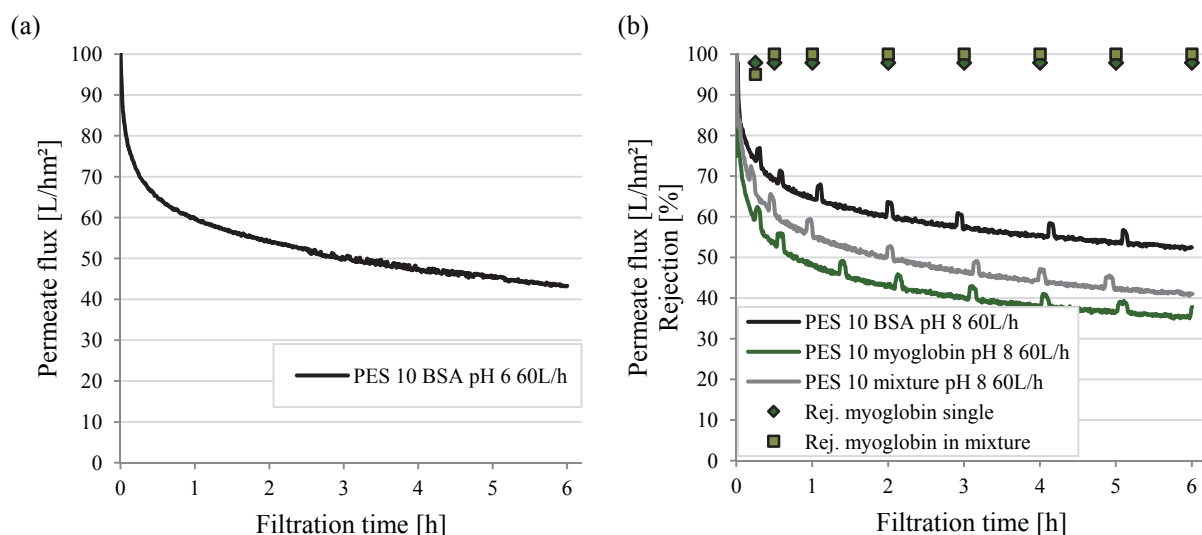


Figure 5.68 Permeate flux and rejection during the CF filtration of BSA, myoglobin and their mixture through virgin PES 10 at 60 L/h CF; (a) pH = 6; (b) pH = 8.

At pH = 6 (Figure 5.68(a)), the permeate flux of BSA changed over time like at 20 L/h CF but was found to be slightly higher. The fluxes measured at pH = 8 resembled the data observed at pH = 6 but the rejection of myoglobin alone increased to 100 % (Figure 5.68(b)).

Flux recovery from cleaning experiments is summarised in Appendix A, Figure 30 and Figure 31. Higher flux recovery from mechanical cleaning was measured at pH = 8. In contrast, the contribution of chemical treatment to the increase in flux recovery was lower.

5.3.5.2.2 PES 30

The performance of PES 30 was tested in similar experiments (see Section 5.3.5.2.1). Results from filtration runs at 20 L/h CF are visualised in Figure 5.69.

At pH = 6 (Figure 5.69(a)), BSA permeate flux decreased strongly in the early stage of the filtration. After 3 hours, the BSA flux approached the permeate flux of myoglobin and remained similar over the tested period of 6 hours. The permeate flux of protein mixture was slightly lower. BSA was completely rejected by PES 30. Myoglobin rejection in single solution after 15 minutes was 30 % but increased rapidly and reached 85 % after 4 hours. In mixture, myoglobin was firstly rejected to 70 % and after 2 hours to 90 %.

At pH = 8 (Figure 5.69(b)), higher permeate fluxes were obtained. Furthermore, the initial rejection of myoglobin in single solution increased to more than 60 %; in mixture, myoglobin was rejected to the same extent as in single solution.

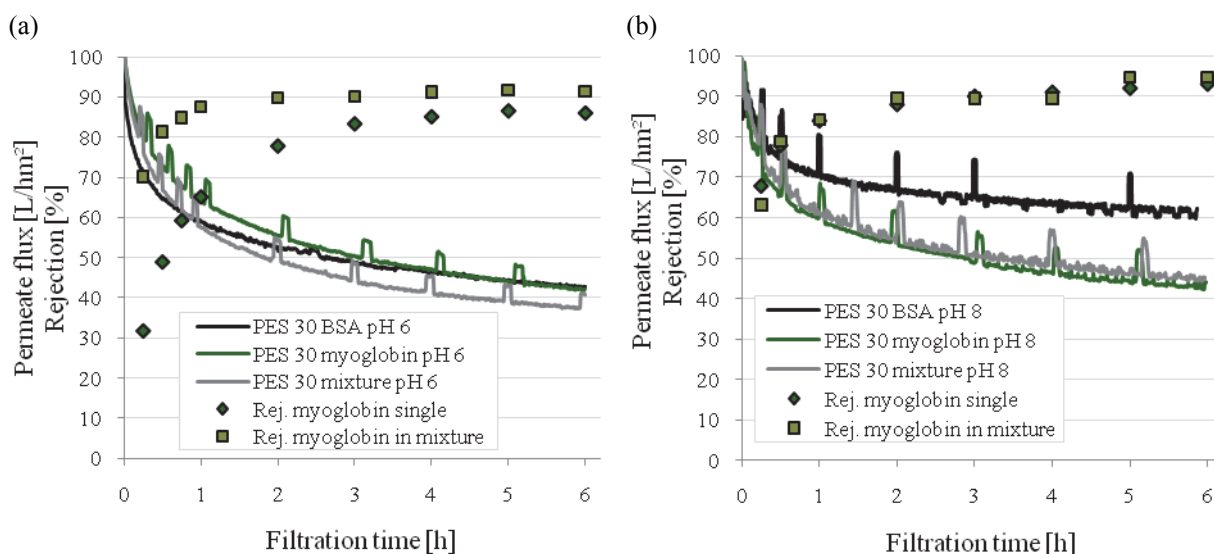


Figure 5.69 Permeate flux and rejection during the CF filtration of BSA, myoglobin and their mixture through virgin PES 30 at 20 L/h CF; (a) pH = 6; (b) pH = 8.

When filtration experiments were performed at pH = 8 and 60 L/h CF, similar permeate fluxes to 20 L/h were measured, as it can be taken from Figure 5.70. Slightly higher rejection values for myoglobin were observed at this CF.

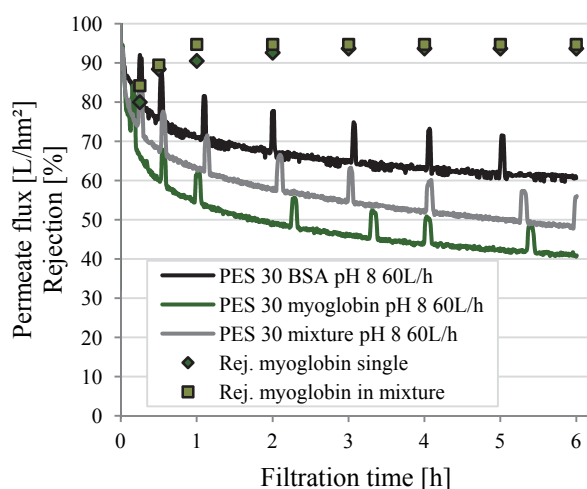


Figure 5.70 Permeate flux and rejection during the CF filtration of BSA, myoglobin and their mixture through virgin PES 30 at 60 L/h CF and pH = 8.

During the cleaning tests with PES 30, similar results to the findings for PES 10 were obtained (summarised in Figure 32 and Figure 33 in Appendix A).

5.3.5.2.3 PES 50

5.3.5.2.3.1 Virgin membranes

CF filtration experiments were done with virgin PES 50. At the accordant low operating pressure (see Table 5.15), a CF of 60 L/h could not be adjusted due to technical limitations. The permeate flux and rejection results at 20 L/h CF are shown in Figure 5.71.

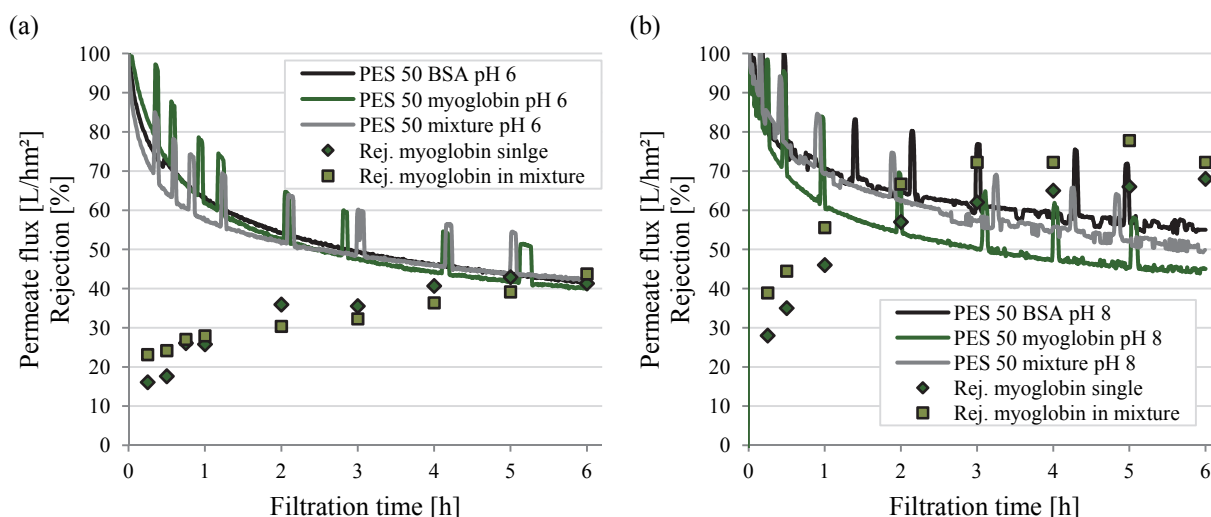


Figure 5.71 Permeate flux and rejection during the CF filtration of BSA, myoglobin and their mixture through virgin PES 50 at 20 L/h CF; (a) pH = 6; (b) pH = 8.

At pH = 6, the permeate curves of the tested solutions differed in their initial slopes but after 2 hours similar fluxes were obtained over the analysed period (Figure 5.71(a)). BSA was rejected to 100 % by virgin PES 50, whereas myoglobin rejection in single solution increased from around 15 % to 40 % over 6 hours. Slightly higher rejection of myoglobin in mixture was also detected. The permeate flux increased when filtration tests were performed at pH = 8 (Figure 5.71(b)). This effect was less pronounced during filtration of single myoglobin solution: myoglobin exhibited lower flux compared to BSA and mixture. Single myoglobin was rejected to 30 % at the beginning of the process and further to 70 %. Again, slightly higher rejection values were measured for myoglobin in mixture.

Cleaning with water increased the water flux slightly. Chemical cleaning was more effective and led to flux recovery up to 80 %. In general, higher values were measured for membranes used at pH = 8. The conducted data can be found in Figure 34 in Appendix A.

5.3.5.2.3.2 Functionalised membranes

PEGMA functionalised membranes (40/0) prepared with 5 J/cm² and 11 J/cm² UV irradiation dose were tested in CF filtrations. Here, solution pH and CF were also varied. Permeate flux and rejection data from filtrations at 20 L/h CF are presented in Figure 5.72.

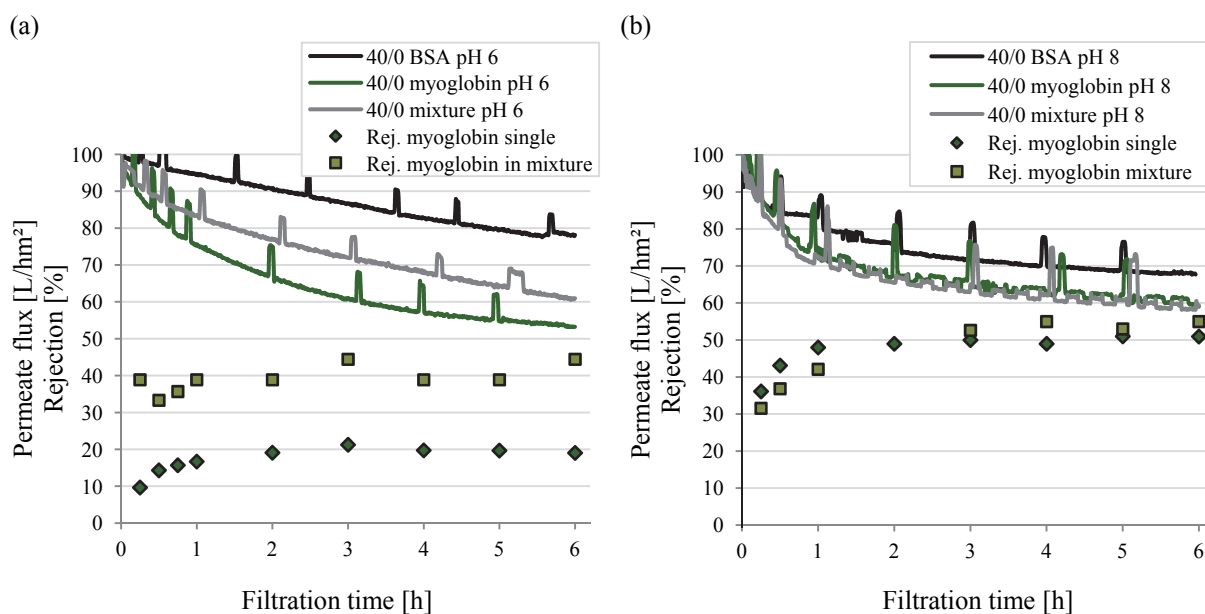


Figure 5.72 Permeate flux and rejection during the CF filtration of BSA, myoglobin and their mixture through PES 50 modified with 40/0 5 J/cm² at 20 L/h CF; (a) pH = 6; (b) pH = 8.

At pH = 6 (Figure 5.72(a)), linear flux curve from filtration of BSA was observed. The flux decreased to 80 L/hm² after 6 hours. BSA was rejected completely by the tested membranes. The permeate flux of single myoglobin solution decreased stronger to 53 L/hm² and the curve behaved non-linear. Myoglobin in single solution was rejected initially to 10 %. After 1 hour the rejection increased to 20 % and did not change further over the filtration period. The almost linear curve obtained for the permeate flux of mixture reached 60 L/hm² after 6 hours. The myoglobin rejection in mixture was nearly constant around 40 % over 6 hours. During filtrations at pH = 8 presented in Figure 5.72(b), permeate flux behaviour did not change significantly. The rejection of myoglobin in single solution was initially 30 % and increased further to 50 %. Slightly stronger change in rejection over filtration time was obtained for myoglobin in mixture.

CF filtration test of protein mixture was performed with PES 50 modified with 40/0 and 11 J/cm². The obtained permeate flux is presented in Figure 5.73.

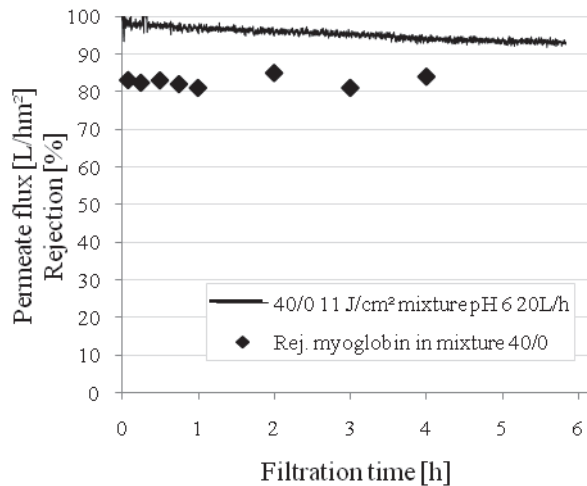


Figure 5.73 Permeate flux during CF filtration of mixture through PES 50 40/0 11 J/cm² at 20 L/h CF.

As it can be seen, very high flux was obtained with this membrane. The flux decreased linearly only to 93 L/hm³ for 6 hours of filtration and the rejection of myoglobin remained stable around 80 %.

The performance of the modified membranes at 60 L/h CF is presented in Figure 5.74.

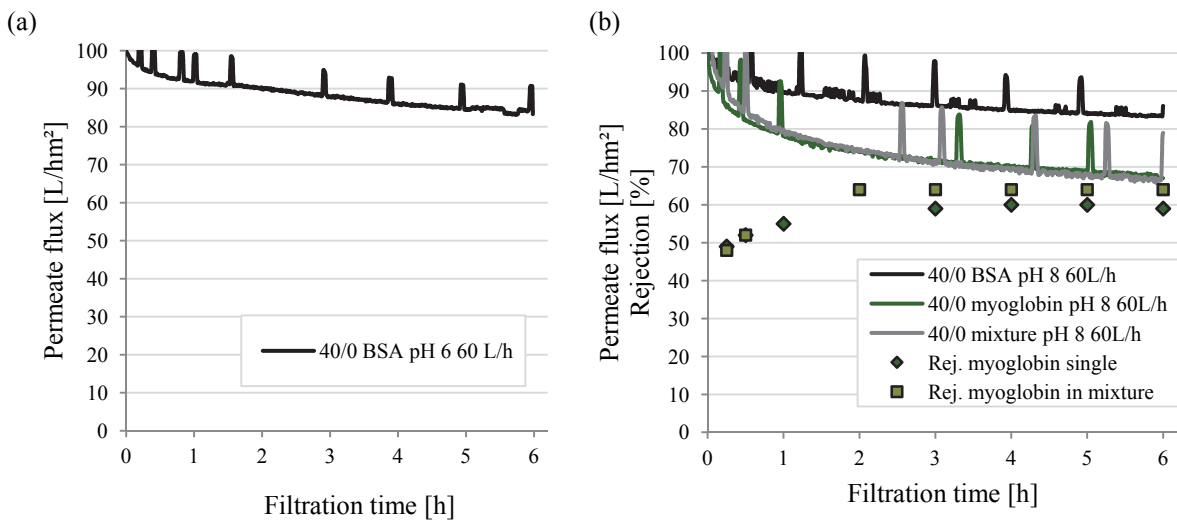


Figure 5.74 Permeate flux and rejection during the CF filtration of BSA, myoglobin and their mixture through PES 50 modified with 40/0 5 J/cm² at 60 L/h CF; (a) pH = 6; (b) pH = 8.

The permeate flux during filtration of BSA at pH = 6 decreased non-linearly and after 6 hours reached 85 L/hm² (Figure 5.74(a)). Similar flux behaviour was found when BSA was filtered at pH = 8 (Figure 5.74(b)). Here, myoglobin and mixture permeate fluxes reached 68 L/hm² with myoglobin rejection increasing from 50 % to 60 % over the filtration period of 6 hours.

Results from the performed cleaning tests of functionalised membranes are summarised in Figure 35 and Figure 36 (Appendix A). The obtained data were similar to the findings from cleaning after DE filtrations – compared to virgin membranes, higher flux recovery was measured.

5.3.5.3 Stability

Stability tests with virgin and modified membranes were performed in order to estimate the membrane behaviour after several cleaning procedures. Here, three cycles of filtration and cleaning were carried out with BSA, myoglobin and their equimolar mixture at pH = 6.

5.3.5.3.1 Virgin membranes

The stability of virgin PES 10 during filtration of BSA, myoglobin and their mixture at pH = 6 was investigated. The obtained results for resistance during filtration and flux recovery during cleaning are presented in Figure 5.75.

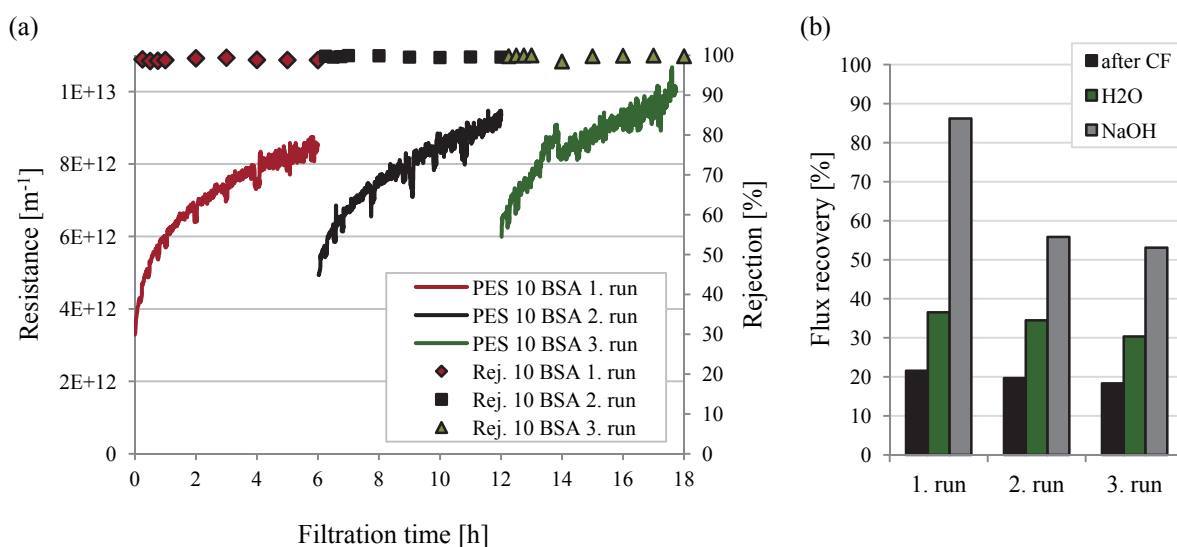


Figure 5.75 Filtration stability test of virgin PES 10 with BSA at 20 L/h CF; (a) resistance and rejection; (b) flux recovery after the cleaning procedures.

In the first run (Figure 5.75(a), red line), the resistance increased over time, as it can be derived from the decrease in permeate flux (Figure 5.67(a)). The second run (black line) started after 6 hours with higher resistance compared to the first run. The resistance increased further and at the end of the run (12 hours) reached higher value than at the end of the first run (after 6 hours). Similar behaviour was found during the third run. The rejection of BSA remained 100 % over the whole cycle. From the flux recovery data obtained after each filtration run presented in Figure 5.75(b), it was found that the flux recovery after chemical cleaning decreased after every run. After the third cleaning run, flux recovery

of around 50 % was achieved. This finding corresponded to the decreasing initial flux (increasing resistance) at every further run.

Similar results were obtained from stability test with BSA at 60 L/h shown in Figure 37 (Appendix A). The behaviour of increasing resistance during stability tests was also found when myoglobin and mixture were tested. The results can be found in Figure 38 and Figure 39 in Appendix A.

5.3.5.3.2 Functionalised membranes

PES 50 modified with PEGMA (40/0) and 5 J/cm² were also tested in three subsequent filtration and cleaning runs. Resistance and flux recovery obtained from experiments with BSA at pH = 6 and 20 L/h are summarised in Figure 5.76.

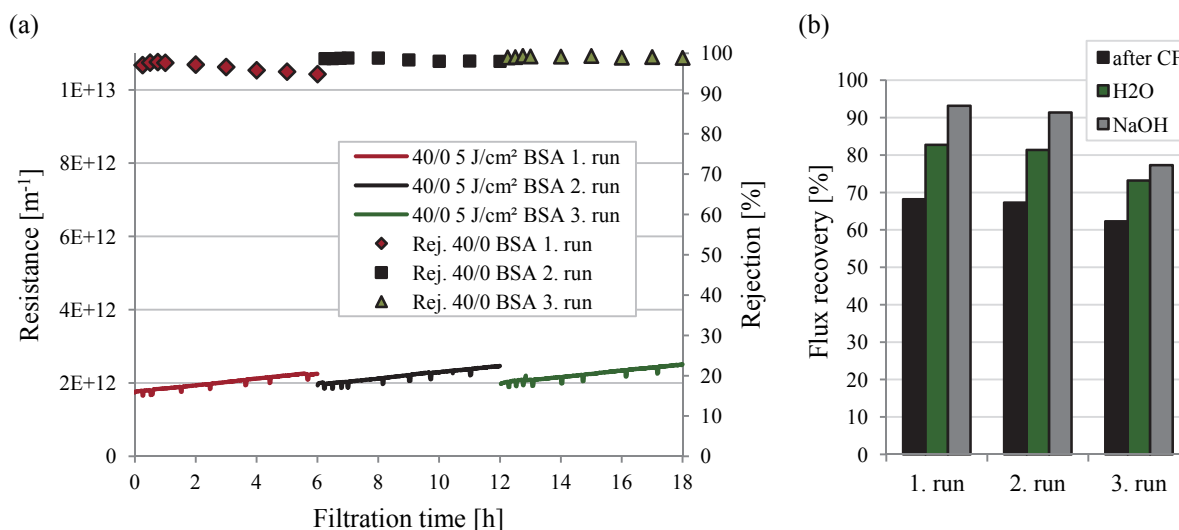


Figure 5.76 Filtration stability test of PES 50 modified with 40/0 5 J/cm² with BSA at 20 L/h CF; (a) resistance and rejection; (b) flux recovery after the cleaning procedures.

In Figure 5.76(a) can be seen that the resistance increased slightly and linearly during each filtration run. Only slight increase in the initial resistance in each run was detected. BSA rejection remained stable over the complete test. The obtained cleaning data showed slight decrease in the flux recovery after every cleaning run (Figure 5.76(b)). After the third run, 80 % flux recovery was measured.

Stability tests were also performed with myoglobin and protein mixture. The summarised data in Figure 40 and Figure 41 (Appendix A) for modified membranes showed stable resistance behaviour over three filtration and cleaning runs. The rejection of myoglobin remained unchanged during the test at 20 % for single solution and 40 % in mixture.

5.3.6 FILTRATION OF HUMIC ACID

The complete spectrum of virgin and modified membranes was used in filtration experiments with HA. The operating parameters, membrane characteristics and measured rejection and mass of deposits from the performed experiments are listed in Table 5.16.

Table 5.16 Summary of the operating parameters and measured data from the DE filtration of humic acid through virgin and modified membranes

Membranes	UV irradiation dose [J/cm ²]	Water permeability [L/hm ² bar]	Cut-off [kDa]	Pressure [bar]	Initial flux [L/hm ²]	Rejection [%]		Mass of deposited layer [g/m ²]	
						8 µm	0.45 µm	8 µm	0.45 µm
PES 5 virgin		7.5	7	4	30	83	n.d.	27	n.d.
PES 10 virgin		190	42	0.5	95	82	48	51	1.63
PES 50 virgin		940	95	0.1	95	78	n.d.	31	n.d.
PES 100 virgin		680	350	0.15	102	80	49	54	5.07
PES 300 virgin		1360	900	0.1	136	80	n.d.	51	n.d.
PES 5 modified	5	3.5	n.d.	4	14	95	n.d.	8.5	n.d.
PES 10 modified	5	30	20	3.5	104	91	88	46	6.2
PES 50 modified	9	130	30	0.75	100	79	48	22	6.99
PES 100 modified	11	280	120	0.35	99	77	47	42	5.98
PES 300 modified	14	750	bt	0.15	113	76	n.d.	30	n.d.

n.d.: not determined/experiment not done

bt: breakthrough

Similar to the experiments in protein filtration, the operating pressure was varied in order to adjust initial flux of 100 L/hm². As it can be taken from the data in Table 5.16, this value was not reached for PES 5 and PES 300 due to pressure limitations by the used set-up.

5.3.6.1 Virgin membranes

When HA solution prefiltered through 8 µm filter was used in experiments with virgin membranes, rejection values of about 80 % were obtained. They were slightly higher for membranes with lower nominal MWCO. From filtration experiments with 0.45 µm prefiltered feed through virgin PES 10 and PES 100, similar rejection was observed for both membranes (~ 50 %).

In the following Figure 5.77, permeate fluxes over 24 hours filtration period are shown. Results from filtrations of 8 µm prefiltered feed are presented in Figure 5.77(a) as relative flux due to the varied initial permeate fluxes, while fluxes from filtrations of 0.45 µm prefiltered solutions are visualised in Figure 5.77(b).

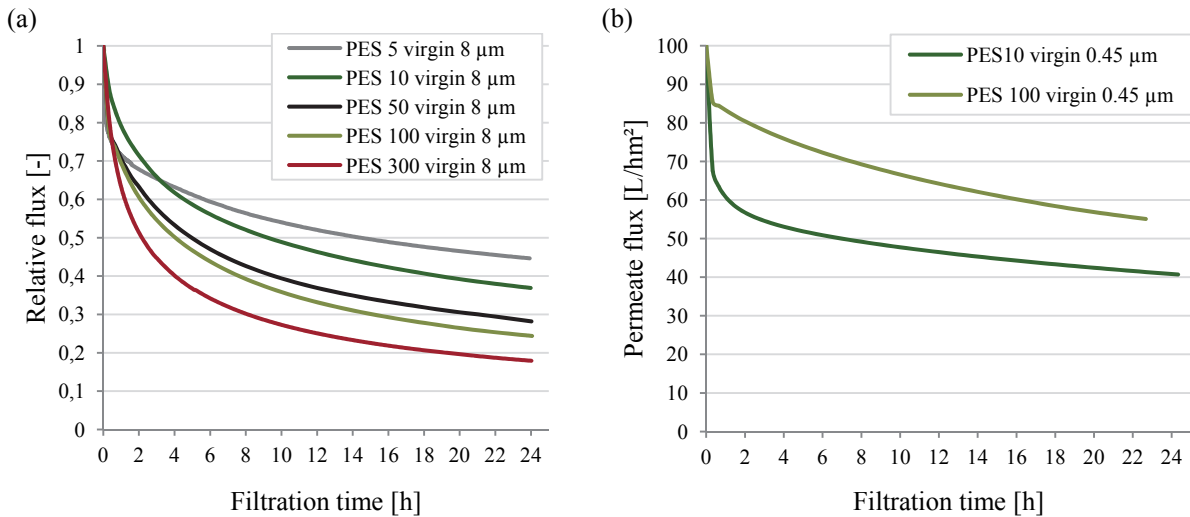


Figure 5.77 Flux behaviour during the DE filtration of humic acid through virgin membranes; prefiltration through (a) 8 µm and (b) 0.45 µm filter.

The filtrations of 8 µm prefiltered solution occurred with pronounced permeate flux decrease in the early stages of the processes. Stronger initial flux decrease was found for PES 5. Nevertheless, this membrane exhibited higher permeate flux in later stages. Furthermore, the flux depended on the nominal MWCO of the used membranes, i.e., less permeate flux was measured with increasing nominal MWCO so that PES 300 had the lowest flux. This tendency was not found during the filtration of 0.45 µm prefiltered HA solution. In contrast to the findings in [62], the filtration with PES 100 occurred with higher permeate flux compared to PES 10. In addition, flux decreased rapidly at the beginning of these filtrations. Comparing the results with the data from filtrations of 8 µm prefiltered solution, higher fluxes were obtained when 0.45 µm prefiltered solution was filtered [163].

Flux recovery data from mechanical and chemical cleaning after filtration of HA prefiltered through 8 µm and 0.45 µm filters are presented in Figure 5.78(a) and Figure 5.78(b), respectively.

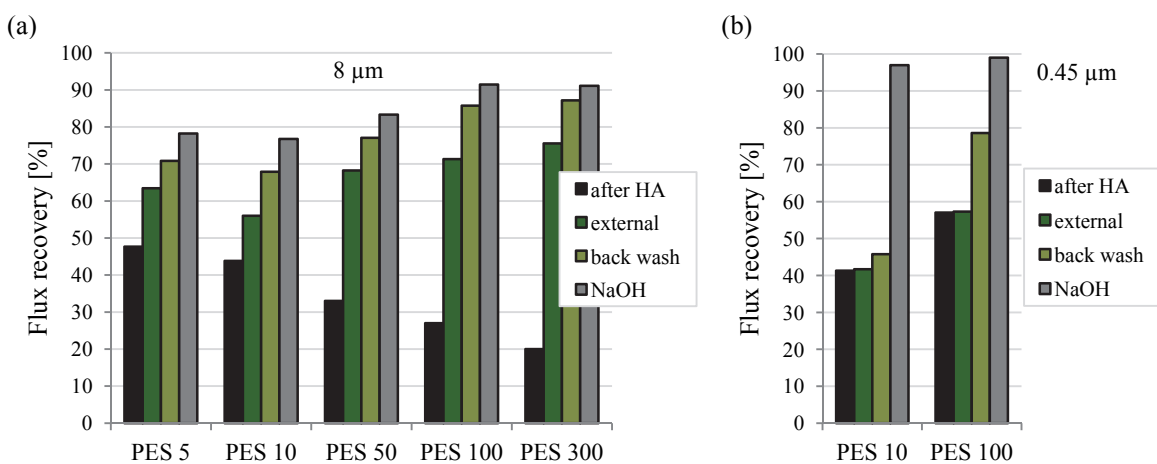


Figure 5.78 Flux recovery after cleaning; prefiltration through (a) 8 µm and (b) 0.45 µm filter.

In case of 8 μm prefiltered feed, external cleaning increased the membrane water flux leading to higher flux recovery. The effect of this first step in the cleaning procedure was found to be stronger for membranes with higher nominal MWCO. Subsequent back wash with water also increased the membrane flux resulting in recovery of more than 70 %. The membrane flux was further improved by chemical cleaning, where PES 100 and PES 300 reached 90 % of their initial flux. The external cleaning with water of membranes used in filtration of 0.45 μm prefiltered solutions did not increase the flux. However, back wash improved the membrane flux and was more effective for PES 100. After treatment with NaOH water flux was recovered to nearly 100 %.

5.3.6.2 Functionalised membranes

As it can be seen in Table 5.16, for filtration tests with HA, virgin membranes were modified at varied UV irradiation doses between 5 J/cm² and 14 J/cm² in order to avoid strong flux decline for membranes with smaller nominal MWCO due to modification (deduced from water flux measurements of membranes with varied nominal MWCO modified with same UV irradiation dose (cf. relative flux data in Table 5.4)).

The rejection of HA decreased with increasing nominal MWCO. PES 5 and PES 10 showed higher rejection compared to the corresponding virgin membranes. In contrast, PES 100 and PES 300 rejected less HA than the virgin membranes.

The relative fluxes during filtration of 8 μm prefiltered solution and the permeate fluxes for filtration of 0.45 μm prefiltered HA are further presented in Figure 5.79(a) and Figure 5.79(b).

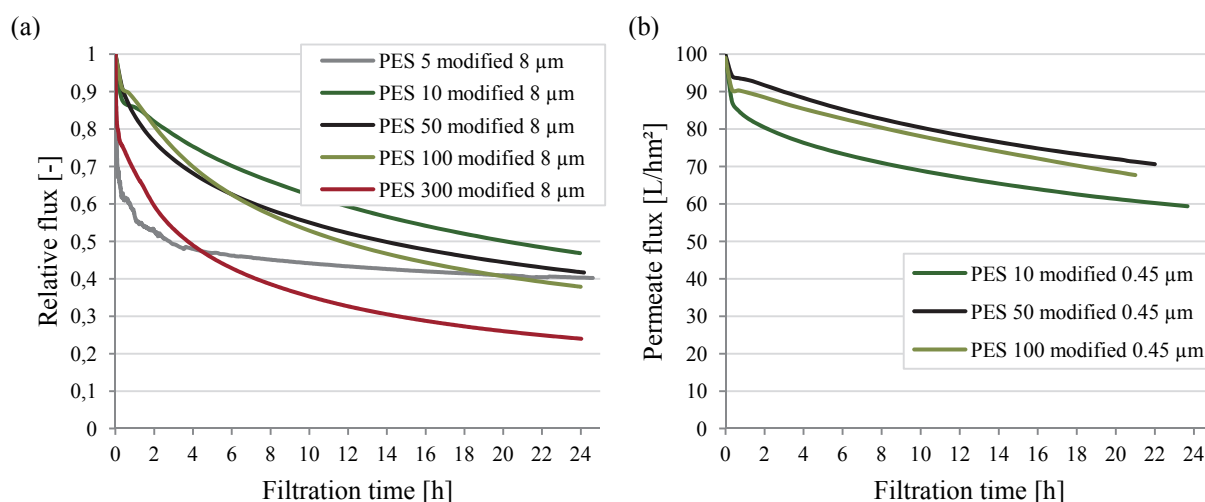


Figure 5.79 Flux behaviour during the DE filtration of humic acid through modified membranes; prefiltration through (a) 8 μm and (b) 0.45 μm filter.

During experiments with 8 μm prefiltered HA solutions, PES 5 lost permeate flux very rapidly at the beginning of the filtration process but the flux did not decrease significantly in the further examined period. With exception of PES 5, the relative flux decreased with increasing nominal MWCO in analogical way to the results for virgin membranes. When experiments were performed with 0.45 μm prefiltered solution, higher permeate fluxes were observed. Best performance was found for modified PES 50 followed by PES 100 and PES 10.

Flux recovery data from cleaning tests of modified membranes are summarised in Figure 5.80.

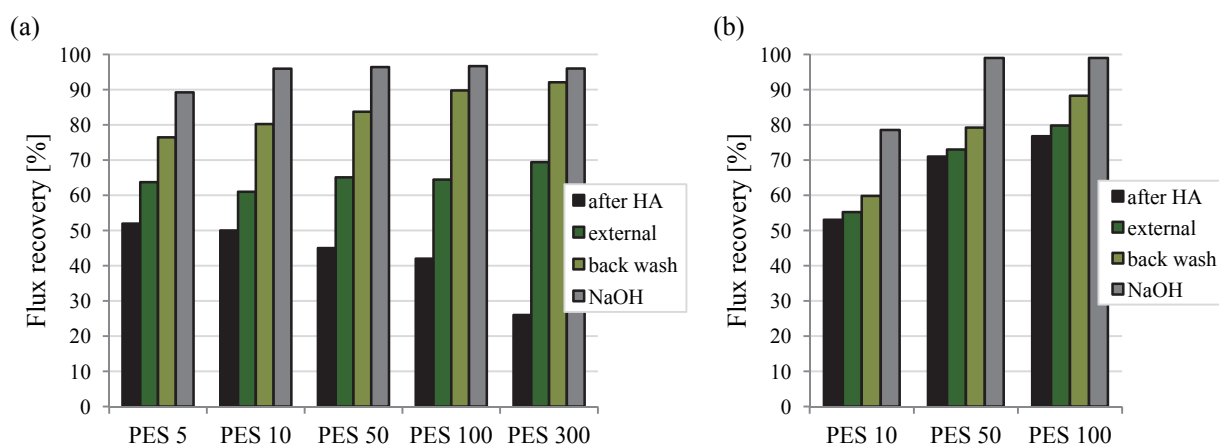


Figure 5.80 Flux recovery after cleaning; prefiltration through (a) 8 μm and (b) 0.45 μm filter.

From Figure 5.80(a) can be taken, that mechanical cleaning increased the flux of membranes used in filtration of 8 μm prefiltered solutions. The effect was stronger for membranes with higher nominal MWCO, where PES 100 and PES 300 reached 90 % of their initial flux. After chemical cleaning, the flux recovery averaged 95 %. The contribution of mechanical cleaning was not so pronounced for membranes used with 0.45 μm prefiltered HA (Figure 5.80(b)). It contributed only to 10 % flux increase. After chemical cleaning, PES 50 and PES 100 reached their initial water fluxes.

Mechanical cleaning was more effective for membranes used in experiments with 8 μm prefiltered solutions. This fact was also evident from photographic images. Exemplarily, the outer surface of modified PES 10 after each cleaning step is visualised in Figure 5.81.

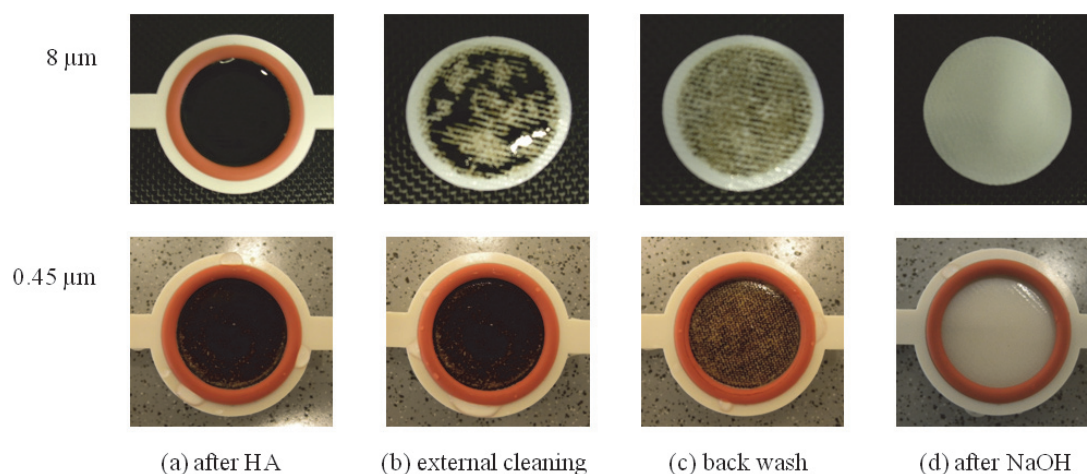


Figure 5.81 Photographic images of the membrane outer surface of modified PES 10 after each stage of the cleaning procedure; up – prefiltration through 8 μm filter; down – prefiltration through 0.45 μm filter; (a) after HA, (b) external cleaning, (c) back wash, (d) chemical cleaning with NaOH at pH = 13.

From the photographs of membrane which was used with 8 μm prefiltered solution, it can be recognised that the deposits were removed in big pieces by external cleaning; further back wash removed also big amount of deposited mass. The external cleaning of membrane from experiments with 0.45 μm prefiltered solutions was visibly not detectable but back wash removed some deposits [163]. After chemical cleaning, the membranes exhibited visibly clean surfaces.

5.3.7 FILTRATION OF POLYPHENOLICS

Polyphenolics extracted from green tea were filtered in DE and CF mode. In this section, the results are focused on virgin PES 5 and PES 50 as well as PES 50 modified with PEGMA 400.

5.3.7.1 Short stirred dead-end filtration

Short DE filtrations with two fold volume reduction were performed. Beside virgin membranes, modified membranes with varied amount of MBAA and UV irradiation dose were tested.

The obtained fouling resistance data from these experiments are presented in Figure 5.82 for virgin and modified membranes 40/0 and 40/4. Very low fouling resistance has been found for virgin PES 5. Unmodified PES 50 performed better with fouling resistance of nearly 0.6. Similar tendency has been found during static adsorption experiments with PES 10 and PES 100 [164]. Modified membranes showed improved fouling resistance to polyphenolics. At moderate UV irradiation doses (5 J/cm^2) $R_f > 1$ was obtained for several membranes. This means that the water flux after filtration of polyphenolics exceeded the initial value. Further modification (higher UV irradiation doses) led to a decrease in the fouling resistance.

The average permeability data during filtration can be found in Figure 42 (Appendix A). The obtained results showed that the permeability decreased with increasing UV irradiation dose.

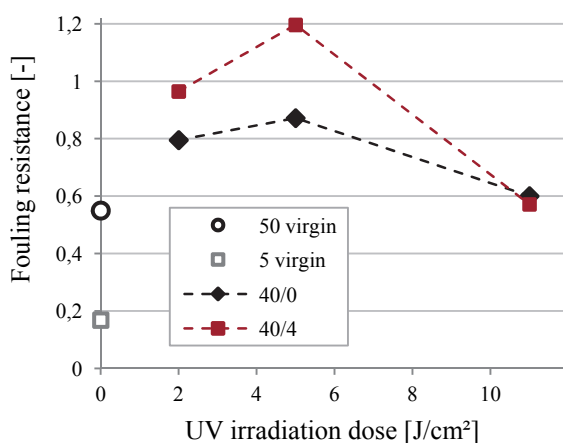


Figure 5.82 Fouling resistance to polyphenolics of virgin and modified membranes depending on the UV irradiation dose.

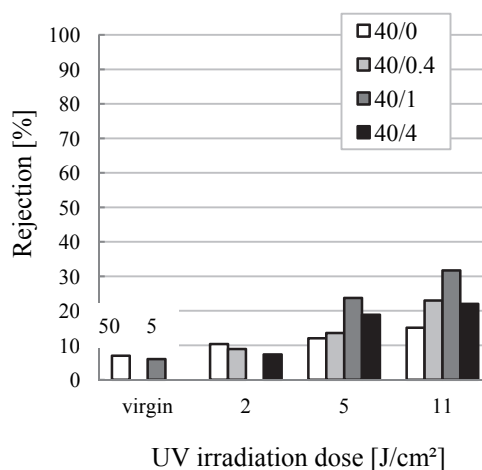


Figure 5.83 Polyphenolics apparent rejection of virgin and modified membranes vs. UV irradiation dose.

Moreover, the apparent rejection of the tested membranes was measured. As presented in Figure 5.83, both virgin membranes rejected polyphenolics to less than 10%. Modified samples showed higher rejection, where MBAA slightly affected the polyphenolics retention. The rejection increased with

increasing amount of MBAA and reached maximum at membrane modifications with 40/1. Nevertheless, the polyphenolics were not rejected to more than 30 %.

5.3.7.2 Cross-flow filtration

CF filtrations with virgin and modified PES 50 were carried out.

From experiments with virgin membranes, a critical pressure of 0.18 bar and a critical flux of 90 L/hm² were measured. The effect of operation pressure was examined in filtration runs at 0.25 bar, 0.5 bar, 1 bar and 3 bar. The obtained results in terms of relative flux are presented in Figure 5.84. The initial permeate flux values corresponding to the applied pressure are included in the legend. The filtrations were performed at higher initial fluxes than the observed critical flux (the critical flux was measured during the pressure increase to the desired operating value). The relative flux decreased initially and after 40 minutes remained constant over the studied 4 hours. As it can be seen, the increase of operation pressure caused lower relative fluxes.

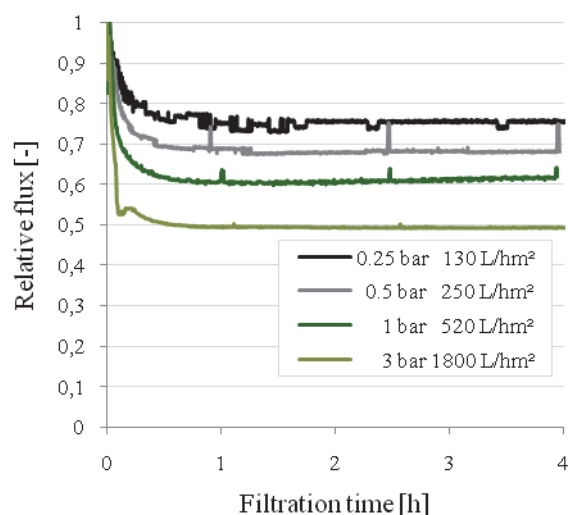


Figure 5.84 Permeate flux ratio during the CF filtration of polyphenolics through virgin PES 50 depending on the operating pressure.

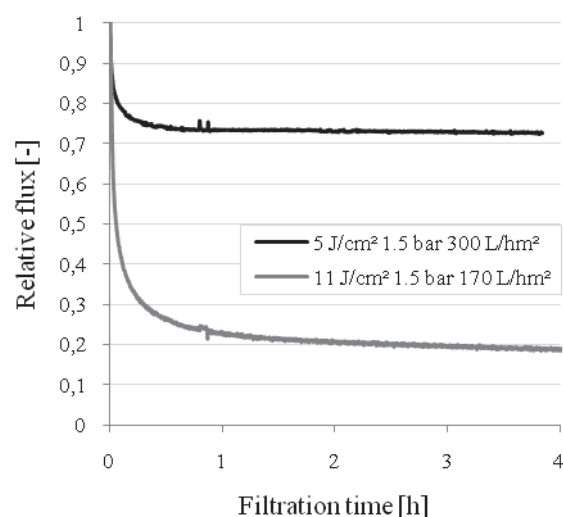


Figure 5.85 Permeate flux ratio during the filtration of polyphenolics through PES 50 modified with 40/0 under variation of the UV irradiation dose.

Experiments with modified membranes with varied UV irradiation dose were performed at 1.5 bar (Figure 5.85). Modification with PEGMA 400 without MBAA was applied. The obtained relative flux curves had similar shape to the curves for virgin membranes. For modified membrane with 5 J/cm², higher relative flux was measured in comparison to the result at 0.5 bar for virgin membranes (similar initial flux). Lower relative flux has been found for modified PES 50 with 11 J/cm².

6 DISCUSSION

6.1 MEMBRANE CHARACTERISATION

In this section, results obtained from the performed characterisation experiments with virgin and functionalised membranes will be discussed. The effects of membrane morphology and additives on the properties of virgin membranes will be explained based on the results obtained from wettability and surface charge measurements. Moreover, the flux reduction due to membrane compaction will be described by means of membrane morphology. Regarding functionalised membranes, the contribution of the virgin membranes to water flux and wettability of composite membranes will be explained. Further, the impact of UV intensity and crosslinking on membrane water flux and rejection will be discussed. Finally, the improvement of membrane properties by the applied functionalisation will be validated by comparison with virgin membranes with similar water flux and dextran rejection.

6.1.1 VIRGIN MEMBRANES – MEMBRANE MORPHOLOGY AND CHEMISTRY

In this work, the effect of membrane morphology by means of pore size and structure is studied. The membrane morphology is found to affect the membrane properties. As already seen in Table 5.1, contact angles decrease with increasing membrane nominal MWCO. Similar results have been reported and explained to be a result from the increasing surface roughness with increasing MWCO [165,166]. However, in this work, surface roughness was not measured in dependence of the membrane MWCO. This finding could be explained by the interactions between membrane, water and air bubble during the wettability measurement. The sample is preconditioned in water, i.e., the pores are filled with water. When air bubble is introduced to the membrane surface, it tends to contact to a lesser extent more hydrophilic surfaces. Thus, when more water is in contact with the air bubble, i.e., in case of relatively bigger pores, the membrane surface appears more hydrophilic.

The contribution of the membrane pores and structure to the measurement of surface charge with consideration of the cell conductivity is also studied. Experiments with variation of the cell gap height are performed according to [155]. The results in Figure 5.7 show that the zeta potential of membranes with sponge-like structure is affected stronger by the cell gap height than the zeta potential of membranes with finger-like structure or non-porous surfaces. The convection of KCl solution in the porous structure contributes to the apparent surface charge, which is measured at relatively small gap heights. This effect is more pronounced for sponge-like surfaces due to their larger, interconnected pores and more open pore structure, compared to finger-like membranes with small pores on the membrane surface limiting the diffusion. These findings are supported by the extrapolation of the

streaming current coefficient and the cell conductivity to zero (shown in Figure 5.8 and Figure 5.9, respectively). Nevertheless, the effect of pores on the streaming current coefficient is not so strong pronounced compared to the results presented in [155]. In contrast, the cell conductivity is affected by the sample morphology. The more open structure of sponge-like membranes contributes to the cell conductivity, since the conductivity of KCl solution in the membrane pores is measured.

From membrane compaction experiments, another effect of the membrane cross-section structure is found. As it can be seen in Table 5.4, due to compaction, the water flux of PES 100 is reduced to lower extent compared to membranes with finger-like structure. From these results can be concluded that the structure of sponge-like membranes behaves in a more stable manner against high pressure than finger-like membranes.

The effect of the additive PVP on the membrane behaviour is also studied. Bigger pores are observed for the membrane without PVP classified by the producer as PES 30 (from SEM (Figure 5.14) and rejection experiments with dextrans (Table 5.5)) but less water flux (Table 5.4) compared to the corresponding membrane prepared with PVP. In addition, this additive increases the membrane hydrophilicity (CA data in Table 5.1). From here can be concluded that the addition of PVP enhances the membrane prewetting behaviour, which leads to increased water flux. The presence of PVP reduces the membrane fouling tendency to dextrans due to the increased hydrophilicity (fouling resistance to dextran, Table 5.5), as reported in [81], and to proteins (cf. Table 5.8).

6.1.2 FUNCTIONALISED MEMBRANES

6.1.2.1 Effect of the UV irradiation on membrane structure

The impact of UV irradiation on the membrane material itself will be discussed by means of membrane water flux, fouling and rejection of dextran. UV irradiation of PES 50 in water with 11 J/cm² reduces the water flux approximately to 85 % (Table 5.4); same irradiation does not influence the rejection curve significantly (Figure 5.30), since the curve shift is within the tolerance limit (Appendix A, Figure 10). In addition, SEM images of a skin layer cross-section show change in the polymer of membranes irradiated in water (Table 5.16), which may be contributed to crosslinking taking place. In contrast, modification with PEGMA at same UV irradiation dose leads to crossing of the rejection curves of virgin and modified membranes for some membranes, as it can be seen in Figure 5.32 from results obtained with PES 10. This effect is evidence for occurred pore degradation in the barrier layer due to UV irradiation. In addition, the extent of pore degradation can be controlled by the UV irradiation dose, i.e., the hydrogel layer thickness (e.g., results obtained with PES 50, Figure 5.35). The occurred pore degradation detectable in the rejection curve for 8 J/cm² is shielded by

the applied hydrogel layer with 11 J/cm^2 . Nevertheless, a quantitative estimation of the pore degradation effect by means of dextran rejection cannot be done due to the stronger fouling tendency of virgin membranes to dextran shown in Table 5.5 (the fouling resistance does not exceed 0.8, whereas composite membranes show R_f of 0.99).

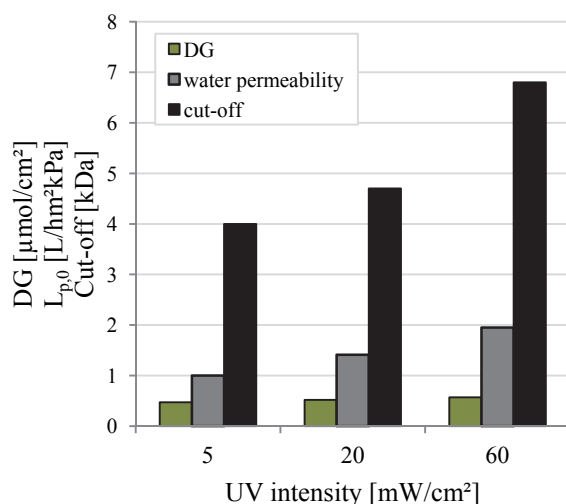


Figure 6.1 Effect of the UV intensity on DG, water permeability and cut-off of PES 50 40/0 11 J/cm².

Furthermore, the influence of the UV intensity is evaluated. Comparing the obtained results for DG, water permeability and cut-off from modification of PES 50 with 11 J/cm^2 at varied UV intensity, in Figure 6.1 can be seen that permeability and cut-off increase accompanied by a slight increase in DG as higher UV intensity is used. This means that at higher UV intensity the synthesis of more hydrogel on the membrane surface does not lead to lower membrane cut-off. He et al. [167] have prepared methacrylate based hydrogels via UV excitation and discussed that higher UV intensity provides more energy for initiation, leading to higher initial concentration of free radicals and a faster polymerisation rate, resulting in higher relative rates of intramolecular to intermolecular reactions. Higher UV intensity facilitates more intramolecular cyclisation, leading to a more “loose” or open hydrogel structure; while lower UV intensity induces more intermolecular reactions and thus, a more compact hydrogel structure. The obtained results from water uptake and MWCO of photopolymerised PVP/MBAA films by Wu et al. [168] support this statement: it has been found that both water uptake and MWCO increase when using high UV intensity. Another reason for these findings may be the assumption that the higher radicals concentration on the membrane surface caused by too high UV intensity possibly leads to pore degradation in the barrier layer, i.e. more open pore structure. To summarise, the increased radicals concentration on the PES surface may cause changes in the hydrogel layer structure (more “open” hydrogel structure) or termination reaction on the PES surface leading to pore degradation (more open pore structure). These findings are supported by the obtained protein rejection data from performed DE filtrations at two fold volume reduction (Table 5.9).

6.1.2.2 Effect of the crosslinker type and amount

The type and amount of the used crosslinkers have an impact on the membrane performance as well. As shown in Figure 5.24 and Figure 5.25, membrane water flux decreases for modifications with MBAA, whereas functionalisation with PETAE as crosslinker leads to higher fluxes. These effects are stronger pronounced when increasing the crosslinker concentration. Corresponding to these results, the rejection curves with dextrans shift. In general, MBAA decreases the membrane cut-off, whereas PETAE induces higher cut-off values. An increase in the concentration of the crosslinking agents amplifies these effects, as shown for PES 50 in Figure 5.40 and for PES 100 in Figure 5.42. These findings are confirmed by the rejection results from two fold volume reduction protein filtrations (cf. Section 5.3.5.1.1.1). Thus, grafted hydrogels crosslinked with MBAA exhibit much tighter structure (in particular, SEM images of the skin layer cross-section of modified PES 100 with MBAA in Figure 5.16 showed the build-up of thither skin layer with increasing the MBAA amount), whereas modification with PETAE leads effectively to more open, presumably surface covered pores.

Furthermore, the membrane morphology plays a role for the membrane behaviour depending on the crosslinking conditions. As shown in the results from water flux measurements (Section 5.3.1), dextran rejection analysis for PES 50 and for PES 100 in Figure 6.2 and protein rejection experiments (Section 5.3.5.1.1.1), the effects are most pronounced in the results for PES 50, i.e., stronger water flux decline, shift of the rejection curves and changes in the protein rejection due to the functionalisation and the applied crosslinkers. Similar trend is found for modified PES 50 and PES 100 with other UV irradiation doses, as presented in Appendix A, Figure 43.

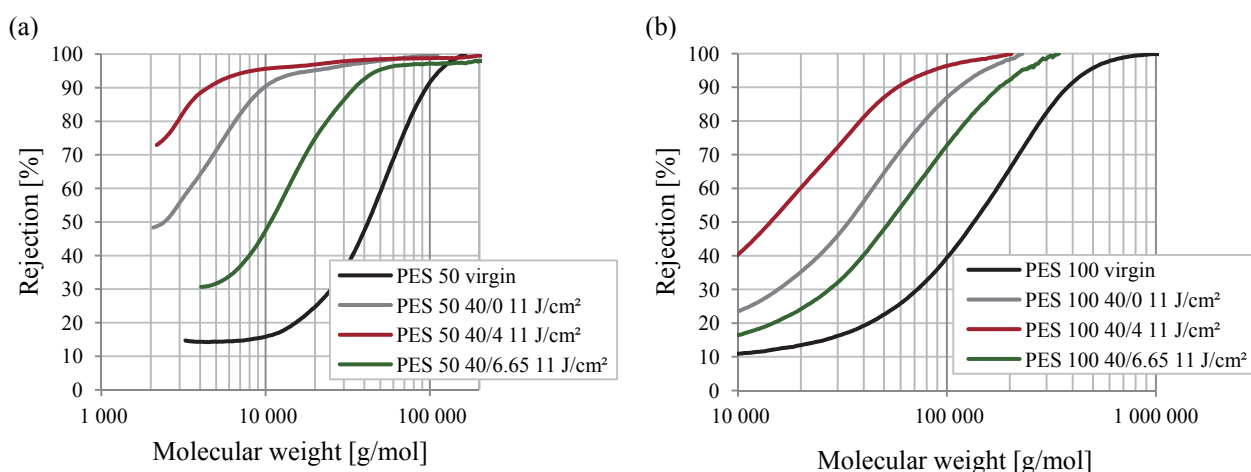


Figure 6.2 Effect of the crosslinking type on the rejection curves of modified membranes with 11 J/cm²; (a) PES 50; (b) PES 100.

In order to describe the mechanisms which govern the membrane selectivity behaviour, swelling data obtained with bulk hydrogels will be discussed. As shown in Figure 5.1, synthesised hydrogels with

MBAA swell less, with further decreasing swelling degree by increasing the MBAA amount. In contrast, hydrogels with PETAE as crosslinker swell more strongly and the increase in crosslinker amount amplifies this effect.

On the basis of these results, the hydrogel properties on the membrane surface and in the pore openings can be explained. Figure 6.3 is a schematic view of the proposed structures. Grey lines represent the polyPEGMA chains, whereas red and green lines visualise MBAA and PETAE containing segments, respectively.

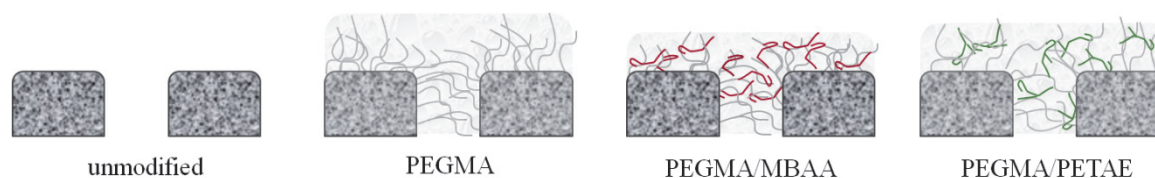


Figure 6.3 Schematic view of the effect of the crosslinking type on hydrogel structure.

Surface functionalisation only with PEGMA occurs on the membrane surface and in the pore openings. Thus, polyPEGMA grows at higher density and to longer chain lengths with increasing UV irradiation dose. The consequences are with increasing UV time an increasing coverage of the PES surface and narrowing or even blocking of the membrane pores. This effect is less pronounced for modifications with PEGMA 200 due to its shorter PEG chains (slightly lower rejection of BSA and myoglobin, cf., Figure 5.50). Even when the hydrogel layer completely covers the pores, it is permeable for convective flux but has significant hydraulic resistance and solute rejection which are a function of the polymer volume fraction in the same pore or a film of the same thickness, i.e., inversely proportional to hydrogel swelling degree. When MBAA is added, the polyPEGMA chains get simultaneously crosslinked during their growth. The layer topology is not significantly changed as compared to the not crosslinked case but the degree of swelling or mesh size (relevant for water flux and rejection) has a specific impact on membrane performance. In contrast, hydrogels prepared with addition of PETAE swell more than hydrogels prepared with PEGMA/MBAA or PEGMA only. It should be mentioned that the preparation of gel using only PEGMA may be possible by physical chains entanglement as well as by present impurities of PEGDA (caused by the synthesis path of PEGMA) [169] which can act as a chemical crosslinker.

The varied swelling of hydrogels prepared with different crosslinkers can be explained by the relative distance between the crosslinking points. In case of PEGMA/MBAA gels, the relative distance between the crosslinking points is smaller compared to hydrogels prepared with PETAE, since the MBAA molecule is smaller than PETAE.

Further point for the discussion of these results is the functionality of the applied crosslinkers and the conversion of the crosslinking points. Due to sterical hindrance, it may be assumed that the third double bond of PETAE may be not completely implemented into the hydrogel network leading to lower crosslinking efficiency. Hence, the PEGMA/PETAE hydrogel structure would be more swollen than the structure of the other hydrogels.

Another aspect which affects the swelling degree is the conversion of the monomers during the polymerisation. According to Table 1(c) in Appendix A, the conversion of the gel composition 40/6.65 decreased to 69 % compared to the conversion of gel 40/0. This means that the amount of polymer in the crosslinked gel PEGMA/PETAE is lower than the one in the PEGMA gel, which can lead to stronger swelling of the hydrogel network and to higher membrane water flux and lower rejection, respectively. However, the conversion of PEGMA hydrogels with lower PETAE amount is similar to the conversion of pure PEGMA hydrogel but the obtained results from hydrogel swelling (Figure 5.1), membrane water flux (Figure 5.25), some rejection curves (e.g., Figure 14(b), Appendix A) and protein rejection (Figure 5.51) show more “open” hydrogel network structure at higher DG (cf. Table 5.2) compared to pure PEGMA. From this point of view, it can be concluded that lower conversion can be a reason for less rejection, but the overall performance of the crosslinked membranes is governed by the PETAE crosslinking behaviour.

Furthermore, the molecule structure of the crosslinking agent may have an influence on the hydrogel behaviour. MBAA has more rigid structure compared to PETAE. In general, the molecule of MBAA shows limited flexibility due to the double bond character of the peptide bonds (caused by + M effect of N and – M effect of O). This can result in more rigid hydrogels with less swelling ability. The molecule of PETAE is relatively bigger and consists mostly of single C–C bonds, which makes PETAE more flexible. Thus, this leads to more flexible overall structure of the network, resulting in a stronger swelling.

6.1.3 VALIDATION OF THE IMPROVEMENT OF MEMBRANE PERFORMANCE BY COMPOSITE MEMBRANES

6.1.3.1 Fouling and rejection during rejection curve measurements

In Table 5.5 is shown that the cut-off obtained from PEG filtrations is lower than the cut-off obtained with dextrans. Reason for this variation can be the different hydrodynamic diameter of the tested solutes. It has been shown that at similar MWs, the hydrodynamic radius of PEG is bigger than that of a dextran molecule [158]. In other words, for similar hydrodynamic radii, the MW of dextran is higher than the MW of PEG. From this point of view, the cut-off of a certain membrane obtained with

dextran should be higher than the cut-off from PEG filtration. Another interesting point is the effect of the membrane functionalisation on this variation. For virgin membranes, the obtained cut-off values from filtration of PEG solutions are in average 10 fold lower than the cut-offs from dextran filtration, while for modified membranes, this factor is 3.5. When the apparent pore diameters calculated from the dextran and PEG cut-off values are compared (Table 5.5), i.e., the effect of the molecular shape on the cut-off values is eliminated, the factor for virgin membranes is 3 and for modified membranes – nearly 1. Moreover, the pore size values obtained with dextran are more close to the nominal pore sizes given by the producer. To explain these findings, fouling resistance data from the PEG and dextran filtration should be discussed. As already mentioned in Section 5.3.2.1, filtration of PEG through virgin membranes causes stronger flux decline in comparison to dextran. The flux decline can be caused by reversible adsorption of PEG, as reported by [170] from filtration experiments of PEG through PSf membranes. In other works [81,171], fouling of dextran on PES membranes due to adsorptive interactions has been reported. A comparison study about filtration of PEG and dextran solutions at same conditions [172] reported that the polarisation time for dextran filtration, i.e., the time necessary to reach 50 % flux decline was much higher than the polarisation time for PEG. Another work reported lower flux when PEG was filtered through PVDF membranes [173]. The results from [172,173] are in agreement with the stronger flux decline from PEG filtrations found in this work. It can be summarised that PEG causes stronger fouling on PES membranes than dextrans.

The operating conditions and feed composition are other important factors which may affect the rejection results. The occurring CP and possible fouling influence the membrane selectivity. Consequently these phenomena should be minimised by choosing the right CF rate/stirring conditions and operating pressure in order to characterise the membrane selectivity properly [174]. Thus, CP hinders the solute permeation increasing the rejection. Fouling (which is enhanced by increasing pressure (cf. Table 5.6)) may lead to pore blockage (especially of smaller pores), which can explain the increased rejection of PEG and (in general) the higher rejection of small molecules which are expected to pass the membrane unhindered. On the other hand, high pressure may lead to deformation of the solutes and consequently to increased transmission, which is confirmed in this study (cf. Figure 5.29(a)). Indeed, short-term filtrations of proteins support the upper observations, i.e., the applied hydrogel layer reduces the membrane fouling tendency (cf. Section 5.3.5.1.1.1).

To conclude, the evaluated results confirm that the performed surface functionalisation improves the fouling behaviour by shielding the membrane surface and reducing the membrane-solute interactions.

6.1.3.2 Rejection properties of membranes with similar water fluxes

In the following, the obtained water permeabilities and cut-off values for virgin and modified membranes will be compared. Aim is the evaluation of optimum performance depending on the requirements for the functionalised membranes. If high throughput at certain selectivity is necessary, the water flux of virgin and functionalised membranes with similar rejection properties can be compared. If high rejection and/or selectivity are needed, the rejection properties of membranes with similar initial water permeabilities should be analysed. Regardless the requirements (based on the membrane application), the functionalised membranes will have higher fouling resistance due to the grafted hydrogel. Therefore, evaluation of the performance of modified membranes compared to virgin ones in terms of dextran rejection and water flux is necessary. In Table 6.1, the collected data for water permeability, fouling resistance, permeate concentration (as measure for the selectivity when membranes with similar cut-off are compared) and cut-off are listed. The comparison will be done on the basis of water permeabilities of compacted membranes (in Table 6.1 marked with ^b).

Table 6.1 Determined parameters from dextran rejection tests with virgin and modified membranes

Membrane	Water permeability [L/hm ² bar]	Fouling resistance [-]	Concentration in permeate ^c [g/L]	Cut-off [kDa]
PES 5 virgin	17 ^a (8) ^b	0.63	0.07	7
PES 10 virgin	230 ^a (100) ^b	0.76	0.46	42
PES 30 virgin	580 ^a (200) ^b	0.75	0.63	92
PES 30 40/0 11 J/cm ²	30	0.99	0.16	7
PES 50 40/0 5 J/cm ²	165	0.98	0.40	31
PES 50 40/4 5 J/cm ²	71	0.95	0.29	23
PES 50 40/6.65 5 J/cm ²	312	0.99	0.48	44
PES 50 40/0 11 J/cm ²	100	0.99	0.42	10
PES 100 40/0 11 J/cm ²	195	0.99	0.63	120
PES 100 40/0 14 J/cm ²	169	0.98	0.62	110

^a water permeability of non-compacted membrane

^b water permeability of compacted membrane

^c feed concentration of 1 g/L

Direct comparison of the rejection properties for virgin and modified membranes with similar cut-off or initial water flux can be done with the help of the rejection curves plotted in Figure 6.4.

From the gathered data presented in Table 6.1 and Figure 6.4(a) can be deduced that modified PES 30 40/0 11 J/cm² show similar cut-off like virgin PES 5 but higher water flux, higher fouling resistance and better selectivity. Similar conclusions can be made for PES 50 40/6.65 5 J/cm² and virgin PES 10 (rejection curves are compared in Appendix A, Figure 44).

Another case can be discussed on the basis of Figure 6.4(b) and Figure 6.4(c). At similar water permeabilities, functionalised membranes show higher dextran rejection with better fouling resistance. The fouling tendency of these membranes is improved by the surface hydrophilisation with polyPEGMA. Similar results from the comparison of hydrophobic PES and hydrophilic cellulose-based membranes are presented in [81].

It should be noted that in the discussed examples, none of the functionalised membranes has apparent pore degradation effects in the rejection curves. From here can be concluded that the membrane surface functionalisation should be performed by choosing appropriate UV irradiation conditions and applying a sufficient amount of polyPEGMA layer in order to shield (or minimise) the occurred pore degradation.

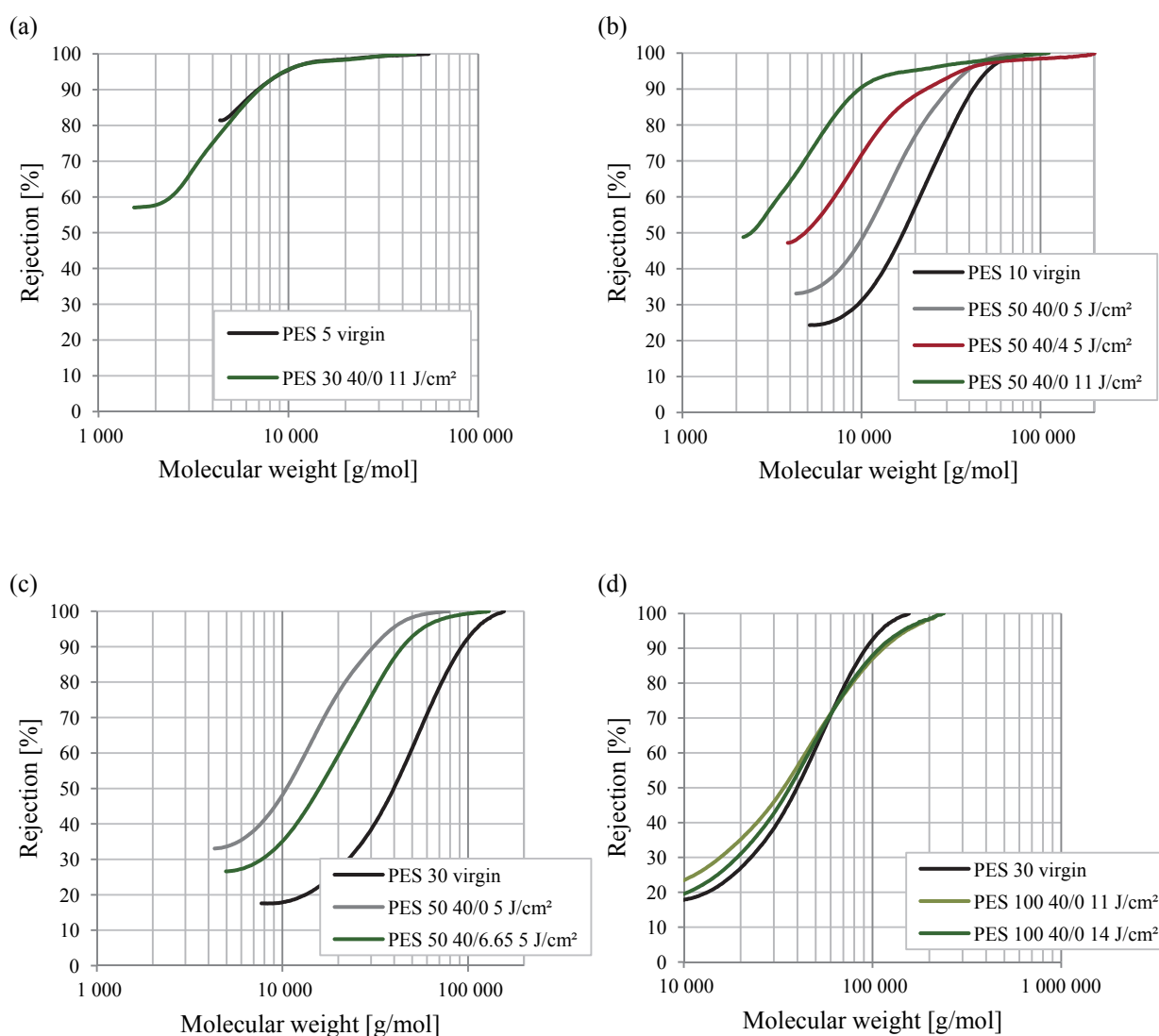


Figure 6.4 Comparison of rejection curves; (a) virgin PES 5 vs. modified PES 30; (b) virgin PES 10 vs. modified PES 50; (c) virgin PES 30 vs. modified PES 50; (d) virgin PES 30 vs. modified PES 100.

Interesting effects can be found when modified PES 100 membranes are compared with virgin PES 30. In this case, the virgin membrane has slightly higher water flux than the modified PES 100. As it can be seen in Figure 6.4(d), the rejection curves of the functionalised membranes are steeper than the rejection curve of virgin PES 30, resulting in higher cut-off. In comparison, modified PES 50 40/0 5 J/cm² with similar water flux shows higher dextran rejection (Figure 6.4(c)). This finding can be explained by the contribution of the membrane morphology to the water flux and selectivity. By combining the data from Table 5.4 and Table 5.5, the water permeability of virgin PES 100 is 1.5 times higher than that of virgin PES 50 but the cut-off is 4 times higher. When virgin membranes PES 10 and PES 50 with finger-like cross-section structures are compared, PES 50 shows 5 times higher water flux but only 2.5 times higher cut-off. From here can be concluded that membranes with sponge-like structure exhibit relatively lower water fluxes in comparison to membranes with finger-like structure. The porous support of finger-like membranes ensures high fluxes, while sponge structure increases the hydraulic resistance. In addition, by examining the rejection curves presented in Figure 5.28(a), relatively steeper curve is observed for virgin PES 100 compared to finger-like membranes, thus this is an indication for worse selectivity.

The contribution of the performed membrane functionalisation in terms of water flux reduction should be also taken into account. From Table 5.4 can be taken that modification with same UV irradiation dose leads to 1.4 fold higher relative water flux for modified PES 100 compared to modified PES 50. From the combination of the facts explained above emerges the effect that after modification with 11 J/cm² the cut-off for modified PES 100 is measured to be 12 times higher than the cut-off of functionalised PES 50. In comparison to that, modification of PES 10 with same UV irradiation dose leads to 4 times lower relative water flux and 2.5 times lower cut-off compared to PES 50. Hence, in case of similar water fluxes, sponge membrane will appear with higher cut-off and steeper rejection curve compared to membrane with finger-like cross-section structure. It should be considered in addition, that pore density and membrane thickness also affect the membrane performance. These parameters are not studied in the present work. Furthermore, considering all tested membranes with finger-like structure, it is found that the smaller the pores the stronger the contribution of the grafted hydrogel to the hydraulic resistance is. Nevertheless, from the presented results can be concluded again that the contribution of the functionalisation to the rejection curve shift for finger-like membranes is more pronounced compared to sponge-like membranes with similar water fluxes (i.e., productivity).

6.2 PROTEIN FILTRATION

6.2.1 GENERAL

In this section, the impact of feed properties (concentration, composition, solutes charge and MW) and membrane characteristics (charge, pore size, morphology, chemistry) on the filtration performance will be discussed. Hence, the contribution of membrane-solute and solute-solute interactions to the predominant fouling mechanisms will be explained. Furthermore, the filtration mode and the applied hydrodynamic conditions play an important role. Consequently, the effect of the varied parameters and conditions on membrane fouling, rejection and cleaning behaviour can be analysed. Finally, the contribution of the membrane functionalisation with hydrophilic agents to the improvement of the membrane performance will be investigated. In particular, performance comparison by means of productivity will be done with virgin and modified membranes with similar water flux and cut-off.

6.2.1.1 Charge effects

During filtrations of protein solutions, the filtration performance is affected by the type of protein solution and its properties, such as composition and pH. In order to discuss the obtained results, first, the protein nature and its contributions to the protein behaviour in aquatic solutions should be explained. Due to their amphiphilic character, proteins exhibit an IEP. Below the IEP they are positively charged, whereas above the IEP they exhibit negative charge. The charge of BSA and myoglobin depending on the pH is schematically viewed in Figure 6.5.

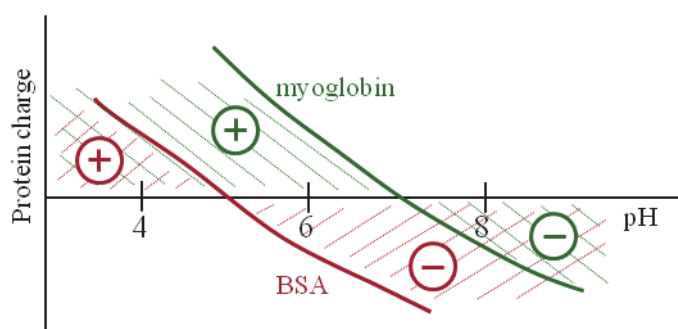


Figure 6.5 Protein charge of BSA and myoglobin depending on pH.

Due to the fact that BSA has its IEP at pH ~ 5 [83,175] and myoglobin at pH = 7 [176], their charge vary in the performed experiments (with pH variation). It is expected that at pH = 4 and pH = 8 both proteins have the same charge – both are positive or negative, respectively. At pH = 6, BSA is negatively charged, whereas myoglobin shows positive charge. Thus, attraction forces between the oppositely charged proteins can occur, which would lead to the presence of agglomerates in the protein mixture. The results from DLS measurements (Figure 6.6) confirm this statement.

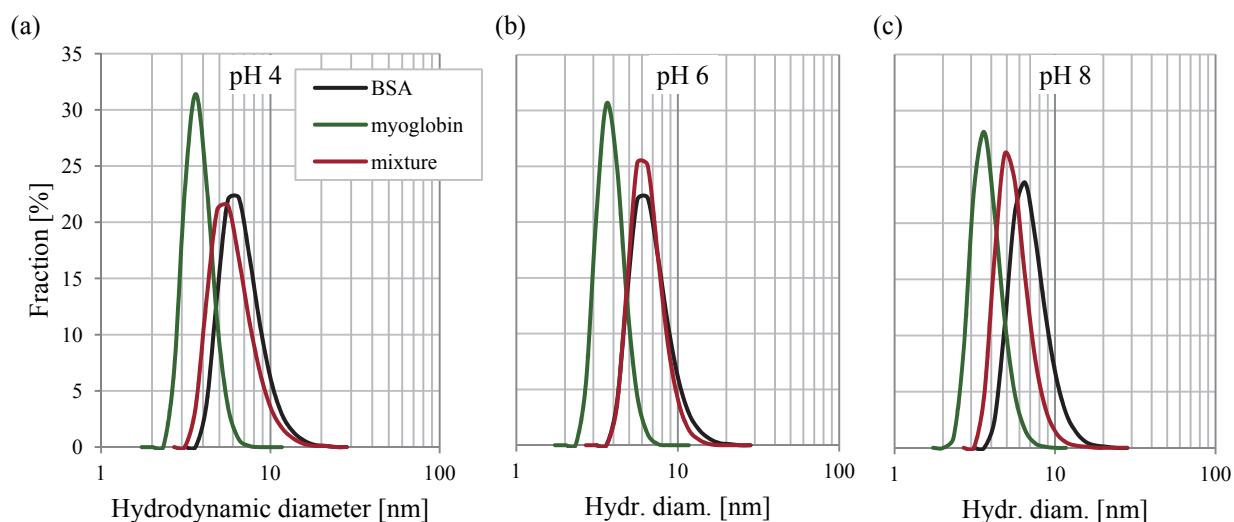


Figure 6.6 Effect of pH on the hydrodynamic diameter of BSA, myoglobin and mixture; (a) pH = 4; (b) pH = 6; (c) pH = 8.

At pH = 4 (Figure 6.6(a)) and pH = 8 (Figure 6.6(c)), myoglobin has the smallest hydrodynamic diameter, and BSA the largest, whereas the mixture is characterised with median hydrodynamic diameter. The apparent molecule size in mixture can be explained by contribution of both proteins to light scattering during the DLS measurement (since the hydrodynamic diameter distributions of the protein fractions are relatively close, the result for protein mixture resembles an overlapping). In contrast, at pH = 6, the protein mixture exhibits an apparent hydrodynamic diameter similar to BSA. Reason for that can be the presumable agglomeration of the oppositely charged proteins due to attraction. Nevertheless, an increase in the hydrodynamic diameter of the mixture measured by DLS was not detected. If agglomeration of oppositely charged molecules is assumed, the net charge of the agglomerate would differ from the charges of both proteins (expected to be less negatively charged compared to BSA). This will probably lead to another shape and hydrodynamic size which can be similar to the measured size of BSA. It should be considered that in mixtures, there is dynamic equilibrium between agglomerated and single proteins. At pH = 6, this equilibrium is shifted to the aggregate state, while at pH = 4 and pH = 8 it is more to the single state. Moreover, the results show that at pH = 6 the rejection of myoglobin increases when in mixture but no complete rejection is reached (e.g., through virgin PES 10 (cf. Table 5.10) and PES 30 (sc. Table 5.11)). From here can be inferred that the equilibrium in mixture is disturbed during filtration and myoglobin is still present to some extent as single molecules, which will contribute to the DLS result.

In all performed filtration experiments, the tested membranes are negatively charged (to varied extent). Thus, BSA attraction to the membrane surface can be predicted at pH = 4, and repulsion at pH = 6 and pH = 8. In contrast, myoglobin will be attracted by the membrane surface at pH = 4 and pH = 6, and repelled at pH = 8. More complicated is the case of filtration experiments with mixture.

First, effects of sterical hindrance can appear when mixture is filtered (BSA is much bigger), which will affect the protein transmission. Moreover, at pH = 6, complex interactions can be claimed. Here, if solutes agglomeration occurs partially, myoglobin and BSA will be present in the solution both as single and agglomerate (as explained before), where each species will interact differently with the membrane surface, i.e., attraction (myoglobin), low repulsion (agglomerate) and repulsion (BSA). This trend can be observed when results from diffusion experiments are discussed. At pH = 6, myoglobin can be transported preferentially through the membrane not only due to its smaller size but probably also due to attraction. In contrast, the transport of BSA is hindered by repulsive forces. In case of mixture, BSA transmission is enhanced due to the less negative charge of the agglomerates compared to single BSA (which can explain the slight increase of the BSA diffusion coefficient in mixture in Table 5.7 and the slight decrease in rejection during two fold and 20 fold short DE filtrations (Figure 5.50 and Figure 5.57)).

6.2.1.2 Fouling mechanisms study

The collected data from dead-end filtration experiments were analysed with the help of the standard classical blocking model proposed by [41] (cf. Eq.(2.4)). In order to clarify the meaning of the presented data from this analysis, the performed data conversion will be explained first (Figure 6.7).

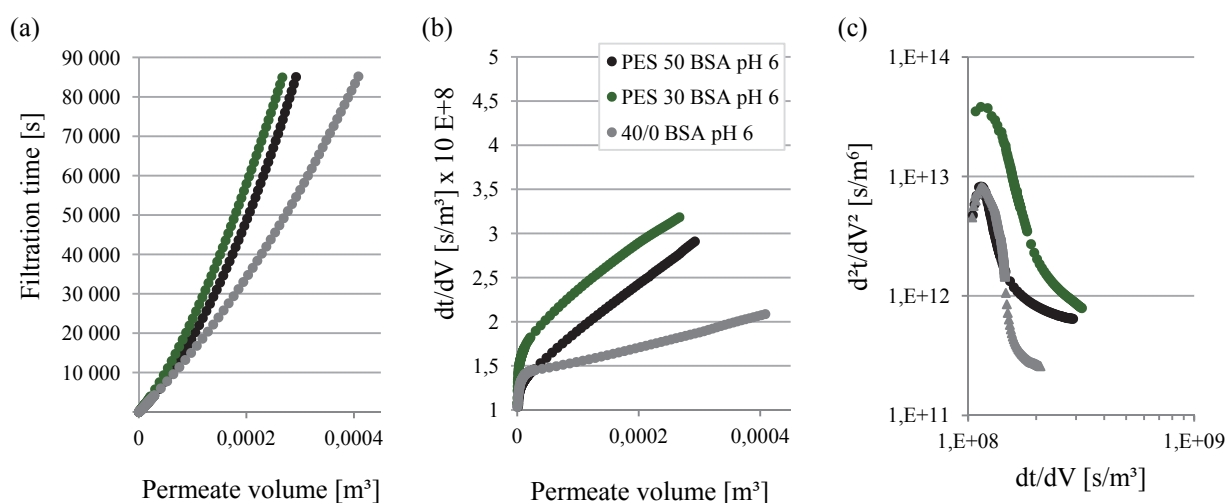


Figure 6.7 Translation of the filtration results into fouling mechanism analysis data.

Figure 6.7(a) is plot of the filtration time against the collected permeate volume. From these data, the slope dt/dV and its change with permeate volume (d^2t/dV^2) were calculated. As it can be seen in Figure 6.7(a), the less time necessary to collect certain permeate volume, the better the filtration performance is, i.e., less flux decline. This means that the small change in filtration time with permeate volume, i.e., small dt/dV , indicates slow flux decline. As a consequence, more permeate volume will be collected when dt/dV is lower (Figure 6.7(b)). In other words, high dt/dV values mean less permeate fluxes. In

general, dt/dV increases with increasing permeate volume, i.e. with time. The slope of the plots in Figure 6.7(b) is d^2t/dV^2 . In this case, lower slope in the early stages of the filtration process corresponds again to larger amount of the collected permeate, i.e., higher flux. In Figure 6.7(c), the change of d^2t/dV^2 with dt/dV is visualised. At low dt/dV (initial stages), high d^2t/dV^2 means fast change of dt/dV . More important is the initial slope in this graphic. The higher the slope, the faster d^2t/dV^2 increases. This means that the influence of the solutes on the change in permeate flux in the early filtration stages becomes more pronounced with filtration time (especially during pore blocking [41,58]). Further fast decrease of d^2t/dV^2 indicates the already occurred pore blocking and the transition to cake formation [56], where the effect of the deposits on permeate flux change decreases. The more negative slope of the curve, i.e., the fast decrease in d^2t/dV^2 reflects large reduction in the rate of flux decline [59]. The smaller the slope, the faster the transition to cake formation occurs [177]. When no further change in d^2t/dV^2 is measured, i.e. the slope of the plots is zero, dt/dV increases constantly indicating filtration regime with increasing hydraulic resistance (can be caused by growing cake layer as well as increasing CP due to concentration increase in the feed during DE filtration if high rejection is present). If stage III (Figure 2.1) in filtration is reached, i.e., filtration occurs with constant flux, dt/dV goes towards infinity.

6.2.2 VIRGIN MEMBRANES

Impact of the relationship pore size/solute size and pH

The protein size and charge as well as the membrane pore size and charge have an impact on the performance of virgin membranes during filtration. The relationship pore size to solute size plays an important role for the membrane performance. As shown in Figure 5.58 (PES 10), Figure 5.59 (PES 30) and Figure 5.60 (PES 50), the protein solutions cause strong flux decline. For better comparison, Figure 6.8 summarises the obtained results by means of relative permeate flux after 16 hours.

Comparing the relative fluxes for BSA and myoglobin at defined pH, it can be concluded that in most cases myoglobin causes stronger flux decline than BSA. Same trend is observed from the performed static adsorption experiments (Figure 5.43) – membranes after static adsorption with myoglobin show lower fouling resistance. Influence on this result will have also the fouling regime, the state of the CP and cake layers (governed by electrostatic forces and membrane rejection) as well as the ratio pore size/solute size.

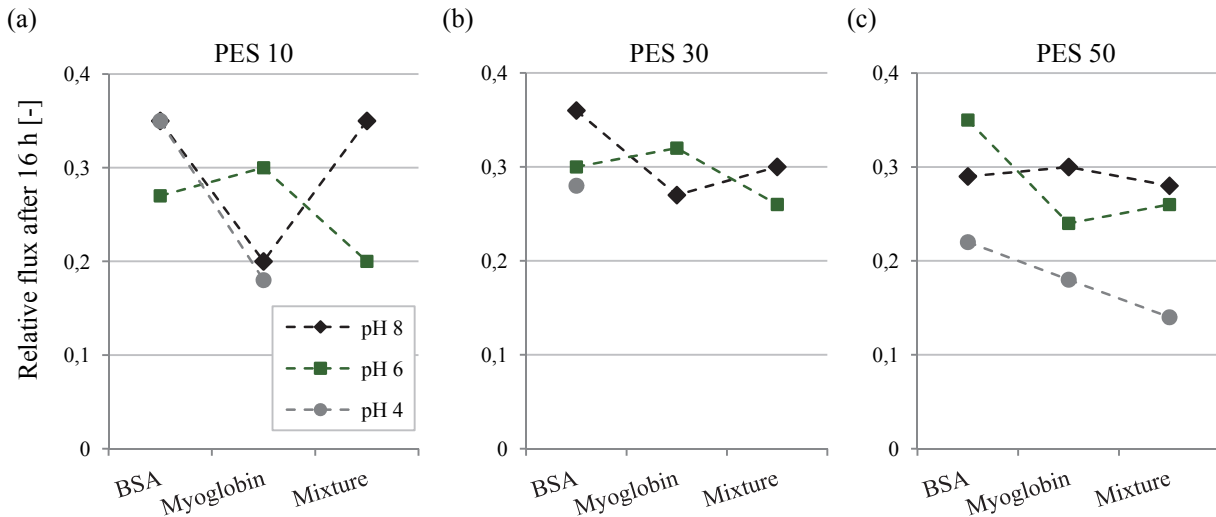


Figure 6.8 Relative flux after 16 hours filtration of proteins at varied pH value through virgin membranes.

As it can be seen from Figure 6.8, the obtained relationships are very complex. In order to clarify these results, the discussion will start with the results collected at pH = 6. The impact of the membrane pore size on the permeate flux during the filtration of BSA is shown in Figure 6.9.

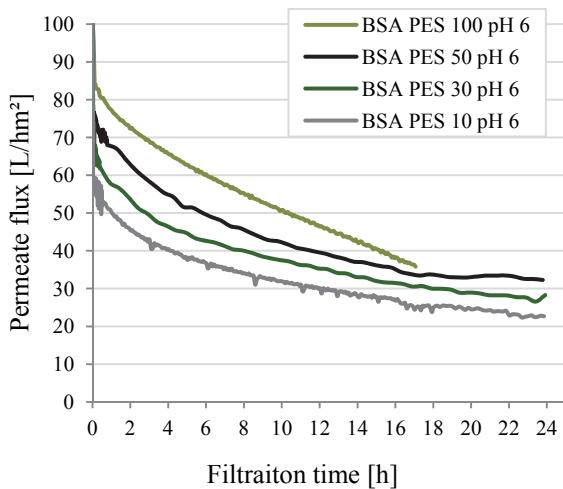


Figure 6.9 Effect of the membrane pore size on the permeate flux and rejection during dead-end filtration of BSA at pH = 6.

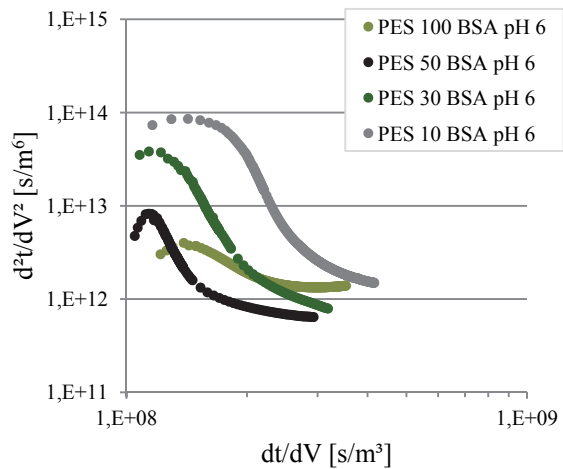


Figure 6.10 Fouling mechanism analysis for dead-end filtration of BSA with virgin membranes at pH = 6.

Obviously, the smaller the pores, the stronger the flux decline is. Furthermore, in Figure 6.10 can be seen that the initial slope n of the curves increases with increasing nominal MWCO (the first measure point is taken after 30 seconds from the beginning of the filtration; for PES 10 and PES 30 it seems that for this time the region for transition to cake filtration is reached, i.e., the pore blocking regime characterised with fast flux decline is not detected, since it occurs very fast). From here can be inferred that the flux decline at the initial filtration stages is stronger and faster with decreasing pore size. After

the plateau is reached in Figure 6.10, slopes of $n < 0$ are obtained. n is more negative for membranes with smaller nominal MWCO, which means that the transition to cake formation regime occurs faster for these membranes.

Interesting is the behaviour of PES 100. The permeate flux of this membrane is the highest but the slope of the curve in Figure 6.9 is not reduced during the filtration which leads to higher dt/dV values (Figure 6.10). This finding is an indication for possible deterioration of the filtration performance of PES 100 for longer process duration. Responsible for this discrepancy could be the membrane morphology. It has been reported that isotropic membranes exhibit higher fluxes during filtration of BSA [178], but the experiments were not performed long term. It should be noticed that BSA is not completely rejected by PES 100 (cf. Table 5.14), thus, different fouling mechanism (internal fouling) may be a further reason for the flux behaviour of this membrane.

The different flux decline caused by varied pore sizes (PES 10, PES 30 and PES 50) can be explained with the help of the schematic representation in Figure 6.11.

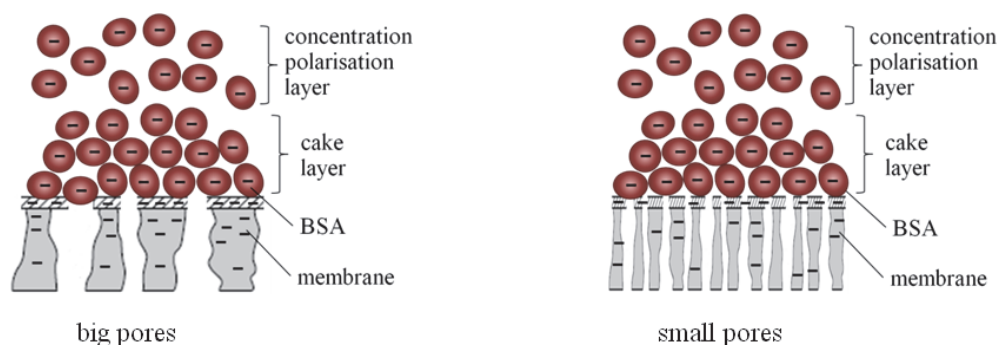


Figure 6.11 Effect of the membrane pore size on fouling for the filtration of BSA at pH = 6. A schematic view.

When the solute is completely rejected by the membranes, the CP and cake layers which are built on the top of the membranes would have similar characteristics when built on membranes that have variable pore sizes but still exhibit complete rejection. Thus, the membrane pore size, i.e. the membrane hydraulic resistance will determine the flux. This explains the stronger flux decline for membranes with smaller pores at pH = 6.

In contrast, at pH = 8, PES 50 exhibits lower flux than PES 10 (cf. Figure 6.8). If the solute molecules have stronger charge, e.g., at pH = 8, the layers on the top of the membrane would be less dense, meaning that the flux will also increase. Indeed, the permeate fluxes of both membranes increase compared to experiments at pH = 6 but to various extent. Here, the balance between electrostatic repulsion and hydrophobic interactions is of great importance, i.e., the protein deposition on the membrane surface caused by hydrophobic interaction should be also taken into account. For smaller

pores, the cake layer porosity would affect the flux, whereas pore plugging of membranes with higher nominal MWCO (the pore size of PES 50 is similar to the size of BSA) would still play a role, in combination with the cake layer properties. Consequently, this would lead to more reduced flux of PES 50 compared to membranes with smaller pore size. Similar results have been found by Martin et al. [179].

The lower values of relative flux of BSA at pH = 4 with increasing membrane pore size can be explained by the membrane-solute interactions. BSA is attracted by the membrane surface due to the opposite charge, causing protein deposition. If $d_{solute} \sim d_{pore}$ (cf. Figure 2.3(b)), pore blocking occurs resulting in stronger disruption of the flux rather than by deposition ($d_{solute} \gg d_{pore}$, cf. Figure 2.3(c)).

Different is the case when the solute is not completely rejected by the membrane. In this case, if membranes with different pore sizes are compared, i.e., different solute rejection, the fouling mechanisms will change with changing pore size (again, pH will play an important role). In the following, the observed data from the filtration of myoglobin at pH = 6 through membranes with varied nominal MWCO will be discussed. Figure 6.12 presents the permeate fluxes through these membranes and the rejections during CF filtration (DE filtration exhibits similar results (cf. Figure 48 in Appendix A); the results from CF are selected here in order to allow discussion of the rejection during filtration).

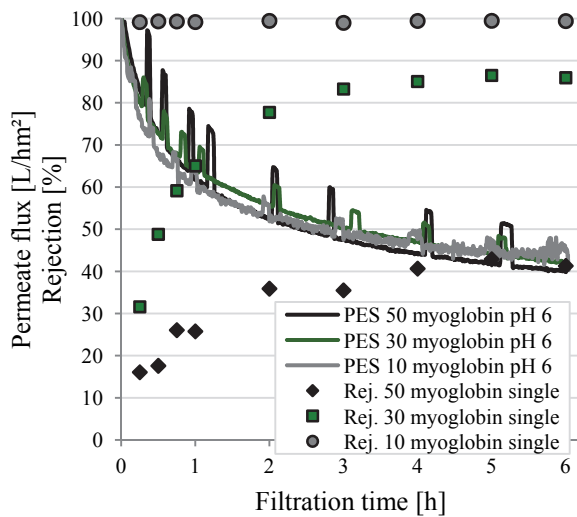


Figure 6.12 Effect of the membrane pore size on the permeate flux and rejection during cross-flow filtration of myoglobin at pH = 6.

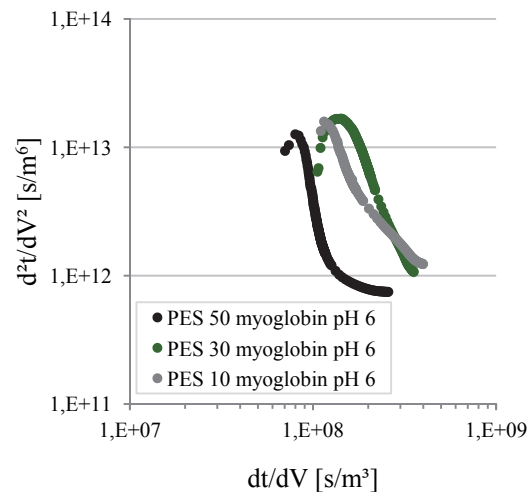


Figure 6.13 Fouling mechanism analysis for dead-end filtration of myoglobin with virgin membranes at pH = 6.

The collected flux curves behave very differently, i.e., stronger flux decline for PES 10 at the beginning of the process, but higher and more stable flux in the later stages; the initial slope for PES 30 and PES 50 are similar, but later PES 50 shows stronger flux decline. Moreover, PES 30

increases its rejection very rapidly, indicating fast pore narrowing, whereas PES 50 remains still permeable for myoglobin. The initial slopes of the curves presented in Figure 6.13 also indicate the faster pore narrowing of PES 30 compared to PES 50. Here, the fouling mechanisms are the key for the explanation. In case of $d_{solute} \ll d_{pore}$ (cf. Figure 2.3(c)), pore narrowing occurs. The pores of PES 30 are almost completely blocked by the deposits in the pores, whereas PES 50 also undergoes pore narrowing but the pores are not closed (see rejection data). This means that the inner pore surface of PES 50 has more contact with myoglobin molecules than PES 10 and PES 30. At pH = 6, myoglobin is attracted to the membrane and in combination with the previous considerations, this can result in lower flux through PES 50 which is more permeable for solutes. The positive charge of myoglobin facilitates the solutes' transport through the membrane. PES 10 ends up with the highest permeate flux due to the presence of only outer surface fouling (complete rejection of myoglobin). In addition to that, from diffusion experiments is established that due to the less solute contact with the membrane inner surface of membranes with smaller pores (decreasing diffusion coefficients with decreasing membrane nominal MWCO), less protein is adsorbed (cf. Figure 5.46). Figure 6.14 shows schematically the build up of fouling deposits of small molecules (myoglobin) depending on the membrane pore size.

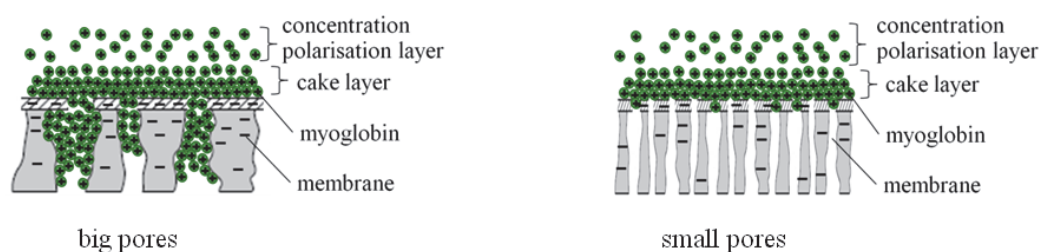


Figure 6.14 Effect of the membrane pore size on fouling for the filtration of myoglobin at pH = 6. A schematic view.

In contrast, at pH = 8, the flux decline increases with smaller pore sizes (cf. relative flux in Figure 6.8). At this pH myoglobin is repelled by the membrane. Thus, the rejection of myoglobin increases for all membrane nominal MWCOs (cf. Table 5.10, Table 5.11, Table 5.12). First, the increase in rejection leads to increased CP near the membrane surface, i.e., the higher the rejection the more strongly the permeate flux would be disturbed by the CP layer. Second, since myoglobin is not attracted by the membrane surface, no strong interactions will be present in the membrane interior. Thus, PES 10 has the lowest permeate flux due to the strongest CP. Considering the increased rejection of myoglobin by PES 10 and PES 30 at pH = 8, more pronounced CP could be the reason for the lower permeate fluxes in comparison to pH = 6. In contrast, the rejection by PES 50 is also higher at pH = 8, but still 40 %.

At pH = 4, PES 10 and PES 50 behave similarly during filtration of myoglobin. Here, myoglobin exhibits strong positive charge, which can result in strong solute deposition on the membrane surface. Moreover, at pH = 4, the lowest relative fluxes are measured (Figure 6.8) indicating the strongest fouling. Hence, both membranes exhibit similarly poor performance.

The effect of pH and pore size on the flux behaviour and rejection during filtration of an equimolar mixture of BSA and myoglobin is more complex due to the varying solution properties influenced by the pH. At all pH values, the effect of pore size on the flux decline followed the trend of single BSA solution. Due to the presence of myoglobin in the mixture, combined fouling can be expected, which may result in lower fluxes. The rejection data from these results are of more interest. Myoglobin in mixture is rejected differently than single myoglobin. At pH = 8, single myoglobin is more strongly repelled by the membrane than in mixture (see Table 5.10, Table 5.11, Table 5.12). Explanation could be given by the extent of fouling (pore narrowing) depending on the myoglobin amount in the feed. Since the concentration of myoglobin is much lower in the mixture (0.02 g/L in mixture, 0.1 g/L as single), less pore narrowing could be caused by myoglobin, thus, during the filtration higher fraction of myoglobin from the feed could pass through the membrane (the myoglobin rejection in mixture is lower than in single solution but its concentration in permeate is also lower).

At pH = 6, the rejection of myoglobin in the mixture increases compared to single solution (Figure 5.57, Table 5.10, Table 5.11, Table 5.12). It has been found that the proteins concentration in the CP layer is higher, if the proteins are oppositely charged [42,46]. This will result in stronger effect of the CP on the flux. Furthermore, as already explained in 6.2.1.1, due to the opposite charge of BSA and myoglobin at pH = 6, solute agglomeration may occur. Hence, less myoglobin can penetrate the membrane.

Both proteins exhibit positive charge at pH = 4, which would lead to strong fouling due to attraction to the membrane surface. Here, combined fouling may be the reason for increased myoglobin rejection in the mixture (in comparison to myoglobin as single solute).

All displays about the influence of the membrane pore size on the permeate flux over time during filtration of BSA, myoglobin and mixture at varied pH in DE and CF modes which are not shown here, are summarised in Figure 45 – Figure 55 in Appendix A. The effects of pH during filtration of each solute system in DE and CF mode are shown in Figure 58 – Figure 64 in same Appendix.

The reversibility of fouling is tested during mechanical and chemical cleaning experiments. Flux recovery from cleaning after filtration of BSA at varied pH is shown in Figure 6.15. Flux recoveries after filtrations of myoglobin and mixture can be found in Figure 56 and Figure 57 in Appendix A, respectively.

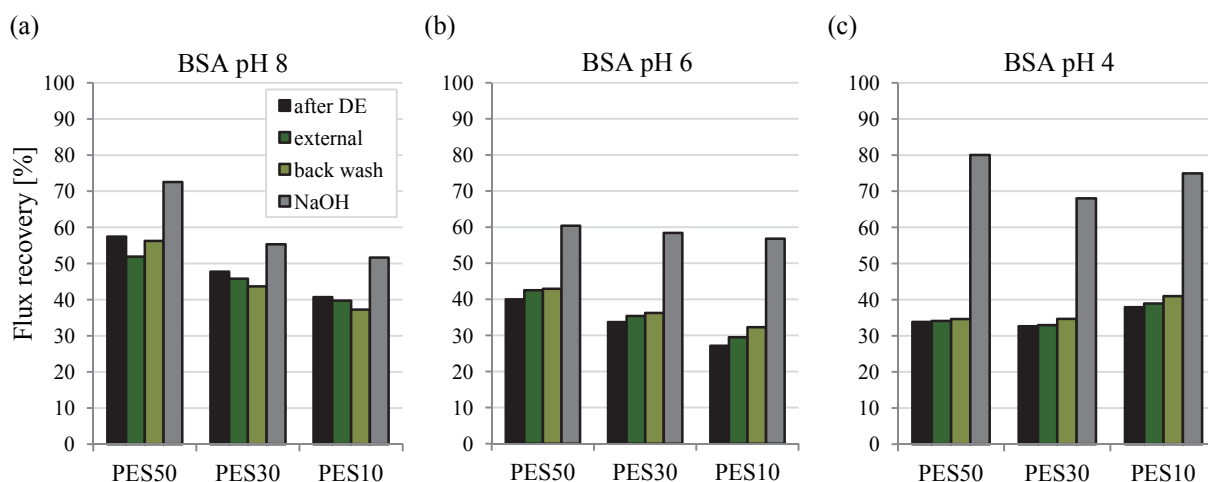


Figure 6.15 Effect of the pore size on the flux recovery after the cleaning of virgin membranes; dead-end filtrations of BSA at: (a) pH = 8; (b) pH = 6; (c) pH = 4.

In some cases the membrane water flux decreases after each cleaning step (e.g., cf. Figure 6.15(a)). These results can be explained by the possible membrane compaction during the cleaning procedures, since, in most cases, they are performed at higher pressure than the filtration experiments (cleaning is performed at 1 bar). Negative membrane flux recovery appears when the effect of membrane compaction on the flux is stronger than the rinsing effect.

In general, as already mentioned, mechanical cleaning is not very successful for unmodified membranes, i.e., the foulants deposit irreversibly on/in the membrane. It is shown that chemical cleaning is able to remove the deposits. However, treatment with NaOH at pH = 13 does not recover the membrane water flux completely. Increasing the concentration of NaOH and the temperature during cleaning would increase the flux recovery [180].

Effect of the cross-flow velocity

The CF/stirring is an important factor for improving the filtration performance, since the CP layer thickness and the cake growth can be reduced by increasing the turbulence [17,18,40]. Some examples from the performed CF filtrations with virgin PES 10 at varied CF are presented in Figure 6.16.

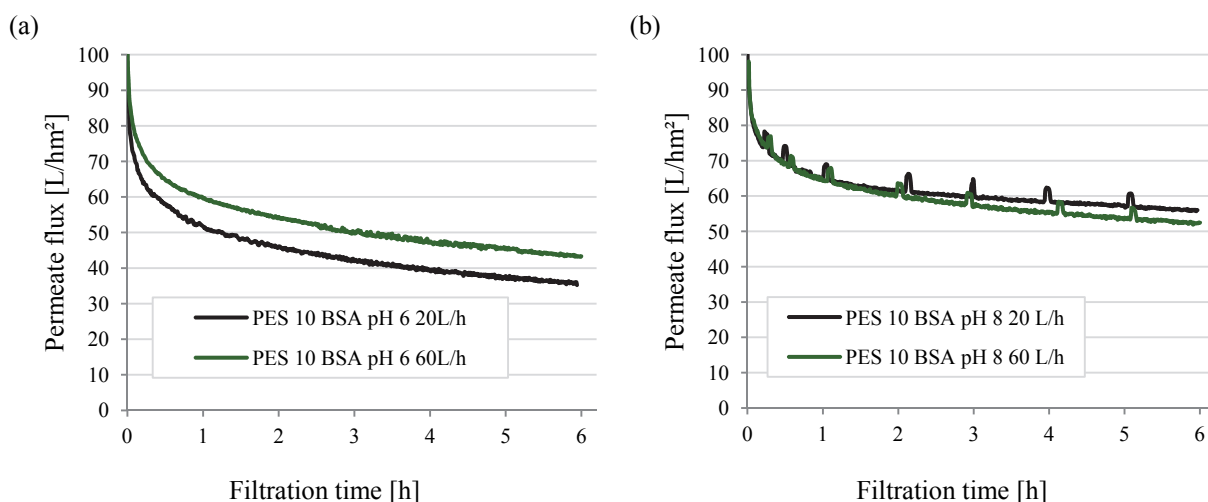


Figure 6.16 Effect of the CF on the permeate flux during cross-flow filtration of BSA through virgin PES 10 at varied pH; (a) pH = 6; (b) pH = 8.

The performed experiments show that increasing the CF from 20 L/h (0,157 m/s) to 60 L/h (0.471 m/s) results in increased flux at pH = 6 (Figure 6.16(a)). In contrast, at pH = 8 the permeate flux is deteriorated (Figure 6.16(b)). It seems that the permeate flux through virgin membranes could be increased, if no strong membrane-solute interactions are present (at pH = 8 the repulsive membrane-solute interactions are stronger than at pH = 6). When the fouling tendency is more pronounced (pH = 6), increasing the CF velocity reduces the extent of building layers on the membrane, whereas, if strong repulsive forces are present, higher CF does not reduce further the build-up of CP and cake layers further. Moreover, at pH = 8 and 60 L/h CF, reduction in flux is found. This can be explained by possible protein aggregation caused by strong turbulence [99].

All obtained results from variation of the CF velocity with PES 10 and PES 30 are to find in Figure 65 and Figure 66 in Appendix A.

Generally, it can be concluded, that increasing the CF is not very effective for virgin membranes.

6.2.3 COMPOSITE MEMBRANES

Effect of the hydrogel layer properties

In this section, the impact of the hydrogel layer properties on the membrane performance will be discussed on the basis of filtration experiments with proteins. First, the fouling and rejection behaviour of functionalised membranes resulting from the varied hydrogel layer structure will be explained by means of filtration experiments with two fold feed volume reduction.

The chain length of the PEG residue in the molecule of PEGMA is found to influence the hydrogel layer properties. When modifications are performed with pure PEGMA or small amounts of MBAA (i.e., 0.4 g/L), membranes with PEGMA 200 exhibit lower protein rejection, as shown in Figure 5.50, whereas similar rejection is obtained for modifications with PEGMA 200 and PEGMA 400 with 1 g/L and 4 g/L of MBAA. These results correspond to the swelling data in Figure 5.1: higher swelling is observed for PEGMA 200 alone and with 0.4 g/L MBAA, while bulk hydrogels prepared from PEGMA 200 with higher amounts of MBAA behave similarly to hydrogels from PEGMA 400. From here it is obvious that the rejection properties of the hydrogel layer are governed by the crosslinking agent (if present in sufficient amount). It is well known that in the hydrogel network physical entanglement of polymer chains is present. Thus, in less crosslinked networks the PEG chain length, i.e., the physical entanglement dictates the rejection properties, while at higher chemical crosslinking these affects become negligible. Here, it should be noted that the impurity of PEGDA acting as chemical crosslinker [169] has different molecule size corresponding to the PEG chain length (PEGMA 200 vs. PEGMA 400). Hence, the crosslinking effect of PEGDA in the hydrogels of PEGMA 200 and PEGMA 400 would be different. It should be taken into account that higher DG values are observed for modifications with PEGMA 200 in comparison to modifications with PEGMA 400 due to the higher molecule diffusivity (resulting from the lower MW) of PEGMA 200. Thus, higher DG may contribute to the rejection and anti-fouling properties of these membranes.

Regarding the amount of crosslinker monomer, two effects are found depending on the modification level. At 4 J/cm², decrease in the rejection with increasing MBAA amount up to 1 g/l and further increase at 4 g/l MBAA are observed (see Figure 5.50). This could be related to the grafted chains' behaviour at this modification level: when the chains are relatively short compared to the pore size of the membrane, the crosslinking of the polyPEGMA chains leads to confined swelling, i.e., the effective pore size increases. Higher amount of MBAA could lead to an increasing probability that crosslinked polyPEGMA chains cover pores. At 5 J/cm², the rejection increases systematically with increasing amount of MBAA. At this level, the chains seem to be long enough to be able to shield the pore openings and further crosslinking increases the network density, i.e., the rejection increases [160]. These findings are in agreement with the discussed effects in Section 6.1.2.2.

Looking at the results for myoglobin (Figure 5.50(b)), both increase of UV irradiation dose and crosslinker amount cause systematic increase in protein rejection, e.g., from ~ 5 % (PEGMA 400, 2 J/cm²) to 80 % (PEGMA 400, 11 J/cm²) and 99 % (PEGMA 400/MBAA = 40/4, 11 J/cm²). Especially, the results at 5 J/cm² are of large interest: at this UV irradiation dose, the increase of crosslinker amount could shift the rejection of myoglobin from 10 % to 90 %, i.e., the selectivity of the hydrogel PES composite membranes is adjusted by MBAA very properly, and this is combined with very good anti-fouling properties [160] (also in long term experiments, cf. below).

The protein rejection of membranes modified with PEGMA/PETAE follow the behaviour obtained from dextran filtrations. In Figure 5.51 about the rejection properties of PES 50 is shown that a very systematic decrease of BSA rejection with increasing crosslinker content is observed at 11 J/cm^2 . Analogous effects are found for the rejections to myoglobin but with very pronounced changes only at the highest irradiation level (11 J/cm^2), apparently due to the smaller MW of the solute [160]. The results are analogous to the obtained rejection curves with dextran and are consequence of the hydrogel layer behaviour when crosslinked with PETAE, as already described in Section 6.1.2.2.

Another contribution to the explanation of the hydrogel network properties depending on the crosslinking type can be found in the results from static adsorption with BSA (Figure 5.44). In order to avoid pore structure effects, modified PES films are tested. It is observed that more BSA is adsorbed on films modified with PEGMA/PETAE, while PEGMA/MBAA films adsorb minimum amount of protein. This can be explained by the hydrogel network mesh size. The tighter PEGMA/MBAA layer is not permeable for BSA, whereas the more “open” PEGMA/PETAE layer structure allows BSA molecules to reach the membrane surface.

In all cases discussed above, the described effects are more strongly pronounced for PES 50 compared to PES 100 and PES 300 (as already discussed by means of dextran rejection in Section 6.1.2.2).

Impact of the solute size and charge

The crosslinking degree (i.e., effective pore size) as well as the solute size and charge influence the filtration performance of functionalised membranes. An overview of the relative fluxes after 16 hours of DE filtration of BSA, myoglobin and their mixture through functionalised PES 50 with PEGMA/MBAA and 5 J/cm^2 is presented in Figure 6.17. First, the effect of solutes and solution composition on permeate flux at defined pH (i.e., depending on their charge) will be discussed.

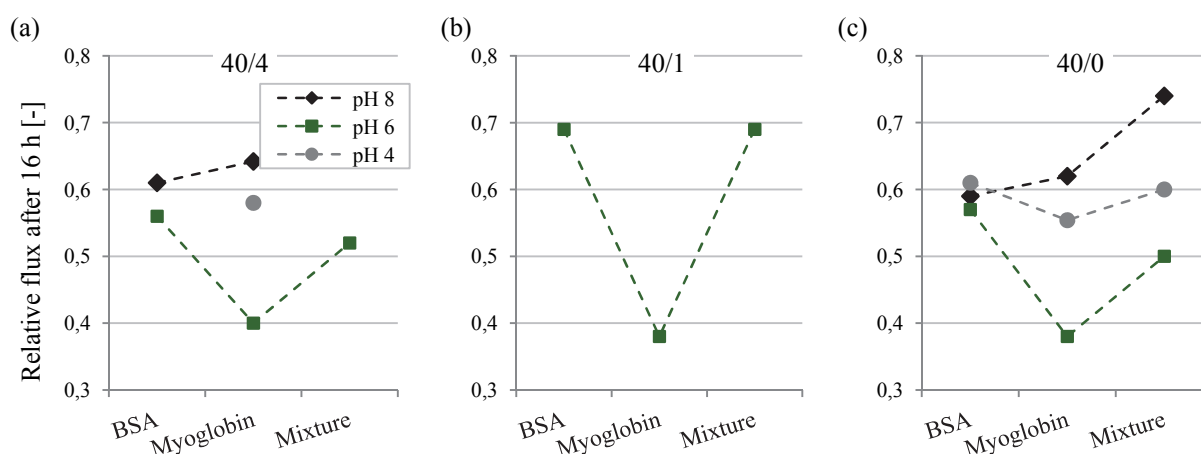


Figure 6.17 Relative flux after 16 hours filtration of proteins at varied pH value through modified membranes with 5 J/cm^2 .

At pH = 8, in all functionalisation cases, BSA caused stronger flux decline compared to other solutes. At this pH, both solutes are negatively charged, thus the solutes size influences the filtration behaviour. Regarding feed solutions of single proteins, it can be concluded that the larger size of BSA combined with the built CP layer due to the high rejection is the reason of stronger flux decline. Higher flux is measured during the filtration of myoglobin due to the anti-fouling properties of the grafted hydrogels combined with the lower influence of the CP layer due to smaller molecule size (higher diffusivity and lower rejection decrease CP [43]). In case of protein mixture, the proteins concentration in the CP is expected to be lower due to the same charge of the proteins [42] and the less amount of BSA in mixture compared to single solution (note that myoglobin in mixture is rejected to 42 % (Table 5.13), which may lead to higher permeate fluxes. The increased myoglobin rejection in mixture compared to single solute may be attributed to the sterical hindrance of BSA and the resulting competition in mixture.

According to Figure 6.5, at pH = 6 myoglobin is positively charged. Hence, myoglobin is attracted by the slight negatively charged membrane (the grafted hydrogel layer does not shield the charge of the virgin membrane completely, cf. ZP in Figure 5.10), solute deposition may occur, leading to deteriorated permeate flux. The filtration of protein mixture gives flux behaviour similar to BSA, which can be explained by the predicted slight negative charge of the protein agglomerates (cf. Section 6.1.2.1) and the low contact of the membrane inner surface with positively charged myoglobin single molecules (less amount of myoglobin and increased myoglobin rejection in mixture compared to single solution).

The effect of solutes on filtration performance at pH = 4 can be evaluated only for functionalised membranes with PEGMA (40/0) due to the incomplete test series. As it can be taken from Figure 6.17, the effect of different solutes can be explained with the solutes charge. Both proteins are positively charged but to various extent, i.e., myoglobin may exhibit stronger positive charge, since its IEP of 7 is farther from pH = 4 than the IEP of BSA (~ 5). Therefore, myoglobin may cause stronger flux decline during filtration. The different flux behaviour depending on the feed solute may be also connected to the retention of these proteins by the membrane. Since myoglobin is rejected to a lower extent than BSA, interactions with the internal membrane surface (which is less modified, cf. modification depth in Figure 5.18) can be predicted. Hence, the impact of the virgin membrane on the filtration flux can be intensified.

Interesting is the impact of solute charge on the filtration performance for defined solute. In Figure 6.17 can be seen that the membrane performance during filtration of BSA is not influenced by the pH significantly. After 16 hours of filtration run, the relative flux of BSA at pH = 4 is slightly higher than at other pH values, which is unexpected. Feasible explanation may be a possible conformational

structure change in the BSA molecule due to charge alteration, which may lead to less dense CP layer as a result of sterical effects. In case of myoglobin, the effect of solute charge is more pronounced, but the expected trend cannot be found. The higher relative flux at pH = 4 than at pH = 6 could be explained in the same way.

Graphical comparison of permeate flux and rejection during DE filtration of BSA, myoglobin and mixture depending on the pH is included in Appendix A, Figure 67(a), Figure 68(a) and Figure 69(a), as well as in Figure 70 and Figure 71 (Appendix A) for CF filtrations. As already mentioned, the charge of the virgin membranes influences the behaviour of the functionalised membranes. Indeed, increased rejection of myoglobin is measured for filtrations at pH = 8 compared to pH = 6 (cf. Table 5.13 for DE and Figure 71 in Appendix A for CF filtrations).

The solute size had an effect on the cleanability of functionalised membranes. From the flux recovery data for PES 50 40/0 5 J/cm² presented in Figure 5.62, it can be concluded, that myoglobin deposits on the membrane outer surface and especially within the pores (expected from the rejection data) and can be removed by cleaning with water, mostly by back wash. This effect is less pronounced at pH = 8 due to the lower amount of deposits. Deposition of molecules is also possible in the hydrogel network but no special indications are found for this statement. The effect of cleaning with water of membranes after BSA filtration is only measurable for the sample used at pH = 6 after external washing, indicating that the protein deposition occurs mostly on the membrane outer surface, while no effects are detected with membranes used for filtration at pH = 4 and at pH = 8. After filtration of mixture, during cleaning with water the tested membranes behave similarly to myoglobin contaminated membranes but the flux recovery is less pronounced due to the lower amount of myoglobin in the mixture compared to single solution. Chemical cleaning contributes to the membrane flux recovery, mostly delivering 10 % increase in flux. The application of more aggressive cleaning conditions may increase the membrane water flux to its initial value.

A direct comparison of flux recoveries at varied pH can be done using Figure 67(a), Figure 68(a) and Figure 69(a) in Appendix A.

Further scope of investigation is the impact of the effective pore size (i.e., crosslinking degree) on the flux and rejection during filtration with functionalised membranes. In Figure 6.18, permeate fluxes from filtration of BSA through modified membranes with varied amount of MBAA at pH = 6 are presented.

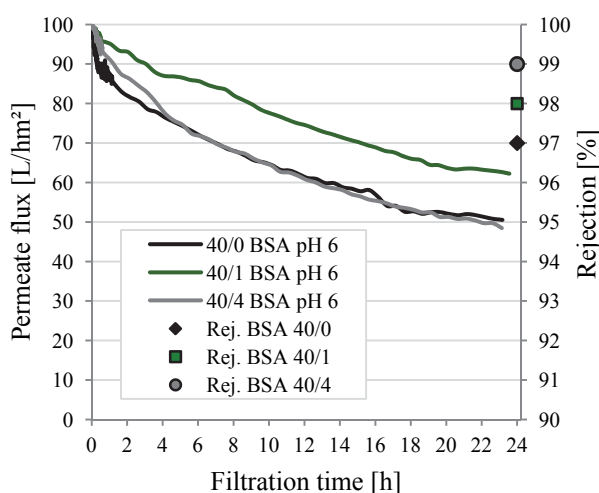


Figure 6.18 Effect of the crosslinking degree on the permeate flux during dead-end filtration of BSA at pH = 6.

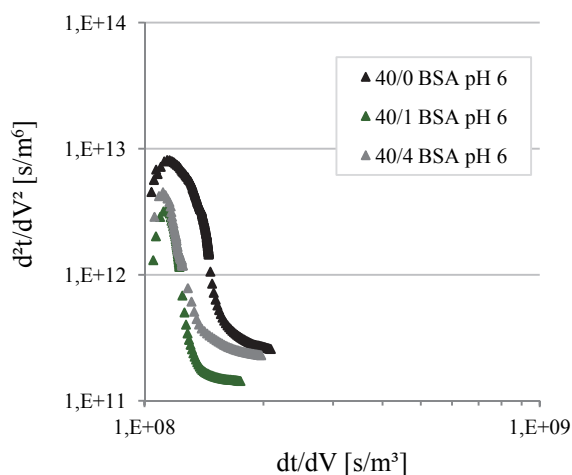


Figure 6.19 Fouling mechanism analysis for dead-end filtration of BSA with modified membranes at pH = 6.

Surprisingly higher flux is obtained during filtration with membrane 40/1. The permeate curves differ from each other in the initial stage of the filtration and proceed later almost parallel. It seems that the CP layer exhibits different properties during this run, which may be related to incidentally different stirring conditions (since the operative design is the same and the rejection is similar for all membranes).

Further information delivers the fouling mechanism analysis displayed on Figure 6.19. The initial slopes of the curves increase with increasing crosslinker amount indicating faster “pore” blocking for membranes with higher MBAA amount. Nevertheless, 40/0 exhibits the highest values for d^2t/dV^2 , which means the fastest change in the flux decline rate. This value is at minimum for 40/1, corresponding to the observed gradual decrease in flux. In the later filtration stages, the curves proceed almost parallel, i.e., the transition to cake formation occurs with similar rate.

Different is the case of myoglobin filtration with membranes with varied hydrogel crosslinking degree. As it can be seen in Figure 6.20 from permeate flux and Figure 6.21 from fouling analysis, 40/0 and 40/1 behave similarly within 16 hours of the filtration process, despite the different rejection.

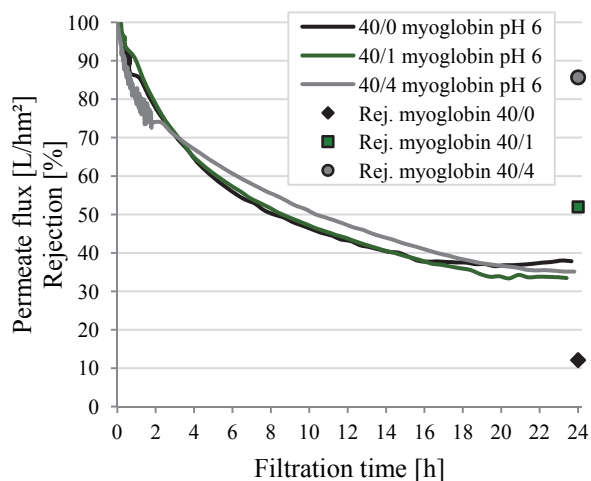


Figure 6.20 Effect of the crosslinking degree on the permeate flux and rejection during dead-end filtration of myoglobin at pH = 6.

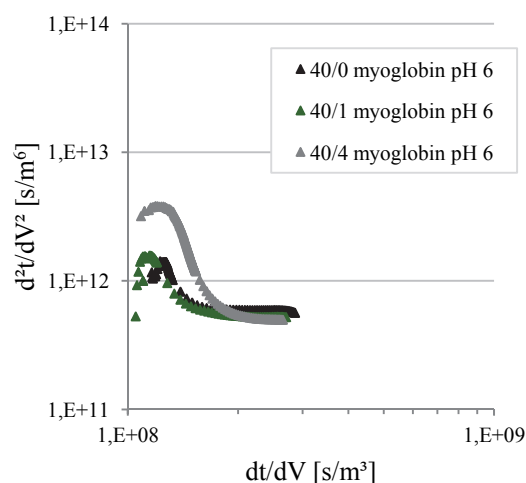


Figure 6.21 Fouling mechanism analysis for dead-end filtration of myoglobin with modified membranes at pH = 6.

Contrarily, fast flux decrease is measured in the initial filtration stage for membrane 40/4, followed by slighter further decline. In this case, pore plugging due to the smaller hydrogel network mesh size of 40/4 may occur, indicated by the very high myoglobin rejection measured. After that, cake formation would have less impact on the rate of flux decline. In general, the discussed differences in flux due to the assumed variation in the flux decline mechanisms may be denoted as less significant in terms of membrane productivity. Nevertheless, it should be noted that the higher the crosslinking degree, the less the water flux is, i.e., the higher the operation pressure (in order to reach the initial flux of 100 L/hm² for better productivity comparisons). It is known that higher flux increases CP; in combination with high rejection, the influence of CP on the membrane performance may be amplified [43]. From this point of view, 40/4 may behave better if other operation conditions are applied.

In case of a mixture, an effect of the crosslinking similar to the one from the experiments with BSA is found (graphical comparison can be found in Figure 72 in Appendix A). 40/1 exhibits the best flux, whereas 40/4 performs worst. Comparing the rejections of myoglobin as single solute and in mixture, the rejection increased in mixture to varied extent depending in the hydrogel crosslinking ratio. The lower the crosslinking degree, i.e., the lower the myoglobin rejection in single solution, the stronger the rejection increase in a mixture is. This effect is caused by the protein agglomeration in mixture at pH = 6. When certain amount of myoglobin agglomerates with BSA and cannot penetrate the membrane anymore, the effect on the rejection value is much stronger for membranes with low myoglobin rejection, because the rejection is calculated according to the whole amount of myoglobin (since the agglomerated myoglobin is not measured in this work).

Further comparison can be done on the basis of membrane cleanability. Flux recovery data from cleaning of membranes after filtrations of BSA and myoglobin are directly compared in Figure 6.22 (the data for mixture are included in Figure 72(c) in Appendix A).

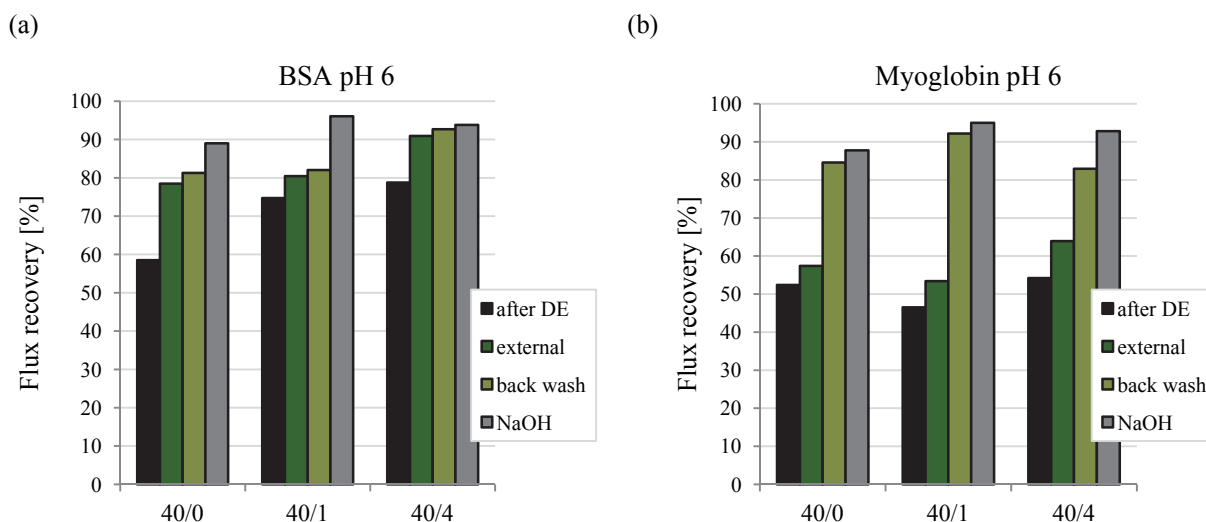


Figure 6.22 Effect of the crosslinking degree on the flux recovery from the cleaning of PES 50 5 J/cm² modified membranes after dead-end filtration at pH = 6; (a) BSA; (b) myoglobin.

As expected, BSA is removed by external cleaning (Figure 1.24(a)), more flux is recovered for membrane functionalised without crosslinker. This is due to the fact that BSA may “stick” into the uncrosslinked hydrogel causing stronger flux decline. In case of myoglobin, the contribution of external cleaning to the flux recovery increases with increasing crosslinking degree, as a consequence of the increasing rejection. Back wash recovers less flux for 40/4 because of the lower contact of the inner hydrogel and membrane surface (fewer deposited molecules due to higher rejection). Interestingly, the strongest contribution of back wash to the membrane flux is found for 40/1. Obviously, myoglobin is removed most efficiently from this membrane. Reason may be the higher rejection of myoglobin by 40/1 compared to 40/0 resulting in smaller contact of the membrane with protein, therefore, lower amount of deposits. Chemical cleaning at pH = 13 does not contribute strongly to further flux increase.

Effect of the cross-flow velocity

The CF influences the filtration behaviour of modified membranes. As it can be seen from the direct comparison of the permeate fluxes during filtration of BSA (Figure 6.23), myoglobin (Figure 6.24) and mixture (Figure 73, Appendix A) at 20 L/h and 60 L/h, higher fluxes are obtained at increased CF velocity. Reason for this is the effect of reducing CP by increased turbulence [43].

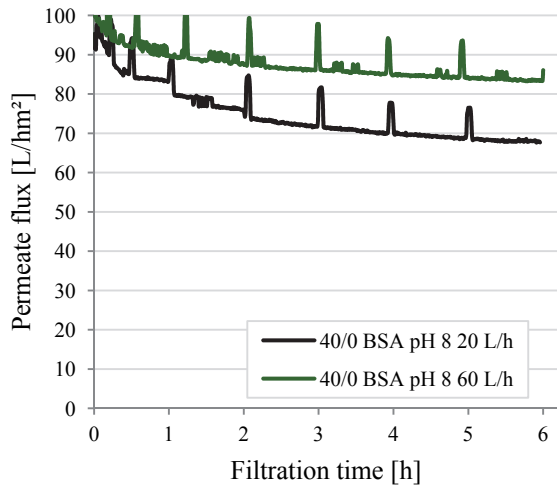


Figure 6.23 Effect of the CF on the permeate flux during cross-flow filtration of BSA through PES 50 40/0 5 J/cm² at pH 8.

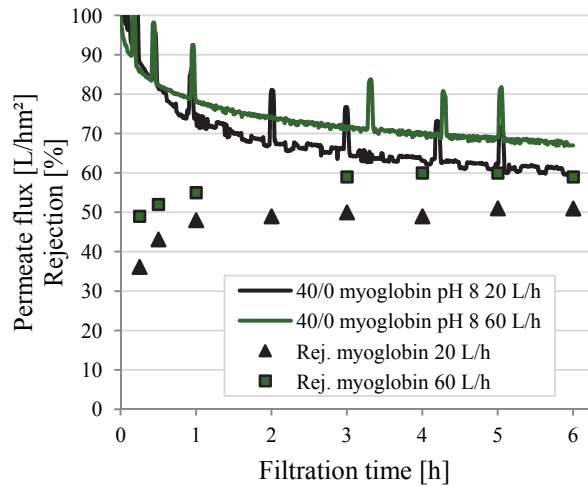


Figure 6.24 Effect of CF on permeate flux and rejection during CF filtration of myoglobin with PES 50 40/0 5 J/cm², pH = 8.

Furthermore, from the plotted rejection data for myoglobin in Figure 6.24 and Figure 73 (Appendix A) can be concluded that the reduced CP increases the protein rejection due to the lowered protein concentration on the membrane surface [2].

6.2.4 VALIDATION OF THE IMPROVEMENT OF MEMBRANE PERFORMANCE BY COMPOSITE MEMBRANES

In this study, it is confirmed that modification with polyPEGMA increases the surface hydrophilicity, resulting in enhanced fouling resistance to proteins and humic substances. In the following sections, the observed improvements will be discussed in terms of general effect of the modification on protein fouling behaviour, effect of the solution properties, the operating parameters and the operation mode.

6.2.4.1 Effect of the modification on fouling behaviour

In general, surface hydrophilisation improves the fouling resistance of the tested membranes (cf. relative fluxes after 24 hours of DE filtration in Table 2, Appendix A). Exemplarily, the fouling resistance after static adsorption with BSA is increased due to the applied modification for all tested membranes, as it can be seen in Figure 6.25.

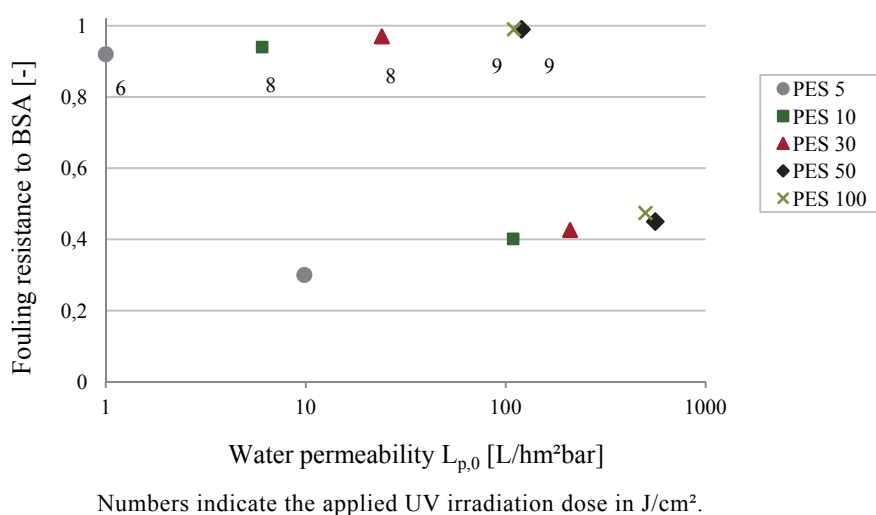


Figure 6.25 Fouling resistance of virgin and modified membranes after static adsorption.

Proteins are preferentially adsorbed on virgin membranes. This is concluded not only from the filtration tests but also from the performed ZP and diffusion measurements. From ZP measurements with virgin and modified samples before and after static adsorption with BSA, it is observed that the charge of fouled membranes (after the contact with BSA) shifts to the net charge of BSA, as shown in Figure 5.11. Moreover, this effect is more strongly pronounced for virgin membranes indicating the higher BSA adsorption on their surface. During diffusion experiments, it is found that the diffusion coefficient through virgin membranes decreases with time as a result of the occurring pore narrowing, whereas through functionalised membranes it remains stable over 48 hours (Figure 5.45).

In order to evaluate the improvement of membrane performance, the behaviour of membranes with similar water flux and rejection properties (from dextran rejection) during contact with foulants has to

be compared. The obtained relationships between virgin and modified membranes in terms of water flux and dextran rejection properties are described in Section 6.1.3.2. Table 6.2 summarises the obtained relative fluxes after 24 hours of DE filtration experiments for virgin and modified membranes with similar water fluxes and rejection curves (with dextran).

Table 6.2 Comparison of the relative permeate flux after 24 hours dead-end filtration of virgin and modified membranes with similar water flux and cut-off. An overview.

Membrane pair		pH	BSA		Myoglobin		Mixture	
virgin	functionalised		virgin	functionalised	virgin	functionalised	virgin	functionalised
PES 30	PES 50 40/0 5 J/cm ²	8	0.32	0.53	0.24	0.55	0.30	0.69
		6	0.25	0.51	0.25	0.39	0.20	0.40
		4	0.26	0.71		n.d.		n.d.
PES 10	PES 50 40/4 5 J/cm ²	8	0.31	0.53	0.20	0.51		n.d.
		6	0.20	0.45	0.21	0.32	0.20	0.42
		4		n.d.	0.16	0.50		n.d.
PES 30	PES 100 40/0 11 J/cm ²	6	0.25	0.76		n.d.		n.d.

n.d.: at least one of the experiments not done

Indeed, all functionalised membranes exhibit higher relative fluxes compared to the corresponding virgin membranes. Figure 6.26 allows further discussion of the obtained results.

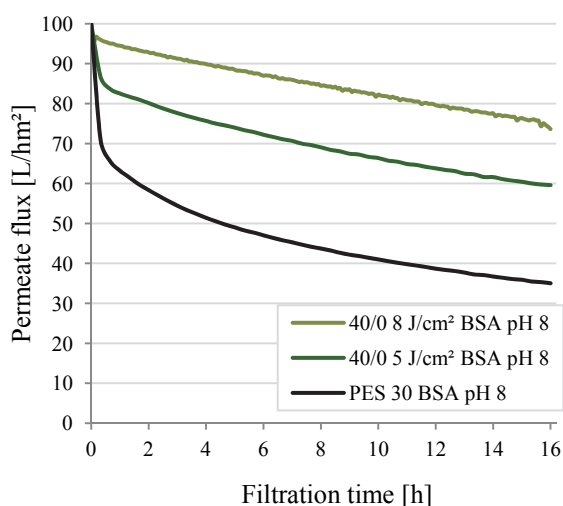


Figure 6.26 Effect of modification on permeate flux during DE filtration of BSA, membranes with similar water flux and cut-off.

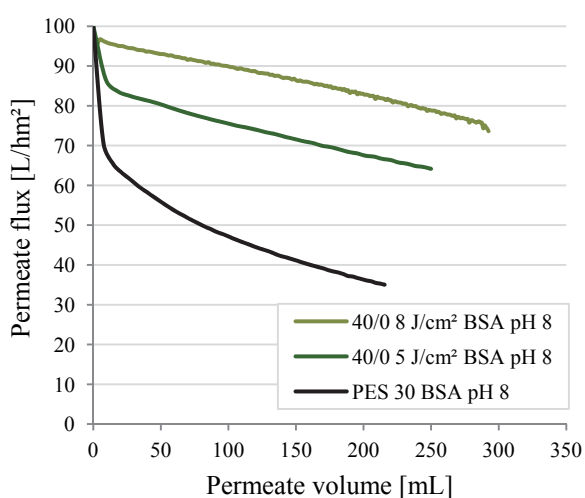


Figure 6.27 Effect of the modification on permeate volume, comparison of membranes with similar water flux and cut-off.

On the basis of the exemplary results from DE filtrations at pH = 8 presented in Figure 6.26 for the comparison pairs virgin PES 30 vs. PES 50 40/0 5 J/cm², it can be inferred that the grafted hydrophilic layer increases the permeate flux. Moreover, further surface modification improves the membrane performance even more (e.g., permeate flux of PES 50 40/0 8 J/cm² presented in Figure 6.26). In

addition, the MWCO of more modified membranes decreases (see dextran rejection curves in Section 5.3.2.2). It should be noted, that in most cases, virgin membranes with smaller pores exhibit similar or worse performance during filtration compared to virgin membranes with bigger pores (cf. Figure 6.8), while the opposite is observed for the hydrogel composite membranes.

For better comparison of the membrane productivity, Figure 6.27 presents the permeate fluxes of the discussed membranes shown in Figure 6.26 against the collected permeate volume for same filtration duration. Obviously, by beginning the test at the same flux for all samples, more permeate can be collected with the composite membranes.

These findings are confirmed also during CF filtration experiments. Figure 6.28 shows examples for filtrations at $\text{pH} = 6$. It can be seen that the permeate flux of modified PES 50 during filtration of BSA is much higher than the obtained flux with virgin PES 30. An initial strong flux drop is not measured with functionalised membranes, which indicates the strong shielding effect of the membrane surface by the applied hydrogel layer.

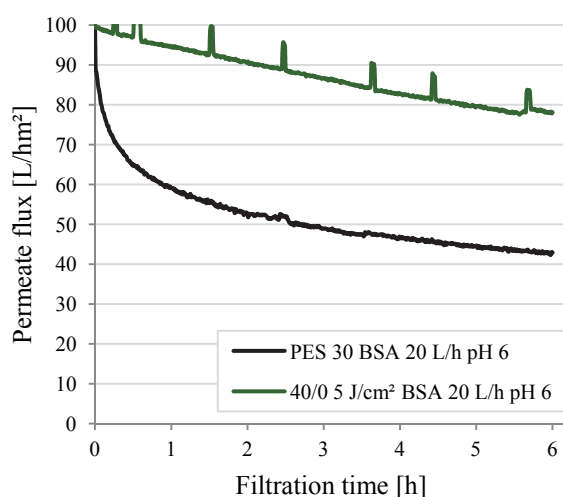


Figure 6.28 Comparison of virgin PES 30 and PES 50 40/0 5 J/cm²: permeate flux and rejection during cross-flow filtration of BSA.

Nevertheless, a constant flux decline for modified membranes during CF filtration of BSA is observed. This behaviour can be explained by insufficient CF (which should minimise (stabilise) CP and cake layers) or by denaturation and aggregation of BSA molecules caused by mechanical impact during CF [96,97] (confirmed by DLS measurements (cf. Figure 4.12)).

In order to describe the principal of (low)-fouling behaviour when membranes exhibit very high or complete rejection to the feed solute(s), Figure 6.29 visualises the occurring membrane-solute interactions during filtration of BSA through virgin membranes with relatively small pores and composite membranes.

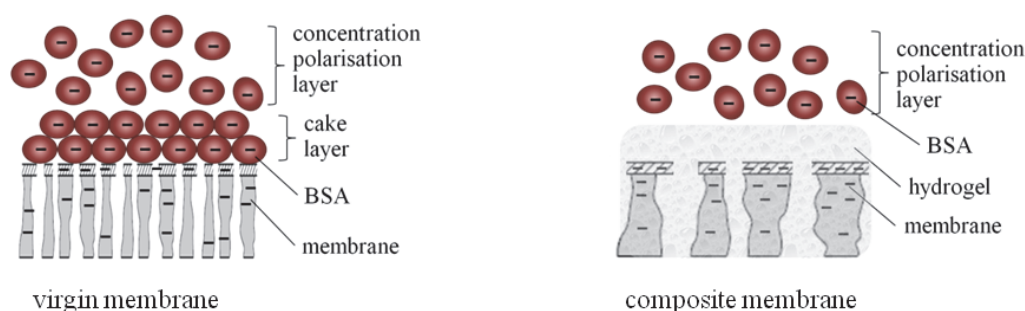


Figure 6.29 Effect of the membrane modification on fouling for the filtration of BSA at pH = 6. A schematic view.

In case of virgin membranes, hydrophobic interactions govern the foulant deposition on the membrane surface. Reason for that is the water structure close to hydrophobic surfaces described as “less-dense”; hence, water molecules close to the surface can be replaced by solutes [138]. Further, due to solute-solute interactions, a cake layer is built. The present CP deteriorates further the permeate flux decline. Even more, when appropriate conditions are present, fouling and consequently flux decline may be enhanced to such extent that the membrane loses flux. By application of a hydrophilic layer on the membrane surface (and within the pores), the membrane-solute interactions can be reduced since the water structure close to the surface is similar to the bulk water structure and no attraction between surface and solutes exists [138]. Nevertheless, CP will still affect the permeate flux.

Higher flux is also measured during CF filtrations of myoglobin through functionalised membranes (example in Figure 6.30(a)). Moreover, the obtained rejection is much more stable over time compared to the rejection of virgin membranes which increases drastically during the process. An example for the filtration performance improvement by the performed surface functionalisation for filtration of protein mixture can be found in Figure 74 (Appendix A).

It is observed, that further surface modification (higher DG) improves the permeate flux much stronger. The example for filtration of protein mixture through PES 50 40/0 11 J/cm² in Figure 6.30(b) shows very high permeate flux and stable myoglobin rejection for the modified membrane, compared to the enormous flux decay of virgin PES 10.

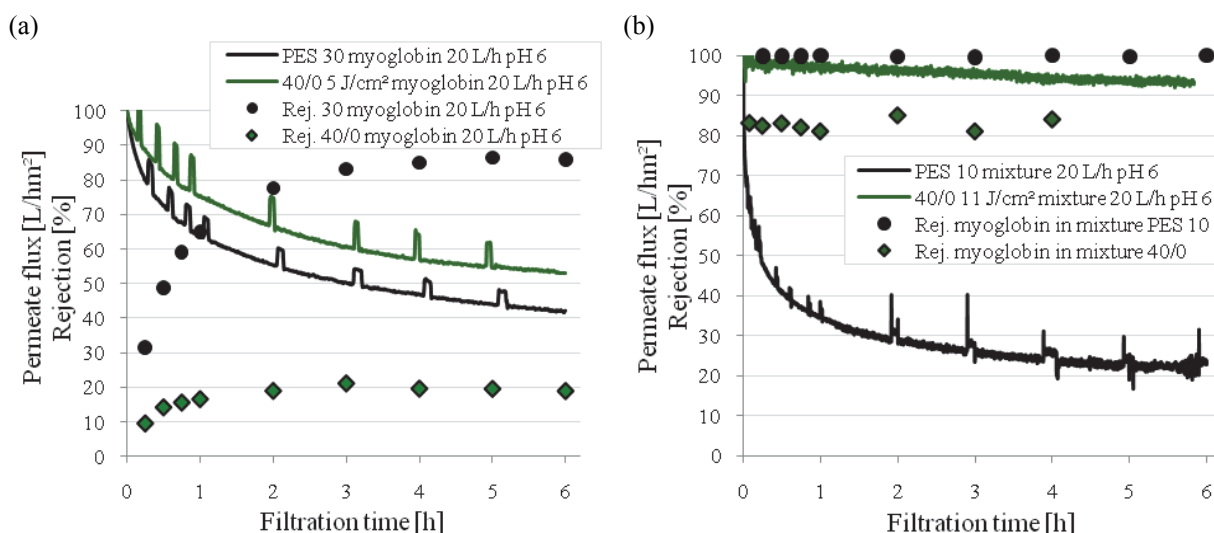


Figure 6.30 Comparison of permeate flux and rejection during cross-flow filtration of (a) myoglobin through virgin PES 30 and PES 50 40/0 5 J/cm²; (b) mixture through virgin PES 10 and PES 50 40/0 11 J/cm².

The effect of membrane-solute and solute-solute interactions in case of filtrations of more permeable solutes is schematically represented in Figure 6.31.

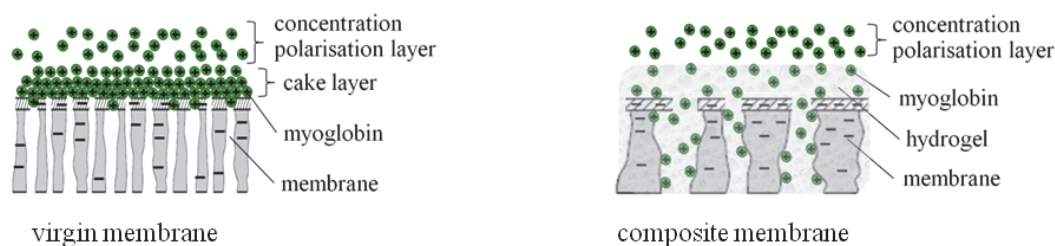


Figure 6.31 Effect of the membrane modification on fouling for the filtration of myoglobin at pH = 6. A schematic view.

When small solutes reach the membrane surface, depending on the relationship solute size/pore size ($d_{\text{solute}}/d_{\text{pore}}$), deposition in the pore openings and membrane inner surface resulting in pore narrowing as well as pore plugging (as shown in Figure 6.31, left) may occur. Further cake layer growth is possible. Depending on the solute permeability of the membrane, CP would influence the flux to varied extent. Since the membrane is modified with hydrophilic polyPEGMA, the strong hydration of the hydrogel reduces the membrane-solute interactions leading to reduced fouling and enhanced flux. Nevertheless, if the hydrogel mesh size is comparable to the solute size, solutes may be caught in the hydrogel network and this would affect the membrane flux and selectivity. Therefore, the hydrogel network has to be well adapted to the solutes to be filtered. CP would influence the permeate flux, since it cannot be affected by the membrane modification (for same rejection).

In general, the fouling mechanism analysis of the data from DE filtrations for virgin and modified membranes shows faster transition from pore plugging to cake formation for functionalised membranes (compared to virgin ones) which does not reduce the permeate flux seriously. In contrast, virgin membranes do not reach steady state of the curve d^2t/dV^2 indicating that the cake filtration regime is not reached during the 24 hours of analysis. The analysis is included in Appendix A (Figure 75 and Figure 76).

6.2.4.2 Effect of the test solution properties

The solution affects the filtration performance of virgin and modified membranes differently. In particular, the solution composition and the solutes' charge cause changes in the permeate flux and rejection of both types of membranes.

Figure 6.32 shows an example for filtrations of single myoglobin solution and mixture through virgin and modified membranes at pH = 6.

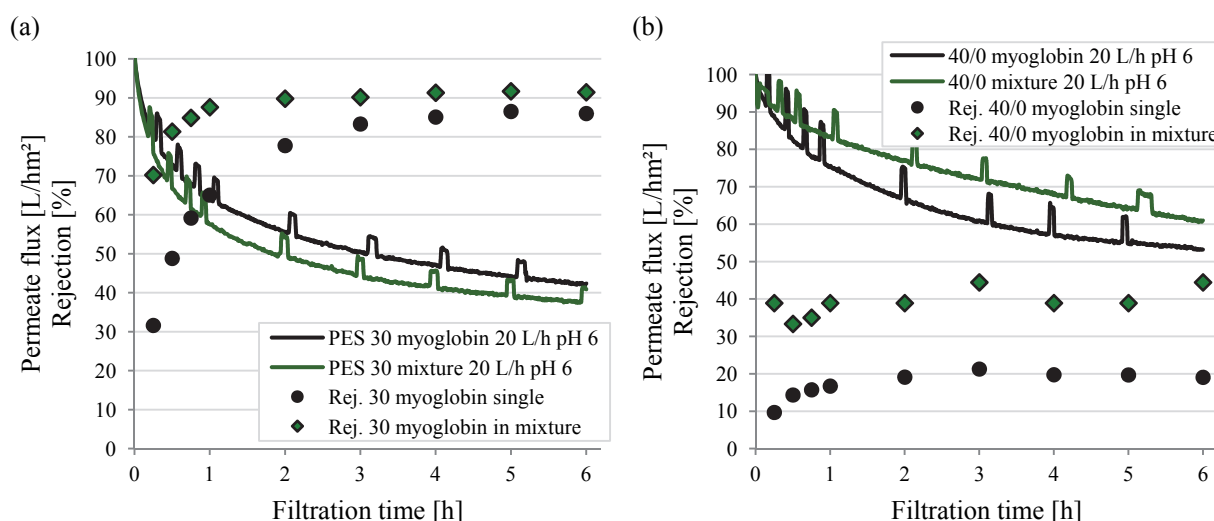


Figure 6.32 Effect of the test solution composition on permeate flux and rejection behaviour during the filtration with virgin and modified membranes; (a) virgin PES 30; (b) PES 50 modified with 40/0 5 J/cm².

When filtrations of solutions of single compounds and mixtures are compared, in many cases virgin membranes deteriorate their permeate fluxes when filtering protein mixture. Contrarily, functionalised membranes exhibit higher fluxes during filtration of mixture (compared to filtration of single solutions). Reason for that are the membrane-solute interactions. In mixtures, the deposition of the bigger BSA molecules on the surface of virgin membranes hamper the penetration of the smaller myoglobin molecules leading to lower flux compared to filtrations of single solutes. Oppositely, BSA deposition is hindered by the hydrogel layer in the composite membranes allowing the myoglobin

transport (cf. Figure 3.2). Since the concentration of myoglobin in mixture is lower than its concentration as single solute in the feed, the permeate flux of mixture increases in comparison to single myoglobin solutions.

As it was already discussed, the solute charge plays an important role for the filtration performance as it may control the membrane selectivity. An example for the effect of pH on permeate flux and rejection during filtrations of myoglobin under variation of its charge through virgin and modified membranes is presented in Figure 6.33(a) and Figure 6.33(b), respectively.

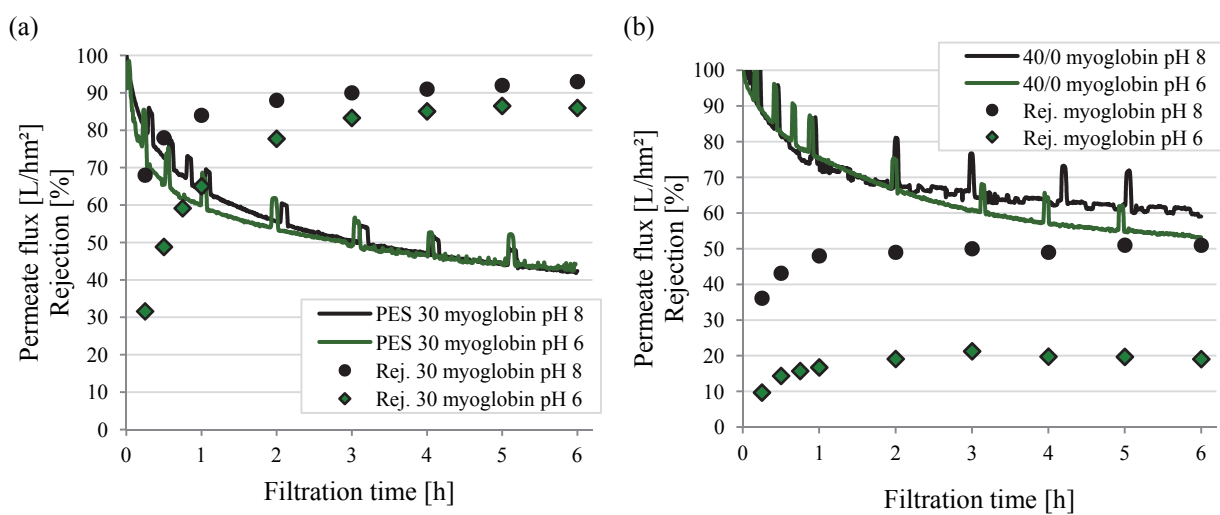


Figure 6.33 Effect of the pH value on permeate flux and rejection during the filtration of myoglobin with virgin and modified membranes; (a) virgin PES 30; (b) PES 50 modified with 40/0 5 J/cm².

For virgin membranes (Figure 6.33(a)), the flux at pH = 6 decreases very rapidly at the beginning of the process but simultaneously with the increasing rejection, the flux decrease is further less pronounced (since the rejection is high, internal fouling is reduced). In the displayed case, after 4 hours both fluxes (at pH = 6 and pH = 8) equalise. Taking into account the results in Figure 6.16 that increase in the CF improves the flux at pH = 6 (but not at pH = 8), it may be assumed that CF is the reason for the relatively good performance of the membrane at pH = 6. In case of modified membranes (Figure 6.33(b)), the obtained rejections of myoglobin at both pH values becomes stable after 1 hour. Due to the fact that the applied hydrogel does not shield the virgin membrane completely, confirmed by the larger CA of modified PES 30 without PVP compared to PES 30 with PVP at same modification degree (cf. Table 5.1), the charge of the virgin membrane plays a role and contributes to the lower myoglobin rejection at pH = 6. Since more myoglobin is in contact with the membrane inner surface at that pH (penetration into the hydrogel is possible), the composite membrane may suffer further flux decline.

6.2.4.3 Effect of the operating parameters

Cross-flow

The operation parameters influence the filtration performance. For all tested membranes and feed solutions, the flux improvement for the functionalised membranes due to increased CF velocity is much stronger pronounced than in the case of virgin membranes. Exemplarily, the effect of the CF on the permeate flux behaviour will be discussed on the basis of results from filtrations of BSA, since this solute is completely rejected by the tested membranes. Figure 6.34 displays the results from filtrations performed at 20 L/h (0.157 m/s) and 60 L/h (0.471 m/s) CF velocity for virgin PES 10 and PES 50 40/0 5 J/cm² at pH = 6 and pH = 8.

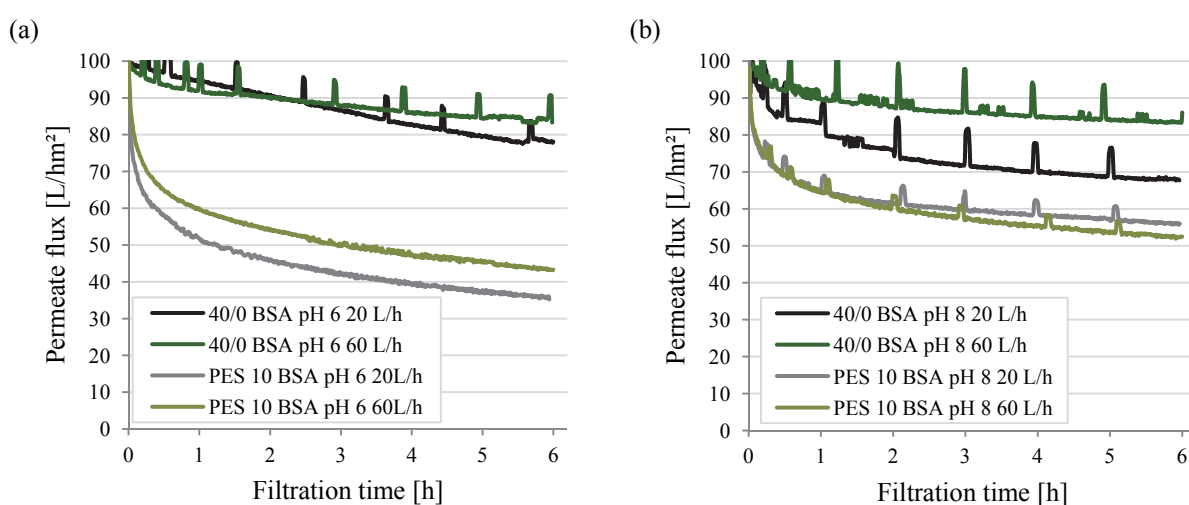


Figure 6.34 Effect of the CF on the flux behaviour of PES 10 virgin and PES 50 modified with 40/0 5 J/cm². Effect of pH; (a) pH = 6; (b) pH = 8.

At pH = 6 (Figure 6.34(a)), for both virgin and modified membranes, the permeate flux is improved by increasing the CF velocity. At pH = 8, better improvement of flux is observed for hydrophilised membranes (Figure 6.34(b)). In studies on the CF effect on CP with hydrophobic PSf and hydrophilic CAC membranes, it has been observed that for hydrophilic membranes the CP was much more minimised due to the less pronounced interactions between BSA and the hydrophilic CAC [28]. According to this work, in case of hydrophilic modified membranes, stronger effect of the CF on flux is found. The effect of CF on the performance of diverse virgin and functionalised membranes during filtrations with BSA, myoglobin and mixture at pH = 8 is shown in Figure 77 – Figure 80 in Appendix A.

Filtration mode

The filtration mode also affects the membrane flux during filtration. In Table 6.3, the relative fluxes of several virgin and functionalised membranes after 6 hours of DE and CF filtrations at similar feed velocities (DE: 0.165 m/s and CF: 0.157 m/s) are summarised.

Table 6.3 Relative fluxes after 6 hours of filtration, comparison of dead-end and cross-flow modes

Membrane pair	pH	BSA		Myoglobin		Mixture	
		dead-end ^a	cross-flow ^b	dead-end ^a	cross-flow ^b	dead-end ^a	cross-flow ^b
PES 50	8	0.40	0.55	0.42	0.45	0.40	0.50
	6	0.49	0.42	0.38	0.40	0.31	0.41
PES 30	8	0.47	0.62	0.36	0.43	0.42	0.45
	6	0.43	0.43	0.39	0.43	0.35	0.41
PES 10	8	0.42	0.56	0.27	0.36	0.53	0.40
	6	0.37	0.33	0.38	0.30	0.36	0.23
40/0 5 J/cm ²	8	0.72	0.68	0.77	0.60	0.87	0.59
	6	0.72	0.78	0.55	0.53	0.76	0.61

^a 0.165 m/s linear feed velocity

^b 0.157 m/s linear feed velocity

The data where CF showed better relative fluxes than DE are presented in black; in red are the data where DE exhibited better fluxes. At first sight, no clear trend can be found about the influence of the operation mode. In general, better performance is expected when using CF, since there is no increasing in the feed concentration due to the recirculation of concentrate and permeate. In DE mode, if high solute rejection is present, the feed concentration increases over time leading to increasing CP, i.e., decreasing permeate flux. However, taking into account the observed protein aggregation due to shear stress in pumps and valves in the CF set-up, deterioration of the performance of CF can be assumed. Hence, if the effect of protein aggregation is more pronounced than the improvement by CF mode, DE appears more lucrative. Looking at the results from the comparison for virgin PES 30 and PES 50 40/0 5 J/cm² in Figure 81 (Appendix A), it can be seen that the initial flux decline during DE is much stronger than that in CF mode due to the increasing CP. The decrease in filtration performance in the later stages of CF mode may be attributed to the assumed protein aggregation. In this work the effect of protein aggregation on membrane fouling and flux is not estimated, therefore, the effect of the CF mode itself cannot be quantified exactly.

Volume reduction

If high solute rejection is present, the volume reduction leads to increase in the feed concentration. The increase in feed concentration may result in stronger CP and fouling or cause enhanced solute transport through the membrane. In Figure 6.35(a), the rejection of myoglobin from DE filtrations with two fold and 20 fold volume reduction in DE filtration is presented.

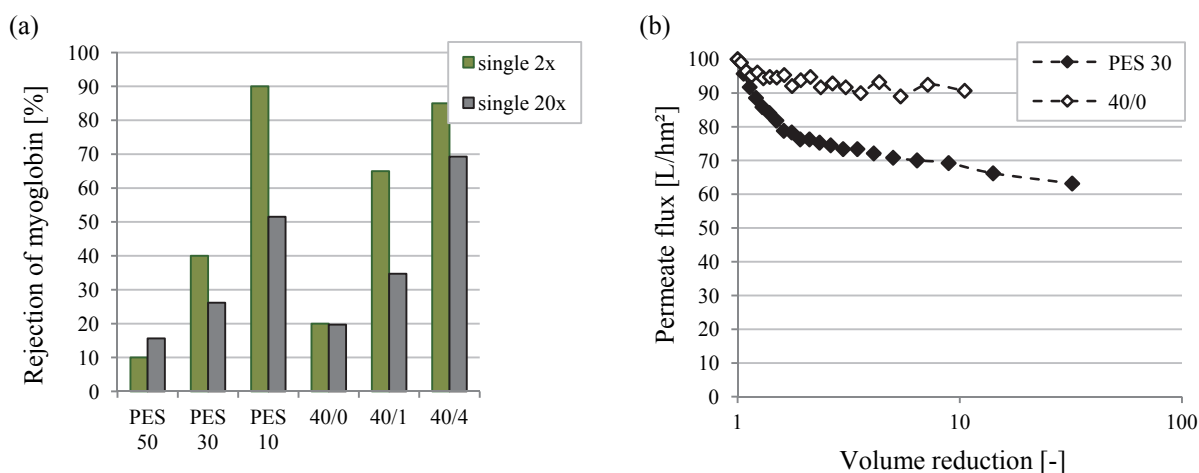


Figure 6.35 Effect of the volume reduction during dead-end filtration with virgin and modified membranes; (a) rejection of myoglobin as single solution; (b) permeate flux of virgin PES 30 and PES 50 40/0 5 J/cm² during 20 fold volume reduction in DE filtration of BSA.

For membranes exhibiting high rejection (virgin PES 30, virgin PES 10, PES 50 40/1 5 J/cm² and PES 50 40/4 5 J/cm²), lower rejection of myoglobin is observed during 20 fold volume reduction in comparison to two fold, caused by the increased CP [2]. Due to the strong accumulation of solute inside the membrane, pore narrowing may be the reason for the obtained opposite effect with virgin PES 50. Modified membrane with 40/0 did not exhibit different behaviour from filtrations with two fold and 20 fold volume reductions. Reason for this can be the low rejection of virgin PES 50 and PES 50 40/0. In this case, CP is less pronounced and therefore, it affects the solute permeation to less extent.

Figure 6.35(b) shows more stable flux during concentration of BSA for modified membrane with 40/0 compared to experiment with virgin PES 30 as a result of the weak interactions between BSA and the hydrogel. Further data for other membranes from rejection of myoglobin in mixture and permeate fluxes during filtration of BSA are summarised in Figure 82, Appendix A.

6.2.4.4 Effect of cleaning and long term stability

The conducted cleaning experiments show that cleaning with water is not effective for virgin membranes. In contrast, the performed external cleaning and back wash with water improve the membrane water flux of functionalised membranes significantly. The hydrophilic layer reduces the irreversible solutes deposition on the surface and within the pores. Furthermore, the stability tests confirm that the grafted hydrogel is stable and reduces fouling even after treatment with NaOH at pH = 13. After three cycles of protein filtration and cleaning, the functionalised membranes exhibit higher and more stable fluxes (cf. Figure 5.76 for filtration of BSA with PES 50 40/0 5 J/cm²) in comparison to virgin membranes (cf. Figure 5.75 – filtration of BSA through virgin PES 10) which lose 50 % of their initial water flux after three cycles.

6.3 FILTRATION OF HUMIC ACID

During filtration of HA solutions, strong flux decline for virgin membranes is observed. In these experiments, the membrane pore size, feed PSD and the membrane surface wettability were found to influence the filtration performance. In the following section, the effects of these parameters and the obtained behaviour improvement by functionalisation will be discussed in terms of permeate flux over time, HA rejection, fouling mechanisms and flux recovery by cleaning.

6.3.1 EFFECT OF PORE SIZE

In Figure 5.77(a), for the filtration of 8 μm prefiltered HA solution through virgin membranes, a very strong flux decline is measured at the beginning of the filtration with PES 5. In this case, the membrane has very small pores compared to the particle size distribution of the filtered solution; thus, pore blocking occurs immediately after the beginning. This curve has the strongest initial flux decline but later during the filtration process this membrane exhibits better performance. This can be explained by the fact that a direct pore blocking and further cake formation occurs. Since the other membranes have bigger pores, pore constriction could be expected first. In case of pore constriction, subsequent pore blocking and further cake formation, the achieved flux is lower than when pore blocking occurs directly. The pore narrowing seems to affect the flux much more strongly, as also described in [181]. In this regard, the bigger the pores, the more the regime moves from initial pore blocking to pore narrowing. Increasing the membrane nominal MWCO increases the flux decline, which can be explained by the above described effects.

The modified membranes show better performance than the corresponding virgin membranes, except PES 5 (Figure 5.79(a)). In general, the measured fluxes are up to 20 % higher than the fluxes of the virgin membranes. Interestingly, modified PES 5 shows very strong drop in the flux during the initial stages, after that almost constant behaviour and ends with lower flux than the corresponding virgin membrane. Very strong flux drop in the early stage of the filtration is observed also for modified PES 300. The curves give the first indication of changing the fouling mechanism due to the applied surface modification [163]. The modified PES 10 and PES 100 show almost constant flux decrease during the filtration. The occurring cake filtration is supported by increasing HA aggregation (cf. Figure 4.6). This means that the fouling layer changes its properties with time, which may lead to an increasing resistance of the deposits.

To explain better the occurring fouling regimes during the filtration of 8 μm prefiltered HA solutions, the collected data are examined using the filtration model introduced in Eq.(2.4) [41]. The calculated d^2t/dV^2 values for selected membranes are plotted against dt/dV in Figure 6.36.

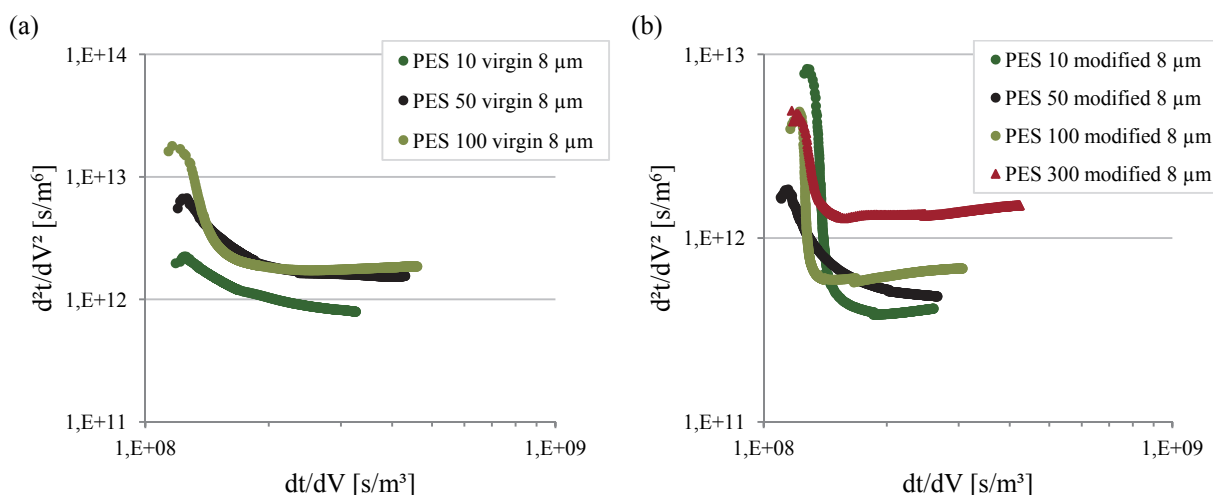


Figure 6.36 Fouling mechanism analysis for the filtration of humic acid with 8 μm prefiltration; (a) virgin; (b) modified membranes.

Figure 6.36(a) presents the results for virgin membranes, whereas results for modified membranes are presented in Figure 6.36(b). Fast pore blocking is found for all examined membranes ($n > 2$). This happens at similar time for the virgin membranes (PES 100 reaches the transition mode earlier than PES 50, which may be due to its different morphology). In contrast, this depends on the pore size for the modified samples. Modified membranes with smaller pores reach the transition mode earlier, e.g., PES 10 (considering the few points with slope $n > 0$).

After that, for all examined filtrations of 8 μm prefiltered HA solutions, a negative slope corresponding to a transition regime from pore narrowing/blocking to cake formation [56] is observed. The slope of the curves during later UF stages changes depending on the pore size, i.e., the fouling regimes of the virgin membranes are influenced by the membrane's nominal MWCO. More negative slope indicates the faster transition to cake formation.

In the later stages of UF, the value for n is $n = 0$ for membranes with smaller nominal MWCO (PES 5, PES 10 and PES 50) and $n > 0$ for PES 100 and PES 300 (the results for PES 5 and PES 300 are shown in Appendix A, Figure 83, since different hydrodynamic conditions were applied, i.e., the initial flux could not be adjusted to 100 L/hm²). This is in contrast to the finding of Taniguchi et al. [56]. It should be mentioned, that PES 100 and PES 300 have sponge-like structure, deviating from the finger-like structure of the membranes with smaller cut-off, which could be also a reason for the different behaviour during UF. Furthermore, the change of the cake properties corresponding to the increase of HA particle size with time (shift of the particle size distribution; cf. Figure 4.6), which could lead to stronger flux decline [23], has an influence on the filtration mode. Taking into account that the cake layer built on the outer surface (due to direct pore blocking) could act as a second membrane, governing the flux and sieving properties, the flux would be more influenced by the

changing cake layer. Membrane with larger pores which are initially narrowed by the foulant, as discussed above, will behave differently.

The cleanability of these membranes is influenced by the membrane pore size (Figure 5.78(a)). The water flux after removing the HA solution increases more for membranes with smaller cut-off, e.g., PES 5 and PES 10. This could be explained with the fact, that CP is stronger for membranes with higher rejection, thus, the elimination of the CP layer increases the flux. External cleaning and back wash with water are more effective with increasing membrane nominal MWCO. This means that the removing of the cake layer by external cleaning recovers more flux for membranes with bigger pores. Reason for that may be the effect of the cake layer on the membrane flux. Assuming that the cake layers have similar properties independent on the membrane type, the membrane pore size and morphology governs the flux behaviour in case of small pores, while for membranes with bigger pores, the porosity and thickness of the cake layer are limiting parameters for the flux. This observation is valid also for modified membranes (cf. Figure 5.80(a)), since cake layer is also built on the hydrogel) [163].

Since HA is better soluble at high pH, chemical cleaning with NaOH is performed. The contribution of the chemical cleaning to the flux recovery is less pronounced for membranes with higher MWCO. The reason is that the effect on flux of removing deposited molecules from the surface of small pores is stronger than for bigger pores because removing a layer of similar thickness from small pores increases the pore diameter more than for big pores.

In case of experiments with 0.45 μm prefiltered HA solutions, both virgin and modified PES 10 exhibit lower fluxes than PES 100 (cf. Figure 5.77(b) and Figure 5.79(b)). It seems that the feed without larger molecules/particles deteriorates the flux of membranes with smaller pores to a higher degree than the flux of membranes with bigger pores. Modified PES 50 performs better than PES 100 probably due to its different morphology. Obviously, membranes with finger-like structure show stronger fouling resistance than membranes with sponge-like structure. More information about the governing fouling mechanisms during these experiments can be obtained from the fouling mechanism analysis displayed on Figure 6.37.

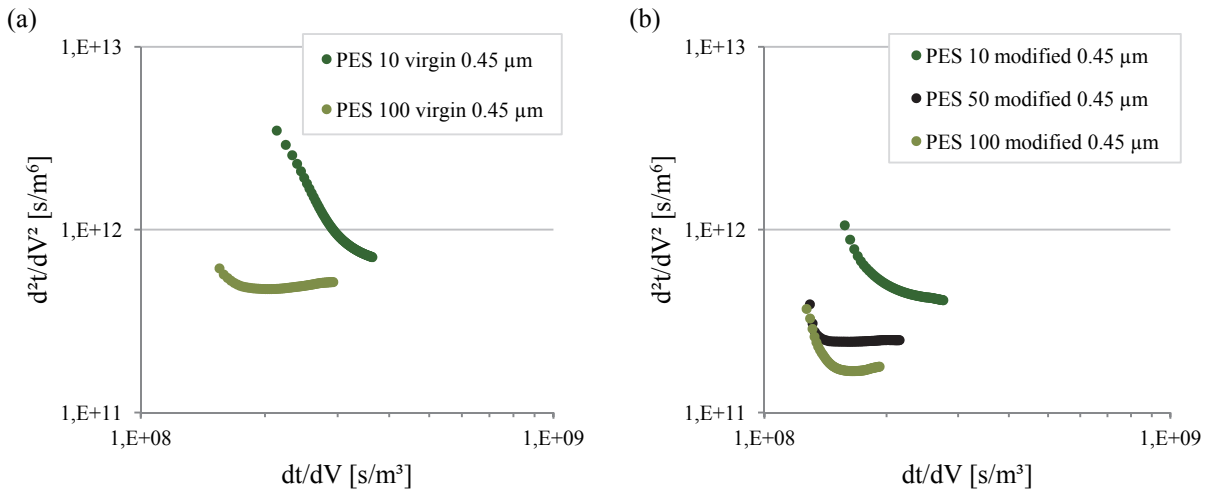


Figure 6.37 Fouling mechanism of filtrations of humic acid with 0.45 μm prefiltration; (a) virgin (b) modified membranes.

For both virgin (Figure 6.37(a)) and modified membranes (Figure 6.37(b)) can be seen that the cake formation regime is not completely reached for PES 10, while PES 100 behaves in cake regime but with increasing cake layer effect possibly due to its morphology ($n > 0$ in the later stages). PES 50 exhibits $n = 0$ corresponding to cake layer regime.

External cleaning induces similar effect on the flux recovery despite the membrane pore size (Figure 5.78(b) and Figure 5.80(b)). In contrast, back wash is more effective for membranes with bigger pores, which can be explained with the possibility for more particles to deposit in the inner surface of membranes with large pores.

6.3.2 EFFECT OF PREFILTRATION

The impact of the prefiltration will be first discussed by means of permeate flux. Figure 6.38 shows a comparison of the permeate fluxes for virgin (Figure 6.38(a)) and modified membranes (Figure 6.38(b)).

Generally speaking, a better flux behaviour is achieved with the solution with smaller HA compounds (prefiltered through 0.45 μm): the curves are less steep, the slopes at the early stages of the filtration are lower. This is valid for both virgin and modified membranes. Regarding the results of the virgin membranes, it is easy to see that the virgin PES 10 shows less improvement (with 0.45 μm prefiltered solution compared to 8 μm): 12 % higher final flux, while the virgin PES 100 has 50 % better performance. Similar is the situation with the corresponding modified membranes. This behaviour could be explained as follows: the aggregates in 8 μm prefiltered solutions could make the cake more permeable to water. The smaller molecules accumulate easily in the cake of big aggregates [10,182]

and could not cause constriction of the small pores of PES 10. The 0.45 μm prefiltered solution has no big aggregates, here, the small molecules that penetrate the membrane inner surface may “stick” together, which could lead to pore constriction and also to the formation of more compact and dense fouling layer [46]. In case of PES 100, pore narrowing is possible with both 8 μm and 0.45 μm prefiltered solutions. Here, the pore constriction would be faster with the 8 μm prefiltered solution due to the relatively bigger particles compared to 0.45 μm prefiltered solution. As a result, the 0.45 μm solution delivers higher flux through PES 100.

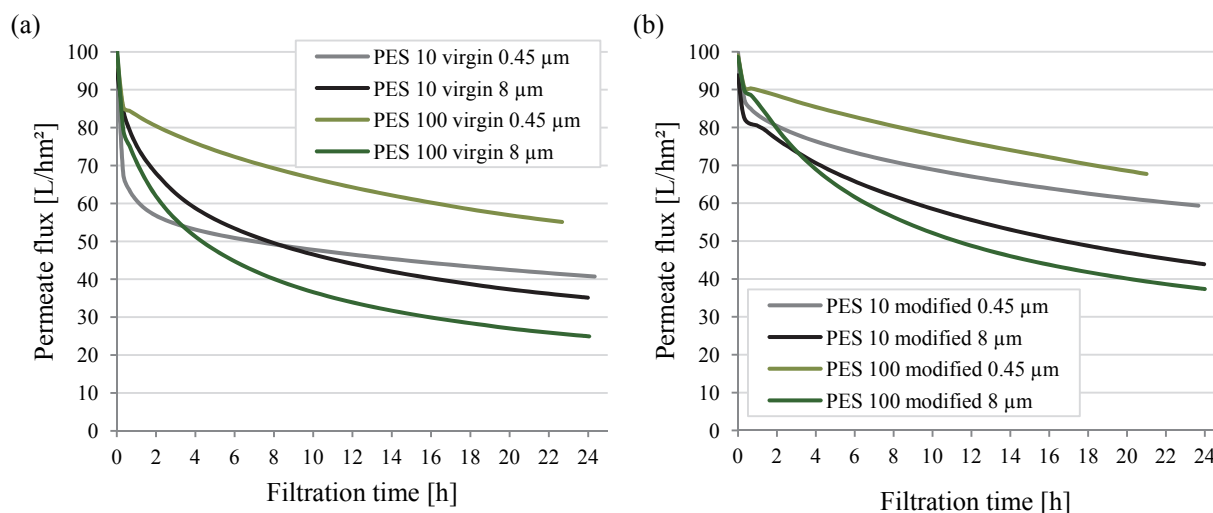


Figure 6.38 Effect of the prefiltration on the permeate flux behaviour; (a) virgin; (b) modified membranes.

Filtration tests with functionalised PES 50 deliver similar curves with slightly higher fluxes compared to PES 100 (a comparison of the results from filtrations with 8 μm and 0.45 μm prefiltered solutions is presented in Figure 84(a) in Appendix A). Similar effect of the prefiltration was reported by Yuan and Zydny [10], where after 2 hours filtration of 2 mg/L HA the 0.16 μm prefiltered solution caused about 0.15 relative flux compared to 100 kDa prefiltered solution with 0.57 relative flux.

Moreover, for modified PES 50 and PES 100 (Figure 6.38(b) and Figure 84(a), Appendix A), a change in the curves' shape is observed. In case of 8 μm prefiltered solution, the curves have the typical fast decrease in flux (in the early stages) and then the slope of the curves decreases with time. Analysis of the curves collected with 0.45 μm prefiltered solutions showed linear decrease already after 20 min filtration time (second point in the diagrams), i.e., the cake filtration regime is reached very fast. The constant decrease in flux means that the changing properties of the cake layer influence the filtrate flux during the 24 hours run [163].

The effect of prefiltration on cleanability is shown exemplarily for PES 10 and PES 100 in Figure 6.39.

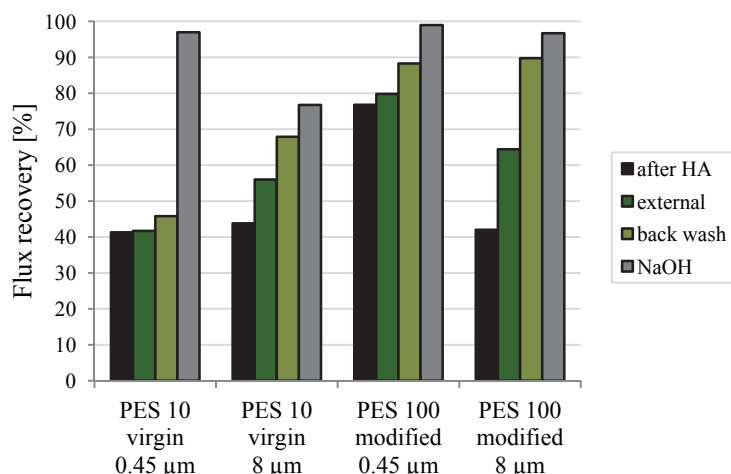


Figure 6.39 Effect of the prefiltration on the cleanability of virgin and modified membranes.

Figure 6.39 shows clearly that the physical cleaning has lower effect on the membranes used for ultrafiltration of 0.45 µm prefiltered solutions. A very small fraction of the deposited fouling layer is removed from the membrane surface, which means that the layer is “stuck” to the membrane. Cleaning with water is not able to remove the deposited HA. Since the smaller HA fraction may be adsorbed more strongly on the membrane surface (irreversible fouling), it would not be removed by physical cleaning. This statement is in agreement with the calculated specific cake resistances (cf. Table 6.4) which are all higher than the values for 8 µm prefiltration. The poor cleanability of the membranes used with 0.45 µm prefiltered solutions can be explained with the physical properties of the fouling layer: bigger aggregates could keep the cake layer porous [55], as explained before, and also trap smaller particles in the cake not allowing them to reach the membrane [10].

Nevertheless, the cleaning of modified PES 100 yields better flux increase compared to virgin PES 10, which means that the hydrogel layer improves the physical cleanability of the membranes. Comparing the contributions of the different cleaning stages to the flux recovery of membranes fouled by 0.45 µm prefiltered solutions, back wash has stronger effect compared to external cleaning. Explanation could be that the layer should be pushed from the back in order to be removed from the surface; furthermore, the inner membrane surface is filled with fouling substances (cf. rejection values for HA in Figure 5.16). The data obtained from cleaning of modified PES 50 are included in Appendix A, Figure 84(b), since similar effects to PES 100 are found.

6.3.3 COMPARISON OF VIRGIN AND MODIFIED MEMBRANES

For comparison of the performance of virgin and functionalised membranes, membranes with similar water flux and dextran rejection properties are selected. The improvements by the applied hydrogel layer will be discussed by means of permeate flux and rejection behaviour, fouling regimes and parameters as well as cleanability. From the data in Figure 5.16, the pairs for comparison are chosen, i.e., virgin PES 5 vs. modified PES 10, virgin PES 10 vs. modified PES 50 and virgin PES 10 vs. modified PES 100.

6.3.3.1 Permeate flux and rejection during filtration

The permeate fluxes of the selected membrane pairs are presented in Figure 6.40. In Figure 6.40(a), the first pair is presented, while Figure 6.40(b) and Figure 6.40(c) show the results of the other two pairs (together) from experiments with 8 μm and 0.45 μm prefiltered HA solutions, respectively.

First, modified PES 10 behaves better than virgin PES 5 but these membranes could not be directly compared, since the hydrodynamic conditions during the experiments are different (initial flux of 100 L/hm² could not be reached for PES 5).

The modified PES 50 has better performance at similar water permeability and MWCO (and also rejection of HA) than the virgin PES 10 in both cases of prefiltration. However, the final flux of the modified PES 50 after filtration of 8 μm prefiltered solution is only by 10 L/hm² higher than the flux of the virgin PES 10, whereas the prefiltration through 0.45 μm filtered solution yields 70 L/hm² for the modified PES 50 and only 40 L/hm² for the virgin PES 10. Comparing the influence of the prefiltration during filtration through the virgin membrane, the prefiltration through 0.45 μm brings 10 L/hm² flux increase. At the same time the performance of modified PES 50 is much more improved – the flux at the end of the filtration increases by 35 L/hm² due to the small feed particle size distribution [163]. The improvement of the resistance towards fouling of modified PES 50 is achieved by the grafted hydrogel layer due to its hydrophilic properties.

In both cases of prefiltration, modified PES 100 exhibits better flux than virgin PES 10 but has higher MWCO.

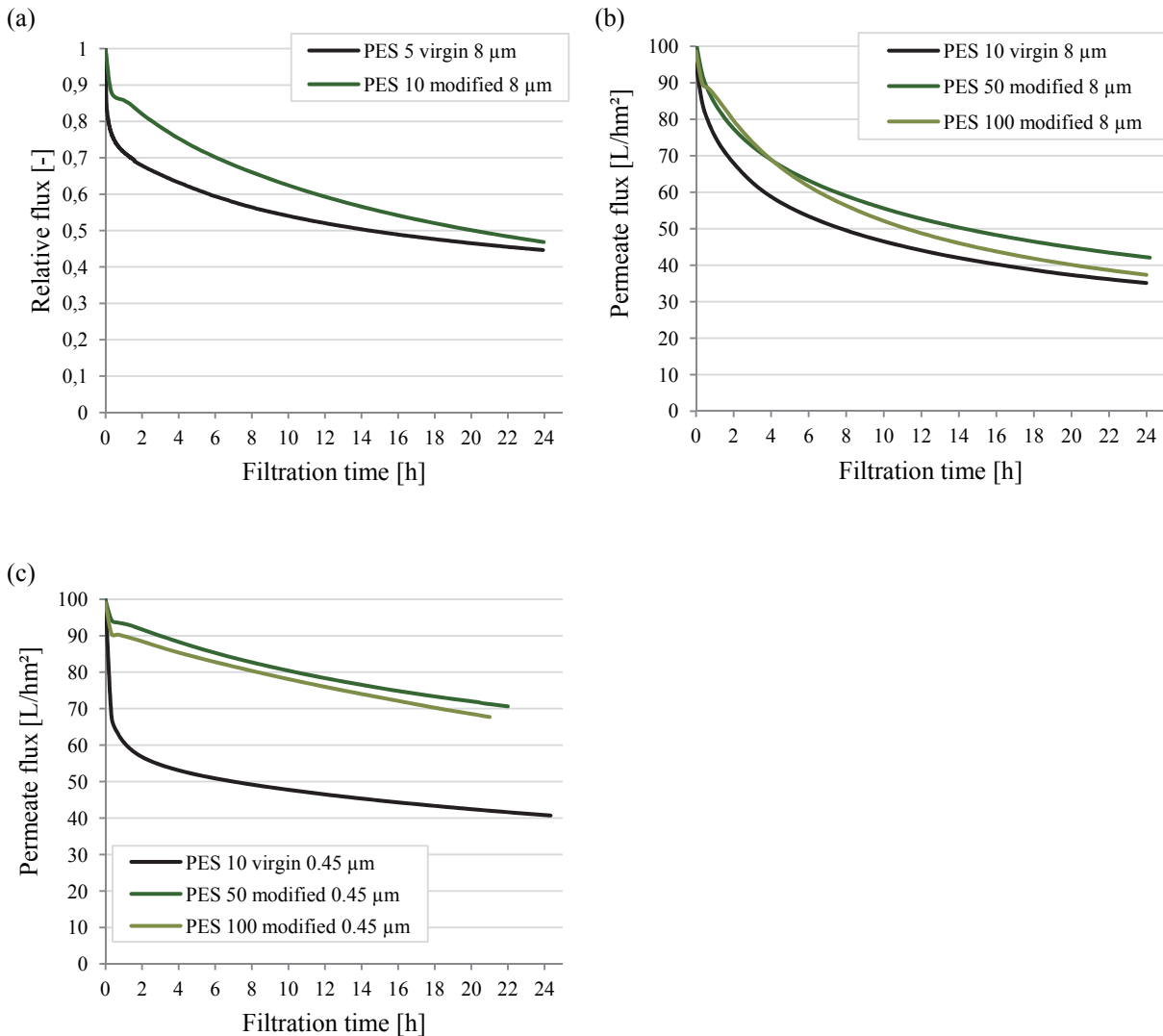


Figure 6.40 Flux during filtration of humic acid. Comparison of virgin and modified membranes with similar water flux and cut-off; (a) virgin PES 5 vs. modified PES 10 (8 μm prefiltration); (b) virgin PES 10 vs. modified PES 50 and PES 100 (8 μm prefiltration); (c) virgin PES 10 vs. modified PES 50 and PES 100 (0.45 μm prefiltration).

Comparing the behaviour of both modified membranes, modified PES 100 shows slightly less performance during filtration compared to PES 50. Reason may be the different morphology of these membranes. PES 100 has higher water permeability and MWCO than PES 50, which means that this membrane has larger pores. Thus, internal fouling will be much more pronounced for PES 100 than for PES 50 leading to lower filtration performance.

6.3.3.2 Fouling regimes and parameters

Furthermore, fouling regime analysis for virgin PES 10 and modified PES 50 and PES 100 after experiments with 0.45 μm prefiltered feeds is performed. A comparison with the data from 8 μm prefiltration is shown in Figure 6.41.

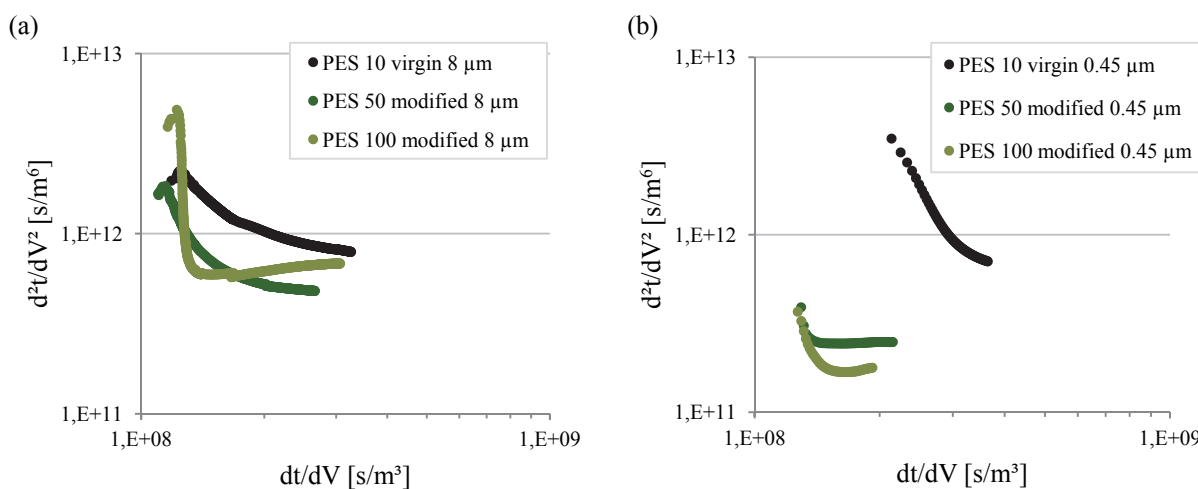


Figure 6.41 Comparison of the fouling regimes for virgin and modified membranes with similar water flux and cut-off; (a) 8 μm ; (b) 0.45 μm prefiltration.

Comparing the results for virgin and modified membranes, the curves for 8 μm prefiltrations lay close to each other, whereas the modified membranes with 0.45 μm prefiltration of HA solution are placed much deeper than the curve of virgin PES 10. This means that the improvement of the filtration properties is more successful for the membranes where the feed is prefiltered through 0.45 μm filter.

The direct comparison of the data for different prefiltrations is not possible, since the first data point for 0.45 μm prefiltration is taken 20 min. after the beginning of the filtration, whereas the interval for 8 μm prefiltration is 0.5 min. Nevertheless, it can be seen, that the modified PES 50 with 0.45 μm prefiltration of the feed solution reaches a plateau, while the curve for feed after prefiltration through 8 μm filter does not show such behaviour.

Specific cake resistance

Further analysis of the collected data is done in order to characterise the built fouling layer and the influence of the surface modification and feed composition on it. The contribution of the cake layer to the total membrane resistance in the form R_c/R_t and the specific cake resistance α are calculated. Therefore, the deposited mass of HA expressed as mass per membrane area m_{dep} is evaluated. The values for selected membranes are summarised in Table 6.4.

Table 6.4 Characteristics of the fouling layer according to the resistance in series model

Membrane type	m_{dep} [g/m ²]		R_m [10 ¹² m ⁻¹]	R_c [10 ¹² m ⁻¹]		R_c/R_t [-]		α [10 ¹¹ m/g]	
	8 μm	0.45 μm		8 μm	0.45 μm	8 μm	0.45 μm	8 μm	0.45 μm
PES 10 virgin	51	1.6	1.89	2.43	7.07	0.56	0.59	0.48	43.3
PES 50 virgin	31	n.d.	0.38	7.77	n.d.	0.67	n.d.	0.25	n.d.
PES 100 virgin	54	5.1	0.53	1.43	0.41	0.73	0.45	0.27	0.81
PES 10 modified	47	6.2	11.9	11.9	11.0	0.50	0.49	2.56	17.7
PES 50 modified	22	7	2.70	3.30	2.60	0.55	0.29	1.50	3.72
PES 100 modified	42	6	1.28	1.76	0.50	0.58	0.32	0.42	0.58

The virgin membranes accumulate more HA from the solution prefiltered through 8 μm than the modified membranes [163]. Furthermore, the ratio R_c/R_t , i.e., the contribution of the cake layer resistance to the total membrane resistance of the virgin membranes is higher.

By comparing the membrane pair virgin PES 10 and modified PES 50, in case of 8 μm prefiltered solutions, the specific cake resistance is lower for the virgin membrane. This means that the contribution of 1 g cake layer to the cake resistance is lower for virgin PES 10. This could be explained with the properties of this cake layer: it would be more “porous” letting the filtrate flow through it. In case of PES 50, the hydrogel layer seems to be “filled up” with relatively small HA fractions; after that on top of the hydrogel layer the cake layer is built.

Regarding the corresponding data of the examined membranes from the filtration of 0.45 μm prefiltered HA solution, the cake layer behaviour seems to be different. In general, the measured specific cake layer resistance after the filtration of 0.45 μm prefiltered solutions is much higher than for 8 μm prefiltered ones. Comparing virgin with modified samples, more mass is accumulated on the modified compared to virgin membranes.

For the virgin PES 10, less deposited mass combined with higher cake layer resistance corresponds to very high specific cake resistance, i.e., the cake layer should be very dense and impermeable. The cake layer which is built on the modified PES 50 seems to be kept away from the membrane surface by the hydrogel layer allowing the permeation. The deposited mass of HA does not affect the liquid flow through the membrane.

6.3.3.3 Effect of cleaning

External cleaning has stronger effect with increasing MWCO. Furthermore, virgin membranes have higher flux recovery due to external cleaning (8 μm prefiltered feed), i.e., it seems that the cake layer is easily removed from the virgin membrane surface. The explanation could be the surface charge of

the membranes. Since the virgin membranes exhibit more negative ZP and HA is prevalently negatively charged, electrostatic repulsion would be the reason for easy removal of the cake layer from virgin membranes.

The impact of back wash on the flux also increases with increasing membrane MWCO. An explanation for this effect is that during back flush at 1 bar TMP more permeate is collected for 10 minutes from membranes with higher MWCO due to their higher flux. In contrast to external cleaning, back flush recovers more flux for the modified membranes. It seems that back flush removes the adhering components from the hydrogel layer, which leads to increase in flux.

Chemical cleaning of modified membranes recovers more flux, thus, they reach mostly more than 95 % of their initial flux. Virgin membranes recover up to 90 % of the initial flux (Figure 5.78 and Figure 5.80).

Generally speaking, physical and chemical cleaning are more effective for the hydrogel layer composite membranes [163]. The comparison of the cleanability of membranes with similar properties (flux and/or MWCO) is displayed on Figure 6.42.

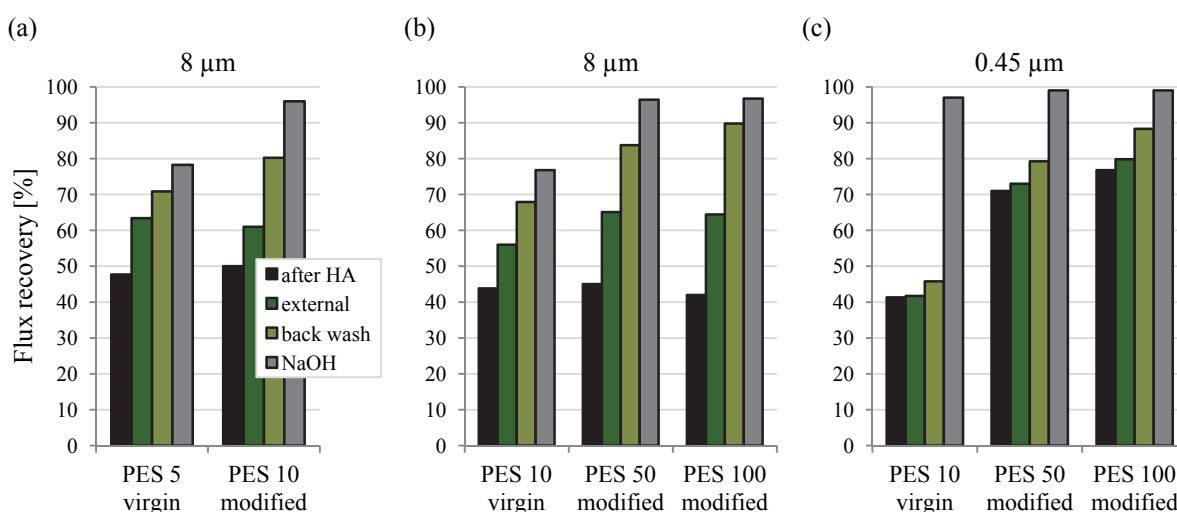


Figure 6.42 Comparison of the cleanability of virgin and modified membranes with similar water flux and cut-off; (a) virgin PES 5 and modified PES 10 (8 µm prefiltration); (b) virgin PES 10 and modified PES 50 and PES 100 (8 µm prefiltration); (c) virgin PES 10 and modified PES 50 and PES 100 (0.45 µm prefiltration).

Comparing virgin PES 10 with modified PES 5, both physical and chemical cleaning are more effective when applied to the modified membrane. The same conclusion could be drawn for the pair virgin PES 10 and modified PES 50, e.g., in case of filtrations with 8 µm prefiltered solution, modified PES 50 increases its water flux with 20 % after each cleaning step.

In conclusion, composite membranes show better performance due to the improved surface properties by the performed hydrophilic functionalisation.

6.4 FILTRATION OF POLYPHENOLICS

The filtration of polyphenolics through virgin membranes shows an influence of the membrane pore size on the fouling resistance. As it can be seen in Figure 5.82, virgin PES 5 exhibits less than 20 % from its initial water flux after short filtration of polyphenolics, while virgin PES 50 maintains almost 60 % of the initial flux. This effect can be explained by the fact that the pore narrowing occurring during the filtration process (both membranes show less than 10 % solutes rejection (Figure 5.83)) affects the flux of smaller pores more strongly than large pores. Moreover, increasing flux causes stronger flux decline during CF filtrations (cf. Figure 5.84) due to the contact of more solutes with the membrane surface at higher solutes throughput. The reasons why these membranes are fouled by polyphenolics may be found in the membrane roughness and chemistry. It has been observed that rougher membranes tend to foul when in contact with polyphenolics [25]. Further, hydrogen bonding between hydroxyl groups of the polyphenolics and oxygen atom from SO₂ group in PES as well as benzene ring-benzene ring interactions via π - π stacking [183] may lead to increased polyphenolics adsorption on the membrane surface. Moreover, polyphenolics bind to PVP via hydrogen bonding [184-186], thus using the high adsorption capacity of PVP towards these compounds, PES/PVP membranes have been already used for selective removal of polyphenolics from apple juice [187,188]. The effect of PVP has been also studied by comparing the flux decrease after static adsorption of polyphenolics on self-made PES membranes with and without PVP with similar cut-off [164]. The fluxes decreased more strongly for the membrane which was prepared without PVP additive.

The modification with polyPEGMA hydrogel at relatively low modification degrees seems to improve the membrane performance, e.g., higher fouling resistance is observed for modified membranes with up to 6 J/cm² UV irradiation energy (Figure 5.82) and higher fluxes are measured during CF filtration with PES 50 40/0 5 J/cm² (Figure 5.85). In fact, even $R_f > 1$ is measured with PES 50 40/0 6 J/cm². Other researchers have already observed this effect and concluded that the adsorption of hydrophilic species (polyphenolics exhibit rather hydrophilic properties due to the presence of many OH groups) may be an advantage for the performance of filtration processes [67].

Further surface modification leads to loss of membrane performance during filtration: modified membranes at 11 J/cm² undergo 80 % of flux decrease during CF filtration (Figure 5.85). Moreover, absorption experiments with hydrogels deliver partitioning coefficients of about $\kappa \sim 10$ (cf. Figure 5.2), showing that polyphenolics have affinity to the hydrogels. Since polyphenolics may be attracted by the hydrophilic composite membrane surface and form hydrogen bonds with the PEG chains, solutes adsorption on the membrane could be expected when more hydrogel is present. On the other hand, modified membranes at same UV irradiation dose but different water fluxes (over varied MBAA amount) were tested in short DE filtrations. The obtained fouling resistances after the performed

experiments were compared by the membranes initial water fluxes. The results for modified membranes PES 50 at three UV irradiation stages are compared with the data from virgin PES 5 and PES 50 in Figure 6.43.

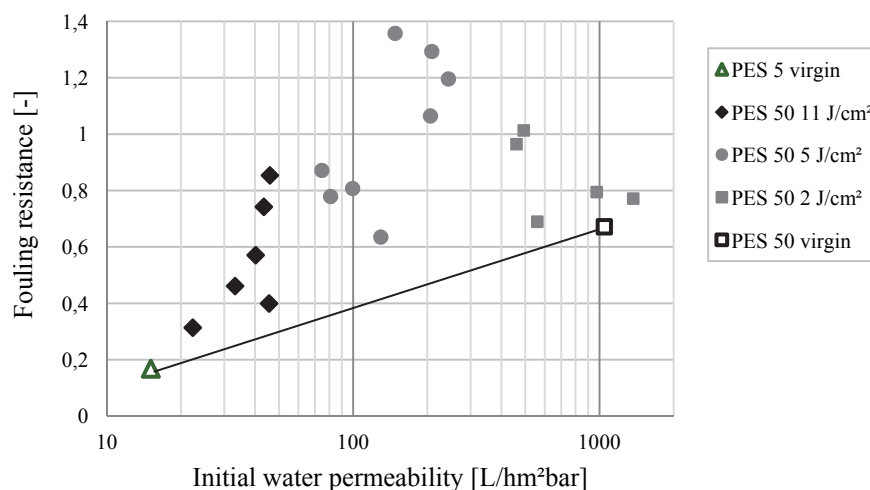


Figure 6.43 Effect of membrane pore size on the fouling resistance to polyphenolics for virgin and modified membranes.

By assuming that the water permeability is governed by the membranes effective pore size, lower permeability can be observed for membranes with smaller pores. As it can be seen, membranes with lower fluxes (assumed to have smaller pores) exhibit lower fouling resistance to polyphenolics. The effect of pore size described for virgin membranes can be found also in the case of functionalised membranes. In addition, from absorption experiments with hydrogels, it is found that PEGMA/MBAA hydrogels adsorb more polyphenolics than PEMGA and PEGMA/PETAE hydrogels ($\kappa \sim 20$; Figure 5.2); furthermore, the rejection of membranes modified with PEGMA/MBAA increases (Figure 5.83). Hence, MBAA may also interact with polyphenolics via H-bonds. Nevertheless, this trade-off analysis shows that in these experiments, all modified membranes exhibit better performance than the virgin membranes, i.e., all data points for modified membranes lay above the trade-off curve for virgin membranes, having higher fouling resistance at higher water permeability.

In conclusion, thin-layer hydrogel composite membranes may be used for separation of polyphenolic compounds when appropriate modification conditions are selected. The selective adsorption or transmission of these compounds can be realised by adjusting the membrane chemistry and hydrodynamic conditions.

7 CONCLUSIONS AND OUTLOOK

Thin-layer hydrogel composite membranes were prepared via UV assisted grafting-from surface modification of commercial PES UF membranes with PEGMA. The resulting membranes had lower water permeability, more neutral surface charge and were more hydrophilic. The functionalisation was performed at mild conditions (low UV intensity and selected UV wavelengths) in order to control the pore degradation occurring due to PES chain scission.

Diverse tests (CA, ZP, SEM, AFM, etc.) showed that the hydrogel layer was successfully grafted on the membrane surface as well as in the membrane pores, until a depth of a few μm relative to the irradiated barrier surface (SEM-EDX). AFM in liquid state delivered very interesting information about the hydrogel layer behaviour. Further optimisation of this characterisation method could yield more information regarding other important properties (e.g., homogeneity in dry and wet state). The effect of the varied grafting conditions was also proved by measuring water permeability, rejection of dextrans and proteins. In this work, variation of the parameters UV irradiation time, UV intensity and crosslinkers type and amount contributed to the preparation of composite membranes with defined structure and properties. Membrane surface modifications with PEGMA/MBAA 40/4 was not successful with larger membrane areas (for CF experiments), thus further investigations of the background of this problem is necessary.

A fine tuning of the desired sieving properties was achieved by the application of suitable crosslinking agents with two or three crosslinking points. Membranes crosslinked with the “two-armed” MBAA showed “tighter” hydrogel structure and enhanced the protein rejection, whereas, in contrast to the expectations, at the same base membrane pore size, hydrogel layers crosslinked with the “three-armed” PETAE swelled more strongly yielding a more open barrier structure and the protein rejection decreased compared to membranes modified with MBAA or without any crosslinker. These effects were less pronounced for modified membranes with larger pores. In this approach, the sieving properties of the functionalised membranes were tailored via controlled crosslinking. By applying the optimised functionalisation conditions, it was possible to prepare membranes with similar water flux and sieving properties compared to virgin membranes but better fouling resistance. The hydrogel is a crucial factor which defines the membrane performance during filtration, whereas the base membrane acts either simply as a permeable support or also contributes to selectivity. The sieving properties of some membranes deteriorated drastically due to the UV excitation (PES 300) or were first deteriorated and then again improved by the growing hydrogel layer after further surface modification. Further investigation of the hydrogel layer mesh size is needed in order to clarify some critical points in this work. Comprehensive study of the behaviour of hydrogel layers prepared with PEGMA/MBAA 40/1

may contribute to understanding the interesting results observed from such composite membranes. The contribution of PETAE to the hydrogel properties was not completely clarified. Experiments with additives in the solvent of the modifiers solution may increase the conversion in gels and lead to more quantitative results.

Since the applied hydrogel layer caused strong membrane flux decline, further experimental study is needed. Aim will be the achievement of good rejection/selectivity properties of modified membranes at higher fluxes. For better understanding of the trends to be achieved, Figure 7.1(a) shows a trade-off analysis of collected representative results by means of myoglobin rejection; i.e., the trade-off between protein rejection (from short DE filtrations with two fold volume reduction) and water permeability of different virgin membranes are compared to the data from functionalised membranes prepared by varied UV irradiation dose and crosslinking. Modified membranes with improved rejection performance and higher water fluxes have to be found above the trade-off curve for virgin membranes; the arrow indicates the target of membrane performance improvement. As it can be seen, most of the modified membranes are below the curve for virgin membranes. Reason is the strong fouling for virgin membranes which shifts the trade-off curve for virgin membranes to higher rejection values. A trade-off analysis between protein selectivity and water permeability [189] would also deliver results overlapped by fouling effects.

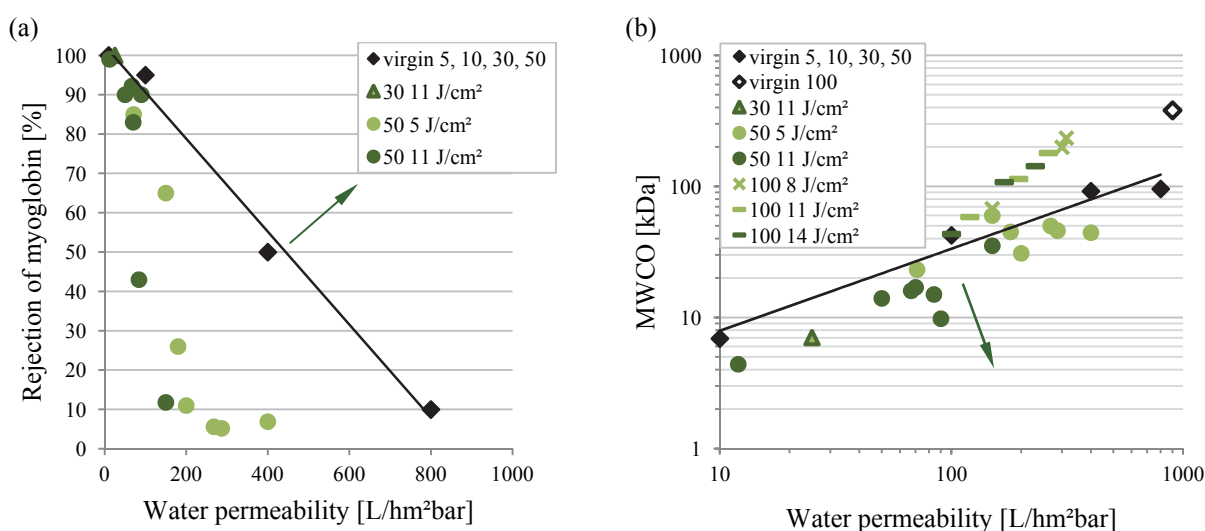


Figure 7.1 Trade-off analysis; (a) myoglobin rejection vs. water permeability; (b) MWCO vs. water permeability.

When the analysis is performed on the basis of MWCO data from dextran rejection experiments (Figure 7.1(b)) where fouling on virgin membranes is relatively low, different trend can be found. Membranes with high dextran rejection and high water flux, i.e., membranes with good performance, can be found below the trade-off curve for virgin membranes; here, the arrow shows again the direction of improved performance. As it can be seen, all data points for functionalised PES 100 are to

find above the trade-off curve for virgin membranes. Here, it should be noticed that the data for virgin PES 100 does not fit the trade-off curve for the other membranes. Since the base membrane PES 100 differs by its structure from the other membranes included in this graphic (PES 100 shows sponge-like membrane structure), the apparent non-satisfying results for modified membranes PES 100 may be due to the different properties of the base membrane. Thus, direct comparison of the performance of these functionalised membranes with virgin membranes with finger-like structure is not appropriate. In contrast, the most other functionalised membranes are below the trade-off curve for virgin membranes. From here it can be concluded that almost all functionalised PES 30 and PES 50 membranes exhibited superior separation performance. The performance improvement by the functionalisation was even larger with feed solutions of stronger fouling potential. For instance, in contrast to the unmodified membranes, it was possible to achieve a stable selectivity between two proteins of different size in the course of long-term ultrafiltration. Nevertheless, it is of great interest to prepare membranes with yet smaller MWCO at same or higher water permeability; i.e., the data points for MWCO have to be shifted down further away from the curve of virgin membranes (note the green arrow).

Furthermore, the membrane performance of virgin and modified membranes was evaluated during filtration experiments with proteins, humic substances and polyphenolics as well as cleaning and long term stability tests.

Regarding the behaviour of virgin membranes, the protein size and charge as well as the membrane pore size and charge influenced the membrane performance during filtration. If membrane and solute were oppositely charged, attraction forces caused strong fouling. In case of similar charge, repulsion minimised fouling. The relationship pore size/solute size played an important role for the membrane performance. If the size of solute was much bigger than the membrane pore size, this led also to lower membrane performance for solutes with charge close to zero. When solute and membrane were oppositely charged, the enhanced pore plugging by attraction forces combined with cake formation led to low performance. Pore narrowing enhanced fouling, when $d_{solute} \ll d_{pore}$.

The modification with hydrophilic agent increased the fouling resistance of the membranes against proteins. Modified membranes with similar water flux and cut-off to virgin ones showed higher fluxes and more stable rejection properties during protein filtration. The CF had more pronounced effect on membrane flux for modified membranes, i.e. when fouling was not strongly pronounced. Mechanical cleaning with water was successful only for modified membranes; the water flux of virgin membranes could be slightly recovered only by using chemical cleaning. In long term application, after more cleaning steps, functionalised membranes showed more stable behaviour and better filtration performance. Fouling studies with proteins at their IEP are needed for functionalised membranes in order to evaluate the interactions between low charged surfaces and non-charged solutes. Further study

of the filtration behaviour at $\text{pH} = 4$ should be performed due to the incomplete characterisation of the occurring effects during filtration provided by this work.

During the filtration of humic substances, the size distribution of the solute was important. Membranes with higher MWCO exhibited stronger flux decline during UF but better cleanability. Prefiltration through $0.45\ \mu\text{m}$ filter improved the membrane performance during filtration of HA but the cake layer was more difficult to remove from the membranes surface during cleaning. The applied modification improved also in this case the membrane performance during ultrafiltration and facilitated the physical cleaning. The study contributed to a better understanding of the relationships between membrane pore size, solute size and size distribution, membrane surface chemistry and membrane fouling.

From filtration experiments with polyphenolics, at first sight, the increase in membrane hydrophilicity (i.e. increasing of UV irradiation dose) did not lead to better filtration performance. When analysing the membrane effective pore size (by comparing the composite membranes water flux), for same UV irradiation dose membranes with higher fluxes showed better fouling resistance to polyphenolics. At functionalisation conditions where the membrane pore size did not change very strongly, e.g. $5\ \text{J}/\text{cm}^2$ UV irradiation dose, the membranes showed higher permeate fluxes than virgin membranes.

Through varying the degree of crosslinking, membranes with defined characteristics either for the separation of macromolecular mixtures or for the concentration of products were prepared. Moreover, these membranes exhibited improved performance during filtration of natural compounds; the applied hydrogel layer was able to control the membrane-solute interactions minimising fouling. Mixtures of polyphenolics and proteins and sugars may be investigated in filtration experiments in order to collect information relevant to real applications. The application of these new thin-film hydrogel composite membranes would reduce the material costs and increase the throughput of the ultrafiltration process, leading to high quality products, especially for the food and pharmaceutical industries.

REFERENCES

- [1] H. Susanto, Fouling Study in Ultrafiltration: Mechanism and Control via Membrane Surface Modification, Dissertation, Universität Duisburg-Essen, Essen (2007)
- [2] R.W. Baker, Membrane technology and applications, John Wiley & Sons Ltd., Chichester (2004).
- [3] R. van Reis and A. Zydney, Membrane separations in biotechnology, *Current Opinion in Biotechnology* 12 (2001) 208-211.
- [4] J.E. Kilduff, S. Mattaraj, M. Zhou and G. Belfort, Kinetics of Membrane Flux Decline: The Role of Natural Colloids and Mitigation via Membrane Surface Modification, *Journal of Nanoparticle Research* 7 (2005) 525-544.
- [5] R. Molinari, M.G. Buonomenna, A. Cassano and E. Drioli, Recovery and recycle of tannins in the leather industry by nanofiltration membranes, *Journal of Chemical Technology & Biotechnology* 79 (2004) 361-368.
- [6] F. Lipnizki, Industrieller Einsatz der Ultrafiltration in der pharmazeutischen Biotechnologie, *Chemie Ingenieur Technik* 76 (2004) 165-168.
- [7] P. Le-Clech, V. Chen and T.A.G. Fane, Fouling in membrane bioreactors used in wastewater treatment, *Journal of Membrane Science* 284 (2006) 17-53.
- [8] K. Glucina, A. Alvarez and J.M. Laine, Assessment of an integrated membrane system for surface water treatment, *Desalination* 132 (2000) 73-82.
- [9] D. Wu and M.R. Bird, The fouling and cleaning of ultrafiltration membranes during the filtration of model tea component solutions, *Journal of Food Process Engineering* 30 (2007) 293-323.
- [10] W. Yuan and A.L. Zydney, Humic acid fouling during microfiltration, *Journal of Membrane Science* 157 (1999) 1-12.
- [11] M. Kabsch-Korbutowicz, Ultrafiltration as a method of separation of natural organic matter from water, *Materials Science-Poland* 26 (2008) 459-467.
- [12] H.-C. Kim and B.A. Dempsey, Effects of wastewater effluent organic materials on fouling in ultrafiltration, *Water Research* 42 (2008) 3379-3384.
- [13] M. Zhou, H. Liu, J.E. Kilduff, R. Langer, D.G. Anderson and G. Belfort, High-Throughput Membrane Surface Modification to Control NOM Fouling, *Environmental Science & Technology* 43 (2009) 3865-3871.
- [14] G. Amy and J. Cho, Interactions between natural organic matter (NOM) and membranes: Rejection and fouling, *Water Science and Technology* 40 (1999) 131-139.

- [15] R. Ghosh, Study of membrane fouling by BSA using pulsed injection technique, *Journal of Membrane Science* 195 (2002) 115-123.
- [16] J. Liu, J. Lu, X. Zhao, J. Lu and Z. Cui, Separation of glucose oxidase and catalase using ultrafiltration with 300-kDa polyethersulfone membranes, *Journal of Membrane Science* 299 (2007) 222-228.
- [17] W. Youravong, L.S. Grandison and M.J. Lewis, Effect of hydrodynamic and physicochemical changes on critical flux of milk protein suspensions, *Journal of Dairy Research* 69 (2002) 443-455.
- [18] L. Song and M. Elimelech, Theory of concentration polarization in crossflow filtration, *Journal of the Chemical Society, Faraday Transactions* 91 (1995) 3389-3398.
- [19] M. Elimelech, Z. Xiaohua, A.E. Childress and H. Seungkwan, Role of membrane surface morphology in colloidal fouling of cellulose acetate and composite aromatic polyamide reverse osmosis membranes, *Journal of Membrane Science* 127 (1997) 101-109.
- [20] N. Lee, G. Amy, J.-P. Croué and H. Buisson, Morphological analyses of natural organic matter (NOM) fouling of low-pressure membranes (MF/UF), *Journal of Membrane Science* 261 (2005) 7-16.
- [21] M.J. Ariza, A. Cañas and J. Benavente, Electrical and surface chemical characterizations of the active layer of composite polyamide/polysulphone nanofiltration commercial membranes, *Surface and Interface Analysis* 30 (2000) 425-429.
- [22] D.B. Burns and A.L. Zydney, Contributions to electrostatic interactions on protein transport in membrane systems, *AIChE Journal* 47 (2001) 1101-1114.
- [23] W. Yuan and A.L. Zydney, Effects of solution environment on humic acid fouling during microfiltration, *Desalination* 122 (1999) 63-76.
- [24] C. Combe, E. Molis, P. Lucas, R. Riley and M.M. Clark, The effect of CA membrane properties on adsorptive fouling by humic acid, *Journal of Membrane Science* 154 (1999) 73-87.
- [25] P.J. Evans, M.R. Bird, A. Pihlajamäki and M. Nyström, The influence of hydrophobicity, roughness and charge upon ultrafiltration membranes for black tea liquor clarification, *Journal of Membrane Science* 313 (2008) 250-262.
- [26] B. Keszler, G. Kovács, A. Tóth, I. Bertóti and M. Hegyi, Modified polyethersulfone membranes, *Journal of Membrane Science* 62 (1991) 201-210.
- [27] J. Mueller and R.H. Davis, Protein fouling of surface-modified polymeric microfiltration membranes, *Journal of Membrane Science* 116 (1996) 47-60.
- [28] H. Reihanian, C.R. Robertson and A.S. Michaels, Mechanisms of polarization and fouling of ultrafiltration membranes by proteins, *Journal of Membrane Science* 16 (1983) 237-258.

- [29] M. Ulbricht and G. Belfort, Surface modification of ultrafiltration membranes by low temperature plasma II. Graft polymerization onto polyacrylonitrile and polysulfone, *Journal of Membrane Science* 111 (1996) 193-215.
- [30] J.A. Koehler, M. Ulbricht and G. Belfort, Intermolecular Forces between a Protein and a Hydrophilic Modified Polysulfone Film with Relevance to Filtration, *Langmuir* 16 (2000) 10419-10427.
- [31] D. Möckel, E. Staude and M.D. Guiver, Static protein adsorption, ultrafiltration behavior and cleanability of hydrophilized polysulfone membranes, *Journal of Membrane Science* 158 (1999) 63-75.
- [32] T. Amornsakchai and H. Kubota, Photoinitiated grafting of methyl methacrylate on highly oriented polyethylene: Effect of draw ratio on grafting, *Journal of Applied Polymer Science* 70 (1998) 465-470.
- [33] H. Chen and G. Belfort, Surface modification of poly(ether sulfone) ultrafiltration membranes by low-temperature plasma-induced graft polymerization, *Journal of Applied Polymer Science* 72 (1999) 1699-1711.
- [34] I. Gancarz, G. Pozniak and M. Bryjak, Modification of polysulfone membranes 1. CO₂ plasma treatment, *European Polymer Journal* 35 (1999) 1419-1428.
- [35] J. Pieracci, J.V. Crivello and G. Belfort, Photochemical modification of 10 kDa polyethersulfone ultrafiltration membranes for reduction of biofouling, *Journal of Membrane Science* 156 (1999) 233-240.
- [36] M. Ulbricht and G. Belfort, Surface modification of ultrafiltration membranes by low temperature plasma. I. Treatment of polyacrylonitrile, *Journal of Applied Polymer Science* 56 (1995) 325-343.
- [37] M. Ulbricht, H. Matuschewski, A. Oechel and H.-G. Hicke, Photo-induced graft polymerization surface modifications for the preparation of hydrophilic and low-protein-adsorbing ultrafiltration membranes, *Journal of Membrane Science* 115 (1996) 31-47.
- [38] M. Ulbricht, M. Riedel and U. Marx, Novel photochemical surface functionalization of polysulfone ultrafiltration membranes for covalent immobilization of biomolecules, *Journal of Membrane Science* 120 (1996) 239-259.
- [39] J. Mansouri, S. Harrisson and V. Chen, Strategies for controlling biofouling in membrane filtration systems: challenges and opportunities, *Journal of Materials Chemistry* 20 (2010) 4567-4586.
- [40] L. Song, Flux decline in crossflow microfiltration and ultrafiltration: mechanisms and modeling of membrane fouling, *Journal of Membrane Science* 139 (1998) 183-200.
- [41] J. Hermia, Constant pressure blocking filtration laws - application to power law non-Newtonian fluids, *Transactions of the Institution of Chemical Engineers* 60 (1982) 183-187.

- [42] G.B. van den Berg and C.A. Smolders, Flux decline in ultrafiltration processes, *Desalination* 77 (1990) 101-133.
- [43] M. Mulder, *Basic principles of membrane technology*, Kluwer Academic Publishers, Dordrecht (1996).
- [44] H. Chen and A.S. Kim, Prediction of permeate flux decline in crossflow membrane filtration of colloidal suspension: a radial basis function neural network approach, *Desalination* 192 (2006) 415-428.
- [45] S. Bhattacharjee, A.S. Kim and M. Elimelech, Concentration Polarization of Interacting Solute Particles in Cross-Flow Membrane Filtration, *Journal of Colloid and Interface Science* 212 (1999) 81-99.
- [46] J. Rodríguez, C.H. Allibert and J.M. Chaix, A computer method for random packing of spheres of unequal size, *Powder Technology* 47 (1986) 25-33.
- [47] W.J. Koros, Y.H. Ma and T. Shimidzu, Terminology for membranes and membrane processes, *Pure and Applied Chemistry* 68 (1996) 1479-1489.
- [48] A. Asatekin, S. Kang, M. Elimelech and A.M. Mayes, Anti-fouling ultrafiltration membranes containing polyacrylonitrile-graft-poly(ethylene oxide) comb copolymer additives, *Journal of Membrane Science* 298 (2007) 136-146.
- [49] I.H. Huisman, P. Prádanos and A. Hernández, The effect of protein-protein and protein-membrane interactions on membrane fouling in ultrafiltration, *Journal of Membrane Science* 179 (2000) 79-90.
- [50] S.T. Kelly and A.L. Zydney, Mechanisms for BSA fouling during microfiltration, *Journal of Membrane Science* 107 (1995) 115-127.
- [51] P. Bacchin, P. Aimar and R.W. Field, Critical and sustainable fluxes: Theory, experiments and applications, *Journal of Membrane Science* 281 (2006) 42-69.
- [52] G. Belfort, J.M. Pimbley, A. Greiner and K.Y. Chung, Diagnosis of membrane fouling using a rotating annular filter. 1. Cell culture media, *Journal of Membrane Science* 77 (1993) 1-22.
- [53] D. Wu, J.A. Howell and R.W. Field, Critical flux measurement for model colloids, *Journal of Membrane Science* 152 (1999) 89-98.
- [54] S. Metsämuuronen, J. Howell and M. Nyström, Critical flux in ultrafiltration of myoglobin and baker's yeast, *Journal of Membrane Science* 196 (2002) 13-35.
- [55] T.D. Waite, A.I. Schäfer, A.G. Fane and A. Heuer, Colloidal Fouling of Ultrafiltration Membranes: Impact of Aggregate Structure and Size, *Journal of Colloid and Interface Science* 212 (1999) 264-274.
- [56] M. Taniguchi, J.E. Kilduff and G. Belfort, Modes of Natural Organic Matter Fouling during Ultrafiltration, *Environmental Science & Technology* 37 (2003) 1676-1683.

- [57] A.R. Costa, M.N. de Pinho and M. Elimelech, Mechanisms of colloidal natural organic matter fouling in ultrafiltration, *Journal of Membrane Science* 281 (2006) 716-725.
- [58] C.-C. Ho and A.L. Zydney, Protein Fouling of Asymmetric and Composite Microfiltration Membranes, *Industrial & Engineering Chemistry Research* 40 (2001) 1412-1421.
- [59] C.-C. Ho and A.L. Zydney, A Combined Pore Blockage and Cake Filtration Model for Protein Fouling during Microfiltration, *Journal of Colloid and Interface Science* 232 (2000) 389-399.
- [60] P. Bacchin, D. Si-Hassen, V. Starov, M.J. Clifton and P. Aimar, A unifying model for concentration polarization, gel-layer formation and particle deposition in cross-flow membrane filtration of colloidal suspensions, *Chemical Engineering Science* 57 (2002) 77-91.
- [61] W. Yuan, A. Kocic and A.L. Zydney, Analysis of humic acid fouling during microfiltration using a pore blockage-cake filtration model, *Journal of Membrane Science* 198 (2002) 51-62.
- [62] H. Susanto and M. Ulbricht, High-performance thin-layer hydrogel composite membranes for ultrafiltration of natural organic matter, *Water Research* 42 (2008) 2827-2835.
- [63] W.R. Bowen and G. Quan, Properties of microfiltration membranes: Flux loss during constant pressure permeation of bovine serum albumin, *Biotechnology and Bioengineering* 38 (1991) 688-696.
- [64] E.M. Tracey and R.H. Davis, Protein Fouling of Track-Etched Polycarbonate Microfiltration Membranes, *Journal of Colloid and Interface Science* 167 (1994) 104-116.
- [65] S. Loh, U. Beuscher, T.K. Poddar, A.G. Porter, J.M. Wingard, S.M. Husson and S.R. Wickramasinghe, Interplay among membrane properties, protein properties and operating conditions on protein fouling during normal-flow microfiltration, *Journal of Membrane Science* 332 (2009) 93-103.
- [66] A.L. Zydney, C.-C. Ho and W. Yuan, Chapter 2: Fouling phenomena during microfiltration: Effects of pore blockage, cake filtration, and membrane morphology, In: D. Bhattacharyya; D.A. Butterfield, *New insights into membrane science and technology: polymeric and biofunctional membranes*, *Membrane Science and Technology* 8, Elsevier (2003).
- [67] P.J. Evans and M.R. Bird, Solute-Membrane Fouling Interactions During the Ultrafiltration of Black Tea Liquor, *Food and Bioproducts Processing* 84 (2006) 292-301.
- [68] N. Lee, G. Amy, J.-P. Croué and H. Buisson, Identification and understanding of fouling in low-pressure membrane (MF/UF) filtration by natural organic matter (NOM), *Water Research* 38 (2004) 4511-4523.
- [69] R. Chan and V. Chen, The effects of electrolyte concentration and pH on protein aggregation and deposition: critical flux and constant flux membrane filtration, *Journal of Membrane Science* 185 (2001) 177-192.

- [70] C. Velasco, M. Ouammou, J.I. Calvo and A. Hernández, Protein fouling in microfiltration: deposition mechanism as a function of pressure for different pH, *Journal of Colloid and Interface Science* 266 (2003) 148-152.
- [71] A.R. Costa and M.N. de Pinho, Effect of membrane pore size and solution chemistry on the ultrafiltration of humic substances solutions, *Journal of Membrane Science* 255 (2005) 49-56.
- [72] H.-Y. Yu, L.-Q. Liu, Z.-Q. Tang, M.-G. Yan, J.-S. Gu and X.-W. Wei, Mitigated membrane fouling in an SMBR by surface modification, *Journal of Membrane Science* 310 (2008) 409-417.
- [73] A.G. Fane, C.J.D. Fell and A. Suki, The effect of pH and ionic environment on the ultrafiltration of protein solutions with retentive membranes, *Journal of Membrane Science* 16 (1983) 195-210.
- [74] M.M. Rohani and A.L. Zydney, Role of electrostatic interactions during protein ultrafiltration, *Advances in Colloid and Interface Science* 160 (2010) 40-48.
- [75] S. Salgin, Effects of Ionic Environments on Bovine Serum Albumin Fouling in a Cross-Flow Ultrafiltration System, *Chemical Engineering & Technology* 30 (2007) 255-260.
- [76] S.-H. Yoon, C.-H. Lee, K.-J. Kim and A.G. Fane, Effect of calcium ion on the fouling of nanofilter by humic acid in drinking water production, *Water Research* 32 (1998) 2180-2186.
- [77] A. Seidel and M. Elimelech, Coupling between chemical and physical interactions in natural organic matter (NOM) fouling of nanofiltration membranes: implications for fouling control, *Journal of Membrane Science* 203 (2002) 245-255.
- [78] A.D. Marshall, P.A. Munro and G. Trägårdh, The effect of protein fouling in microfiltration and ultrafiltration on permeate flux, protein retention and selectivity: A literature review, *Desalination* 91 (1993) 65-108.
- [79] C.-H. Yu, C.-H. Wu, C.-H. Lin, C.-H. Hsiao and C.-F. Lin, Hydrophobicity and molecular weight of humic substances on ultrafiltration fouling and resistance, *Separation and Purification Technology* 64 (2008) 206-212.
- [80] N.A. Ochoa, M. Masuelli and J. Marchese, Effect of hydrophilicity on fouling of an emulsified oil wastewater with PVDF/PMMA membranes, *Journal of Membrane Science* 226 (2003) 203-211.
- [81] H. Susanto, S. Franzka and M. Ulbricht, Dextran fouling of polyethersulfone ultrafiltration membranes--Causes, extent and consequences, *Journal of Membrane Science* 296 (2007) 147-155.
- [82] W. Xi, W. Rong, L. Zhansheng and A.G. Fane, Development of a novel electrophoresis-UV grafting technique to modify PES UF membranes used for NOM removal, *Journal of Membrane Science* 273 (2006) 47-57.

- [83] D.B. Burns and A.L. Zydney, Effect of solution pH on protein transport through ultrafiltration membranes, *Biotechnology and Bioengineering* 64 (1999) 27-37.
- [84] S. Saksena and A.L. Zydney, Effect of solution pH and ionic strength on the separation of albumin from immunoglobulins (IgG) by selective filtration, *Biotechnology and Bioengineering* 43 (1994) 960-968.
- [85] Y. Wan, R. Ghosh, G. Hale and Z. Cui, Fractionation of bovine serum albumin and monoclonal antibody alemtuzumab using carrier phase ultrafiltration, *Biotechnology and Bioengineering* 90 (2005) 303-315.
- [86] M.-S. Chun, G.-Y. Chung and J.-J. Kim, On the behavior of the electrostatic colloidal interaction in the membrane filtration of latex suspensions, *Journal of Membrane Science* 193 (2001) 97-109.
- [87] L. Palacio, J.I. Calvo, P. Pradanos, A. Hernandez, P. Väisänen and M. Nyström, Contact angles and external protein adsorption onto UF membranes, *Journal of Membrane Science* 152 (1999) 189-201.
- [88] C.-F. Lin, T.-Y. Lin and O.J. Hao, Effects of humic substance characteristics on UF performance, *Water Research* 34 (2000) 1097-1106.
- [89] J.-E. Hwang, J. Jegal and K.-H. Lee, Separation of humic acid with nanofiltration polyamide composite membranes, *Journal of Applied Polymer Science* 86 (2002) 2847-2853.
- [90] K. Katsoufidou, S.G. Yiantsios and A.J. Karabelas, An experimental study of UF membrane fouling by humic acid and sodium alginate solutions: the effect of backwashing on flux recovery, *Desalination* 220 (2008) 214-227.
- [91] J. Cho, G. Amy and J. Pellegrino, Membrane filtration of natural organic matter: factors and mechanisms affecting rejection and flux decline with charged ultrafiltration (UF) membrane, *Journal of Membrane Science* 164 (2000) 89-110.
- [92] V. García-Molina, S. Lyko, S. Esplugas, T. Wintgens and T. Melin, Ultrafiltration of aqueous solutions containing organic polymers, *Desalination* 189 (2006) 110-118.
- [93] Y. Wang, C. Combe and M.M. Clark, The effects of pH and calcium on the diffusion coefficient of humic acid, *Journal of Membrane Science* 183 (2001) 49-60.
- [94] C.Y. Tang, Y.-N. Kwon and J.O. Leckie, Fouling of reverse osmosis and nanofiltration membranes by humic acid--Effects of solution composition and hydrodynamic conditions, *Journal of Membrane Science* 290 (2007) 86-94.
- [95] R.W. Field, D. Wu, J.A. Howell and B.B. Gupta, Critical flux concept for microfiltration fouling, *Journal of Membrane Science* 100 (1995) 259-272.
- [96] K.J. Kim, V. Chen and A.G. Fane, Some factors determining protein aggregation during ultrafiltration, *Biotechnology and Bioengineering* 42 (1993) 260-265.

- [97] R. van Reis and A. Zydney, Bioprocess membrane technology, *Journal of Membrane Science* 297 (2007) 16-50.
- [98] W.R. Bowen, R.S. Kingdon and H.A.M. Sabuni, Electrically enhanced separation processes: the basis of in situ intermittent electrolytic membrane cleaning (IEMC) and in situ electrolytic membrane restoration (IEMR), *Journal of Membrane Science* 40 (1989) 219-229.
- [99] I.C. Kim, J.G. Choi and T.M. Tak, Sulfonated polyethersulfone by heterogeneous method and its membrane performances, *Journal of Applied Polymer Science* 74 (1999) 2046-2055.
- [100] A. Nabe, E. Staude and G. Belfort, Surface modification of polysulfone ultrafiltration membranes and fouling by BSA solutions, *Journal of Membrane Science* 133 (1997) 57-72.
- [101] Y. Chen, L. Ying, W. Yu, E.T. Kang and K.G. Neoh, Poly(vinylidene fluoride) with Grafted Poly(ethylene glycol) Side Chains via the RAFT-Mediated Process and Pore Size Control of the Copolymer Membranes, *Macromolecules* 36 (2003) 9451-9457.
- [102] F. Schacher, T. Rudolph, F. Wieberger, M. Ulbricht and A.H.E. Müller, Double Stimuli-Responsive Ultrafiltration Membranes from Polystyrene-block-poly(N,N-dimethylaminoethyl methacrylate) Diblock Copolymers, *ACS Applied Materials & Interfaces* 1 (2009) 1492-1503.
- [103] B. van den Bruggen, Chemical modification of polyethersulfone nanofiltration membranes: a review, *Journal of Applied Polymer Science* 114 (2009) 630-642.
- [104] H. Susanto, N. Stahra and M. Ulbricht, High performance polyethersulfone microfiltration membranes having high flux and stable hydrophilic property, *Journal of Membrane Science* 342 (2009) 153-164.
- [105] H. Susanto and M. Ulbricht, Characteristics, performance and stability of polyethersulfone ultrafiltration membranes prepared by phase separation method using different macromolecular additives, *Journal of Membrane Science* 327 (2009) 125-135.
- [106] X. Ma, Y. Su, Q. Sun, Y. Wang and Z. Jiang, Preparation of protein-adsorption-resistant polyethersulfone ultrafiltration membranes through surface segregation of amphiphilic comb copolymer, *Journal of Membrane Science* 292 (2007) 116-124.
- [107] D. Rana, T. Matsuura, R.M. Narbaitz and C. Feng, Development and characterization of novel hydrophilic surface modifying macromolecule for polymeric membranes, *Journal of Membrane Science* 249 (2005) 103-112.
- [108] S. Chen, J. Zheng, L. Li and S. Jiang, Strong resistance of phosphorylcholine self-assembled monolayers to protein adsorption: Insights into nonfouling properties of zwitterionic materials, *Journal of the American Chemical Society* 127 (2005) 14473-14478.
- [109] J. Kochan, T. Wintgens, J.E. Wong and T. Melin, Polyelectrolyte-modified polyethersulfone ultrafiltration membranes for wastewater treatment applications, *Desalination and Water Treatment* 9 (2009) 175-180.

- [110] J. Kochan, T. Wintgens, J.E. Wong and T. Melin, Properties of polyethersulfone ultrafiltration membranes modified by polyelectrolytes, *Desalination* 250 (2010) 1008-1010.
- [111] H. Guo and M. Ulbricht, Surface modification of polypropylene microfiltration membrane via entrapment of an amphiphilic alkyl oligoethyleneglycolether, *Journal of Membrane Science* 349 (2010) 312-320.
- [112] H. Guo and M. Ulbricht, Preparation of thermo-responsive polypropylene membranes via surface entrapment of poly(N-isopropylacrylamide)-containing macromolecules, *Journal of Membrane Science* 372 (2011) 331-339.
- [113] M. Ulbricht, Advanced functional polymer membranes, *Polymer* 47 (2006) 2217-2262.
- [114] Q. Yang, N. Adrus, F. Tomicki and M. Ulbricht, Composites of functional polymeric hydrogels and porous membranes, *Journal of Materials Chemistry* 21 (2011) 2783-2811.
- [115] C. Yao, X. Li, K.G. Neoh, Z. Shi and E.T. Kang, Surface modification and antibacterial activity of electrospun polyurethane fibrous membranes with quaternary ammonium moieties, *Journal of Membrane Science* 320 (2008) 259-267.
- [116] D.S. Wavhal and E.R. Fisher, Hydrophilic modification of polyethersulfone membranes by low temperature plasma-induced graft polymerization, *Journal of Membrane Science* 209 (2002) 255-269.
- [117] A. Schulze, B. Marquardt, S. Kaczmarek, R. Schubert, A. Prager and M.R. Buchmeiser, Electron Beam-Based Functionalization of Poly(ethersulfone) Membranes, *Macromolecular Rapid Communications* 31 (2010) 467-472.
- [118] Y.-C. Chiang, Y. Chang, A. Higuchi, W.-Y. Chen and R.-C. Ruaan, Sulfobetaine-grafted poly(vinylidene fluoride) ultrafiltration membranes exhibit excellent antifouling property, *Journal of Membrane Science* 339 (2009) 151-159.
- [119] A. Higuchi, K. Shirano, M. Harashima, B.O. Yoon, M. Hara, M. Hattori and K. Imamura, Chemically modified polysulfone hollow fibers with vinylpyrrolidone having improved blood compatibility, *Biomaterials* 23 (2002) 2659-2666.
- [120] H. Yamagishi, J.V. Crivello and G. Belfort, Development of a novel photochemical technique for modifying poly(arylsulfone) ultrafiltration membranes, *Journal of Membrane Science* 105 (1995) 237-247.
- [121] C. Geismann, F. Tomicki and M. Ulbricht, Block Copolymer Photo-Grafted Poly(Ethylene Terephthalate) Capillary Pore Membranes Distinctly Switchable by Two Different Stimuli, *Separation Science and Technology* 44 (2009) 3312 - 3329.
- [122] A. Friebe and M. Ulbricht, Controlled Pore Functionalization of Poly(ethylene terephthalate) Track-Etched Membranes via Surface-Initiated Atom Transfer Radical Polymerization, *Langmuir* 23 (2007) 10316-10322.

- [123] A. Friebe and M. Ulbricht, Cylindrical Pores Responding to Two Different Stimuli via Surface-Initiated Atom Transfer Radical Polymerization for Synthesis of Grafted Diblock Copolymers, *Macromolecules* 42 (2009) 1838-1848.
- [124] C. Geismann and M. Ulbricht, Photoreactive Functionalization of Poly(ethylene terephthalate) Track-Etched Pore Surfaces with "Smart" Polymer Systems, *Macromolecular Chemistry and Physics* 206 (2005) 268-281.
- [125] D. He, H. Susanto and M. Ulbricht, Photo-irradiation for preparation, modification and stimulation of polymeric membranes, *Progress in Polymer Science* 34 (2009) 62-98.
- [126] M. Ulbricht, K. Richau and H. Kamusewitz, Chemically and morphologically defined ultrafiltration membrane surfaces prepared by heterogenous photo-initiated graft polymerization, *Colloids and Surfaces A: Physicochemical and Engineering Aspects* 138 (1998) 353-366.
- [127] J. Pieracci, J.V. Crivello and G. Belfort, UV-assisted graft polymerization of N-vinyl-2-pyrrolidinone onto poly(ether sulfone) ultrafiltration membranes using selective UV wavelengths, *Chem. Mater.* 14 (2002) 256-265.
- [128] M. Taniguchi and G. Belfort, Low protein synthetic membranes by UV-assisted surface grafting modification: varying monomer type, *Journal of Membrane Science* 231 (2004) 147-157.
- [129] H. Yamagishi, J.V. Crivello and G. Belfort, Evaluation of photochemically modified poly(arylsulfone) ultrafiltration membranes, *Journal of Membrane Science* 105 (1995) 249-259.
- [130] H. Susanto and M. Ulbricht, Photografted thin layer polymer hydrogel layers on PES ultrafiltration membranes: Characterization, stability and influence on separation performance, *Langmuir* 23 (2007) 7818-7830.
- [131] S. Kuroda, I. Mita, K. Obata and S. Tanaka, Degradation of aromatic polymers: Part IV--Effect of temperature and light intensity on the photodegradation of polyethersulfone, *Polymer Degradation and Stability* 27 (1990) 257-270.
- [132] M. Mrksich and G.M. Whitesides, Using Self-Assembled Monolayers to Understand the Interactions of Man-made Surfaces with Proteins and Cells, *Ann. Rev. Biophys. Biomol. Struct.* 25 (1996) 55-78.
- [133] R.G. Chapman, E. Ostuni, S. Takayama, R.E. Holmlin, L. Yan and G.M. Whitesides, Surveying of surfaces that resist the adsorption of proteins, *Journal of the American Chemical Society* 122 (2000) 8303-8304.
- [134] E. Ostuni, R.C. Chapman, R.E. Holmlin, S. Takayama and G.M. Whitesides, A survey of structure-property relationships of surfaces that resist the adsorption of protein, *Langmuir* 17 (2001) 5605-5620.

- [135] A. Asatekin, A. Menniti, S. Kang, M. Elimelech, E. Morgenroth and A.M. Mayes, Antifouling nanofiltration membranes for membrane bioreactors from self-assembling graft copolymers, *Journal of Membrane Science* 285 (2006) 81-89.
- [136] R.S. Kane, P. Deschatelets and G.M. Whitesides, Kosmotropes form the basis of protein-resistant surfaces, *Langmuir* 19 (2003) 2388-2391.
- [137] K. Tasaki, Poly(oxyethylene)-water interaction: A molecular dynamics study, *Journal of the American Chemical Society* 118 (1996) 8459-8469.
- [138] E.A. Vogler, Water and the acute biological response to surfaces, *Journal of Biomaterials Science, Polymer Edition* 10 (1999) 1015-1045.
- [139] E. Uchida, Y. Uyama and Y. Ikada, Grafting of water-soluble chains onto a polymer surface, *Langmuir* 10 (1994) 481-485.
- [140] H. Susanto, M. Balakrishnan and M. Ulbricht, Via surface functionalization by photograft copolymerization to low-fouling polyethersulfone-based ultrafiltration membranes, *Journal of Membrane Science* 288 (2007) 157-167.
- [141] N.A. Peppas, J.Z. Hilt, A. Khademhosseini and R. Langer, Hydrogels in Biology and Medicine: From Molecular Principles to Bionanotechnology, *Advanced Materials* 18 (2006) 1345-1360.
- [142] C. Fänger, H. Wack and M. Ulbricht, Macroporous poly(N-isopropylacrylamide) hydrogels with adjustable size "cut-off" for the efficient and reversible immobilization of biomacromolecules, *Macromolecular Bioscience* 6 (2006) 393-402.
- [143] Y.-H. Wu and B.D. Freeman, Structure, water sorption and transport properties of crosslinked N-vinyl-2-pyrrolidone/N,N'-methylenebisacrylamide films, *Journal of Membrane Science* 344 (2009) 182-189.
- [144] L.-J. Mu and W.-Z. Zhao, Hydrophilic modification of polyethersulfone porous membranes via thermal-induced surface crosslinking approach, *Applied Surface Science* 255 (2009) 7273-7278.
- [145] N. D'Alvise, C. Lesueur-Lambert, B. Fertin, P. Dhulster and D. Guillochon, Removal of Polyphenols and Recovery of Proteins from Alfalfa White Protein Concentrate by Ultrafiltration and Adsorbent Resin Separations, *Separation Science and Technology* 35 (2000) 2453 - 2472.
- [146] K.J. Siebert, N.V. Troukhanova and P.Y. Lynn, Nature of Polyphenol-Protein Interactions, *Journal of Agricultural and Food Chemistry* 44 (1996) 80-85.
- [147] A. Vernhet and M. Moutounet, Fouling of organic microfiltration membranes by wine constituents: importance, relative impact of wine polysaccharides and polyphenols and incidence of membrane properties, *Journal of Membrane Science* 201 (2002) 103-122.

- [148] T. Canal and N.A. Peppas, Correlation between mesh size and equilibrium degree of swelling of polymeric networks, *Journal of Biomedical Materials Research* 23 (1989) 1183-1193.
- [149] T. Uhlich, G. Tomashevski and H. Komber, Synthesis of a hydrophobised and photocrosslinkable prepolymer based on poly(vinyl alcohol), *Reactive and Functional Polymers* 28 (1995) 55-60.
- [150] A.M. Lowman and N.A. Peppas, Analysis of the Complexation/Decomplexation Phenomena in Graft Copolymer Networks, *Macromolecules* 30 (1997) 4959-4965.
- [151] M. Ulbricht, A. Oechel, C. Lehmann, G. Tomaschewski and H.-G. Hicke, Gas-phase photoinduced graft polymerization of acrylic acid onto polyacrylonitril ultrafiltration membranes, *Journal of Applied Polymer Science* 55 (1995) 1707-1723.
- [152] V.N. Kislenco and L.P. Oliinyk, Reaction of Copper(II) with Polyacrylic Acid and Its Copolymers in Dilute Solutions, *Russian Journal of Applied Chemistry* 75 (2002) 1497-1500.
- [153] M. Suzuki, A. Kishida, H. Iwata and Y. Ikada, Graft copolymerization of acrylamide onto a polyethylene surface pretreated with glow discharge, *Macromolecules* 19 (1986) 1804-1808.
- [154] D. Möckel, E. Staude, M. Dal-Cin, K. Darcovich and M. Guiver, Tangential flow streaming potential measurements: Hydrodynamic cell characterization and zeta potentials of carboxylated polysulfone membranes, *Journal of Membrane Science* 145 (1998) 211-222.
- [155] A. Yaroshchuk and T. Luxbacher, Interpretation of Electrokinetic Measurements with Porous Films: Role of Electric Conductance and Streaming Current within Porous Structure, *Langmuir* 26 (2010) 10882-10889.
- [156] G. Schock, A. Miquel and R. Birkenberger, Characterization of ultrafiltration membranes: cut-off determination by gel permeation chromatography, *Journal of Membrane Science* 41 (1989) 55-67.
- [157] C.M. Tam and A.Y. Tremblay, Membrane pore characterization - comparison between single and multicomponent solute probe techniques, *Journal of Membrane Science* 57 (1991) 271-287.
- [158] M.N. Sarbolouki, A General Diagram for Estimating Pore Size of Ultrafiltration and Reverse Osmosis Membranes, *Separation Science and Technology* 17 (1982) 381 - 386.
- [159] A.K. Fritzsche, A.R. Arevalo, M.D. Moore, C.J. Weber, V.B. Elings, K. Kjoller and C.M. Wu, Image enhancement of polyethersulfone ultrafiltration membrane surface structure for atomic force microscopy, *Journal of Applied Polymer Science* 46 (1992) 167-178.
- [160] P.D. Peeva, T. Pieper and M. Ulbricht, Tuning the ultrafiltration properties of anti-fouling thin-layer hydrogel polyethersulfone composite membranes by suited crosslinker monomers and photo-grafting conditions, *Journal of Membrane Science* 362 (2010) 560-568.
- [161] Sartorius-Stedim Biothec, Personal correspondence, (2008)

- [162] French standard Nr. NF 45-103, Rejection of membranes for ultra- and nanofiltration, ARNOR (1997)
- [163] P.D. Peeva, A.E. Palupi and M. Ulbricht, Ultrafiltration of humic acid solutions through unmodified and surface functionalized low-fouling polyethersulfone membranes – Effects of feed properties, pore size and membrane chemistry on fouling behavior and cleanability, *Separation and Purification Technology* (2011) under revision.
- [164] H. Susanto, Y. Feng and M. Ulbricht, Fouling behavior of aqueous solutions of polyphenolic compounds during ultrafiltration, *Journal of Food Engineering* 91 (2009) 333-340.
- [165] M. Han, A. Sethuraman, R.S. Kane and G. Belfort, Nanometer-Scale Roughness Having Little Effect on the Amount or Structure of Adsorbed Protein, *Langmuir* 19 (2003) 9868-9872.
- [166] M. Taniguchi, J.P. Pieracci and G. Belfort, Effect of Undulations on Surface Energy: A Quantitative Assessment, *Langmuir* 17 (2001) 4312-4315.
- [167] H. He, L. Li and L.J. Lee, Photopolymerization and structure formation of methacrylic acid based hydrogels: The effect of light intensity, *Reactive and Functional Polymers* 68 (2008) 103-113.
- [168] Y.-H. Wu, Y.-L. Liu, Y. Chang, A. Higuchi and B.D. Freeman, Effect of UV intensity on structure, water sorption, and transport properties of crosslinked N-vinyl-2-pyrrolidone/N,N'-methylenebisacrylamide films, *Journal of Membrane Science* 348 (2010) 47-55.
- [169] I. Eshet, V. Freger, R. Kasher, M. Herzberg, J. Lei and M. Ulbricht, Chemical and physical factors in design of antibiofouling polymer coatings, *Biomacromolecules* (2011) accepted.
- [170] N.V. Churaev, R.G. Holdich, P.P. Prokopovich, V.M. Starov and S.I. Vasin, Reversible adsorption inside pores of ultrafiltration membranes, *Journal of Colloid and Interface Science* 288 (2005) 205-212.
- [171] H. Susanto and M. Ulbricht, Influence of ultrafiltration membrane characteristics on adsorptive fouling with dextrans, *Journal of Membrane Science* 266 (2005) 132-142.
- [172] S.K. Zaidi and A. Kumar, Effects of ethanol concentration on flux and gel formation in dead end ultrafiltration of PEG and dextran, *Journal of Membrane Science* 237 (2004) 189-197.
- [173] A. Bottino, G. Capannelli, A. Imperato and S. Munari, Ultrafiltration of hydrosoluble polymers. Effect of operating conditions on the performance of the membrane, *Journal of Membrane Science* 21 (1984) 247-267.
- [174] R. Nobrega, H. De Balmann, P. Aimar and V. Sanchez, Transfer of dextran through ultrafiltration membranes: a study of rejection data analysed by gel permeation chromatography, *Journal of Membrane Science* 45 (1989) 17-36.
- [175] U. Böhme and U. Scheler, Effective charge of bovine serum albumin determined by electrophoresis NMR, *Chemical Physics Letters* 435 (2007) 342-345.

- [176] K. Figueiredo, H. Ferraz, C. Borges and T. Alves, Structural Stability of Myoglobin in Organic Media, *The Protein Journal* 28 (2009) 224-232.
- [177] J.-Y. Wang, K.-S. Chou and C.-J. Lee, Dead-End Flow Filtration of Solid Suspension in Polymer Fluid through an Active Kaolin Dynamic Membrane, *Separation Science and Technology* 33 (1998) 2513 - 2529.
- [178] C.-C. Ho and A.L. Zydney, Effect of membrane morphology on the initial rate of protein fouling during microfiltration, *Journal of Membrane Science* 155 (1999) 261-275.
- [179] A. Martín, F. Martínez, J.I. Calvo, P. Prádanos, L. Palacio and A. Hernández, Protein adsorption onto an inorganic microfiltration membrane: Solute-solid interactions and surface coverage, *Journal of Membrane Science* 207 (2002) 199-207.
- [180] N.M. D'Souza and A.J. Mawson, Membrane Cleaning in the Dairy Industry: A Review, *Critical Reviews in Food Science and Nutrition* 45 (2005) 125 - 134.
- [181] M.M. Dal-Cin, C.N. Striez, T.A. Tweddle, C.E. Capes, F. McLellan and H. Buisson, Effect of adsorptive fouling on membrane performance: Case study with a pulp mill effluent, *Desalination* 101 (1995) 155-167.
- [182] V.T. Kuberkar and R.H. Davis, Modeling of fouling reduction by secondary membranes, *Journal of Membrane Science* 168 (2000) 243-258.
- [183] J. Huang, K. Huang, S. Liu, Q. Luo and M. Xu, Adsorption properties of tea polyphenols onto three polymeric adsorbents with amide group, *Journal of Colloid and Interface Science* 315 (2007) 407-414.
- [184] R.A. Andersen and J.A. Sowers, Optimum conditions for bonding of plant phenols to insoluble polyvinylpyrrolidone, *Phytochemistry* 7 (1968) 293-301.
- [185] J.C. Gray, Absorption of polyphenols by polyvinylpyrrolidone and polystyrene resins, *Phytochemistry* 17 (1978) 495-497.
- [186] J.G. Handique and J.B. Baruah, Polyphenolic compounds: an overview, *Reactive and Functional Polymers* 52 (2002) 163-188.
- [187] Z. Borneman, V. Gökmen and H.H. Nijhuis, Selective removal of polyphenols and brown colour in apple juices using PES/PVP membranes in a single-ultrafiltration process, *Journal of Membrane Science* 134 (1997) 191-197.
- [188] V. Gökmen, Z. Borneman and H.H. Nijhuis, Improved Ultrafiltration for Color Reduction and Stabilization of Apple Juice, *Journal of Food Science* 63 (1998) 504-507.
- [189] A. Mehta and A.L. Zydney, Permeability and selectivity analysis for ultrafiltration membranes, *Journal of Membrane Science* 249 (2005) 245-249.

APPENDIX A

Table 1 Characteristics of hydrogels; (a) PEGMA 200/MBAA; (b) PEGMA 400/MBAA; (c) PEGMA 400/PETAE.

(a)

Code PEGMA/MBAA	Conversion [%]	Degree of swelling [-]	Mesh size [nm]
23/0	69	35	
23/0.4	76	24	17.7
23/1	80	14	9.6
23/4	85	8	4.3

(b)

Code PEGMA/MBAA	Conversion [%]	Degree of swelling [-]	Mesh size [nm]
40/0	83	18	
40/0.4	83	15	15.1
40/1	94	13	9
40/4	82	10	4.4

(c)

Code PEGMA/PETAE	Conversion [%]	Degree of swelling [-]
40/0	83	18
40/0.66	89	18
40/1.66	84	19
40/6.67	68	20

Table 2 Summary of relative flux of virgin and modified membranes at 24 h of DE filtration

Membrane	pH 8			pH 6			pH 4		
	BSA	myoglobin	mixture	BSA	myoglobin	mixture	BSA	myoglobin	mixture
PES 50 virgin	0.26	0.25	0.25	0.31	0.26	0.16	0.22	0.26	0.15
PES 30 virgin	0.32	0.24	0.30	0.25	0.25	0.20	0.20		
PES 10 virgin	0.31	0.20	0.29	0.20	0.21	0.20	0.32	0.16	
40/0 5 J/cm ²	0.53	0.55	0.69	0.51	0.39	0.50	0.61	0.58	0.58
40/1 5 J/cm ²				0.62	0.33	0.59			
40/4 5 J/cm ²	0.53	0.51		0.45	0.32	0.40		0.50	
40/0 8 J/cm ²	0.70	0.67					0.84	0.37	0.53
40/4 8 J/cm ²							0.92	0.36	

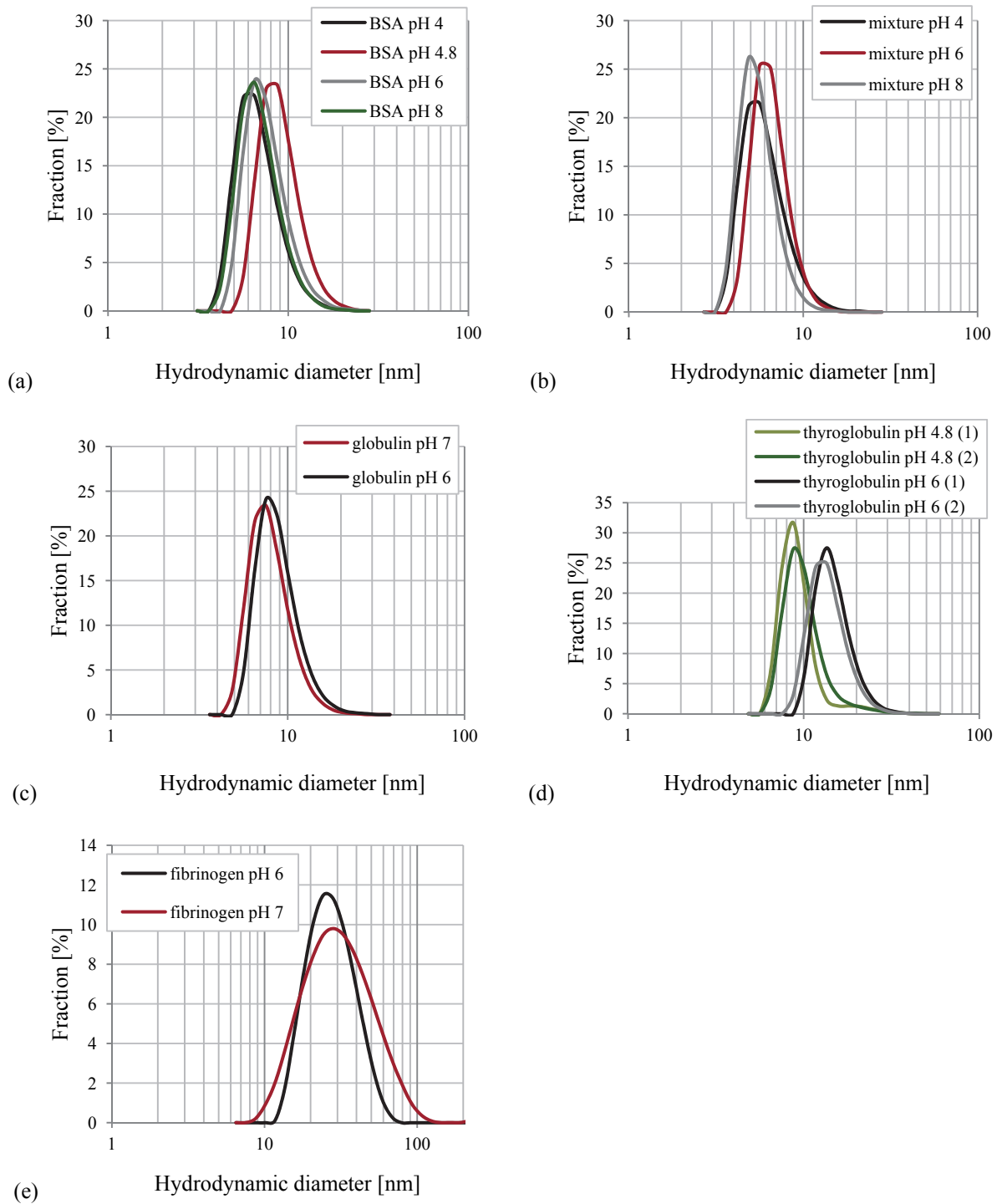


Figure 1 Hydrodynamic diameter of tested substances depending on the pH value; (a) BSA; (b) mixture of BSA and myoglobin; (c) γ -globulin; (d) thyroglobulin (incl. reproducibility); (e) fibrinogen.

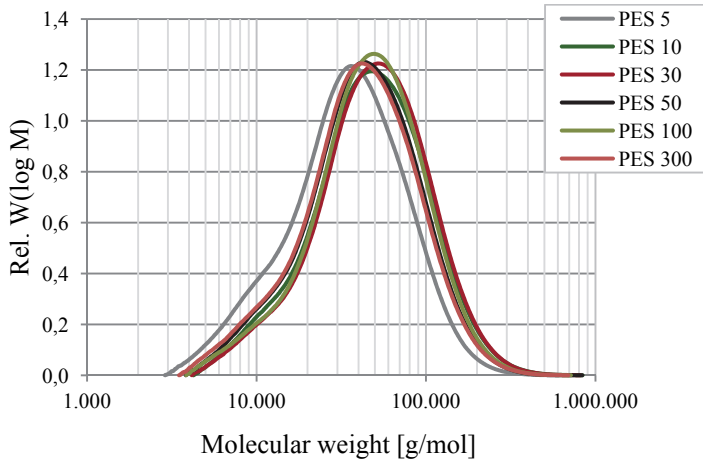


Figure 2 Polymer mixture MWD of the used membranes (universal calibration).

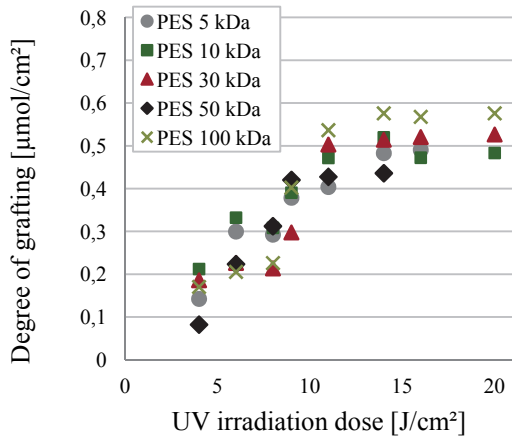


Figure 3 Degree of grafting of membranes depending on the UV irradiation dose.

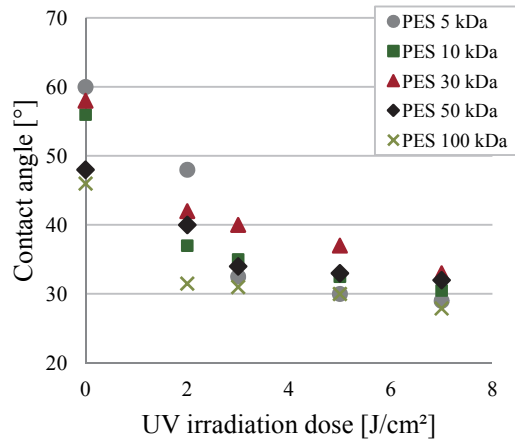


Figure 4 Contact angle of membranes depending on the UV irradiation dose.

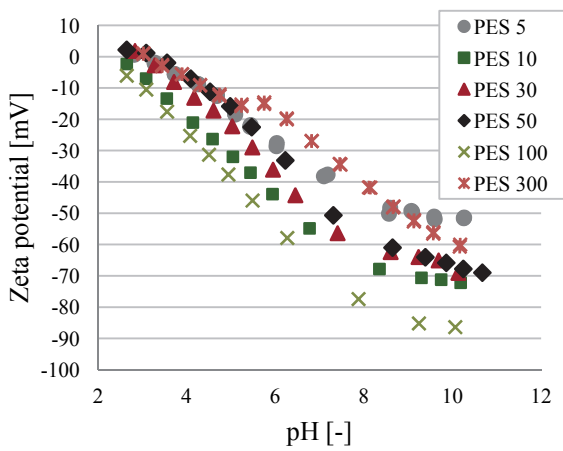


Figure 5 Zeta potential of virgin membranes.

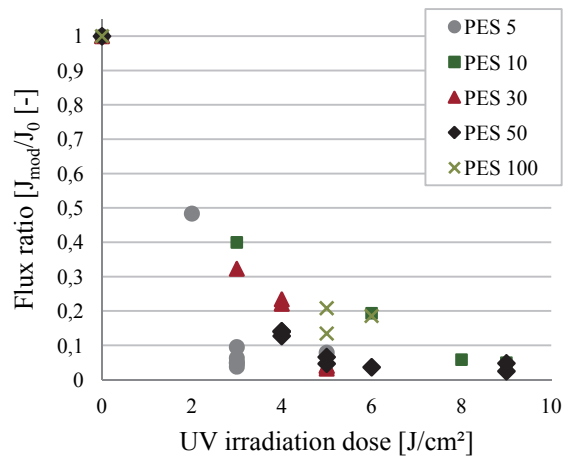


Figure 6 Flux reduction due to the applied modification depending on the UV dose.

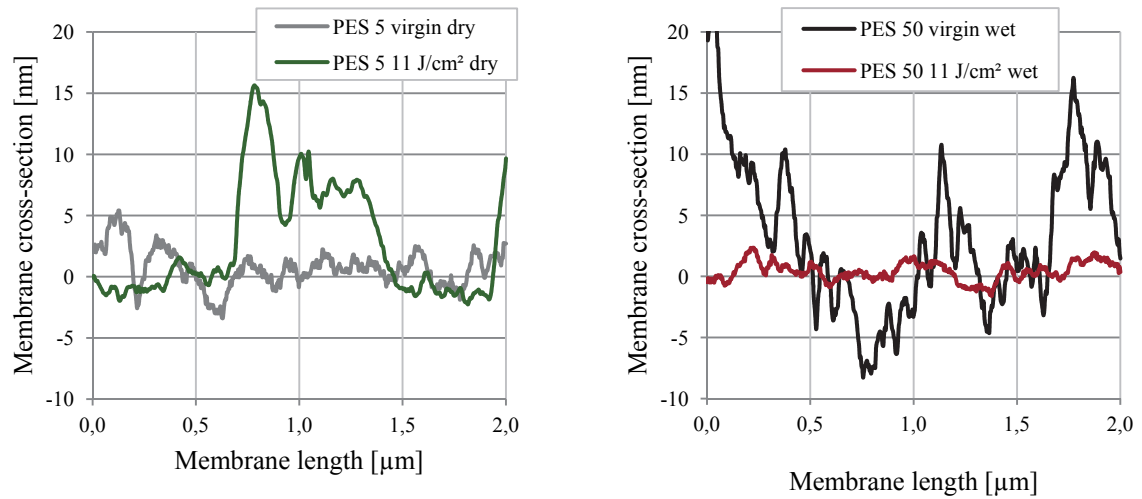


Figure 7 Cross-section profile of virgin and modified membranes measured by AFM in wet and dry state; (a) dry; (b) wet state.

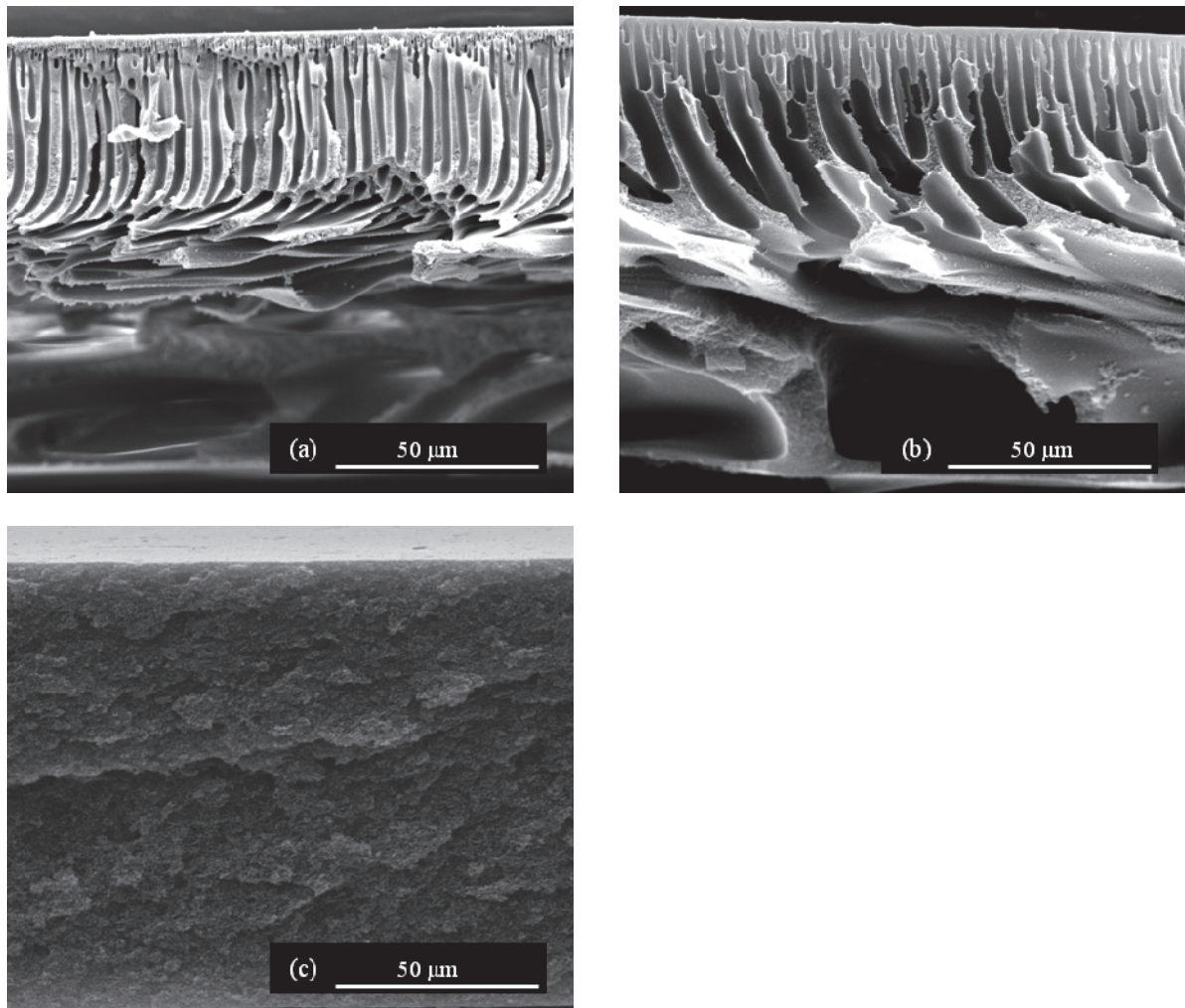


Figure 8 SEM images of cross-sections; (a) PES 5; (b) PES 10; (c) PES 300.

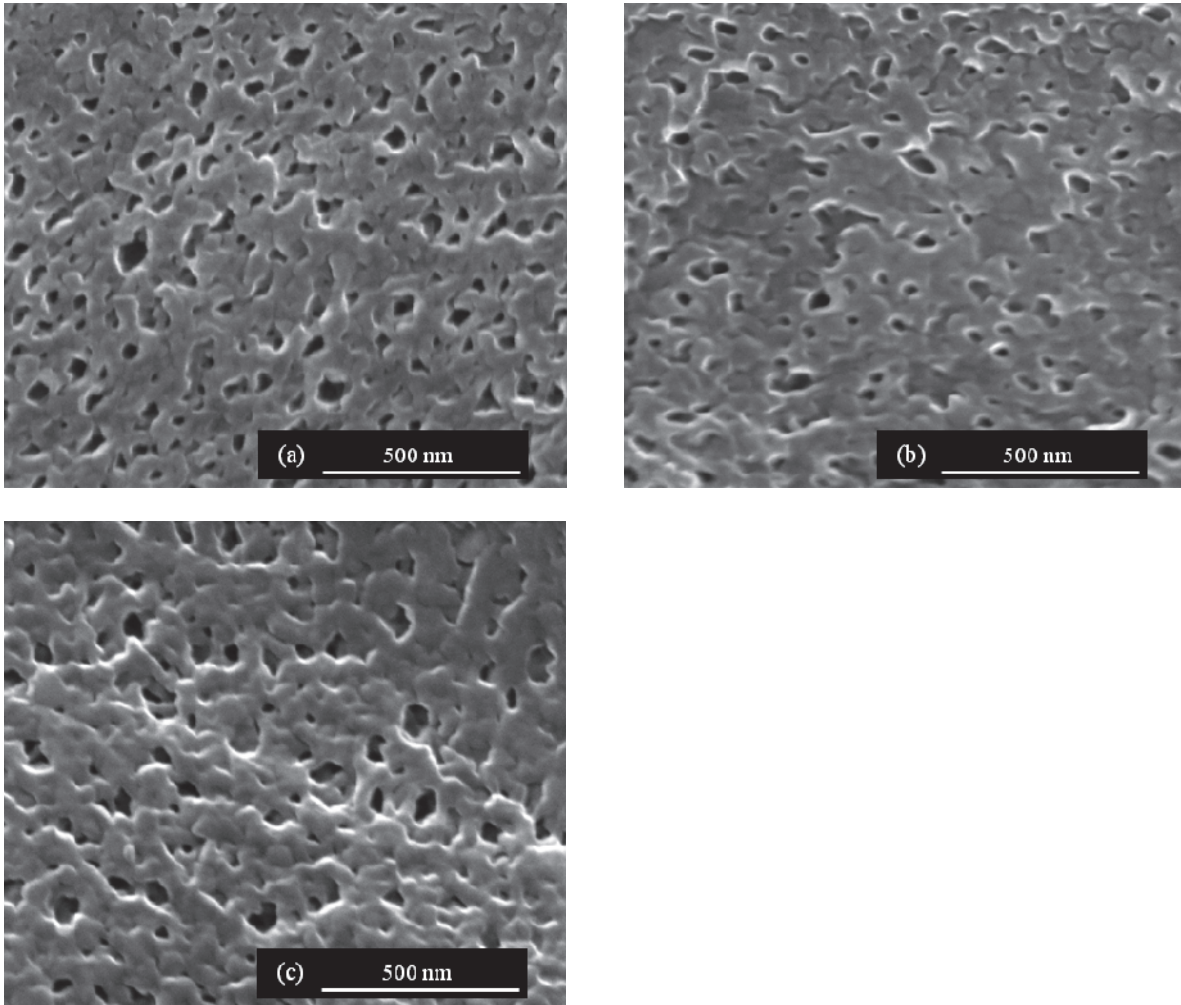


Figure 9 SEM images of skin surface of modified PES 100; (a) 40/0 11 J/cm²; (b) 40/4 11 J/cm²; (c) 40/6.65 11 J/cm².

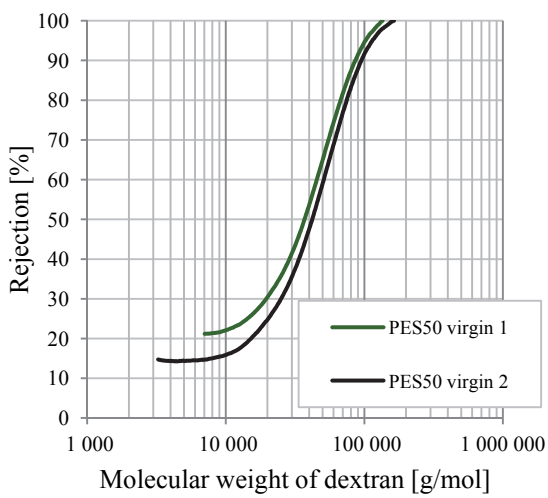


Figure 10 Reproducibility of the rejection curves of virgin PES 50.

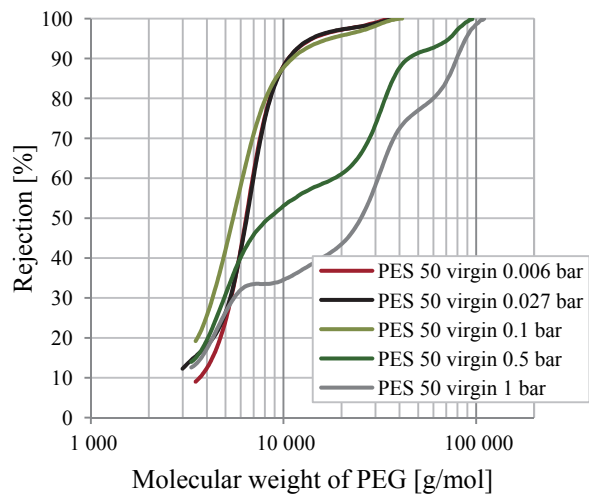


Figure 11 Effect of the initial flux on the rejection curves conducted with PEG.

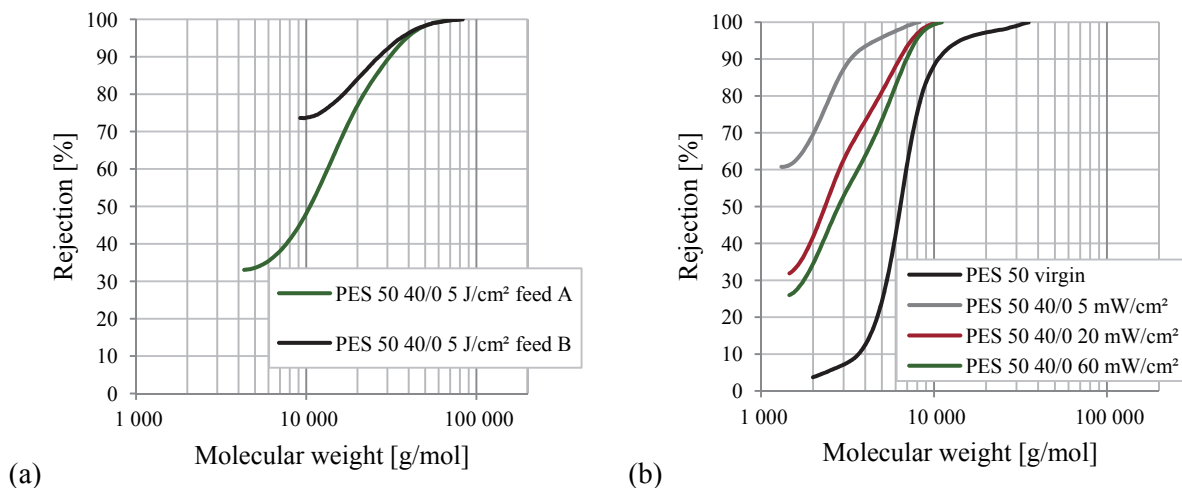


Figure 12 Rejection curves of modified membranes; (a) dextran, effect of feed; (b) PEG, effect of the UV intensity.

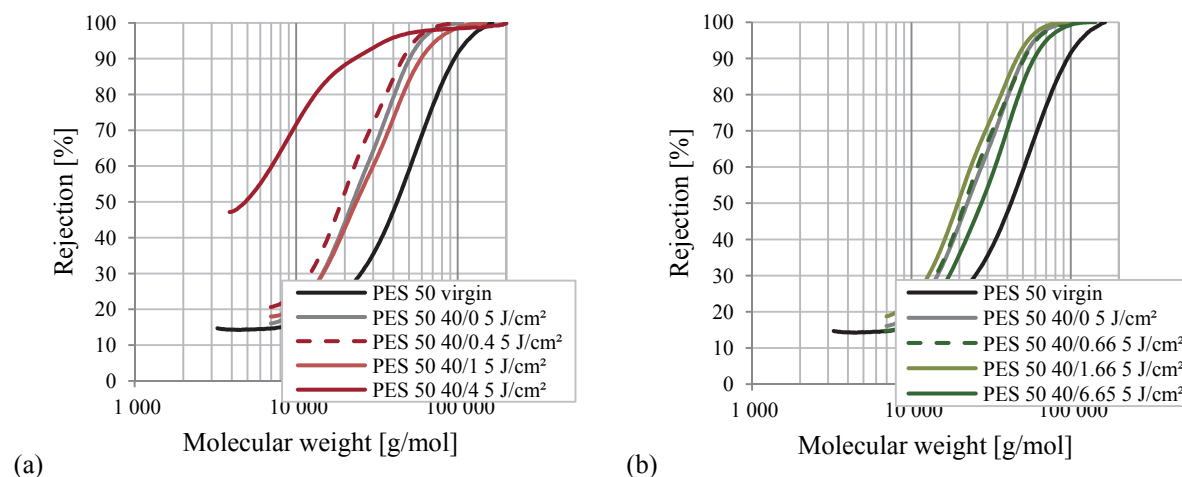


Figure 13 Rejection curves of modified PES 50 at 5 J/cm² under variation of the crosslinking degree; (a) PEGMA 400/MBAA; (b) PEGMA 400/PETAE.

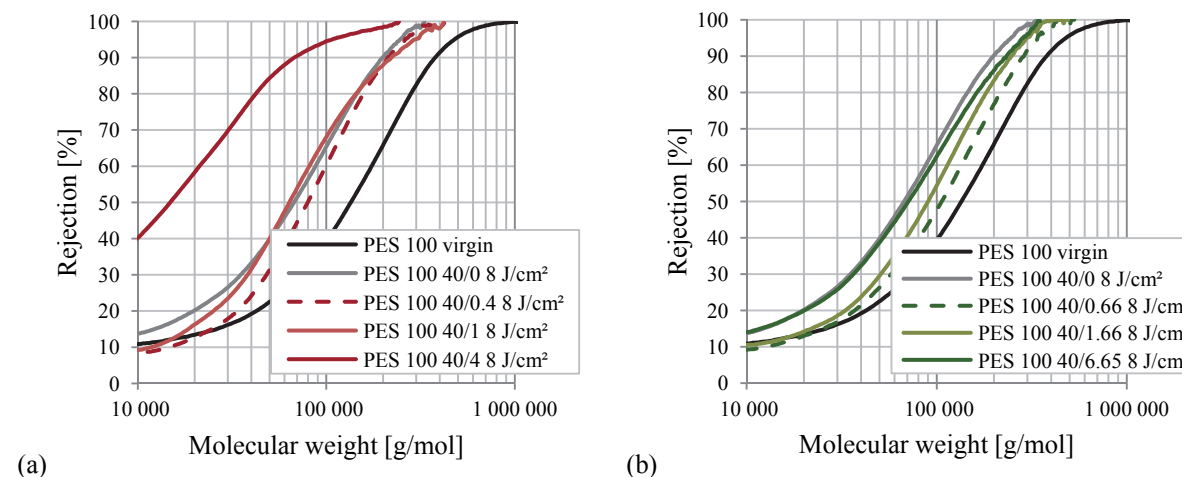


Figure 14 Rejection curves of modified PES 100 at 8 J/cm² under variation of the crosslinking degree; (a) PEGMA 400/MBAA; (b) PEGMA 400/PETAE.

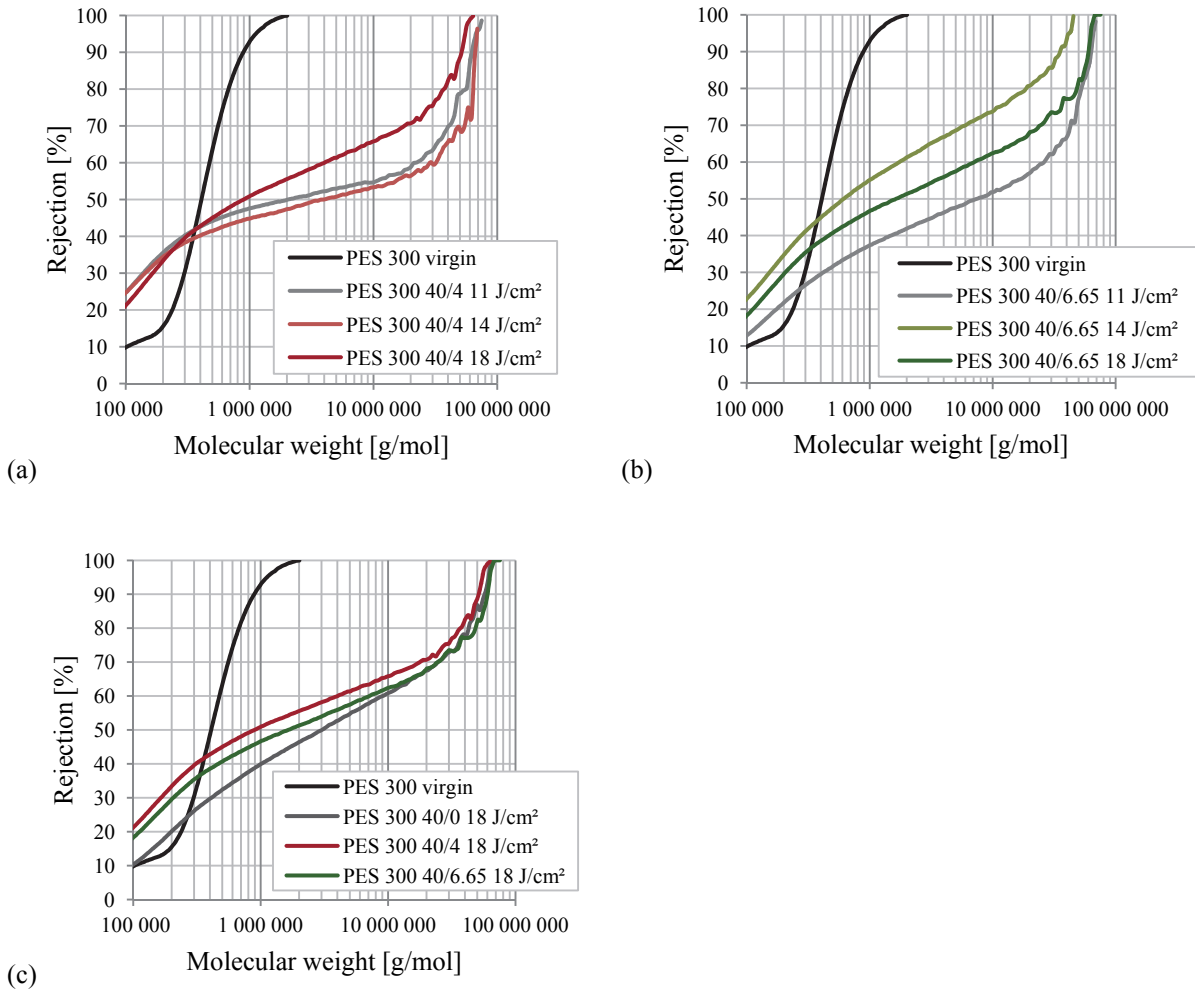


Figure 15 Rejection curves of modified PES 300; (a) PEGMA 400/MBAA; (b) PEGMA 400/PETAE; (c) variation of the crosslinking type at 18 J/cm².

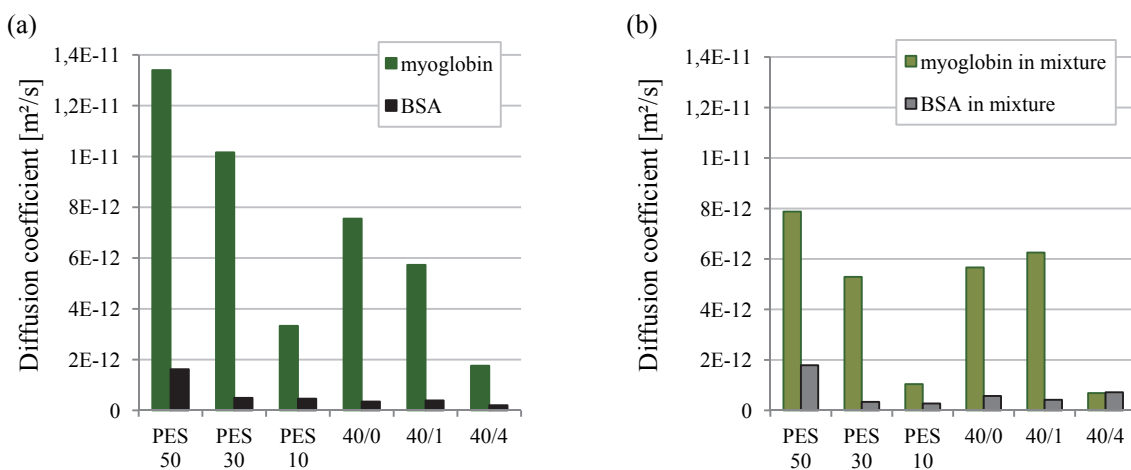


Figure 16 Effective diffusion coefficients of myoglobin and BSA; (a) single solutions; (b) mixture.

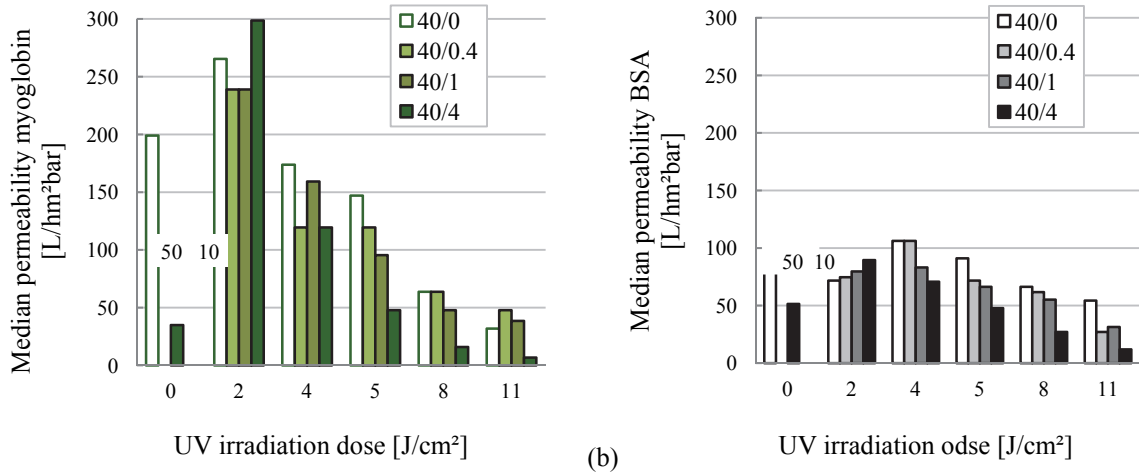


Figure 17 Median permeability during short DE filtration with PES 50 PEGMA 400/MBAA depending on the UV irradiation dose; (a) myoglobin; (b) BSA.

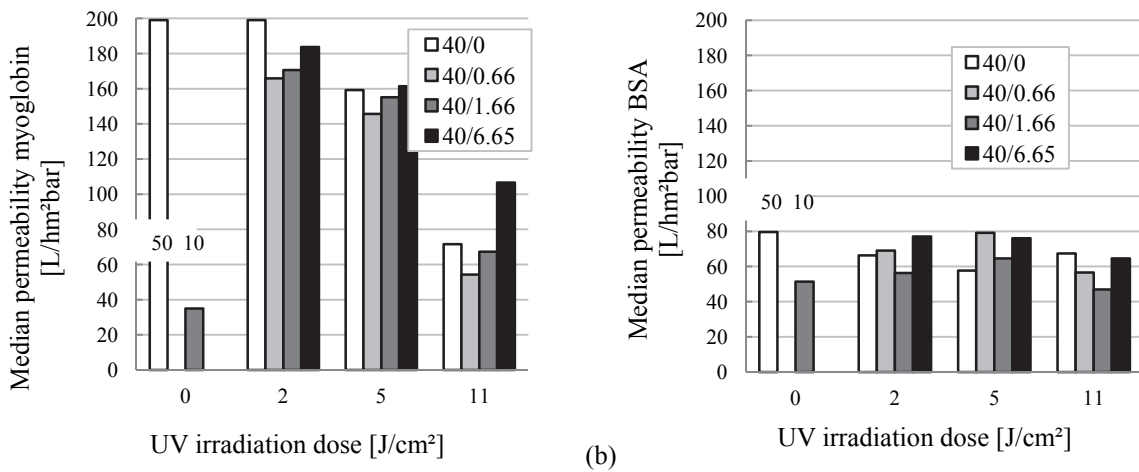


Figure 18 Median permeability during short DE filtration with PES 50 PEGMA 400/PETAE depending on the UV irradiation dose; (a) myoglobin; (b) BSA.

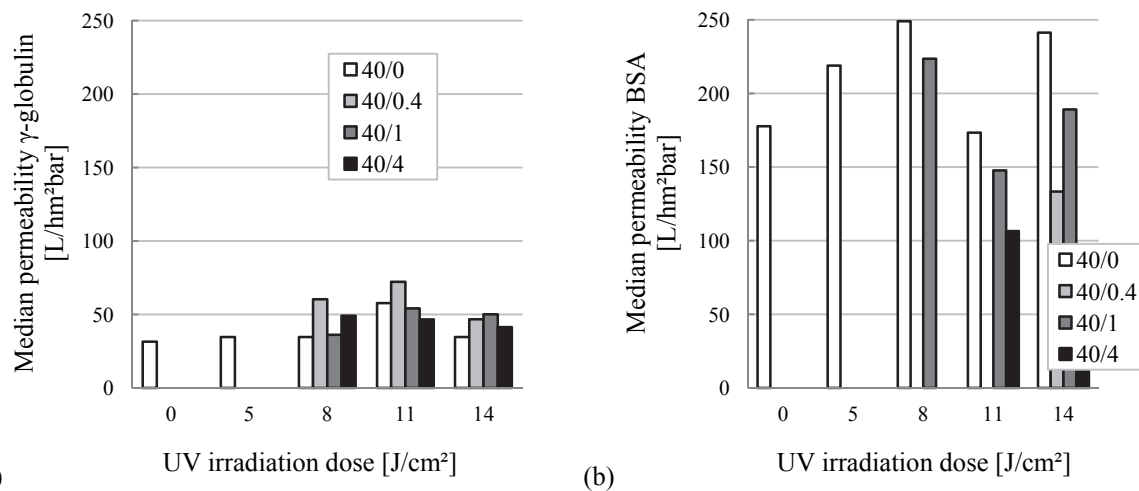


Figure 19 Median permeability during short DE filtration with PES 100 PEGMA 400/MBAA depending on the UV irradiation dose; (a) γ -globulin; (b) BSA.

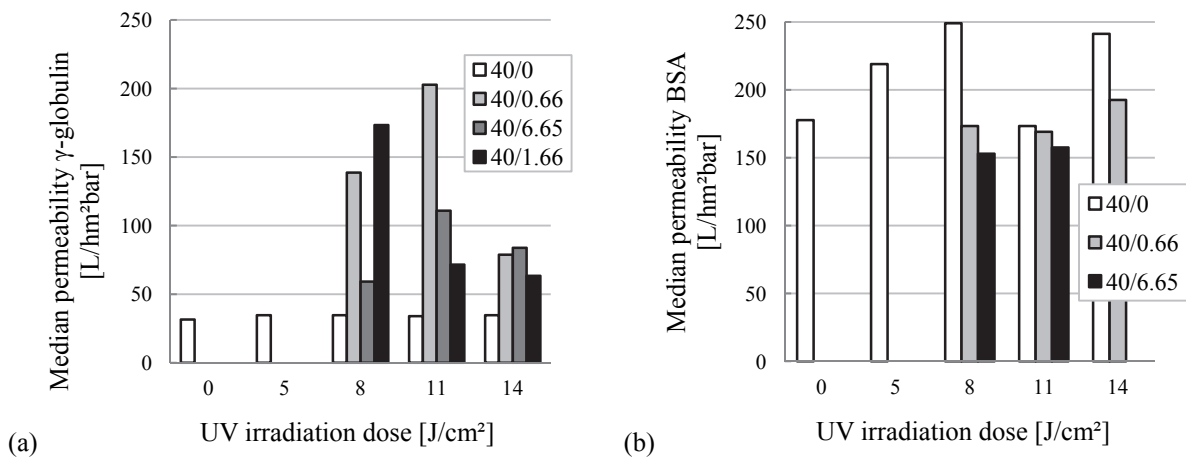


Figure 20 Median permeability during short DE filtration with PES 100 PEGMA 400/PETA depending on the UV irradiation dose; (a) γ -globulin; (b) BSA.

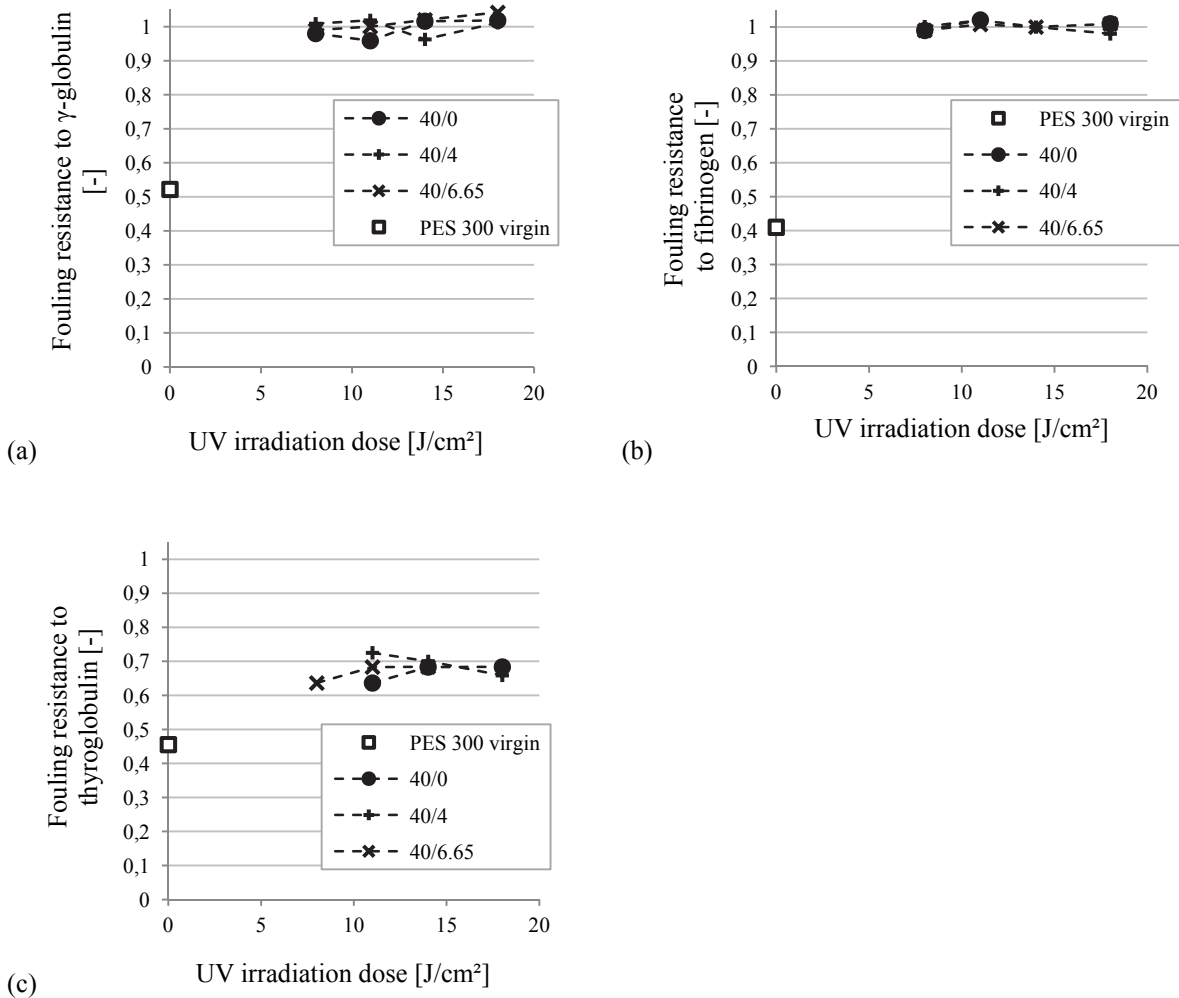


Figure 21 Fouling resistance of PES 300 to tested solutes depending on the UV irradiation dose; (a) γ -globulin; (b) fibrinogen; (c) thyroglobulin.

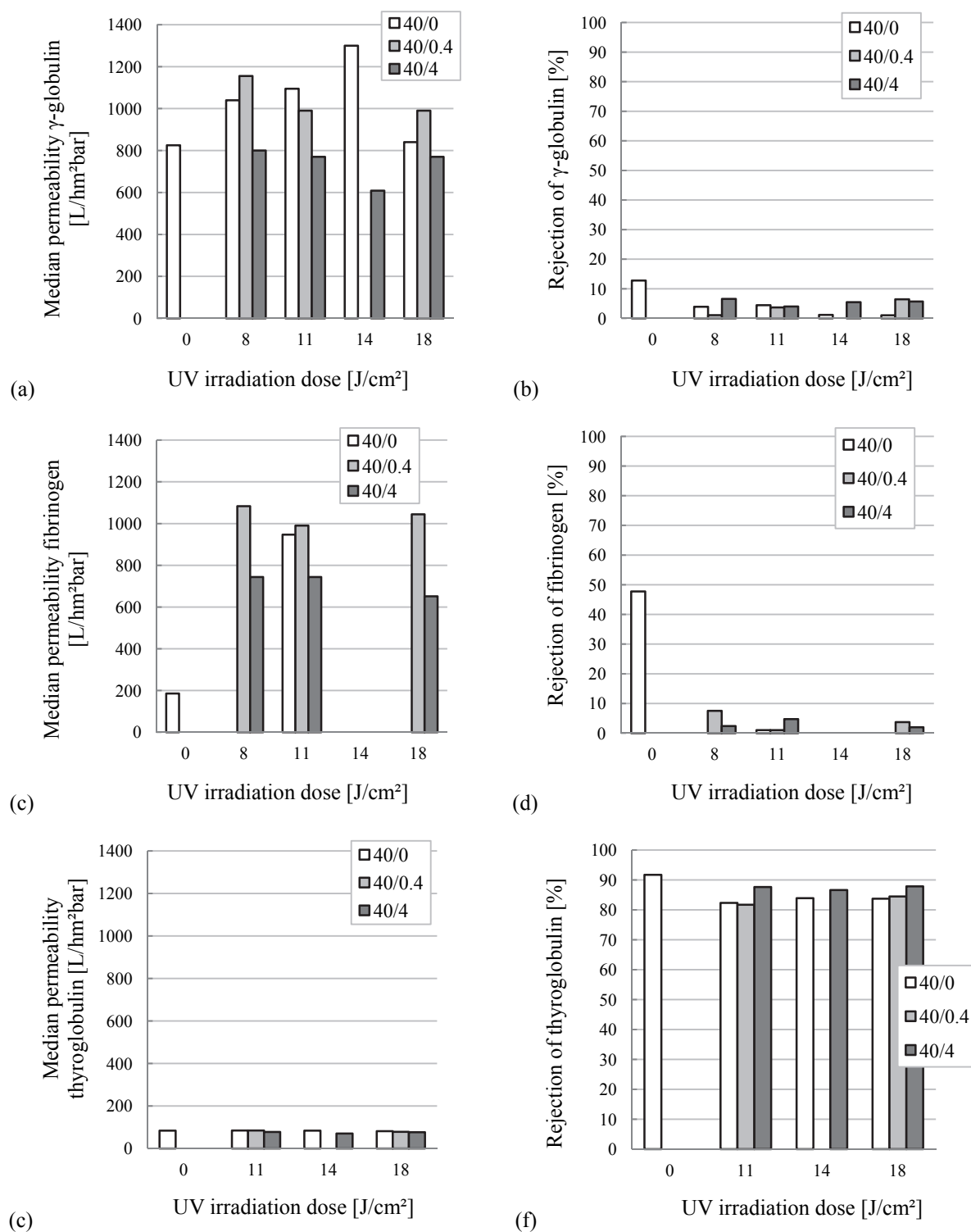


Figure 22 Median permeability and rejection during short DE filtration with PES 300 PEGMA 400/MBAA depending on the UV irradiation dose; (a), (b) γ -globulin; (c), (d) fibrinogen; (e), (f) thyroglobulin.

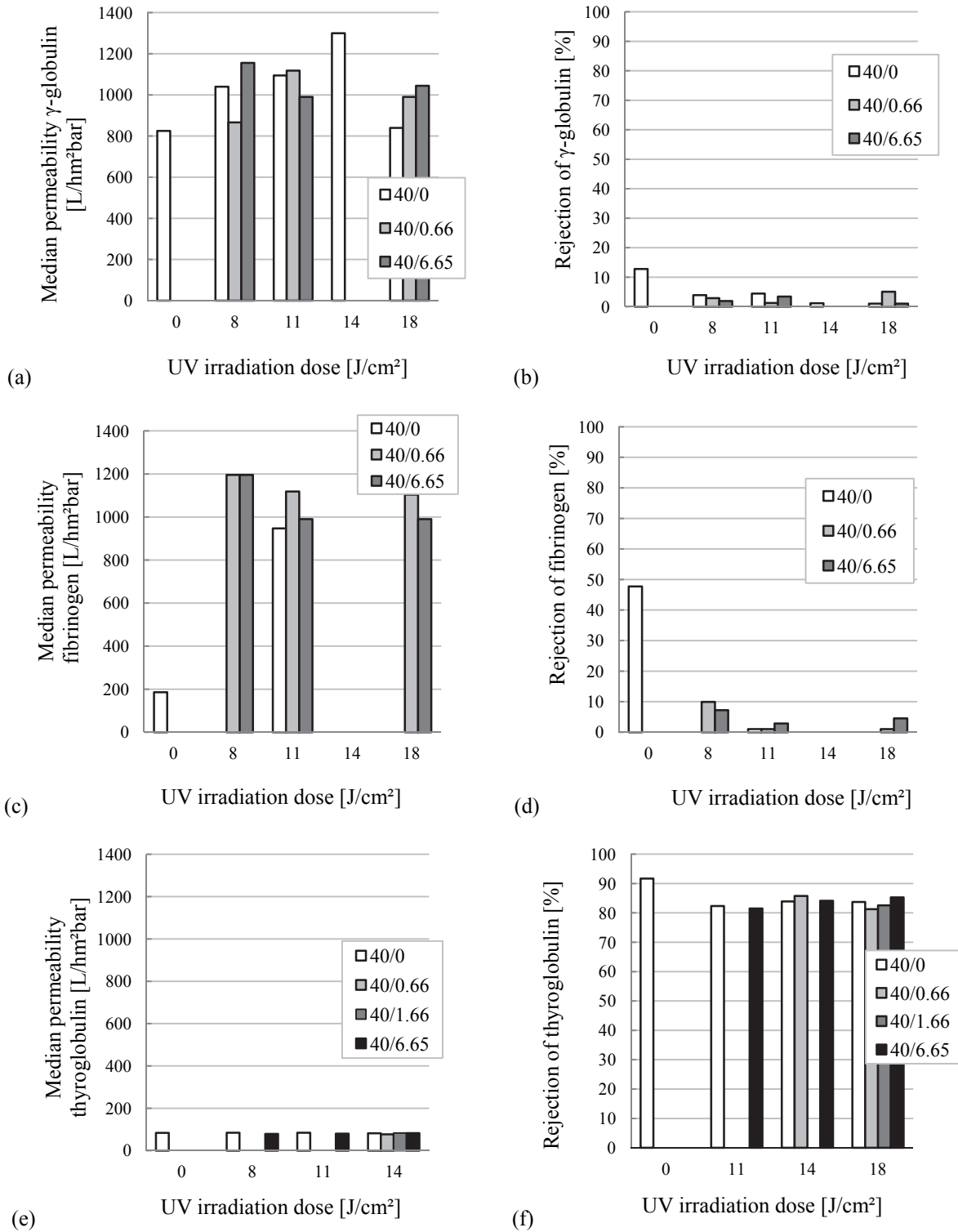


Figure 23 Median permeability and rejection during short DE filtration with PES 300 PEGMA 400/PETAE depending on the UV irradiation dose; (a), (b) γ -globulin; (c), (d) fibrinogen; (e), (f) thyroglobulin.

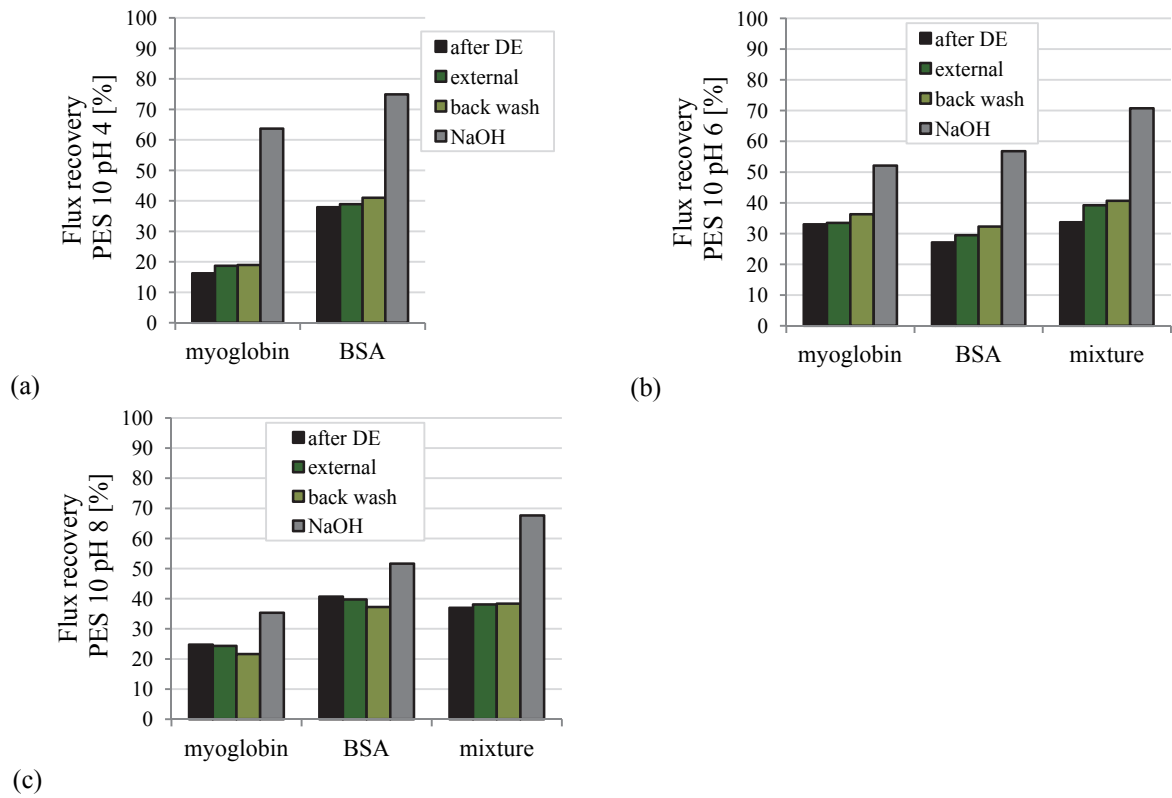


Figure 24 Flux recovery during cleaning of PES 10 after filtration at varied pH value; (a) pH = 4; (b) pH = 6; (c) pH = 8.

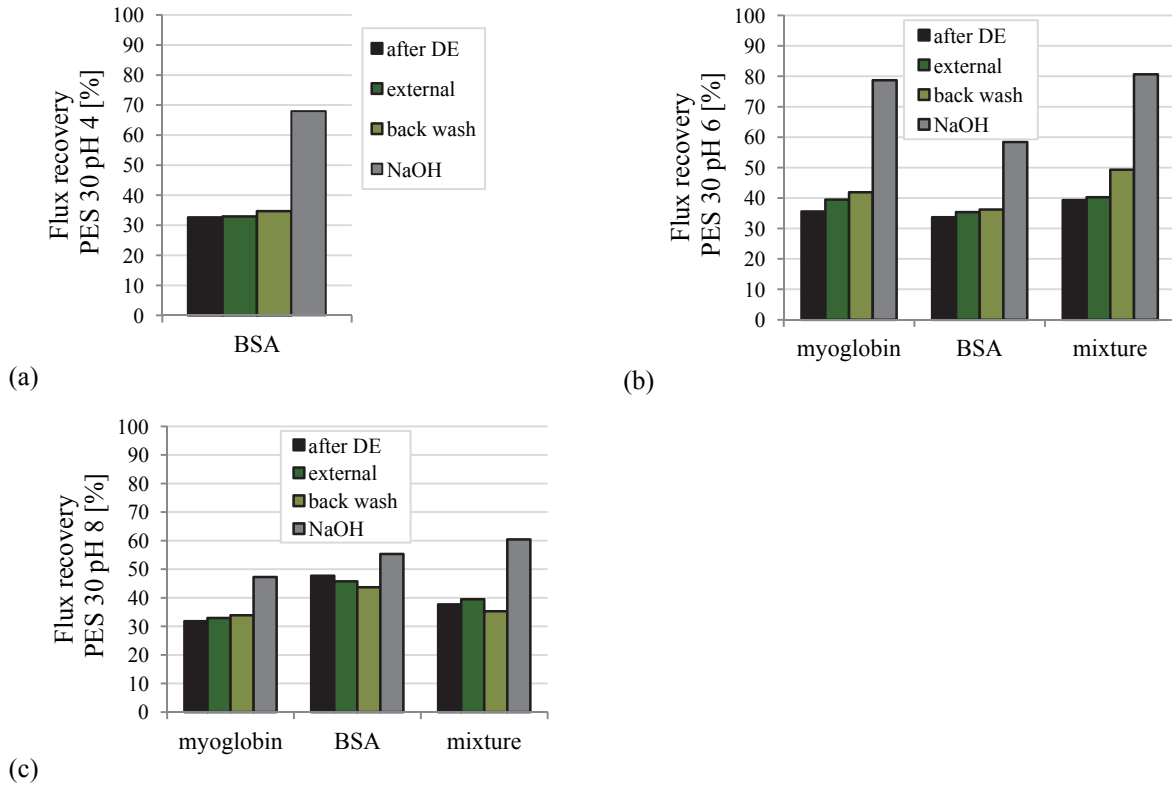


Figure 25 Flux recovery during cleaning of PES 30 after filtration at varied pH value; (a) pH = 4; (b) pH = 6; (c) pH = 8.

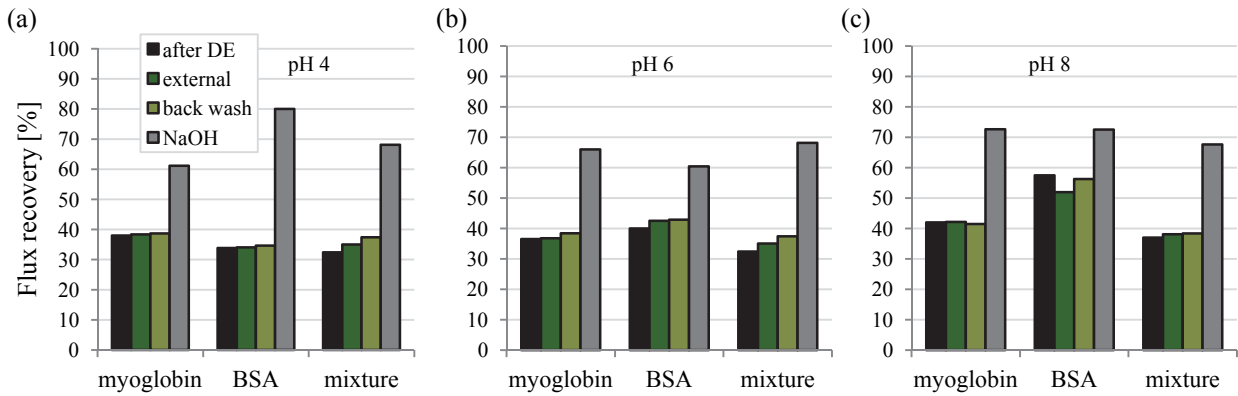


Figure 26 Flux recovery of virgin PES 50 during the cleaning process; (a) pH 4; (b) pH 6; (c) pH 8.

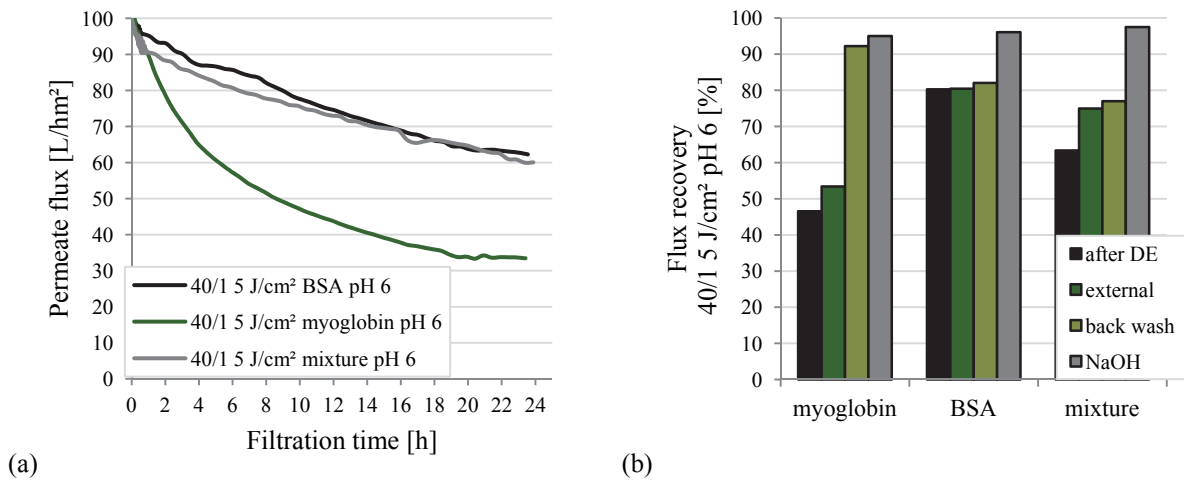


Figure 27 Permeate flux at pH = 6 from DE filtrations and cleanability of PES 50 modified with 40/1 5 J/cm²; (a) permeate flux; (b) flux recovery.

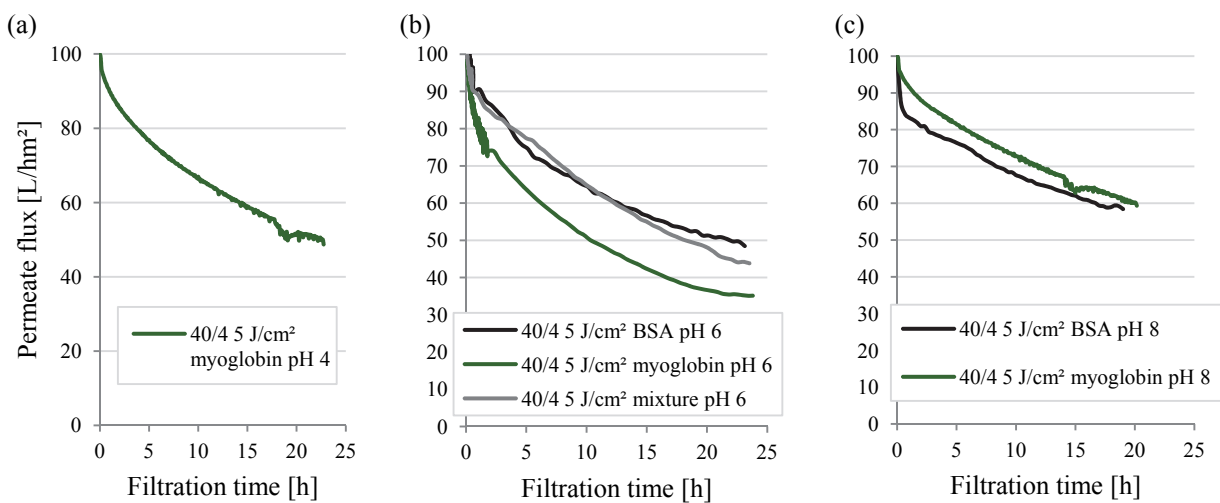


Figure 28 Permeate flux during DE filtration through PES 50 modified with 40/4 5 J/cm² at varied pH value; (a) pH = 4; (b) pH = 6; (c) pH = 8.

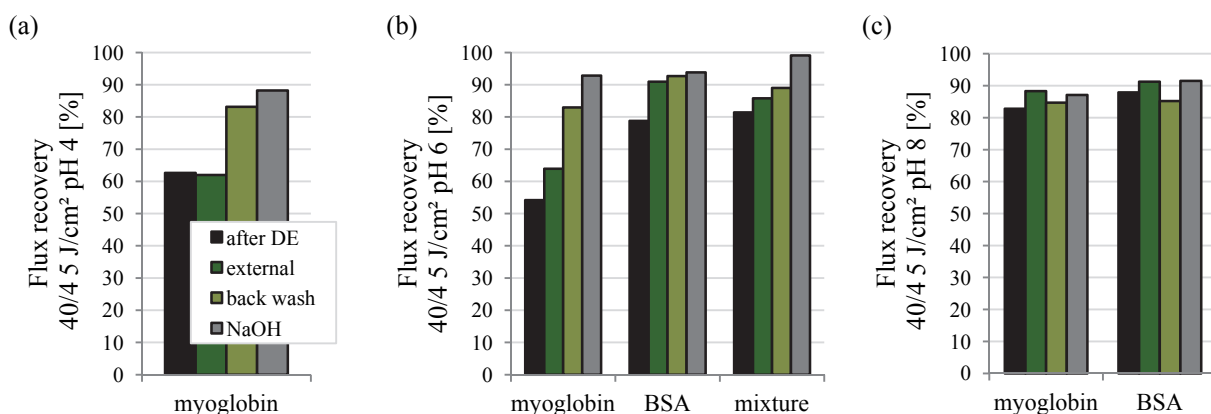


Figure 29 Cleanability after DE filtration through PES 50 modified with 40/4 5 J/cm² at varied pH value; (a) pH = 4; (b) pH = 6; (c) pH = 8.

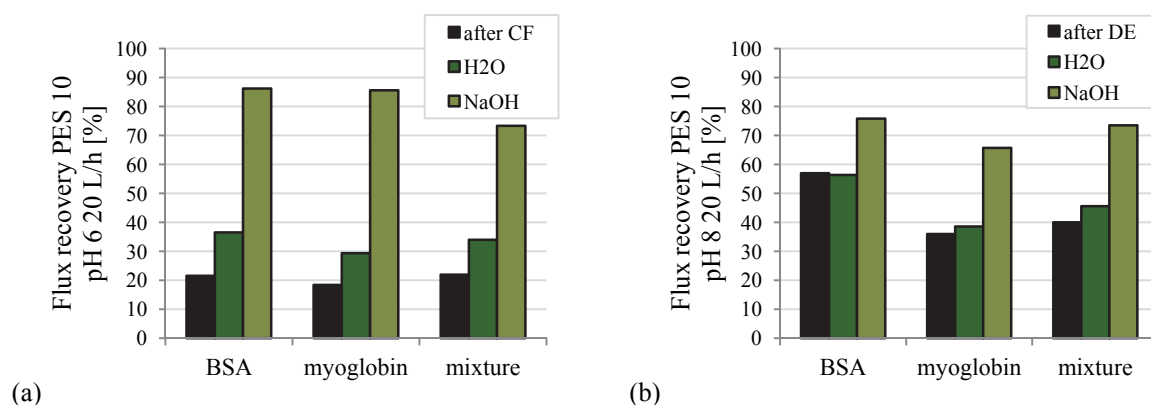


Figure 30 Flux recovery during cleaning after CF filtration through virgin PES 10 at 20 L/h CF; (a) pH 6; (b) pH 8.

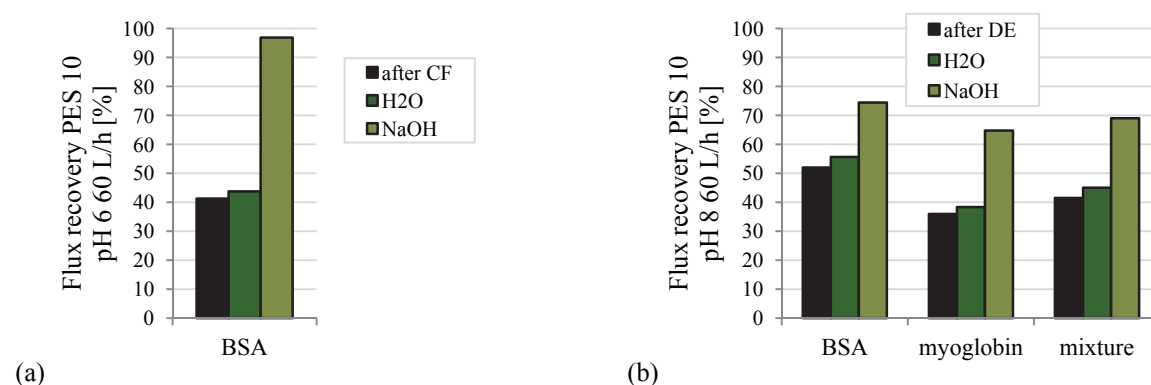


Figure 31 Flux recovery during cleaning after CF filtration through virgin PES 10 at 60 L/h CF; (a) pH 6; (b) pH 8.

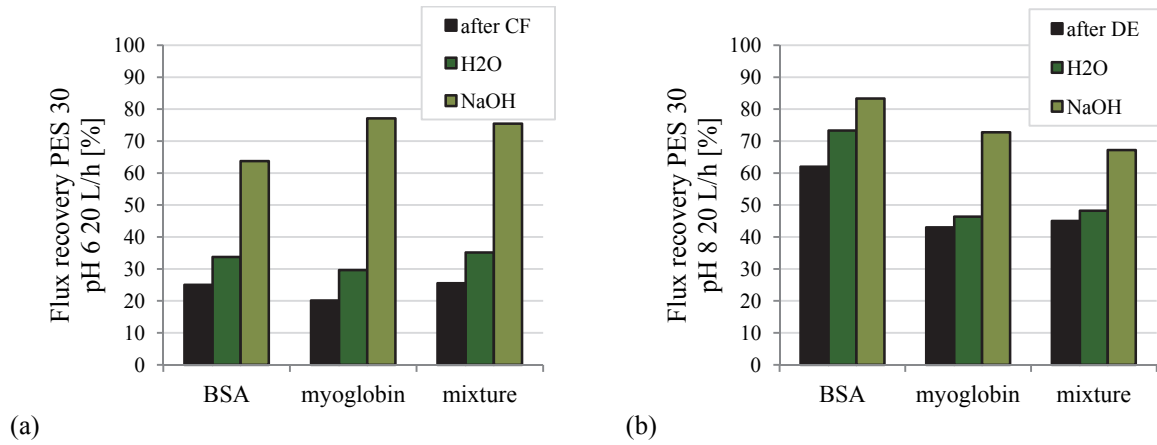


Figure 32 Flux recovery during cleaning after CF filtration through virgin PES 30 at 20 L/h CF; (a) pH 6; (b) pH 8.

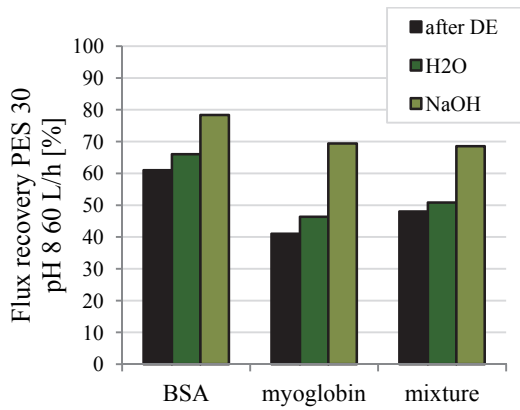


Figure 33 Flux recovery during cleaning after CF filtration through virgin PES 30 at pH = 8 60 L/h CF.

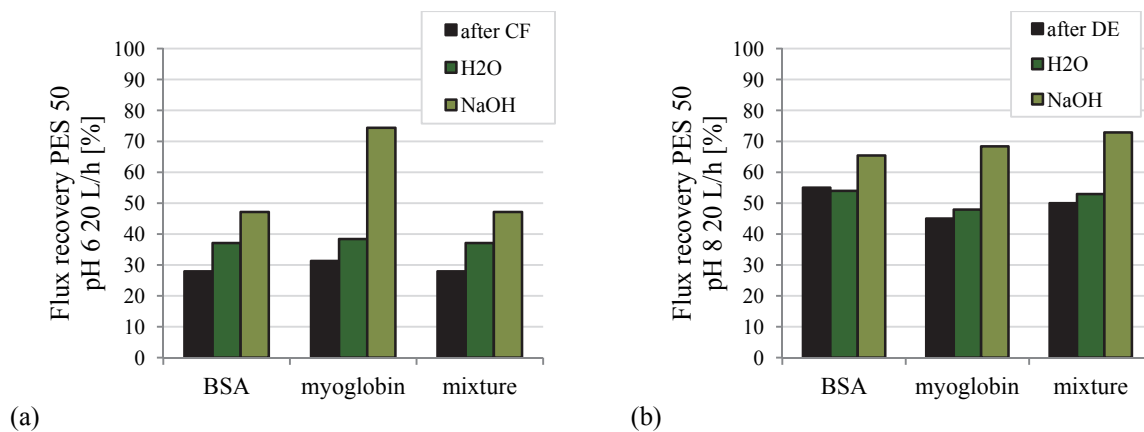


Figure 34 Flux recovery during cleaning after CF filtration through virgin PES 50 at 20 L/h CF; (a) pH 6; (b) pH 8.

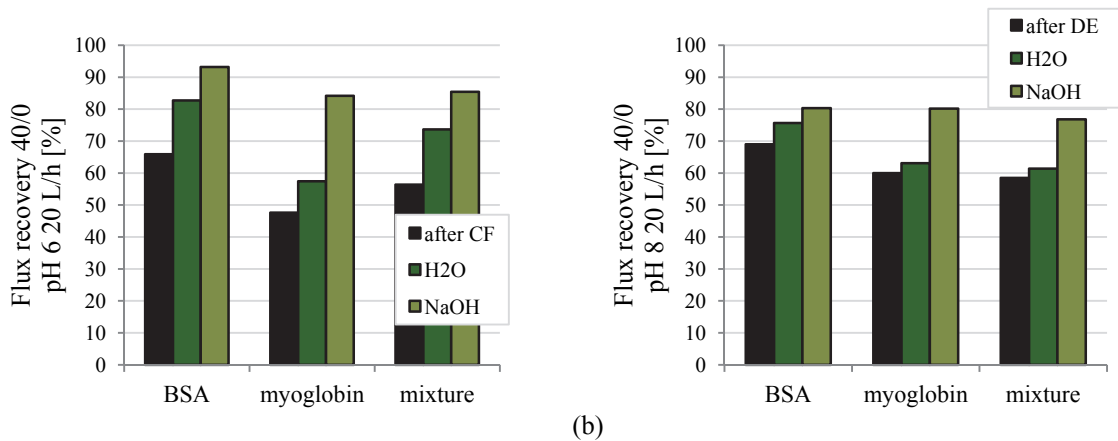


Figure 35 Flux recovery during cleaning after CF filtration through modified PES 50 with 40/0 5 J/cm² at 20 L/h CF; (a) pH 6; (b) pH 8.

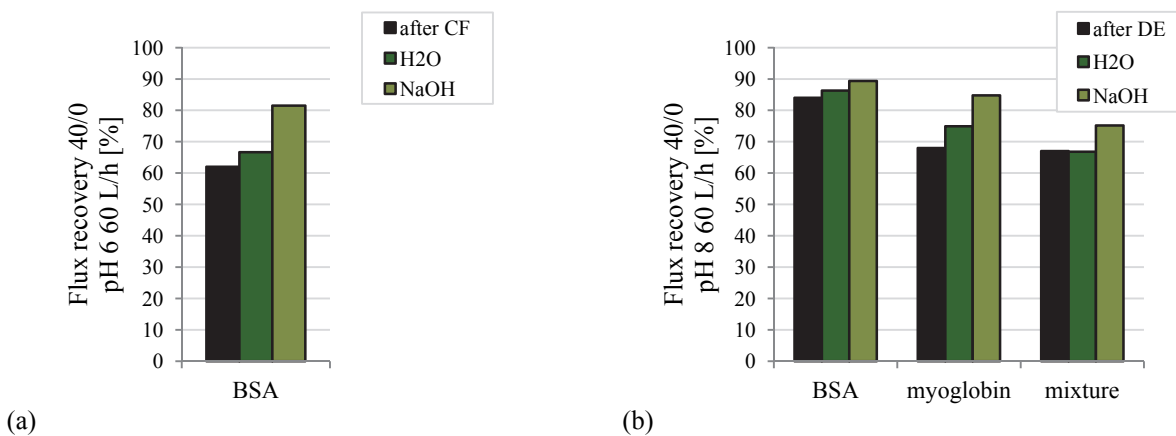


Figure 36 Flux recovery during cleaning after CF filtration through modified PES 50 with 40/0 5 J/cm² at 60 L/h CF; (a) pH 6; (b) pH 8.

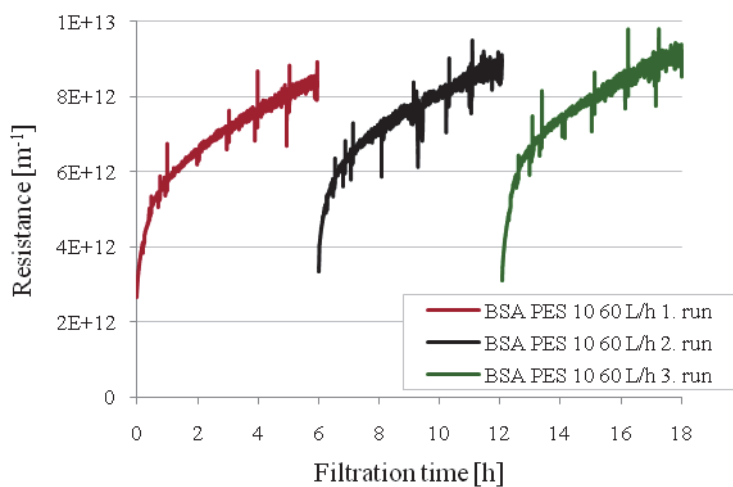


Figure 37 Resistance during filtration stability test with BSA through virgin PES 10 at 60 L/h CF.

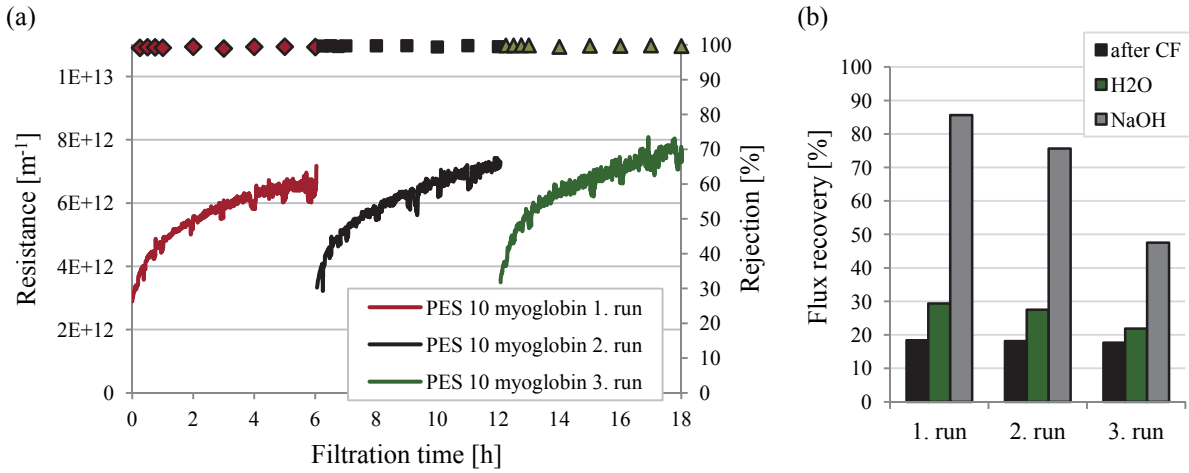


Figure 38 Filtration stability test with myoglobin through virgin PES 10; (a) resistance and rejection; (b) flux recovery after the cleaning procedures.

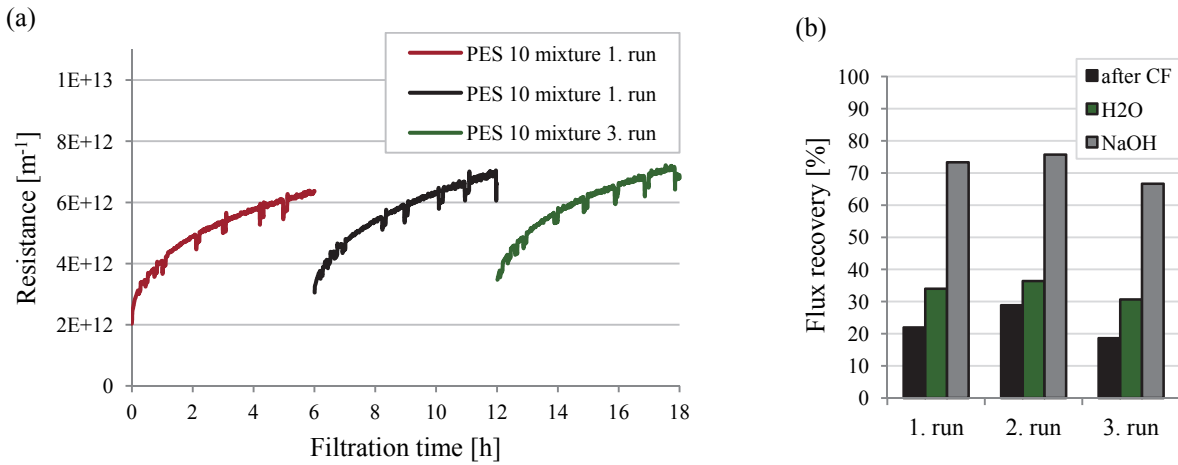


Figure 39 Filtration stability test with mixture through virgin PES 10; (a) resistance and rejection; (b) flux recovery after the cleaning procedures.

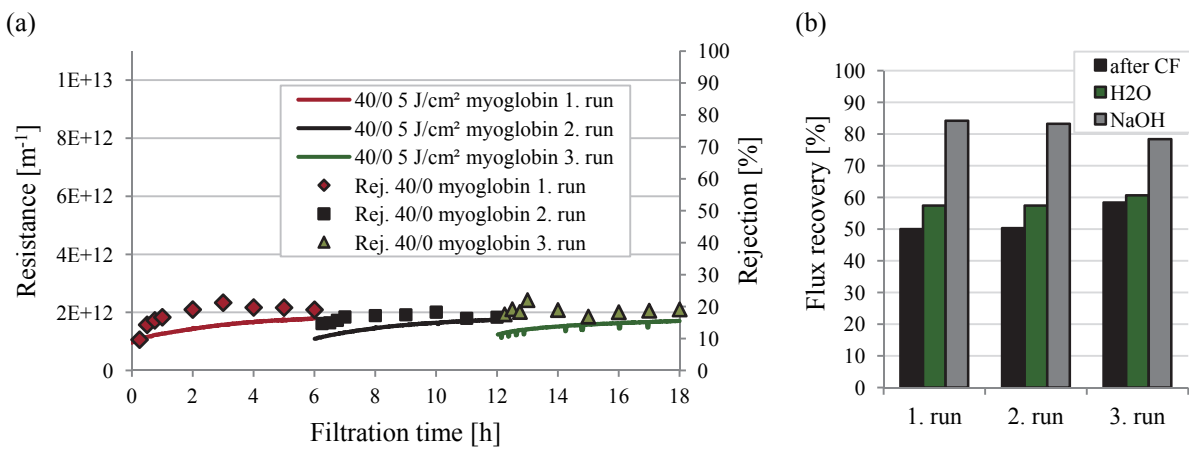


Figure 40 Filtration stability test with myoglobin through PES 50 modified with 40/0 5 J/cm²; (a) resistance and rejection; (b) flux recovery after the cleaning procedures.

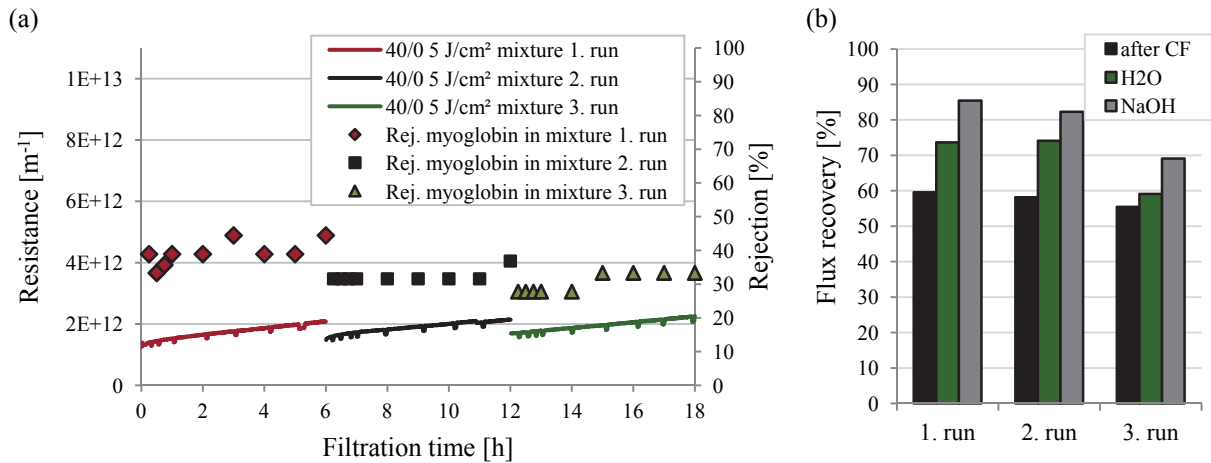


Figure 41 Filtration stability test with mixture through PES 50 modified with 40/0 5 J/cm²; (a) resistance and rejection; (b) flux recovery after the cleaning procedures.

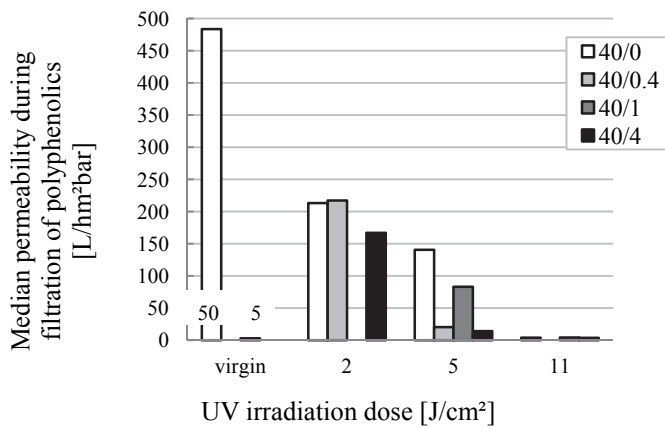


Figure 42 Median permeability during short DE filtration of polyphenolics through modified PES 50 at varied UV irradiation dose.

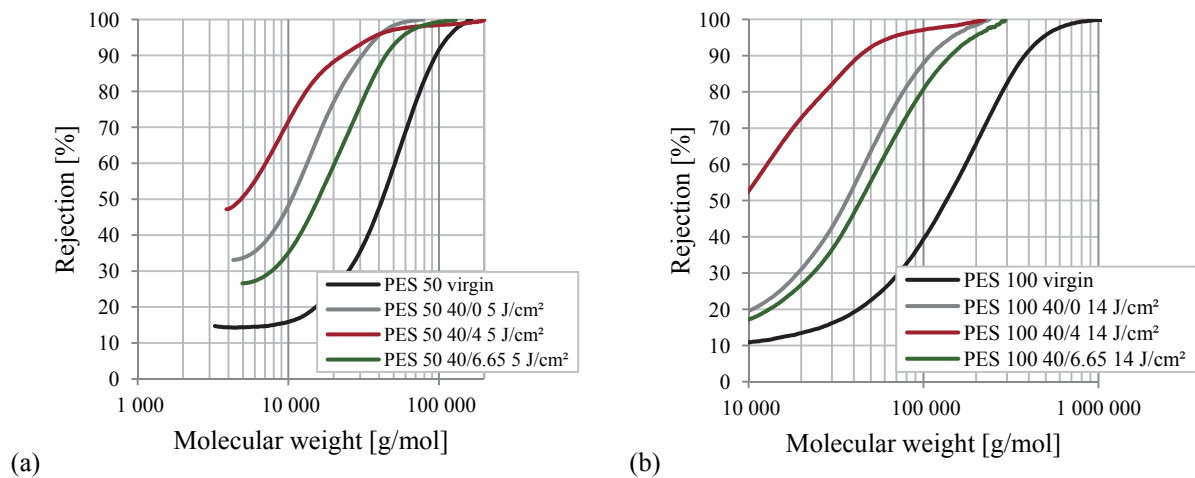


Figure 43 Rejection curves of modified membranes under variation of the crosslinking type; (a) PES 50 5 J/cm²; (b) PES 100 14 J/cm².

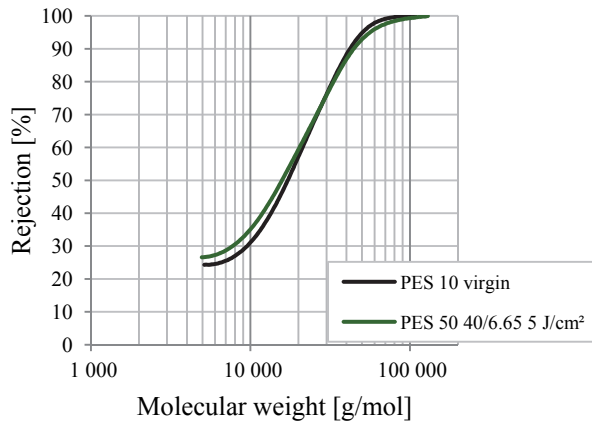


Figure 44 Comparison of rejection curves of virgin PES 10 and modified PES 50 40/6.65 11 J/cm².

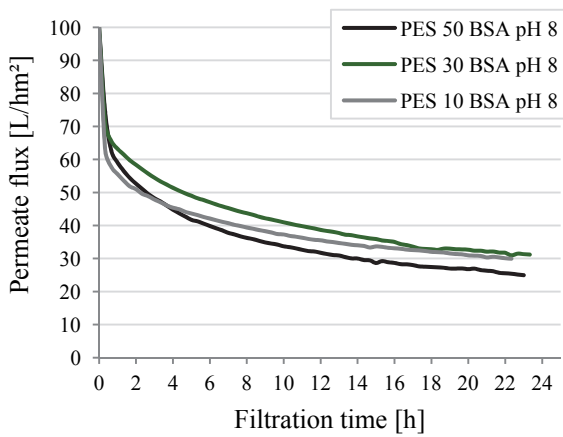


Figure 45 Effect of the membrane pore size on the permeate flux and rejection during DE filtration of BSA at pH = 8.

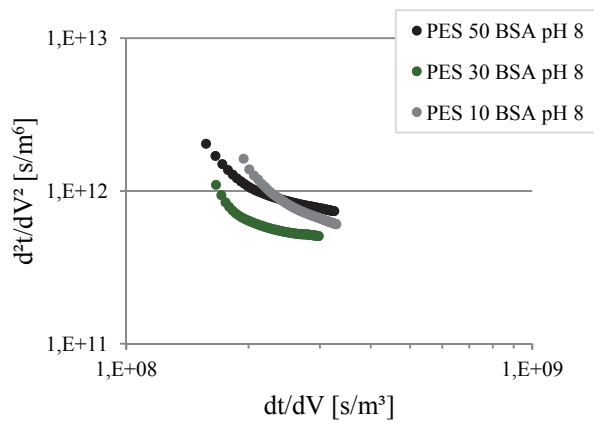
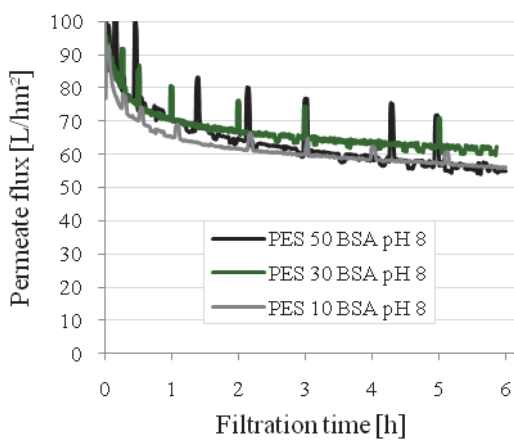
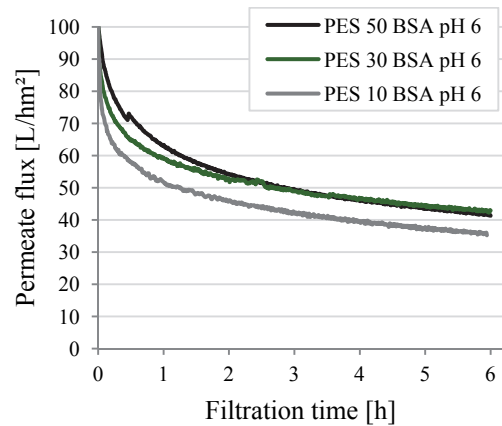


Figure 46 Fouling mechanism analysis for DE filtration of BSA with virgin membranes at pH = 8.



(a)



(b)

Figure 47 Permeate flux during CF filtration of BSA through virgin membranes at varied pH; (a) pH = 8; (b) pH = 6.

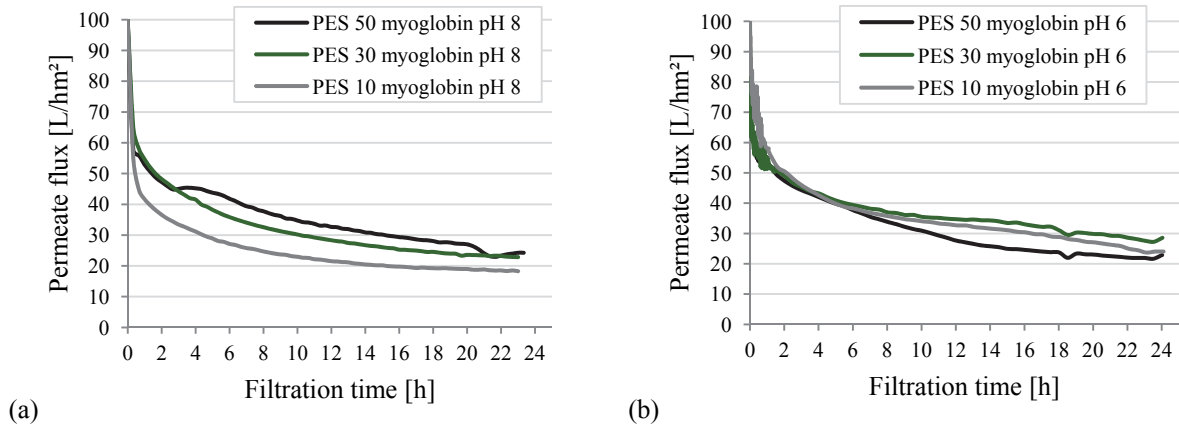


Figure 48 Permeate flux during DE filtration of myoglobin through virgin membranes at varied pH; (a) pH = 8; (b) pH = 6.

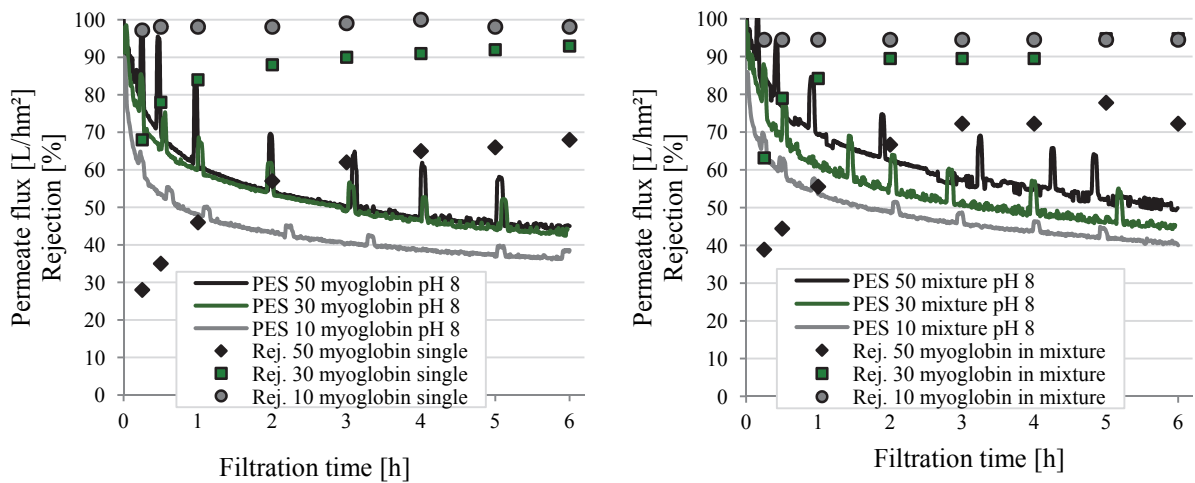


Figure 49 Effect of the membrane pore size on the permeate flux and rejection during CF filtration of myoglobin at pH = 8.

Figure 50 Effect of the membrane pore size on the permeate flux and rejection during CF filtration of mixture at pH = 8.

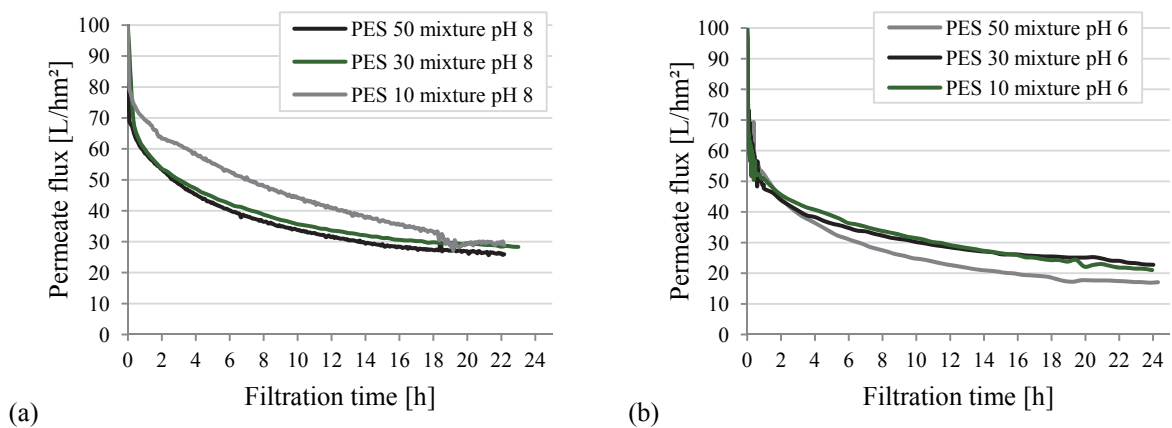


Figure 51 Permeate flux during DE filtration of mixture through virgin membranes at varied pH; (a) pH = 8; (b) pH = 6.

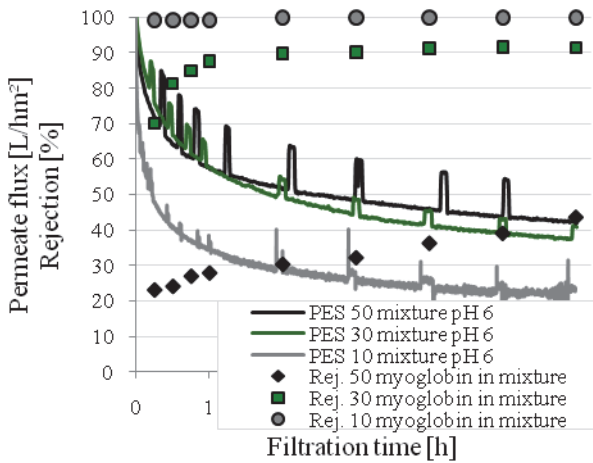


Figure 52 Effect of the membrane pore size on the permeate flux and rejection during CF filtration of mixture at pH = 6.

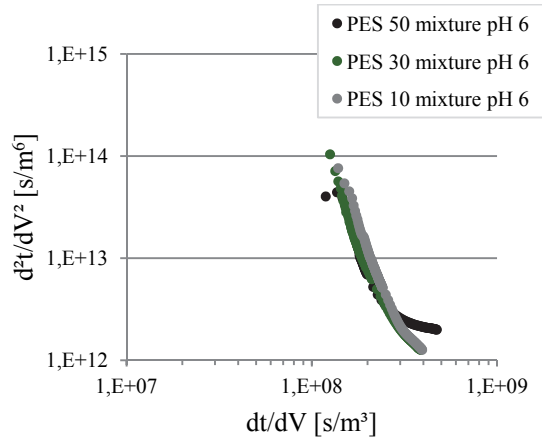
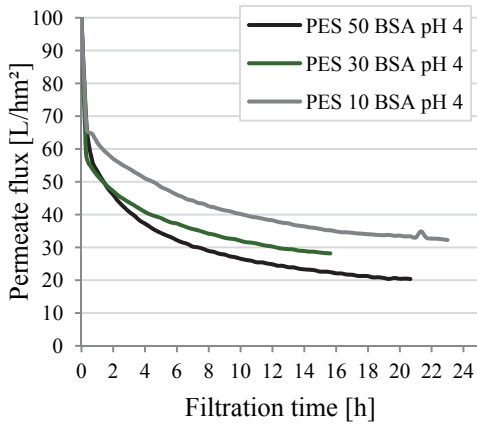
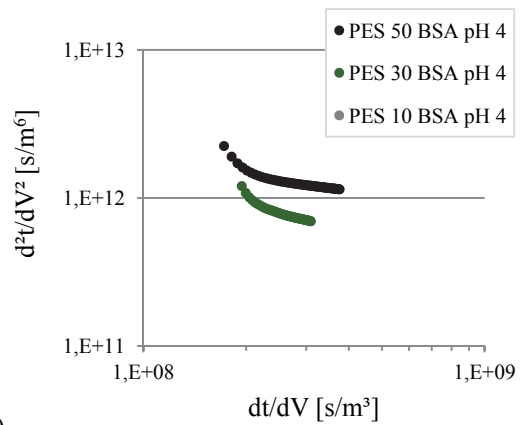


Figure 53 Fouling mechanism analysis for DE filtration of mixture with virgin membranes at pH = 6.

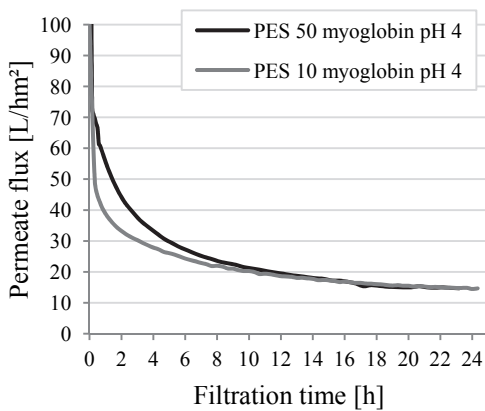


(a)

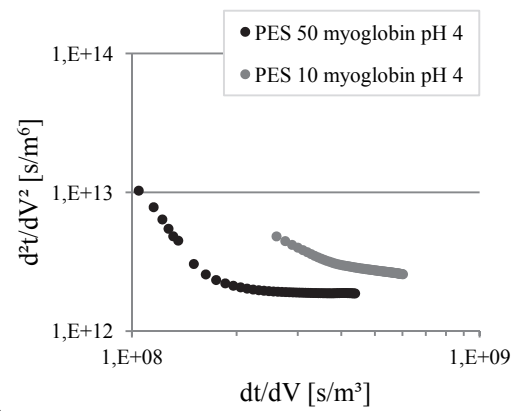


(b)

Figure 54 Effect of the membrane pore size during DE filtration of BSA at pH = 4; (a) permeate flux; (b) fouling mechanism analysis.



(a)



(b)

Figure 55 Effect of the membrane pore size during DE filtration of myoglobin at pH = 4; (a) permeate flux; (b) fouling mechanism analysis.

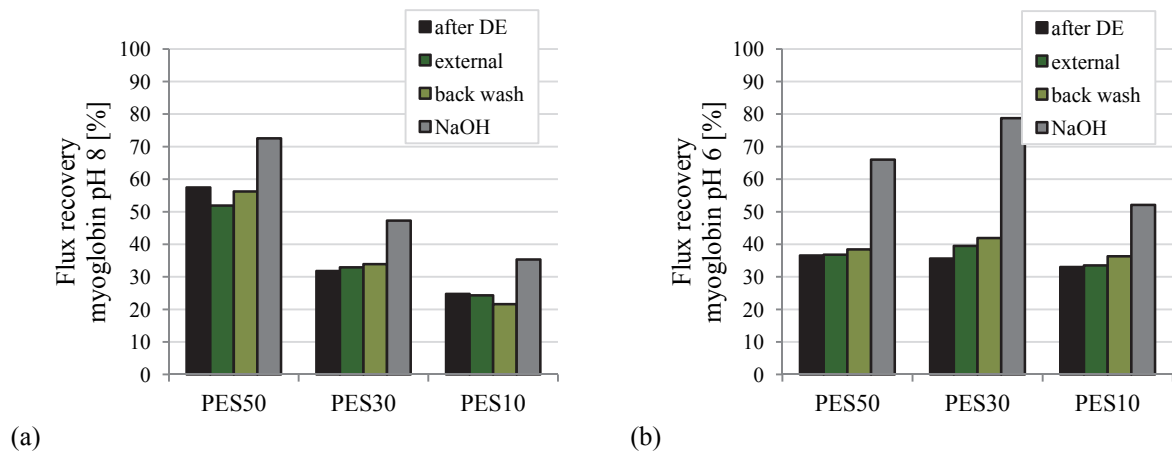


Figure 56 Flux recovery during cleaning after DE filtration of myoglobin through virgin membranes at varied pH; (a) pH = 8; (b) pH = 6.

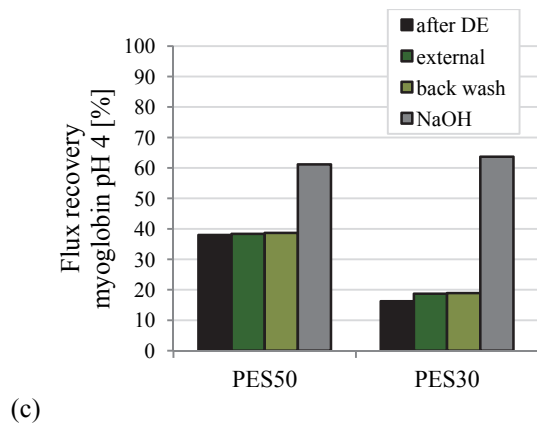
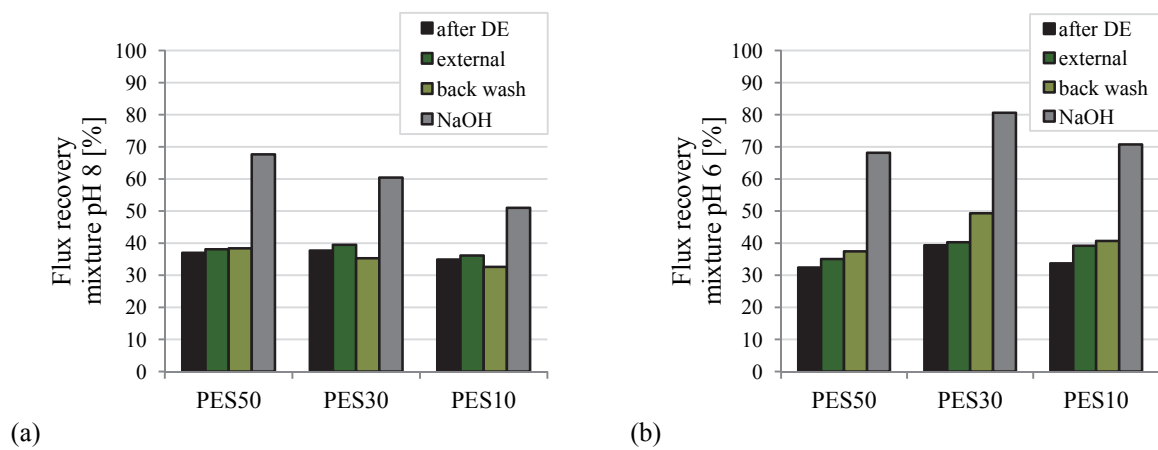


Figure 57 Flux recovery during cleaning after DE filtration of mixture through virgin membranes at varied pH; (a) pH = 8; (b) pH = 6; (c) pH = 4.

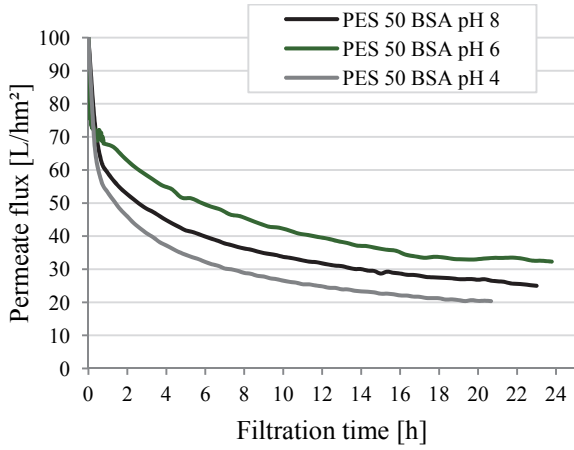
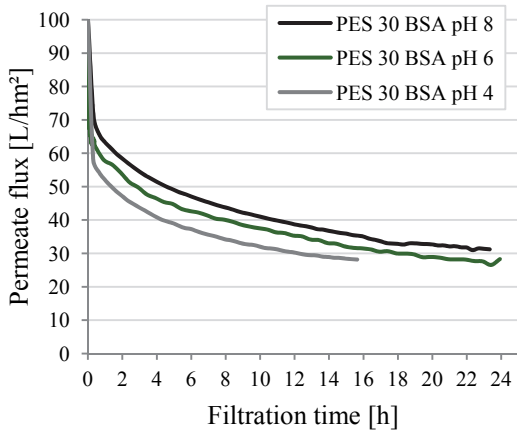
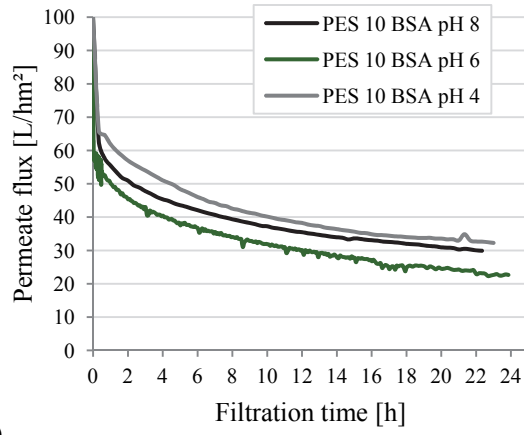


Figure 58 Effect of the pH on the permeate flux during DE filtration of BSA through PES 50.

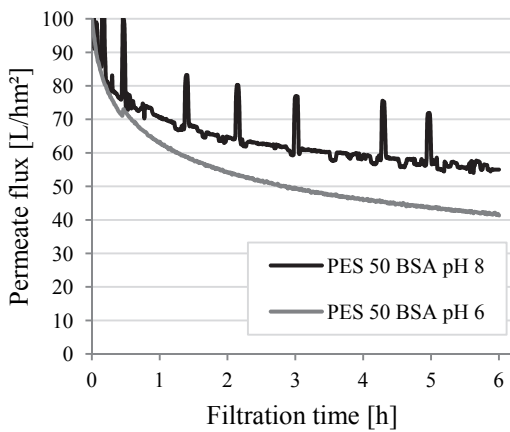


(a)

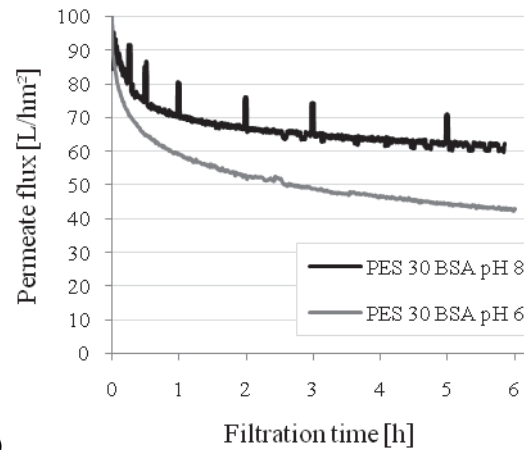


(b)

Figure 59 Permeate flux during DE filtration of BSA through virgin membranes at varied pH; (a) PES 30; (b) PES 10.



(a)



(b)

Figure 60 Permeate flux during CF filtration of BSA through virgin membranes at varied pH; (a) PES 50; (b) PES 30.

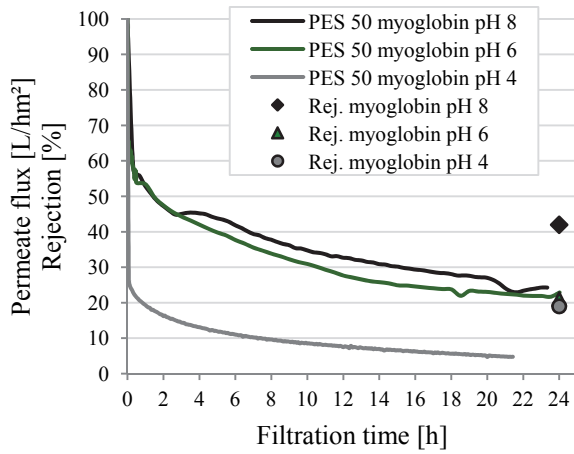


Figure 61 Effect of the pH on the permeate flux and rejection during DE filtration of myoglobin through PES 50.

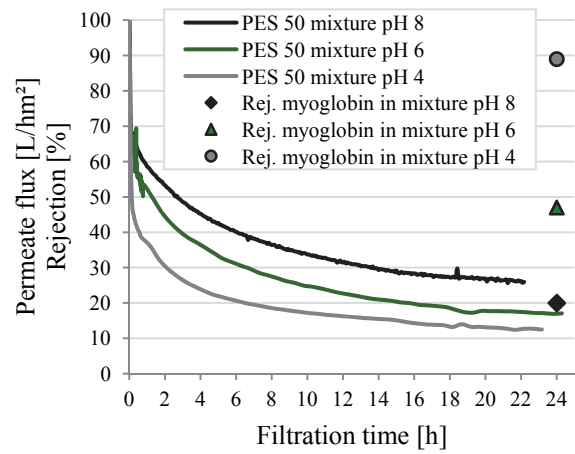


Figure 62 Effect of the pH on the permeate flux and rejection during DE filtration of mixture through PES 50.

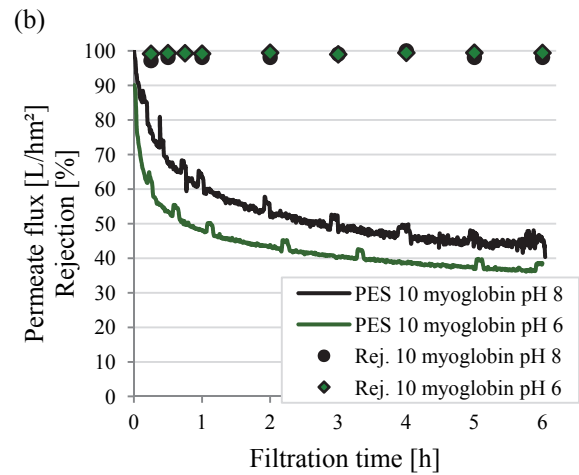
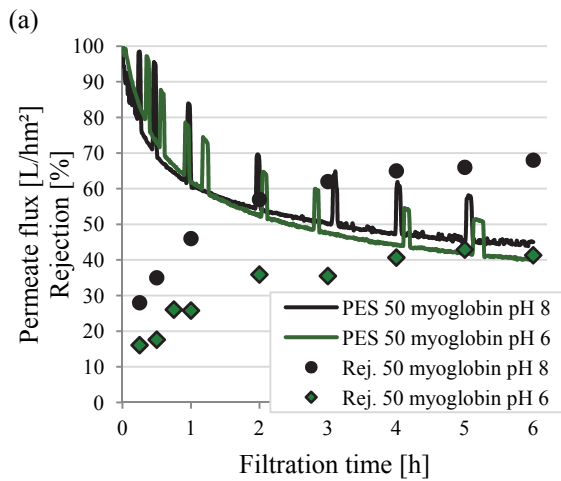


Figure 63 Permeate flux and rejection during CF filtration of myoglobin through virgin membranes at varied pH; (a) PES 50; (b) PES 10.

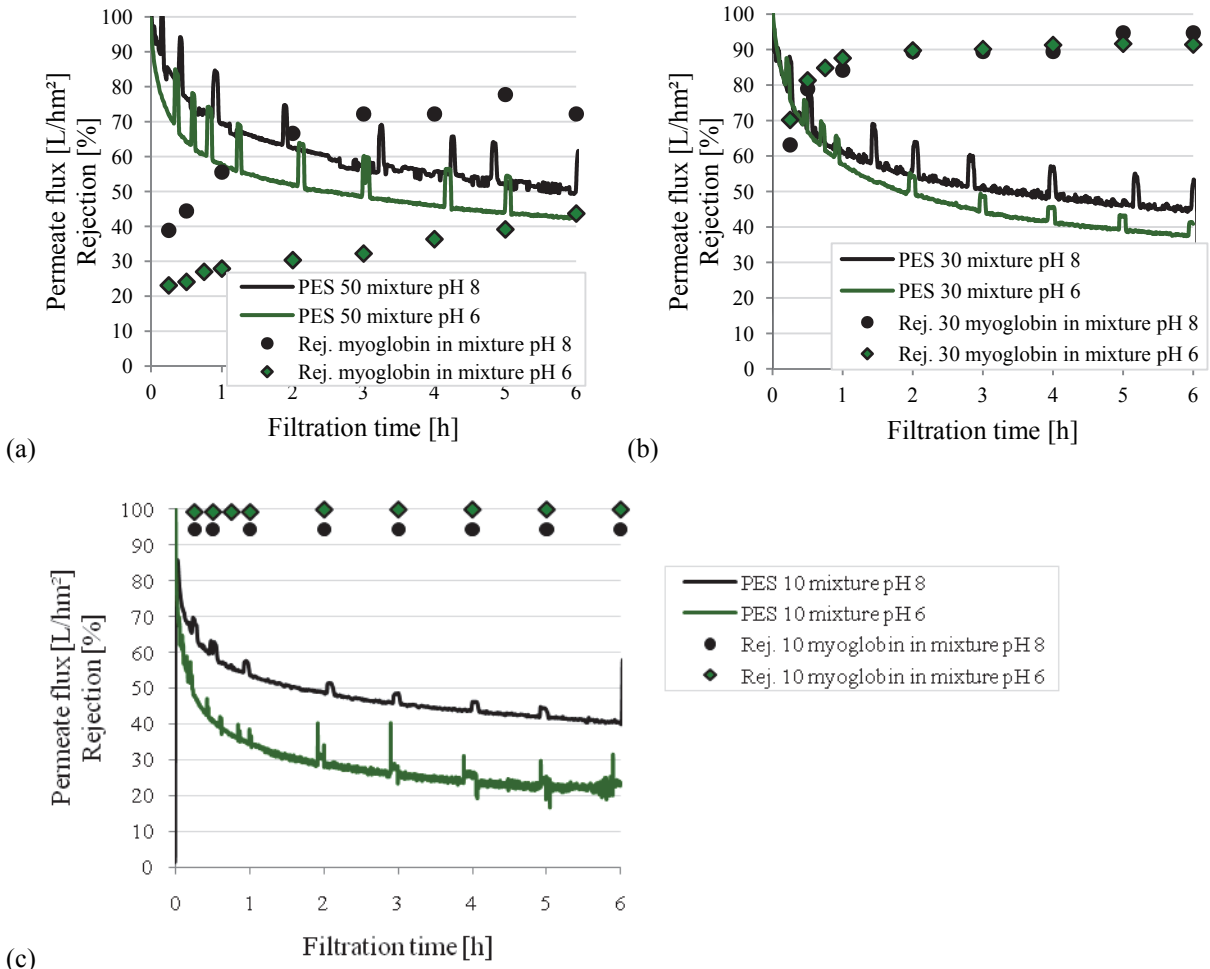


Figure 64 Permeate flux and rejection during CF filtration of BSA through virgin membranes at varied pH; (a) PES 50; (b) PES 30; (c) PES 10.

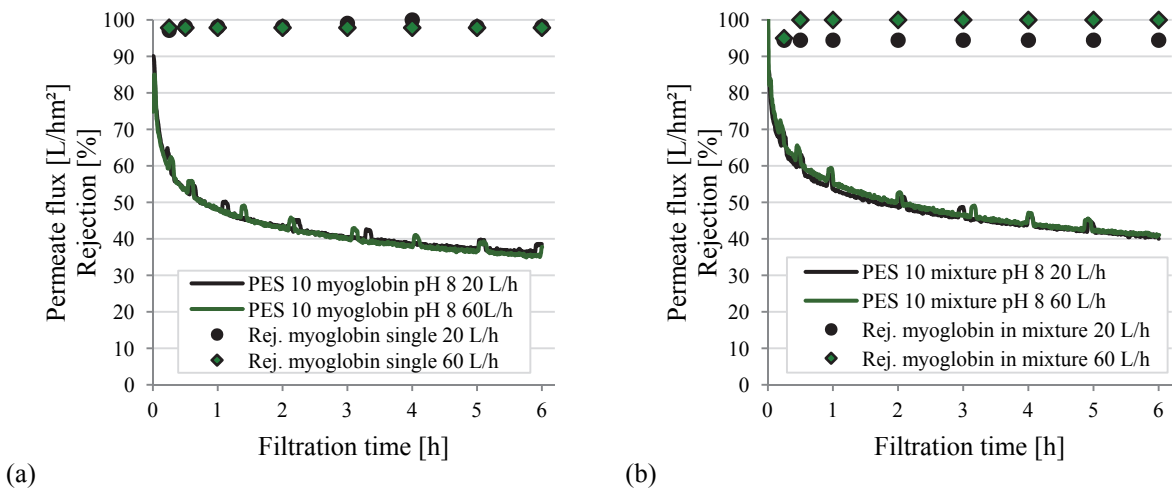


Figure 65 Permeate flux and rejection during CF filtration through virgin PES 10 at pH = 8 and varied CF; (a) myoglobin; (b) mixture.

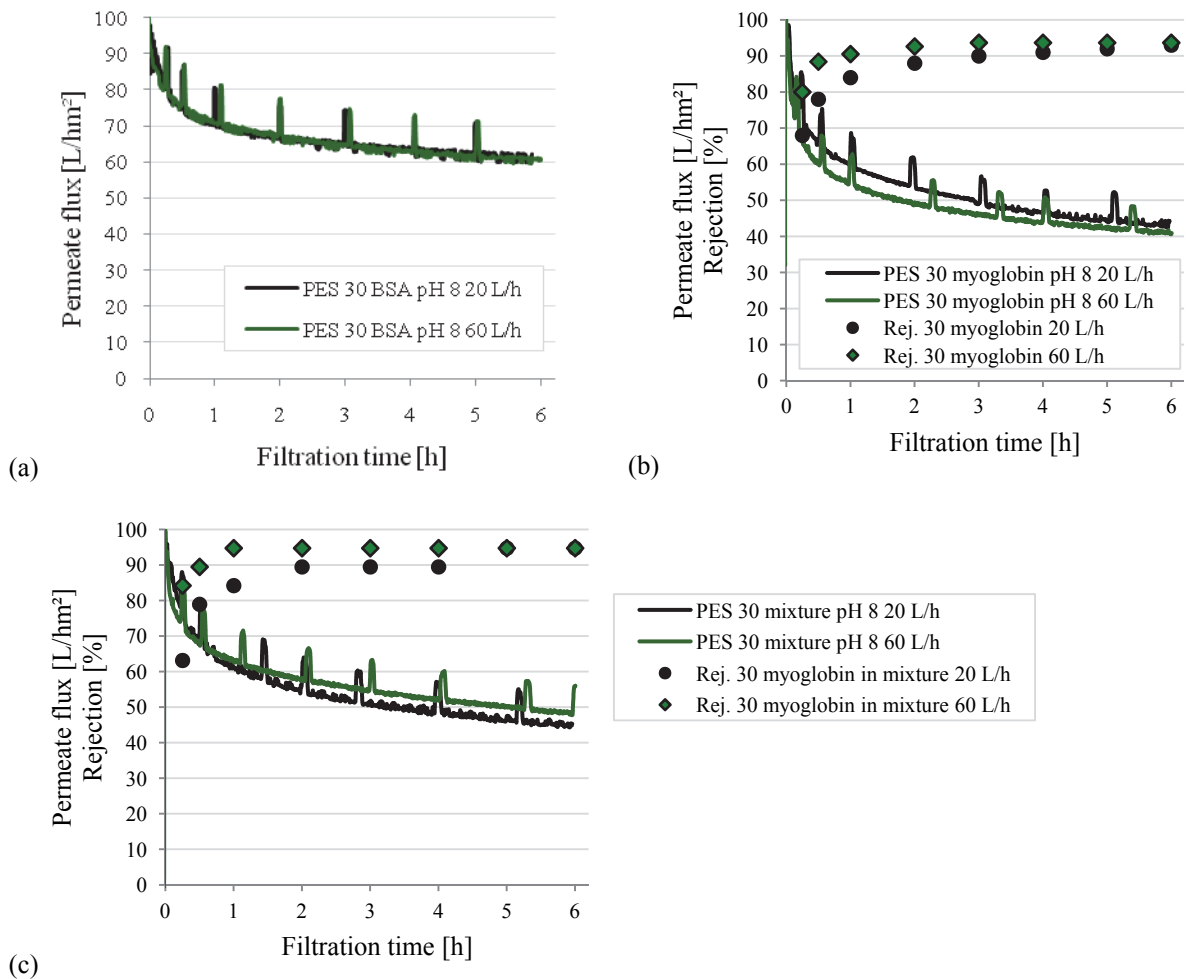


Figure 66 Permeate flux and rejection during CF filtration through virgin PES 30 at pH = 8 and varied CF; (a) filtration of BSA, (b) myoglobin; (c) mixture.

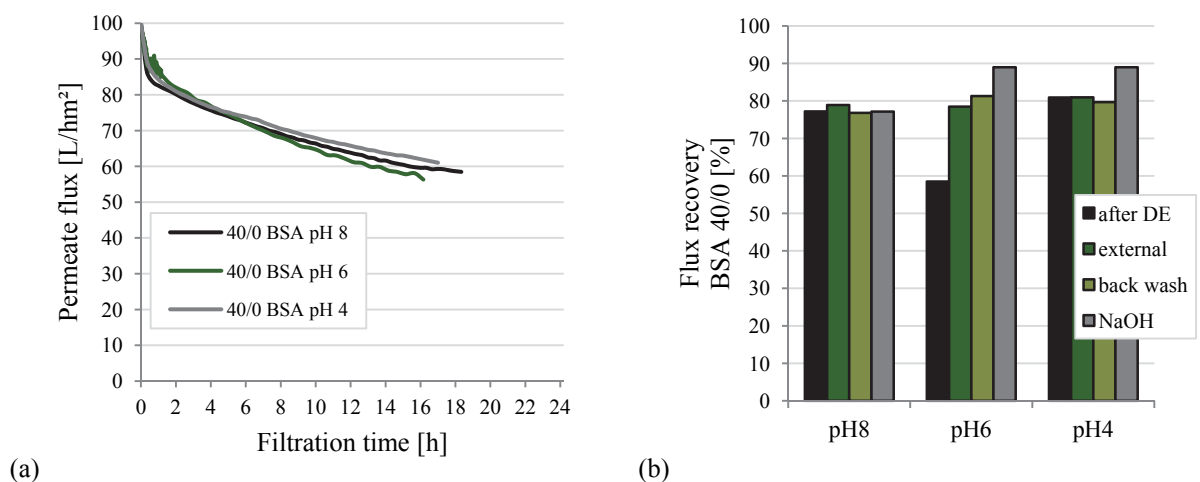
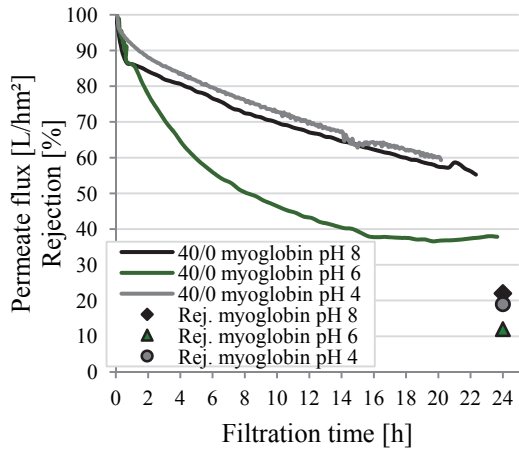
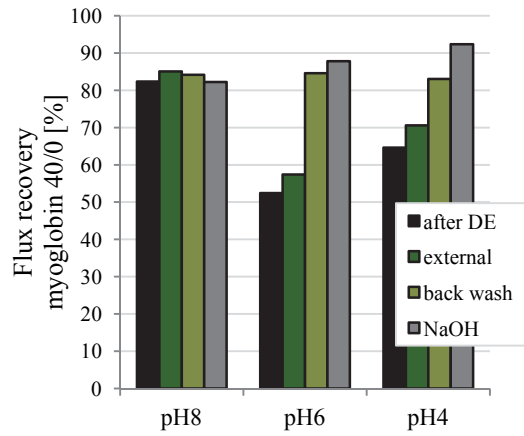


Figure 67 Effect of the pH during DE filtration of BSA through PES 50 40/0 5 J/cm²; (a) permeate flux and rejection; (b) flux recovery during cleaning.

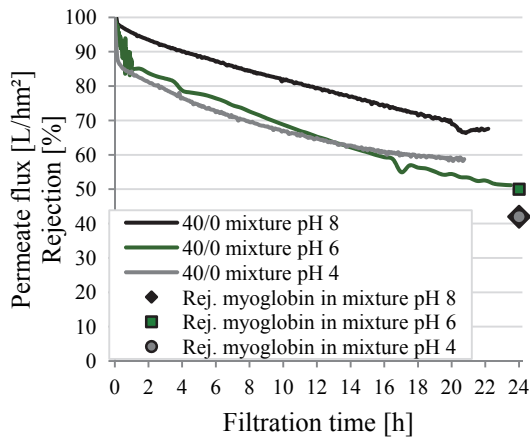


(a)

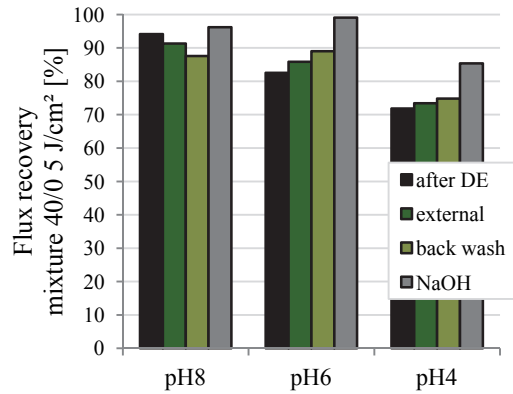


(b)

Figure 68 Effect of the pH during DE filtration of myoglobin through PES 50 40/0 5 J/cm²; (a) permeate flux and rejection; (b) flux recovery during cleaning.

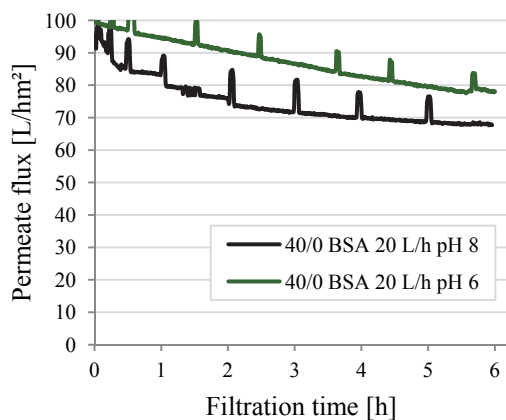


(a)

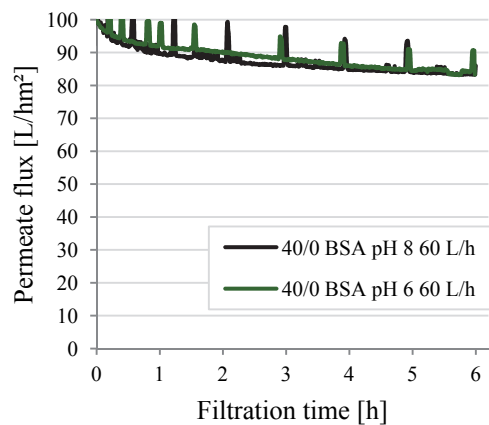


(b)

Figure 69 Effect of the pH during DE filtration of mixture through PES 50 40/0 5 J/cm²; (a) permeate flux and rejection of myoglobin; (b) flux recovery during cleaning.



(a)



(b)

Figure 70 Permeate flux and rejection during CF filtration of BSA through PES 50 modified with 40/0 5 J/cm² at varied CF and pH value; (a) 20 L/h; (b) 60 L/h CF.

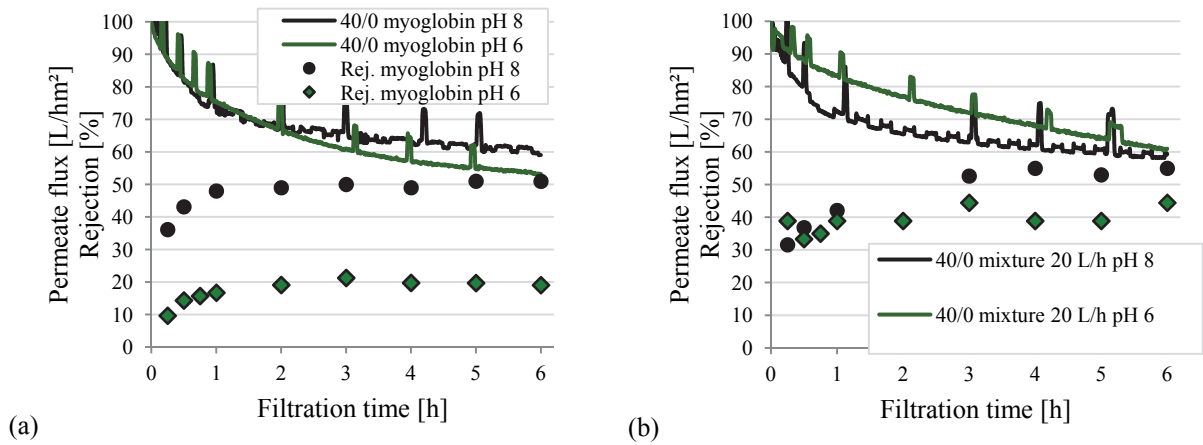


Figure 71 Permeate flux and rejection during CF filtration through PES 50 modified with 40/0 5 J/cm² at 20 L/h CF and varied pH value; (a) myoglobin; (b) mixture.

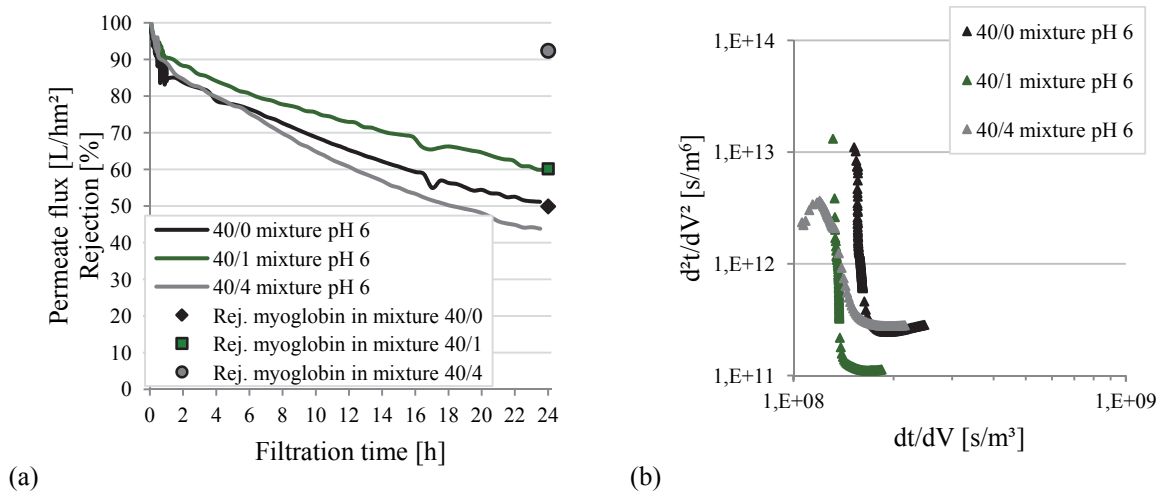


Figure 72 Effect of the crosslinking degree during DE filtration of mixture at pH = 6; (a) permeate flux and rejection of myoglobin; (b) fouling mechanism analysis; (c) flux recovery.

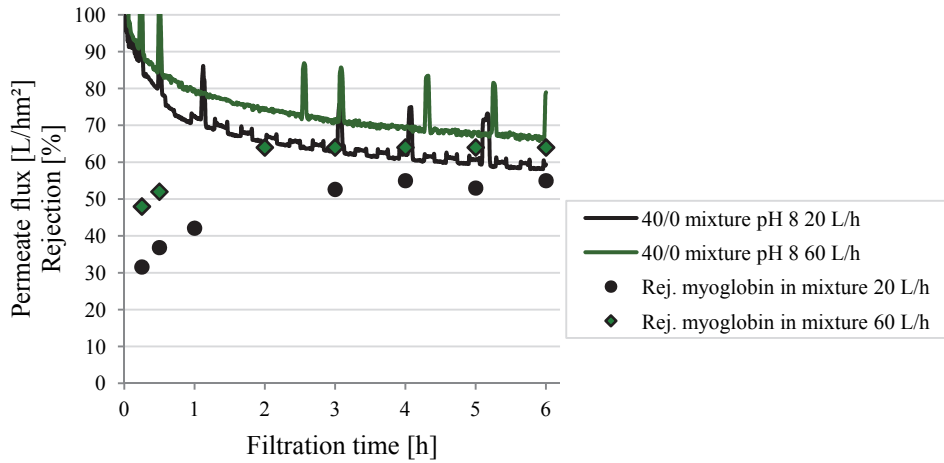


Figure 73 Permeate flux and rejection during CF filtration of mixture through PES 50 modified with 40/0 5 J/cm² at pH = 8 and varied CF.

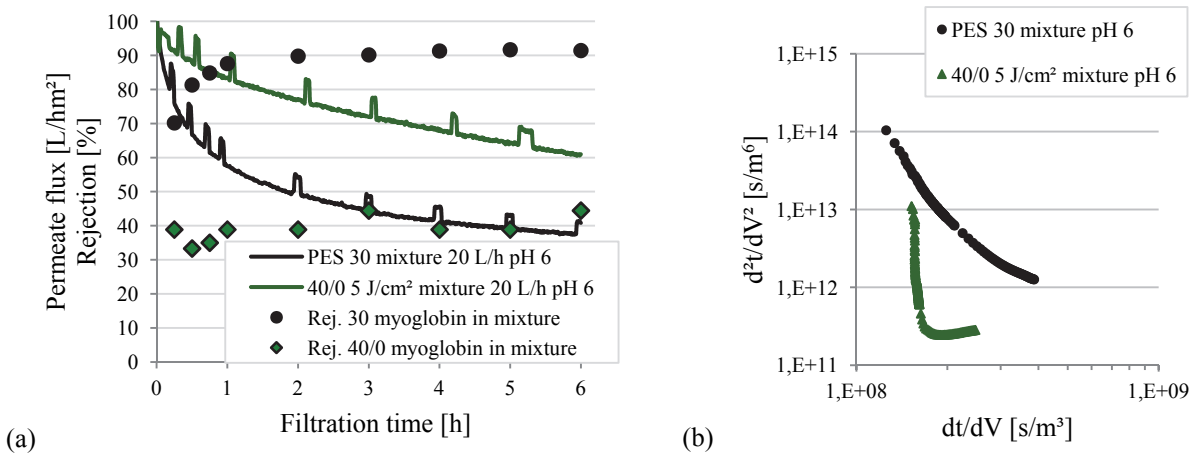


Figure 74 Comparison of virgin PES 30 and PES 50 40/0 5 J/cm², filtration of mixture; (a) permeate flux and rejection during CF filtration; (b) fouling mechanism analysis for DE filtration.

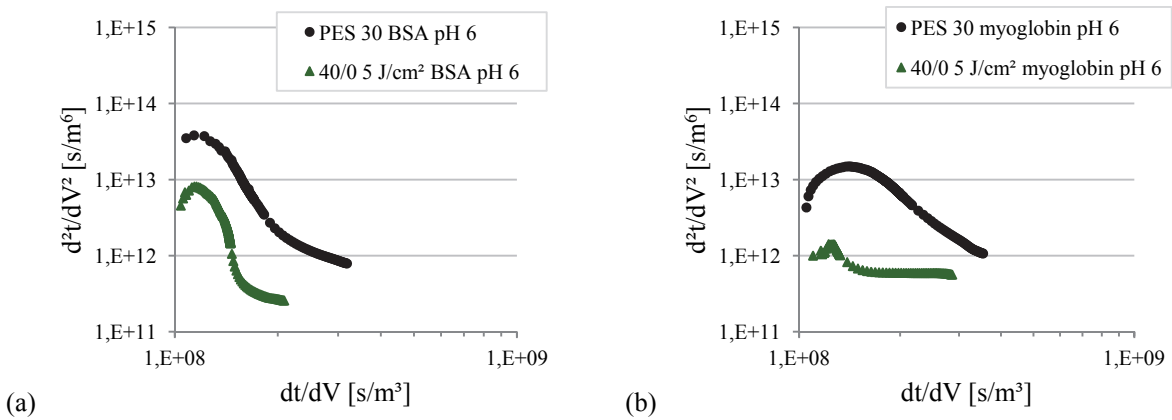


Figure 75 Comparison of virgin PES 30 and PES 50 40/0 5 J/cm²: fouling mechanism analysis for DE filtration of (a) BSA; (b) myoglobin.

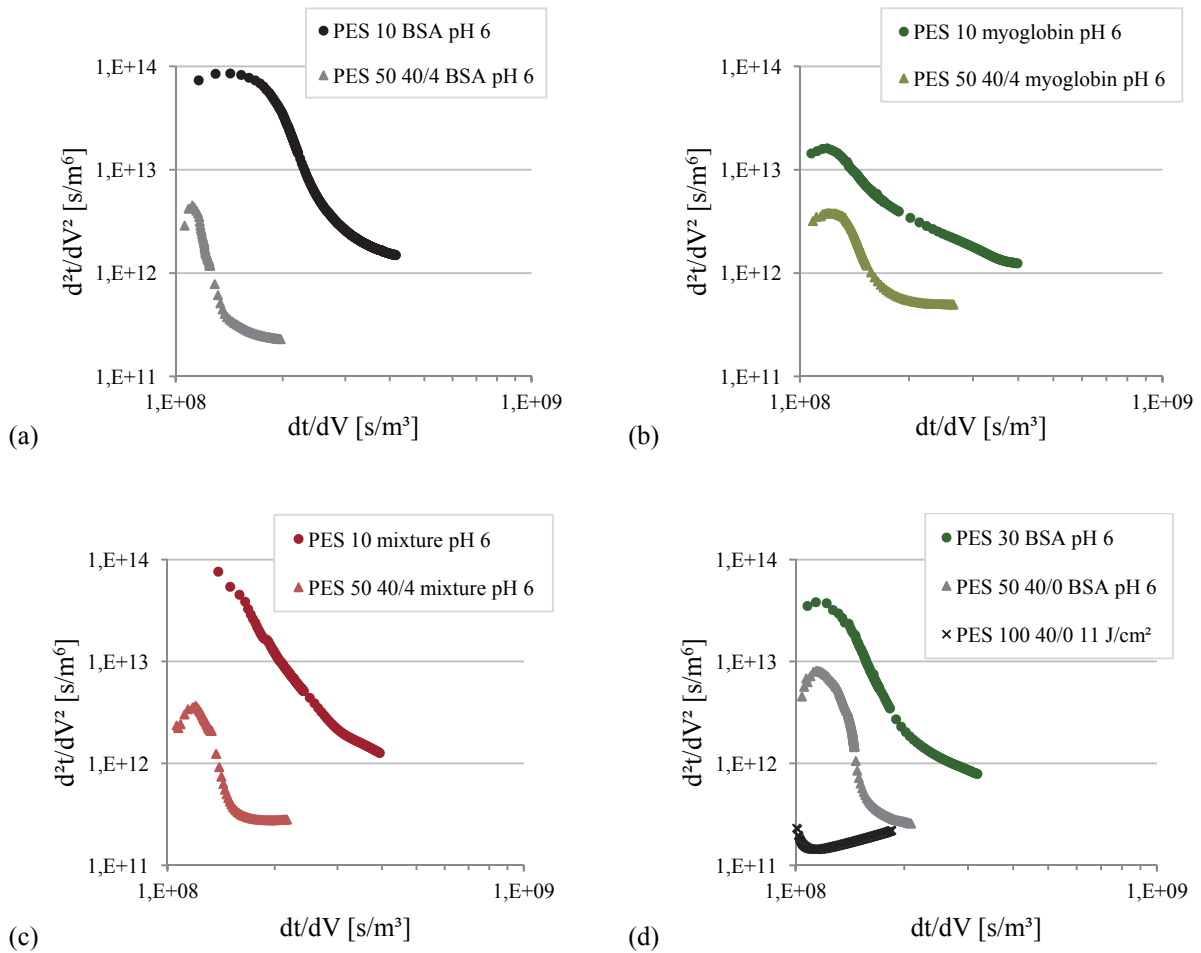


Figure 76 Fouling mechanism analysis. Comparison of DE filtration with virgin and modified membranes with similar water flux and cut-off at pH 6; (a) BSA; (b) myoglobin; (c) mixture; (d) modified PES 100 BSA.

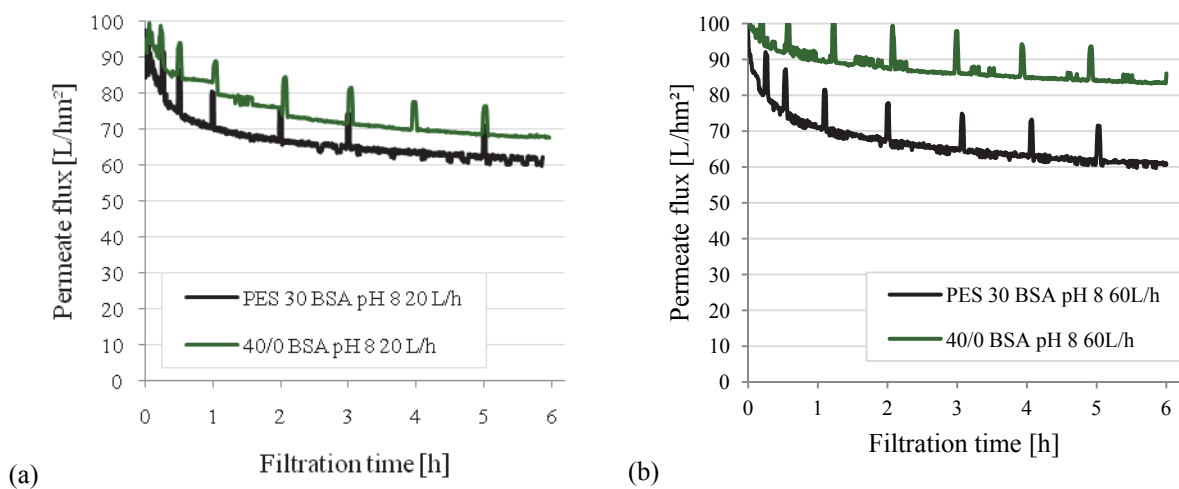
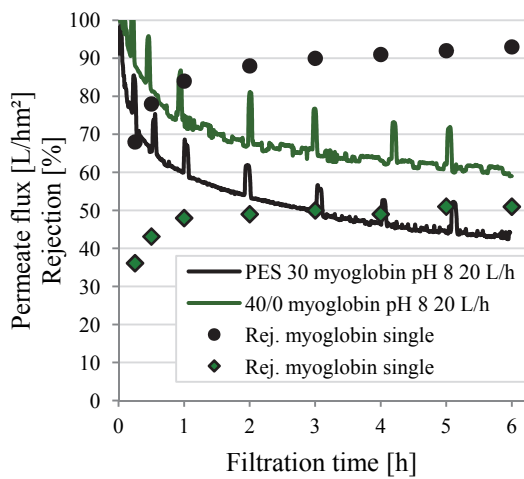
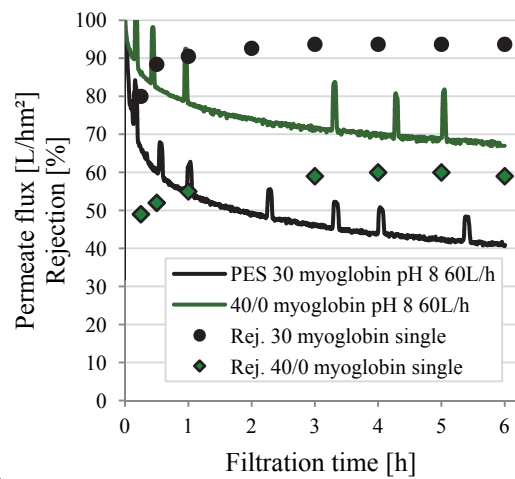


Figure 77 Permeate flux comparison of virgin PES 30 and PES 50 modified with 40/0 5 J/cm² during CF filtration of BSA at pH = 8 and varied CF; (a) 20 L/h; (b) 60 L/h CF.

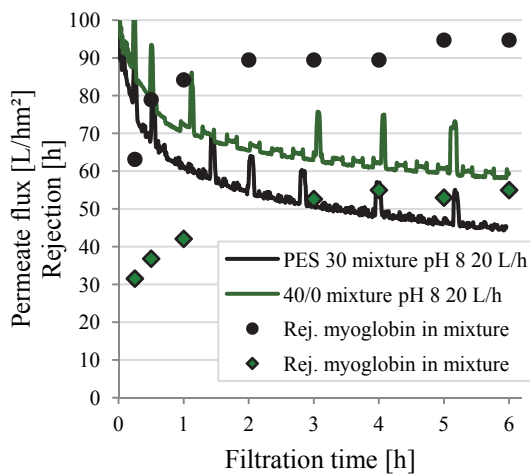


(a)

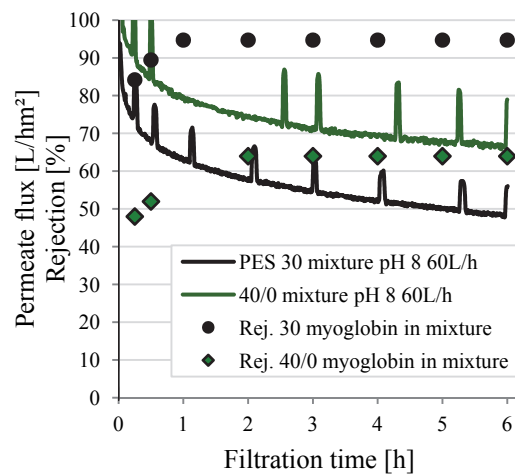


(b)

Figure 78 Permeate flux and rejection comparison of virgin PES 30 and PES 50 modified with 40/0 5 J/cm² during CF filtration of myoglobin at pH = 8 and varied CF; (a) 20 L/h; (b) 60 L/h CF.



(a)



(b)

Figure 79 Permeate flux and rejection comparison of virgin PES 30 and PES 50 modified with 40/0 5 J/cm² during CF filtration of mixture at pH = 8 and varied CF; (a) 20 L/h; (b) 60 L/h CF.

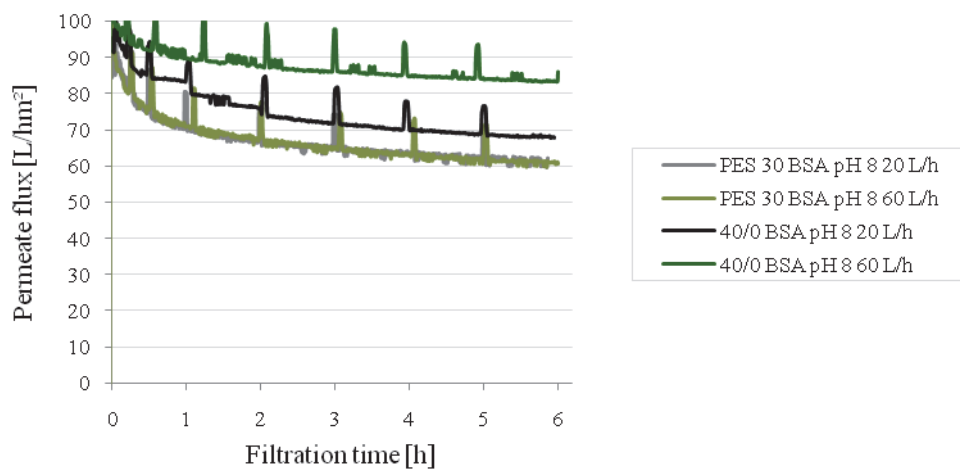


Figure 80 Permeate flux direct comparison of virgin PES 30 and PES 50 modified with 40/0 5 J/cm² during CF filtration of BSA at pH = 8 and varied CF.

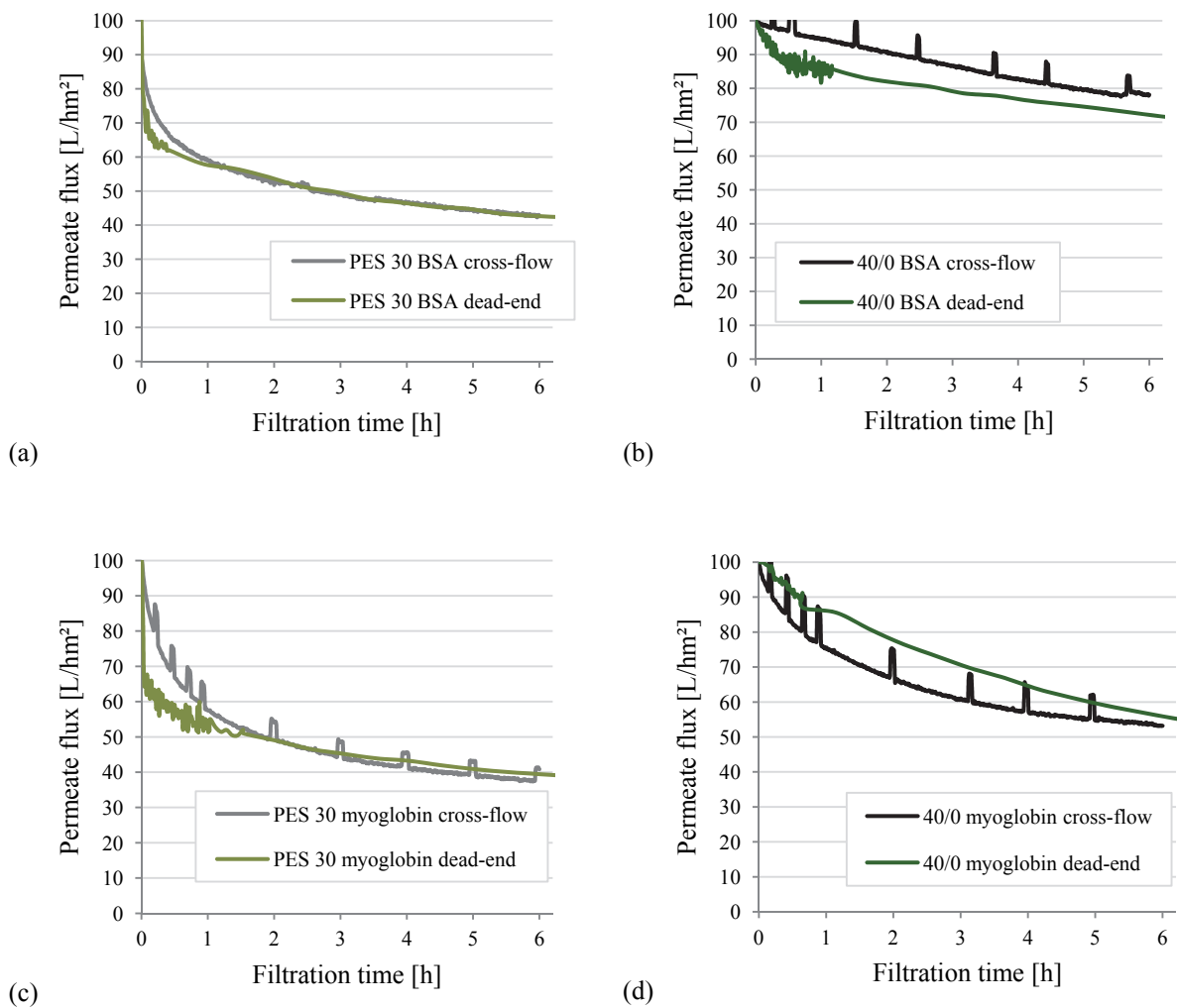


Figure 81 Comparison of permeate fluxes during DE and CF filtration at pH = 6; (a) PES 30 virgin BSA; (b) 40/0 5 J/cm² BSA; (c) PES 30 virgin myoglobin; (d) 40/0 5 J/cm² myoglobin.

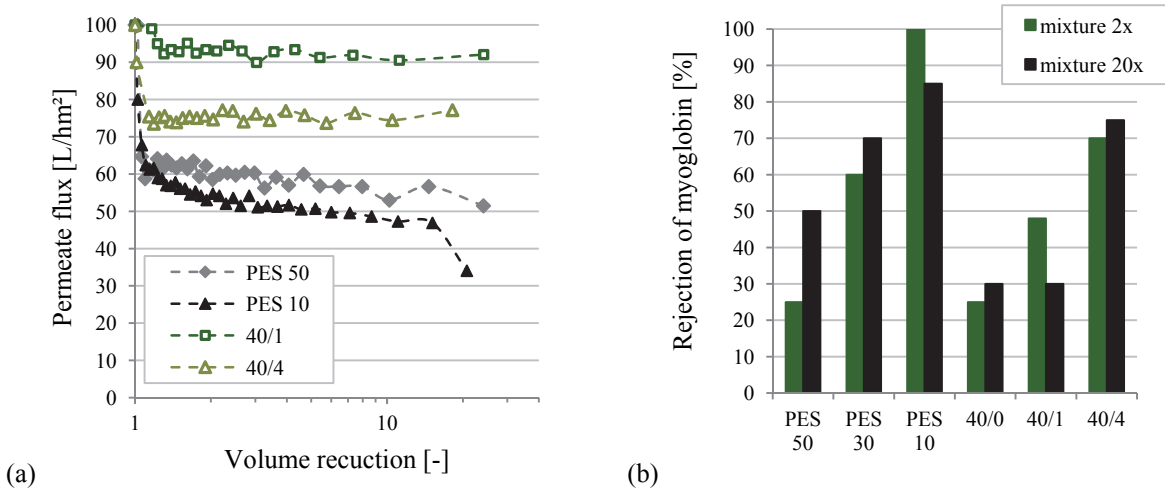


Figure 82 Filtrations with 20 fold volume reduction; (a) permeate flux of BSA; (b) rejection of myoglobin from mixture.

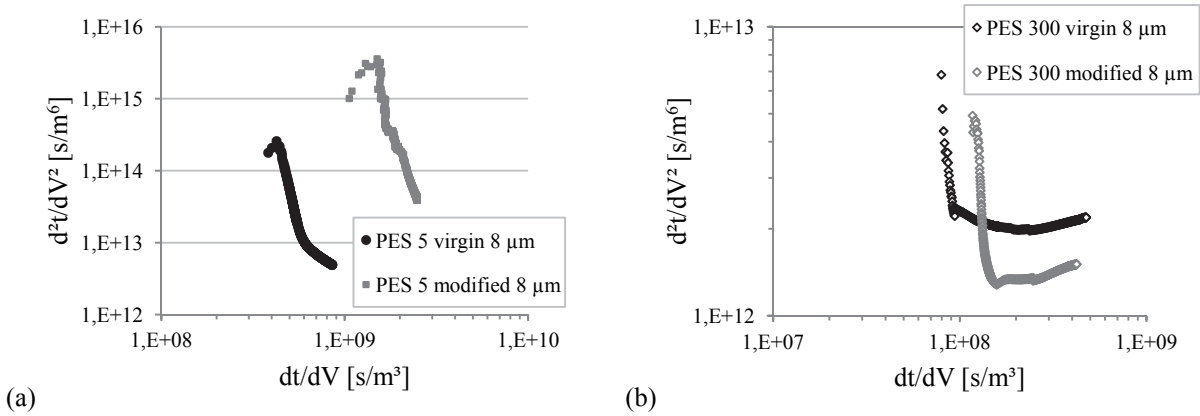


Figure 83 Fouling mechanism analysis for some virgin and modified membranes; (a) PES 5; (b) PES 300.

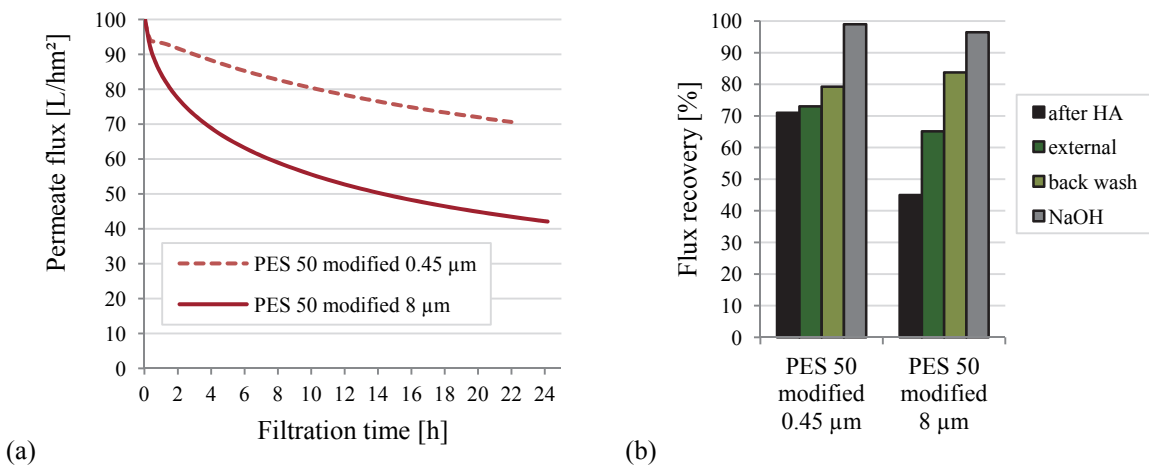


Figure 84 Effect of the HA prefiltration for modified PES 50; (a) permeate flux; (b) flux recovery by cleaning.

APPENDIX B

LIST OF TABLES

Table 4.1	Cross-section structure of the used membranes.....	22
Table 4.2	Molecular weight of the used modifying monomers.....	23
Table 4.3	Concentration of the modifier compositions in g/L.....	23
Table 4.4	Concentration of the hydrogel compositions in g/L.....	24
Table 4.5	Composition of the dextran and PEG mixtures.....	24
Table 4.6	Characteristics of the used test solutions.....	25
Table 5.1	CA and DG of membranes and film after modification at 11 J/cm ² . Variation of the UV intensity.....	43
Table 5.2	CA and DG of modified PES 50 with 11 J/cm ² depending on the crosslinking type and amount.....	44
Table 5.3	Roughness of virgin and modified membranes measured in wet and dry state.....	49
Table 5.4	Water permeability of virgin membranes and relative flux after modification with 11 J/cm ²	55
Table 5.5	Summary of the parameters and characteristics during the measurement of rejection curves with dextran and PEG (initial flux: 10 L/hm ²).....	60
Table 5.6	Characteristics of the rejection curves measurement with dextran and PEG of virgin PES 50 at varied operating pressure.....	61
Table 5.7	Summary of the effective diffusion coefficients through virgin and modified membranes of myoglobin and BSA as single solutions and mixture at pH = 6.....	70
Table 5.8	Obtained data from filtration experiments of BSA through virgin and modified PES 30. Effect of PVP.....	72
Table 5.9	Apparent rejection of myoglobin and BSA after short DE filtration through PES 50 depending on the UV irradiation intensity.....	73
Table 5.10	Operating parameters and apparent rejection of the tested solutes in all performed DE filtration runs with virgin PES 10.....	80
Table 5.11	Operating parameters and apparent rejection of the tested solutes in all performed DE filtration runs with virgin PES 30.....	82
Table 5.12	Operating parameters and apparent rejection of the tested solutes in all performed DE filtration runs with virgin PES 50.....	83
Table 5.13	Operating parameters and apparent rejection of the tested solutes in all performed DE filtration runs with modified PES 50.....	84

Table 5.14	Operating parameters and apparent rejection of the tested solutes in all performed DE filtration runs with virgin and modified PES 100	88
Table 5.15	Operating parameters and measured critical data of all tested membranes at pH 6.....	90
Table 5.16	Summary of the operating parameters and measured data from the DE filtration of humic acid through virgin and modified membranes	99
Table 6.1	Determined parameters from dextran rejection tests with virgin and modified membranes	113
Table 6.2	Comparison of the relative permeate flux after 24 hours dead-end filtration of virgin and modified membranes with similar water flux and cut-off. An overview.	136
Table 6.3	Relative fluxes after 6 hours of filtration, comparison of dead-end and cross-flow modes	143
Table 6.4	Characteristics of the fouling layer according to the resistance in series model.....	154

LIST OF FIGURES

Figure 2.1	Schematic view of the three stages in flux decline.....	3
Figure 2.2	Schematic view of the mass transport within a boundary layer.....	4
Figure 2.3	Fouling mechanisms depending on the relationship pore size/solute size.....	6
Figure 2.4	Possible resistances against solvent transport occurring during filtration processes.....	8
Figure 2.5	Operation modes of filtration; (a) dead-end; (b) cross-flow.....	11
Figure 2.6	Initiation mechanisms for “grafting-from” surface functionalisation; (a) controlled degradation of the membrane polymer; (b) decomposition of an initiator; (c) adsorption of an initiator on the surface.	16
Figure 3.1	Mechanism of the chemical reaction on the membrane surface during “grafting-from” modification of PES with PEGMA.....	18
Figure 3.2	Schematic representation of a filtration process with commercial (left) and thin-layer hydrogel composite membranes (right).	19
Figure 3.3	Schematic view of UF regimes with composite membranes. Influence of: (a) base membrane pore size and (b) hydrogel layer architecture.....	20
Figure 4.1	Structural formula of PES (repeating unit).....	22
Figure 4.2	Structural formulas of the used modifying monomers; (a) PEGMA; (b) MBAA; (c) PETAE.....	23
Figure 4.3	Molecular weight distribution of feeds used for the determination of rejection curves; (a) dextran; (b) PEG.....	25
Figure 4.4	Molecular size distribution of the used proteins at pH = 6.	26
Figure 4.5	Molecular size distribution of myoglobin depending on the pH value.....	26
Figure 4.6	Particle size distribution of humic acid at the beginning and after 24 hours of the filtration runs.	26
Figure 4.7	Experimental set-up for membrane UV irradiation.	29
Figure 4.8	Schematic representation of the SurPASS adjustable gap cell [155].	32
Figure 4.9	Schematic view of DE filtration set-up.....	34
Figure 4.10	Schematic view of diffusion equipment.	36
Figure 4.11	Schematic view of the CF filtration set-up.....	38
Figure 4.12	Molecular size distribution of BSA during CF filtration depending on the filtration time.	39
Figure 4.13	Determination of the critical flux and pressure from CF filtration experiments.	39

Figure 5.1	Hydrogels degree of swelling depending on the crosslinker amount.....	41
Figure 5.2	Partitioning coefficient after 24 hours absorption of test solutes on hydrogels with maximal crosslinking amount.	42
Figure 5.3	DG at varied UV irradiation dose. Example: PES 10 modified with PEGMA 400.....	43
Figure 5.4	CA depending on the UV irradiation dose. Example: PES 10 modified with PEGMA 400.....	43
Figure 5.5	ATR-IR spectra of PES, PEG, virgin and modified membranes.	45
Figure 5.6	ZP of selected virgin membranes and film.	46
Figure 5.7	ZP at pH = 5.6 as function of the cell gap height.....	46
Figure 5.8	Streaming current coefficient of virgin membranes and film vs. cell gap height.	46
Figure 5.9	Cell conductivity during the ZP measurement at varied cell gap height.	46
Figure 5.10	ZP of virgin and modified membranes PES 50 at varied UV irradiation dose and crosslinking type.	47
Figure 5.11	ZP of virgin and modified membranes PES 5 (9 J/cm ²) before and after static adsorption with 10 g/L BSA at pH 4.8.....	47
Figure 5.12	AFM 3D visualisation of membranes; (a) PES 5 virgin, dry state; (b) PES 5 modified, dry state; (c) PES 50 virgin, wet state; (d) PES 50 modified, wet state.....	48
Figure 5.13	SEM cross-section images of selected membranes; (a) PES 50; (b) PES 100.....	49
Figure 5.14	SEM surface images of the used virgin membranes; (a) PES 30; (b) PES 30 without PVP; (c) PES 50; (d) PES 100; (e) PES 300.....	50
Figure 5.15	SEM surface images of PES 50 UV irradiated with 11 J/cm ² at 5 mW/cm ² ; (a) irradiated in water; (b) modified with 40/0; (c) modified with 40/4; (d) modified with 40/6.65.	51
Figure 5.16	SEM cross-section images of the skin layer of PES 100 UV irradiated with 11 J/cm ² ; (a) virgin; (b) irradiated in water at 5 mW/cm ² ; (c) irradiated in water at 60 mW/cm ² ; (d) modified with 40/0 at 5 mW/cm ² ; (e) modified with 40/1 at 5 mW/cm ² ; (f) modified with 40/4 at 5 mW/cm ²	52
Figure 5.17	Cu/S ratio in the cross-section of modified membranes with 11 J/cm ²	53
Figure 5.18	Cu/S ratio in the cross-section of PES 50 modified at varied UV irradiation dose.	53
Figure 5.19	Apparent distance between two radicals for selected membranes and films irradiated with 5 J/cm ²	54
Figure 5.20	Apparent average distance between two radicals for PES 10 and films under variation of the UV irradiation dose.....	54
Figure 5.21	Flux ratio at varied UV irradiation dose. Example: PES 10 modified with 40/0.....	55
Figure 5.22	Water permeability of PES 50 40/0, 11 J/cm ² at varied UV intensity.	55

Figure 5.23 Water permeability of PES 10 as function of the crosslinker amount at varied UV irradiation dose; (a) PEGMA 400/MBAA; (b) PEGMA 400/PETAE.....	56
Figure 5.24 Water permeability of PES 50 as function of the crosslinker amount at varied UV irradiation dose; (a) PEGMA 200/MBAA; (b) PEGMA 400/MBAA.....	57
Figure 5.25 Water permeability of PES 50 modified with PEGMA 400 as function of the PETAE amount at varied UV irradiation dose.....	58
Figure 5.26 Water permeability of PES 100 as function of the crosslinker amount at varied UV irradiation dose; (a) PEGMA 400/MBAA; (b) PEGMA 400/PETAE.....	58
Figure 5.27 Water permeability of PES 300 as function of the crosslinker amount at varied UV irradiation dose; (a) PEGMA 400/MBAA; (b) PEGMA 400/PETAE.....	59
Figure 5.28 Rejection curves of all virgin membranes; (a) with dextran; (b) with PEG.	61
Figure 5.29 Rejection curves of virgin PES 50 with dextran; (a) at varied initial flux; (b) at varied feed.	62
Figure 5.30 Rejection curves with dextran of PES 50. Effect of the irradiation in water.....	63
Figure 5.31 Rejection curves with dextran of PES 50 modified with 40/0 at varied UV intensity.	63
Figure 5.32 Rejection curves of PES 10 modified with varied UV irradiation dose.	63
Figure 5.33 Rejection curve of modified PES 30.....	63
Figure 5.34 Rejection curve of modified PES 30 without PVP.....	64
Figure 5.35 Rejection curves of PES 50 modified with varied UV irradiation dose.	64
Figure 5.36 Rejection curves of PES 100 modified with varied UV irradiation dose.	65
Figure 5.37 Rejection curves of PES 300 modified with varied UV irradiation dose.	65
Figure 5.38 Rejection curves of PES 10 modified with different crosslinker type.....	65
Figure 5.39 Rejection curves of modified PES 50 with varied irradiation dose; (a) PEGMA/MBAA; (b) PEGMA/PETAE.....	66
Figure 5.40 Rejection curves of modified PES 50 with variation of the crosslinker amount; (a) PEGMA/MBAA; (b) PEGMA/PETAE.....	67
Figure 5.41 Rejection curves of modified PES 100 with varied irradiation dose; (a) PEGMA/MBAA; (b) PEGMA/PETAE.....	67
Figure 5.42 Rejection curves of modified PES 100 with variation of the crosslinker amount; (a) PEGMA/MBAA; (b) PEGMA/PETAE.....	68
Figure 5.43 Fouling resistance to myoglobin and BSA of virgin PES 10 and PES 50 and modified PES 50 with varied UV irradiation energy.....	69
Figure 5.44 Adsorbed amount of BSA after 24 h of static adsorption. Effect of the pore size and the functionalisation.....	69

Figure 5.45 Effective diffusion coefficient of BSA over time through virgin and modified membranes.	71
Figure 5.46 Adsorbed amount of solutes as single during 48 h of diffusion.	71
Figure 5.47 Permeate flux behaviour of virgin and modified membranes during short DE filtrations; (a) PES 50; (b) PES 100.	72
Figure 5.48 Fouling resistance of PES 50 modified with PEGMA 200 depending on the UV irradiation dose; (a) myoglobin; (b) BSA.	74
Figure 5.49 Fouling resistance of PES 50 modified with PEGMA 400 depending on the UV irradiation dose; (a) myoglobin; (b) BSA.	74
Figure 5.50 Apparent protein rejection of modified PES 50; (a) PEGMA 200/MBAA, single solutions; (b) PEGMA 400/MBAA, single solutions; (c) PEGMA 400/MBAA, UV irradiation dose: 5 J/cm ² , mixture.	75
Figure 5.51 Apparent protein rejection of PES 50 modified with PEGMA 400/PETAE.	76
Figure 5.52 Fouling resistance of PES 100 modified with PEGMA 400 depending on the UV irradiation dose; (a) BSA; (b) γ -globulin.	77
Figure 5.53 Apparent protein rejection of modified PES 100; (a) PEGMA 400/MBAA; (b) PEGMA 400/PETAE.	77
Figure 5.54 Fouling resistance of PES 300 modified with PEGMA 400 depending on the UV dose. .	78
Figure 5.55 Apparent protein rejection of PES 300 modified with PEGMA 400.	78
Figure 5.56 Permeate flux of BSA during the 20x volume reduction; (a) virgin membranes; (b) modified PES 50.	79
Figure 5.57 Apparent rejection of solutes during 20x volume reduction; (a) single solutions; (b) mixture.	80
Figure 5.58 Permeate flux behaviour during the DE filtration of BSA, myoglobin and their mixture through virgin PES 10; (a) pH 4; (b) pH 6; (c) pH 8.	81
Figure 5.59 Permeate flux behaviour during the DE filtration of BSA, myoglobin and their mixture through virgin PES 30; (a) pH 4; (b) pH 6; (c) pH 8.	82
Figure 5.60 Permeate flux behaviour during the DE filtration of globulin, BSA, myoglobin and their mixture through virgin PES 50; (a) pH 4; (b) pH 6; (c) pH 8.	83
Figure 5.61 Permeate flux behaviour during the DE filtration of BSA, myoglobin and their mixture through modified PES 50; (a) pH 4; (b) pH 6; (c) pH 8.	85
Figure 5.62 Flux recovery of PES 50 modified with 40/0 5 J/cm ² during the cleaning process; (a) pH 4; (b) pH 6; (c) pH 8.	86
Figure 5.63 Permeate flux behaviour during the DE filtration of BSA, myoglobin and their mixture through modified PES 50 with 8 J/cm ² ; (a) 40/0 at pH 8; (b) 40/0 at pH 4; (c) 40/4 at pH 4.	87

Figure 5.64 Flux recovery of modified PES 50 with 8 J/cm ² during the cleaning process after DE filtration; (a) 40/0 at pH 8; (b) 40/0 at pH 4; (c) 40/4 at pH 4.	87
Figure 5.65 Permeate flux behaviour during DE filtration experiments with γ -globulin and BSA through PES 100; (a) virgin PES 100; (b) PES 100 modified with 40/0 11 J/cm ² ; (c) PES 100 modified with 40/0 14 J/cm ²	89
Figure 5.66 Flux recovery of PES 100 during the cleaning process after DE filtration; (a) virgin PES 100; (b) PES 100 modified with 40/0 11 J/cm ² ; (c) PES 100 modified with 40/0 14 J/cm ²	89
Figure 5.67 Permeate flux and rejection during the CF filtration of BSA, myoglobin and their mixture through virgin PES 10 at 20 L/h CF; (a) pH = 6; (b) pH = 8.	91
Figure 5.68 Permeate flux and rejection during the CF filtration of BSA, myoglobin and their mixture through virgin PES 10 at 60 L/h CF; (a) pH = 6; (b) pH = 8.	92
Figure 5.69 Permeate flux and rejection during the CF filtration of BSA, myoglobin and their mixture through virgin PES 30 at 20 L/h CF; (a) pH = 6; (b) pH = 8.	93
Figure 5.70 Permeate flux and rejection during the CF filtration of BSA, myoglobin and their mixture through virgin PES 30 at 60 L/h CF and pH = 8.	93
Figure 5.71 Permeate flux and rejection during the CF filtration of BSA, myoglobin and their mixture through virgin PES 50 at 20 L/h CF; (a) pH = 6; (b) pH = 8.	94
Figure 5.72 Permeate flux and rejection during the CF filtration of BSA, myoglobin and their mixture through PES 50 modified with 40/0 5 J/cm ² at 20 L/h CF; (a) pH = 6; (b) pH = 8.	95
Figure 5.73 Permeate flux during CF filtration of mixture through PES 50 40/0 11 J/cm ² at 20 L/h CF.	96
Figure 5.74 Permeate flux and rejection during the CF filtration of BSA, myoglobin and their mixture through PES 50 modified with 40/0 5 J/cm ² at 60 L/h CF; (a) pH = 6; (b) pH = 8.	96
Figure 5.75 Filtration stability test of virgin PES 10 with BSA at 20 L/h CF; (a) resistance and rejection; (b) flux recovery after the cleaning procedures.	97
Figure 5.76 Filtration stability test of PES 50 modified with 40/0 5 J/cm ² with BSA at 20 L/h CF; (a) resistance and rejection; (b) flux recovery after the cleaning procedures.	98
Figure 5.77 Flux behaviour during the DE filtration of humic acid through virgin membranes; prefiltration through (a) 8 μ m and (b) 0.45 μ m filter.	100
Figure 5.78 Flux recovery after cleaning; prefiltration through (a) 8 μ m and (b) 0.45 μ m filter.	100
Figure 5.79 Flux behaviour during the DE filtration of humic acid through modified membranes; prefiltration through (a) 8 μ m and (b) 0.45 μ m filter.	101
Figure 5.80 Flux recovery after cleaning; prefiltration through (a) 8 μ m and (b) 0.45 μ m filter.	102

Figure 5.81 Photographic images of the membrane outer surface of modified PES 10 after each stage of the cleaning procedure; up – prefiltration through 8 μm filter; down – prefiltration through 0.45 μm filter; (a) after HA, (b) external cleaning, (c) back wash, (d) chemical cleaning with NaOH at pH = 13.	103
Figure 5.82 Fouling resistance to polyphenolics of virgin and modified membranes depending on the UV irradiation dose.	104
Figure 5.83 Polyphenolics apparent rejection of virgin and modified membranes vs. UV irradiation dose.	104
Figure 5.84 Permeate flux ratio during the CF filtration of polyphenolics through virgin PES 50 depending on the operating pressure.	105
Figure 5.85 Permeate flux ratio during the filtration of polyphenolics through PES 50 modified with 40/0 under variation of the UV irradiation dose.	105
Figure 6.1 Effect of the UV intensity on DG, water permeability and cut-off of PES 50 40/0 11 J/cm ²	108
Figure 6.2 Effect of the crosslinking type on the rejection curves of modified membranes with 11 J/cm ² ; (a) PES 50; (b) PES 100.	109
Figure 6.3 Schematic view of the effect of the crosslinking type on hydrogel structure.	110
Figure 6.4 Comparison of rejection curves; (a) virgin PES 5 vs. modified PES 30; (b) virgin PES 10 vs. modified PES 50; (c) virgin PES 30 vs. modified PES 50; (d) virgin PES 30 vs. modified PES 100.	114
Figure 6.5 Protein charge of BSA and myoglobin depending on pH.	116
Figure 6.6 Effect of pH on the hydrodynamic diameter of BSA, myoglobin and mixture; (a) pH = 4; (b) pH = 6; (c) pH = 8.	117
Figure 6.7 Translation of the filtration results into fouling mechanism analysis data.	118
Figure 6.8 Relative flux after 16 hours filtration of proteins at varied pH value through virgin membranes.	120
Figure 6.9 Effect of the membrane pore size on the permeate flux and rejection during dead-end filtration of BSA at pH = 6.	120
Figure 6.10 Fouling mechanism analysis for dead-end filtration of BSA with virgin membranes at pH = 6.	120
Figure 6.11 Effect of the membrane pore size on fouling for the filtration of BSA at pH = 6. A schematic view.	121
Figure 6.12 Effect of the membrane pore size on the permeate flux and rejection during cross-flow filtration of myoglobin at pH = 6.	122
Figure 6.13 Fouling mechanism analysis for dead-end filtration of myoglobin with virgin membranes at pH = 6.	122

Figure 6.14 Effect of the membrane pore size on fouling for the filtration of myoglobin at pH = 6. A schematic view.....	123
Figure 6.15 Effect of the pore size on the flux recovery after the cleaning of virgin membranes; dead-end filtrations of BSA at: (a) pH = 8; (b) pH = 6; (c) pH = 4.....	125
Figure 6.16 Effect of the CF on the permeate flux during cross-flow filtration of BSA through virgin PES 10 at varied pH; (a) pH = 6; (b) pH = 8.....	126
Figure 6.17 Relative flux after 16 hours filtration of proteins at varied pH value through modified membranes with 5 J/cm ²	128
Figure 6.18 Effect of the crosslinking degree on the permeate flux during dead-end filtration of BSA at pH = 6.	131
Figure 6.19 Fouling mechanism analysis for dead-end filtration of BSA with modified membranes at pH = 6.	131
Figure 6.20 Effect of the crosslinking degree on the permeate flux and rejection during dead-end filtration of myoglobin at pH = 6.....	132
Figure 6.21 Fouling mechanism analysis for dead-end filtration of myoglobin with modified membranes at pH = 6.....	132
Figure 6.22 Effect of the crosslinking degree on the flux recovery from the cleaning of PES 50 5 J/cm ² modified membranes after dead-end filtration at pH = 6; (a) BSA; (b) myoglobin.....	133
Figure 6.23 Effect of the CF on the permeate flux during cross-flow filtration of BSA through PES 50 40/0 5 J/cm ² at pH 8.....	134
Figure 6.24 Effect of CF on permeate flux and rejection during CF filtration of myoglobin with PES 50 40/0 5 J/cm ² , pH = 8.	134
Figure 6.25 Fouling resistance of virgin and modified membranes after static adsorption.	135
Figure 6.26 Effect of modification on permeate flux during DE filtration of BSA, membranes with similar water flux and cut-off.	136
Figure 6.27 Effect of the modification on permeate volume, comparison of membranes with similar water flux and cut-off.	136
Figure 6.28 Comparison of virgin PES 30 and PES 50 40/0 5 J/cm ² : permeate flux and rejection during cross-flow filtration of BSA.....	137
Figure 6.29 Effect of the membrane modification on fouling for the filtration of BSA at pH = 6. A schematic view.....	138
Figure 6.30 Comparison of permeate flux and rejection during cross-flow filtration of (a) myoglobin through virgin PES 30 and PES 50 40/0 5 J/cm ² ; (b) mixture through virgin PES 10 and PES 50 40/0 11 J/cm ²	139

Figure 6.31 Effect of the membrane modification on fouling for the filtration of myoglobin at pH = 6. A schematic view.....	139
Figure 6.32 Effect of the test solution composition on permeate flux and rejection behaviour during the filtration with virgin and modified membranes; (a) virgin PES 30; (b) PES 50 modified with 40/0.5 J/cm ²	140
Figure 6.33 Effect of the pH value on permeate flux and rejection during the filtration of myoglobin with virgin and modified membranes; (a) virgin PES 30; (b) PES 50 modified with 40/0.5 J/cm ²	141
Figure 6.34 Effect of the CF on the flux behaviour of PES 10 virgin and PES 50 modified with 40/0.5 J/cm ² . Effect of pH; (a) pH = 6; (b) pH = 8.....	142
Figure 6.35 Effect of the volume reduction during dead-end filtration with virgin and modified membranes; (a) rejection of myoglobin as single solution; (b) permeate flux of virgin PES 30 and PES 50 40/0.5 J/cm ² during 20 fold volume reduction in DE filtration of BSA.....	144
Figure 6.36 Fouling mechanism analysis for the filtration of humic acid with 8 µm prefiltration; (a) virgin; (b) modified membranes.....	146
Figure 6.37 Fouling mechanism of filtrations of humic acid with 0.45 µm prefiltration; (a) virgin (b) modified membranes.....	148
Figure 6.38 Effect of the prefiltration on the permeate flux behaviour; (a) virgin; (b) modified membranes.....	149
Figure 6.39 Effect of the prefiltration on the cleanability of virgin and modified membranes.....	150
Figure 6.40 Flux during filtration of humic acid. Comparison of virgin and modified membranes with similar water flux and cut-off; (a) virgin PES 5 vs. modified PES 10 (8 µm prefiltration); (b) virgin PES 10 vs. modified PES 50 and PES 100 (8 µm prefiltration); (c) virgin PES 10 vs. modified PES 50 and PES 100 (0.45 µm prefiltration).....	152
Figure 6.41 Comparison of the fouling regimes for virgin and modified membranes with similar water flux and cut-off; (a) 8 µm; (b) 0.45 µm prefiltration.....	153
Figure 6.42 Comparison of the cleanability of virgin and modified membranes with similar water flux and cut-off; (a) virgin PES 5 and modified PES 10 (8 µm prefiltration); (b) virgin PES 10 and modified PES 50 and PES 100 (8 µm prefiltration); (c) virgin PES 10 and modified PES 50 and PES 100 (0.45 µm prefiltration).....	155
Figure 6.43 Effect of membrane pore size on the fouling resistance to polyphenolics for virgin and modified membranes.....	157
Figure 7.1 Trade-off analysis; (a) myoglobin rejection vs. water permeability; (b) MWCO vs. water permeability.....	159

ABBREVIATIONS

AA	Acrylic acid
AFM	Atomic force microscopy
APS	Ammonium perfulfate
ATR-IR	Attenuated total reflection infrared spectrometry
BSA	Bovine serum albumin
CA	Contact angle
CAC	Cellulose acetate
CF	Cross-flow
CP	Concentration polarisation
DE	Dead-end
DG	Degree of grafting
DLS	Dynamic light scattering
DPPH	2,2-diphenyl 1-picryl hydrazyl
DS	Degree of swelling
EDX	Energy-dispersive X-ray analysis
GPC	Gel permeation chromatography
HA	Humic acid
IEP	Isoelectric point
MBAA	N,N'-methylene bisacrylamide
MF	Microfiltration
MSD	Molecular size distribution
MW	Molecular weight
MWCO	Molecular weight cut-off
MWD	Molecular weight distribution
NF	Nanofiltration
NMP	N-methyl-2-pyrrolidone
NOM	Natural organic matter
NVP	N-vinyl-2-pyrrolidinone
PAA	Polyacrylic acid
PEG	Polyethylene glycol
PEGDA	Poly(ethylene glycol) dimethacrylate
PEGMA	Poly(ethylene glycol) methacrylate

PEGMEMMA	Poly(ethylene glycol) methyl ether methacrylate
PES	Polyethersulfone
PETAE	Pentaerythritol triallyl ether
PSf	Polysulfone
PSD	Particle size distribution
PVDF	Polyvinyl fluoride
PVP	Polyvinylpyrrolidone
SEM	Scanning electron microscopy
TMP	Transmembrane pressure
TMPTMA	Trimethylolpropane trimethacrylate
TOC	Total organic carbon
UF	Ultrafiltration
UV	Ultraviolet
ZP	Zetapotential

APPENDIX C**CURRICULUM VITAE**

Name	Polina Peeva
Date of birth	29 December 1983
Place of birth	Gabrovo, Bulgaria

Education

2008 – 2011	Doctoral study at the University of Duisburg-Essen, Lehrstuhl für Technische Chemie II
2007 – 2008	Master study in Chemical Engineering at Otto-von-Guericke Universität, Magdeburg
2002 – 2006	Bachelor study in Chemical Engineering at The University of Chemical Technology and Metallurgy, Sofia

Scholarships

2009 – 2011	DBU scholarship for Doctoral study at Universität Duisburg-Essen, Lehrstuhl für Technische Chemie II
2008 – 2009	DBU scholarship at Universität Duisburg-Essen, Lehrstuhl für Technische Chemie II
2006 – 2007	ERASMUS scholarship for Master study at Otto-von-Guericke Universität, Magdeburg
2006	DAAD scholarship for Bachelor thesis at Max-Planck-Institute for Dynamic of Complex Technical Systems, Magdeburg
2005	DAAD scholarship for Practical work at Max-Planck-Institute for Dynamic of Complex Technical Systems, Magdeburg

LIST OF PUBLICATIONS

Papers in journals (peer-reviewed)

1. P.D. Peeva, T. Pieper, M. Ulbricht
Tuning the ultrafiltration properties of anti-fouling thin-layer hydrogel polyethersulfone composite membranes by suited crosslinker monomers and photo-grafting conditions
Journal of Membrane Science 362 (2010) 560-568.
2. P.D. Peeva, A.E. Palupi, M. Ulbricht
Ultrafiltration of humic acid solutions through unmodified and surface functionalized low-fouling polyethersulfone membranes – Effects of feed properties, molecular weight cut-off and membrane chemistry on fouling behavior and cleanability
Separation and Purification Technology 81 (2011) 124-133
3. P.D. Peeva, N. Million, M. Ulbricht
Factors affecting the sieving behavior of anti-fouling thin-layer cross-linked hydrogel polyethersulfone composite ultrafiltration membranes
Journal of Membrane Science 390-391 (2012) 99-112
4. P.D. Peeva, T. Knoche, T. Pieper, M. Ulbricht
Performance of thin-layer hydrogel polyethersulfone composite membranes during dead-end ultrafiltration of various protein solutions
Industrial & Engineering Chemistry Research 2012 under revision
5. P.D. Peeva, T. Knoche, T. Pieper, M. Ulbricht
Cross-flow ultrafiltration of protein solutions through unmodified and surface functionalized polyethersulfone membranes – Effect of process conditions on separation performance
Separation and Purification Technology 2012 under revision

Oral presentations in conferences

- 2010 P.D. Peeva, M. Ulbricht
Tuning the sieving properties of low-fouling thin-layer composite polyethersulfone membranes by suitable crosslinking agents and conditions
19th International Congress of Chemical and Process Engineering, Prague, Czech Republic
- 2010 P.D. Peeva, M. Ulbricht
Preparation of low-fouling thin-layer composite polyethersulfone membranes by suitable crosslinking agents and conditions
XXVII European Membrane Society Summer School, Bucharest, Romania

Poster presentations in conferences

- 2010 P.D. Peeva, M. Ulbricht
Tuning the sieving properties of low-fouling PES composite membranes depending on the membrane pore size
13th Aachener Membran Kolloquium, Aachen, Germany
- 2010 P.D. Peeva, M. Ulbricht
Thin-layer hydrogel composite membranes for ultrafiltration with defined anti-fouling and selectivity properties
NanoMemCourse – Membranes for Health and Sustainable Water, Enschede, The Netherlands
- 2010 P.D. Peeva, M. Ulbricht
Thin-layer hydrogel composite membranes for ultrafiltration with defined anti-fouling and selectivity properties
DECHEMA Informationstag zum Stand der Membrantechnik im industriellen Einsatz, Frankfurt am Main, Germany
- 2009 P.D. Peeva, M. Ulbricht
Investigation in development and application of new low-fouling hydrogel composite ultrafiltration membranes
Euromembrane 2009, Montpellier, France
- 2009 P.D. Peeva, M. Ulbricht
Photografted hydrogel thin-layer composite ultrafiltration membranes with antifouling properties
Advanced Membrane Technology IV: Membranes for Clean and Sustainable Processes, Trondheim, Norway
- 2009 P.D. Peeva, M. Ulbricht
Low-fouling hydrogel thin-layer composite membranes for ultrafiltration
11. JungChemikerForum Frühjahrssymposium, Essen, Germany